# STRUCTURAL AND MOLECULAR ANALYSIS OF ARTERIOLAR ANNULI IN THE RETINA: IMPLICATIONS IN DIABETIC AND HYPERTENSIVE RETINOPATHY

Thesis presented by:

**DAVID RAMOS GONZALEZ**

Bellaterra July, 2013

# STRUCTURAL AND MOLECULAR ANALYSIS OF ARTERIOLAR ANNULI IN THE RETINA: IMPLICATIONS IN DIABETIC AND HYPERTENSIVE RETINOPATHY


Thesis presented by:

**DAVID RAMOS GONZALEZ**


To apply for the degree:

**PhD in BIOTECHNOLOGY**
**by the UNIVERSITAT AUTÒNOMA DE BARCELONA**

This PhD has been carried out under the direction of Dr. Jesús Ruberte París at the Genetics and Microbiology Department of the Universitat Autònoma de Barcelona and at the Center of Animal Biotechnology and Gene Therapy (CBATEG)

Jesús Ruberte París David Ramos González

Bellaterra July, 2013

JESÚS RUBERTE PARÍS, school professor at the Departament de Sanitat i Anatomia Animals of the Veterinary School at the Universitat Autònoma de Barcelona

CERTIFIES THAT:

DAVID RAMOS GONZALEZ has carried out this study about "**STRUCTURAL AND MOLECULAR ANALYSIS OF ARTERIOLAR ANNULI IN THE RETINA: IMPLICATION IN DIABETIC AND HYPERTENSIVE RETINOPATHY"**, under my direction at the Departament de Genètica I Microbiologia of the UAB.

Bellaterra, July, 2013

Dr. JESÚS RUBERTE PARÍS

A mi FAMILIA
(en mayúsculas)

# AGRADECIMIENTOS

Hay momentos en la vida que, pese a pasar desapercibidos, marcan un punto de inflexión. Recuerdo uno de estos momentos perfectamente. Recuerdo estar entre amigos y cervezas y recibir una llamada. Recuerdo también aceptar empezar una tesis. Y recuerdo atragantarme con la cerveza por la ilusión al celebrarlo. Que inocente era... ¡Cuantas veces se me habrá atragantado la tesis desde entonces!

Sin embargo, ahora que se acerca el final, no puedo más que sentir agradecimiento ya que, además de conocimientos, este trabajo me ha regalado gente maravillosa. Personas que me han ayudado a ser más grande que el mayor de los obstáculos, a nacer desde de la dificultad, a luchar, a seguir caminando, a comprender que cualquier momento es bueno para volver a empezar y que ninguno es tan terrible para claudicar, a ser el dueño de mi propio destino. Dice un proverbio oriental que quien camina solo llega antes, pero quien camina acompañado llega más lejos. A vosotros, que me habéis acompañado estos años, GRACIAS.

En primer lugar, quisiera dar las gracias a mi director, el Dr. Jesús Ruberte, por formarme como investigador, por su paciencia, por darme esta oportunidad cuando apenas me conocía, por conseguir que me sienta orgulloso de nuestro trabajo, por hacerme sentir la ilusión de aprender cada día.

Pero también quiero dar las gracias a Jesús, así sin doctorado ni titulo, porque no has sido sólo director. También me has cuidado, acompañado, aconsejado, aguantado y animado. Gracias por abrirme incluso tu casa para acabar este proyecto y sobretodo, gracias por aceptarme como soy, con mi caos y mis locuras.

Gracias también a la doctora Fàtima Bosch, por darme la oportunidad de poder trabajar en unas excelentes instalaciones, gracias a ella y a todo el centro he podido obtener los resultados de esta tesis doctoral.

Quiero dar también las gracias a todos los componentes del grupo, por ser mucho más que compañeros de trabajo...por convertiros en una pequeña familia, por hacerme sentir en casa.

# AGRADECIMIENTOS

Me gustaría agradecer a Ana sus enseñanzas y su ayuda en las clases. Pero sobretodo sus consejos, su comprensión, nuestras bromas en las prácticas, los kebabs cuando acababa a las mil con ganas de llorar, su cariño y su apoyo, gracias.

A Marc, gracias por acompañarme estos meses, por enseñarme, por hacerme reír, por las noches en mi casa y por las noches por ahí...esto no ha hecho más que empezar.

Quisiera agradecer a Víctor su ayuda inestimable con la estadística. Pero también quisiera agradecerte tu bondad y tu paciencia. He aprendido mucho de ti.

A Luísa, obrigado por dar-me a mão desde o primeiro dia e não soltar nunca mais. Obrigado pelas tuas histórias. Obrigado pela nossa história.

A Lore, mi morena, no sólo por las mil o dos mil inmunos que hemos hecho juntos, sinó por todos los momentos que hemos compartido. Por los fines de semana. Y porque, pese a todo, siempre nos vamos a querer.

A mi Vero, por enseñarme todo lo que sé del laboratorio. Pero también por tus consejos, por escucharme y entenderme, por ser tantas veces mi confidente, por hacerme reír, por darme cariño cuando lo he necesitado. Te quiero muchísimo rubia.

A Catita, porque has entrado revolucionándolo todo y sé que va a ser el principio de algo bonito.

A todos los compañeros del CBATEG, de la tercera de la cuarta y de la quinta, del estabulario y el SLIPI, a los que están y a los que han estado, Lore, Gemma, Albert, Carles, Vicky, Cris, Eli...sois tantos que no puedo poneros a todos...gracias por hacer que pasar mil horas en el confocal haya sido tan divertido. Gracias Mary Jane, Teresa, Rosmi, César y tanta gente que ha hecho que este tiempo sea inolvidable...

Quisiera agradecer también a mis amigos el apoyo, la comprensión y la paciencia. Gracias a los que habéis entendido que estos meses era imposible quedar con vosotros, y gracias también a los que no lo habéis entendido y me habéis obligado a salir de casa. Un gracias especial a Jèssica, por aguantar estoicamente mis llamadas de pena, de enfado, de rabia, mis malos humores y escucharme sin rechistar.

# AGRADECIMIENTOS

Ángel y Mari, os pongo entre amigos y familia porque os habéis convertido en parte fundamental de mi vida…y ya no sé ni dónde poneros

More, porque, como toda buena historia, apareciste en mi vida una mañana de tormenta de otoño y desde entonces no me has fallado nunca. Por dejarme crecer a tu lado, por apoyarme siempre, porque son demasiadas cosas, risas e historias para poder escribirlas. Por hacerme padrino de tu hija, por hacerme parte de tu vida. Por estar siempre y para siempre. GRACIAS.

Bro, quien nos lo iba a decir el primer día… Recuerdo que me preguntaste cuando nos hicimos tan amigos, hoy te doy la respuesta: nuestra amistad es algo natural y por tanto no tiene principio ni fin, simplemente es. Gracias por hacer que trabajar sea más divertido que ir al cole, porque son preciosos nuestros chistes a las afueras del CBA, por no halagarme, por no juzgarme, por quererme como soy, por compartir tu todo y mi todo, por aconsejarme, por crecer juntos, por enseñarme, por malgastar tu tiempo conmigo. Te deseo lo mejor en esta nueva etapa de la vida, y me deseo compartirla contigo.

Me gustaría dar el mayor gracias de todos a mi familia. Porque me habéis entendido y apoyado en este momento tan difícil y en todos. Por ser los cimientos de mi vida.

Gracias Mamá, por darme no sólo la vida sinó las herramientas para vivirla. Por apoyarme en todo, aunque no te guste. Por decirme lo que no te gusta, por decirme lo que te gusta. Por levantarme cuando me caigo, por mimarme aunque tenga 32 años, por las cenas de los lunes. Por protegerme, por escucharme, por entenderme, por quererme pese a todo, por ser luz, por ser todo, por ser vida. Sin ti nada sería posible, nada tendría brillo. Te quiero muchísimo más de lo que lo digo.

Gracias MacMasuel. Por estar siempre a mi lado, por vivir tus aventuras conmigo, por vivir mis aventuras conmigo. Por ser mi mejor amigo desde siempre y para siempre. Porque te escogería una y mil veces. Porque contigo siempre es y será como cuando éramos pequeños. Porque me entiendes siempre. Porque me dices la verdad aunque me enfade. Porque me quieres sin medida y yo te quiero sin extremos.

Por ser el faro que siempre brilla en la oscuridad. Por todo. Son demasiadas cosas para un párrafo, son demasiadas cosas para una vida. Te quiero infinito más dos.

Gracias Papá por tu cariño, tus llamadas de ánimo, por preocuparte siempre por mi, por ocuparte siempre de mi, por apoyarme siempre, por mimarme, por mil cosas, por tus consejos, por toda una vida, por lo que escribo y por lo que no, porque sin ti no sería capaz de hacer la mitad de las cosas que hago, porque saber que estás me hace fuerte. Porque te quiero muchísimo. Porque me quieres muchísimo.

También a vosotros, Mª Antonia y Álvaro, por ser familia de verdad, por vuestro cariño, por vuestras llamadas, por los mediodías en la Uni, por preocuparos por mi, por los whatsapp con recetas, por apoyarme y mimarme, por estar a mi lado siempre, por vuestros consejos, vuestros abrazos ¡muchas gracias! os quiero mucho.

Gracias también a ti Luís. Por ser parte de nosotros, por tener siempre algo que me gusta para cenar, por mimarme, por tu cariño, por tu apoyo, por tu calma, por hacerme reír... ¿maantiendes? Por hacer que te quiera un montón. Por muchas cosas, gracias.

Gracias también a ti Lía, por convertirte en mi familia, por cuidarme como un hermano, por convertirte en mi hermana, por compartir todo conmigo, por cuidarme, por adoptarme tantos fines de semana. Gracias también a mis sobrinos favoritos, Pol y Nil, por llenarme de amor y de risas este tiempo, por enseñarme lo que es el valor, por enseñarme a aferrarme a la vida con uñas y dientes.

Finalmente quisiera agradecer a los ratones que han dado la vida por este proyecto. Y a la cerveza, la música y el deporte que me hayan mantenido cuerdo estos meses.

**STRUCTURAL AND MOLECULAR ANALYSIS OF ARTERIOLAR ANNULI IN THE RETINA: IMPLICATIONS IN DIABETIC AND HYPERTENSIVE RETINOPATHY.**

## SUMMARY

Retinal vasculature shows special characteristics in order to minimize the interference with the light path, which passes through the entire retina to reach the external segment of photoreceptors. The small size and sparse distribution of retinal capillaries, together with the high metabolic demand, makes retinal homeostasis highly dependent on blood flow regulation. Retinal blood vessels are not innervated. Thereby, the influence of autonomic nerve stimulation can be excluded. In addition, blood-retinal barrier isolates the retina from the effect of circulating hormones and neurotransmitters. Thus, for its function retinal vasculature must be controlled through finely tuned local regulatory blood flow mechanisms.

Arteriolar annuli are singular structures occurring at side-arm branching sites of retinal arterioles. These structures were defined in the mid last century by the presence of increased PAS-positive material and increased cellularity. Moreover, a recent study has evidenced the specific expression of certain genes at the arteriolar branching points. However, most of the studies dealing with arteriolar annuli are out of date and incomplete. Thus, both structure and function remain to be elucidated.

Our results have confirmed the presence of arteriolar annuli in mouse retina, appearing as a conical hypercellular structure of intensely PAS stained material. Lectin specific binding and salivary amylase digestion have determined that specific PAS stain is mainly due to increased glycogen content in cells forming the arteriolar annuli.

Detailed morphological analyses of arteriolar annuli have evidenced three different components: endothelial, interstitial (ICs) and smooth muscle cells, showing a distinctive structural and molecular phenotype. In this regard endothelial cells show decreased expression of CD31, together with enhanced NADPH diaphorase and von Willebrand factor (vWF) expression. Thus, suggesting that annuli endothelial cells are able to induce vasodilatation and to maintain an antithrombotic milieu. Smooth muscle cells in the annuli appeared reoriented embracing the origin of the collateral arteriole. This particular disposition could indicate a sphincter-like activity by bulging annuli cells to the arteriolar lumen. In addition, ultrastuctural analysis evidenced the existence of peg-and-socket junctions between smooth muscle cells of arteriolar annuli. This result suggests a stretch-coordinated annuli contraction. Furthermore, a possible reinforcement of basement membrane was evidenced by increased expression of its main components, including collagen IV, laminin and fibronectin. A diminished colocalization of collagen IV and laminin, suggest a change in the organization of basement membrane in arteriolar annuli.

ICs have been described as a new cell population in the arteriolar annuli. These cells showed features matching the “gold standard” ultrastructural features established for the intestinal Interstitial Cajal cells identification. In

addition, annuli presuntive Interstitial Cajal cells expressed specific markers of these cells, such as Ano1 and CD44, although c-kit expression could not be observed. A distinctive pattern of distribution of F-actin filaments, together with an increased expression of β-actin and a lack of α-SMA allowed further differentiation between annuli ICs and vascular smooth muscle cells. Functional studies suggest that annuli ICs perform functions of: pacemarker activity, neuromodulation and mechanotransduction.

Blood flow alteration is an early event in retinal diseases, such as diabetic and hypertensive retinopathies, which are the two major causes of blindness and visual impairment worldwide. Thus, the function of arterial annuli and their alterations during retinopathy could be of interest in order to understand the physiopathology of vascular retinopathy.

The analyisis of arteriolar annuli in model of diabetes type II (db/db mice) evidenced impaired glycogen storage in annuli ICs. In addition, the studies in a model of hypertension (KAP transgenic mice) evidenced a decreased expression of Ano1 in annuli ICs during hypertensive retinopathy, suggesting a loss of function of calcium-activated chloride channels. Thus, alterations observed in the retinal ICs could induce an impaired function of arteriolar annuli driving to dysregulation of blood flow during retinopathy.

Moreover, arterial annuli are present in man retina. Preliminary results, as happens in mice, may suggest its alteration during retinopathy

Taken together, obtained results suggest that arteriolar annuli are endowed with specific molecular, structural and functional characteristics which

allow playing a key role in the retinal blood flow regulation in health and during retinopathy.

**ANÁLISIS ESTRUCTURAL Y MOLECULAR DE LOS ANILLOS ARTERIOLARES EN LA RETINA: IMPLICACIONES EN LAS RETINOPATÍAS DIABÉTICA E HIPERTENSIVA**

## RESUMEN

La vasculatura de la retina presenta características especiales ya que es fundamental que los vasos no interfieran el paso de la luz, que debe atravesar la retina para llegar a los fotoreceptores. El pequeño calibre de los capilares retinianos, junto con los elevados requerimientos metabólicos, hace que la regulación del flujo sanguíneo sea fundamental para el correcto mantenimiento de la homeostasis de la retina. La vasculatura retiniana no presenta inervación, por lo que la influencia de estimulación por parte del sistema nervioso autónomo queda excluida. Además, la barrera hematorretiniana aísla a la retina del efecto tanto de hormonas circulantes como de neurotransmisores. Por lo tanto, la función de la vasculatura retiniana debe efectuarse a través mecanismos locales de regulación del flujo.

Los anillos arteriolares son estructuras singulares que aparecen en las ramificaciones laterales de las arteriolas de la retina. Dichas estructuras fueron definidas a mediados del siglo pasado por la presencia de acúmulos de material PAS positivo junto con un aumento de la celularidad. Estudios recientes, evidencian, además, la expresión especifica de ciertos genes en dichas ramificaciones. De todos modos, la mayoría de los estudios que versan

sobre el anillo arteriolar son antiguos e incompletos. Por lo tanto, tanto la estructura como la función de los anillos aun deben ser elucidadas.

Nuestros resultados han confirmado la presencia los anillos arteriolares en la retina del ratón, en la que aparecen como una estructura cónica e hipercelular de material intensamente teñido mediante PAS. La unión especifica de lectinas, junto con la digestión con amilasa salivar, han determinado que esta tinción especifica con PAS se debe a un incremento del contenido en glucógeno en la células que forman el anillo arteriolar.

El profundo análisis morfológico del anillo arteriolar evidenció tres componentes distintos en su estructura: las células endoteliales, las células intersticiales (ICs) y las células musculares lisas. Cada uno de estos componentes presentó un fenotipo estructural y molecular distintivo. De este modo, las células endoteliales mostraron una disminución de la expresión de CD31, junto con un incremento en las expresiones tanto de NADPH diaforasa como del factor de von Willebrand (vWF). Por lo tanto, estos resultados sugieren que las células endoteliales del anillo arteriolar son capaces de inducir vasodilatación así como de mantener un ambiente antitrombótico. En el anillo arteriolar, las células musculares lisas presentaron un cambio en la orientación para abrazar el origen de la arteriola colateral. Esta disposición particular podría indicar una actividad de tipo esfínter mediante un abultamiento de las células del anillo hacia el interior de la luz vascular. Además, el análisis ultraestructural evidenció la existencia de uniones de tipo peg-and-socket entre las células musculares lisas del anillo arteriolar. Este resultado sugiere una contracción del anillo arteriolar coordinada mediante tracción. Asimismo, el

incremento de expresión de los principales componentes de la membrana basal, colágeno IV, laminina y fibronectina, evidenció un posible refuerzo de esta. Del mismo modo, una disminución en la colocalización entre colágeno IV y laminina sugiere un cambio en la organización de la membrana basal en el anillo arterial.

Las ICs se describen como una nueva población celular en el anillo arteriolar. La morfológía de estas células concordó completamente con el "estándar de oro" de características ultraestructurales establecido para la identificación de las células intersticiales de Cajal. Más aun, las presuntas células intersticiales de Cajal encontradas en el anillo expresaron marcadores específicos de éstas tales como Ano1 y CD44, pese a que la expresión de c-kit nunca se observó. El patrón diferencial en la distribución de los filamentos de F-actina, junto con el incremento en la expresión de $\beta$-actina y la falta de $\alpha$-SMA, permitieron diferenciar de forma más evidente las ICs de las células musculares lisas en el anillo arteriolar.

Los estudios funcionales han sugerido que las ICs del anillo arteriolar llevan a cabo funciones de actividad marcapasos, neuromodulación y mecanotransducción.

La alteración del flujo sanguíneo es un evento temprano en enfermedades de la retina como la retinopatía diabética y la retinopatía hipertensa, las mayores causas de ceguera y déficit visual en el mundo. Por lo tanto, la función del anillo arteriolar, así como sus alteraciones durante la

retinopatía, pueden ser de interés para el discernimiento de la patofisiología de las retinopatías vasculares.

El análisis de los anillos arteriolares en un modelo de diabetes tipo 2 (el ratón db/db) evidenció una alteración en el almacenamiento de glucógeno en las ICs del anillo arteriolar. Además, los estudios en un modelo de hipertensión (el ratón transgénico KAP) mostraron un decremento en la expresión de Ano1 en las ICs durante la retinopatía hipertensa, sugierendo una pérdida de función de los canales de cloro activados por calcio. Por lo tanto, las alteraciones observadas en las ICs podrían producir una pérdida de funcionalidad del anillo arteriolar que conduciría a una alteración en la regulación del flujo sanguíneo durante la retinopatía.

Los anillos arteriolares también se han encontrado en la retina humana. Estudios preliminares sugieren que, del mismo modo que ocurre en el ratón, estas estructuras se alteran durante la retinopatía.

En conjunto, los resultados obtenidos sugieren que el anillo arteriolar está dotado de características moleculares, estructurales y funcionales que le confieren un papel clave en la regulación del flujo sanguíneo tanto en condiciones fisiológicas como durante la retinopatía.

| | |
|---|---|
| Ano1 | anoctamin 1 |
| AFP | average fluorescence intensity pixel |
| $Ca^{2+}$ | calcium |
| cDNA | complementary deoxyribonucleic acid |
| $CO_2$ | carbon dioxide |
| Cx43 | connexin 43 |
| DAB | 3,3'-diaminobenzidine tetrahydrochloride |
| DMEM | Dulbecco modified Eagle's medium |
| DNA | deoxyribonucleic acid |
| EC | endothelial cell |
| EGFP | enhanced green fluorescente protein |
| eNOS | endothelial nitric oxide synthase |
| ETs | endothelins |
| FITC | fluorescein isothyocyanate |
| g | grames |
| GFP | green fluorescent protein |
| Gal | galactose |
| GalNac | N-acetyl galactosamine |
| GFAP | glial fibrillary acidic protein |
| GLcNac | N-acetyl glucosamine |
| GS | glutamine synthetase |
| GSA | Griffonia simplicifolia agglutinin |
| HBSS | Hank's balanced salt solution |
| HRP | horseradish peroxidase |
| ICs | interstitial cells |
| ICCs | interstitial Cajal cells |
| KAP | kidney androgen protein |
| Kv | Kilovolts |
| LEA | Licopersicon sculentum agglutinin |
| M | molar |
| ml | mililiters |
| mM | milimolar |
| MOM | mouse on mouse |

| | |
|---|---|
| mRNA | messenger ribonucleic acid |
| NADPH | nicotinamide adenin dinucleotide phosphate |
| NBF | neutral buffer formalin |
| NDS | neutral donkey serum |
| NeuAc | Sialic acid |
| NG2 | neuron-glial 2 chondoritin-sulphate |
| nm | nanometers |
| NO | nitric oxide |
| NOS | nitric oxide synthase |
| $O_2$ | oxygen |
| PAS | periodic acid Schiff |
| PBS | phosphate buffer saline |
| PBI | phosphate buffer igepal |
| PDGF-Rβ | platerived derived growth factor receptor beta |
| PECAM-1 | platelet endothelial adhesion molecule 1 |
| PNA | peanut agglutinin |
| $PGE_2$ | prostaglandin $E_2$ |
| $PGI_2$ | prostaglandin $I_2$ |
| RCA | Ricinus communis agglutinin |
| ROI | region of interest |
| SBA | soybean agglutinin |
| SEM | standard error of the mean |
| SMC | smooth muscle cell |
| SNA | Sambucus nigra agglutinin |
| TRITC | tiol-reactive tetramethylrhodamine-5-(and-6)-isothiocyanate |
| USA | United States of America |
| VEGF | vascular endothelial growth factor |
| VS | versus |
| vWF | von Willebrand factor |
| WB | wash buffer |
| WFA | Wisteria floribunda agglutinin |
| WGA | Triticum vulgaris agglutinin |

| | |
|---|---|
| α-SMA | alpha smooth muscle actin |
| μl | microliters |
| μm | micrometers |
| μM | micromolar |
| ºC | centigrades |

# *PRESENTATION and OBJETIVES*

Retinal vasculature shows special characteristics in order to minimize the interference with the light path, which passes through the entire retina to reach the external segment of photoreceptors. The small size and sparse distribution of retinal capillaries (Wangsa-Wirawan and Linsenmeier, 2003), together with the high metabolic demand (Bristow et al., 2002), makes retinal homeostasis highly dependent on blood flow regulation. Retinal blood vessels are not innervated. Thereby, the influence of autonomic nerve stimulation can be excluded. In addition, blood-retinal barrier isolates the retina from the effects of circulating hormones and neurotransmitters (Laties, 1967; Delaey and van de Voorde, 2000). Thus, retinal blood flow must be controlled through finely tuned local regulatory mechanisms.

Arteriolar annuli are singular structures occurring at side-arm branching points of retinal arterioles. These structures were defined in the mid last century by the presence of increased PAS-positive material and increased cellularity (Kuwabara and Cogan, 1960). Moreover, a recent study has evidenced the specific expression of certain genes at the arteriolar branching points (Lopes et al., 2012). However, most of the studies dealing with arteriolar annuli are out of date and incomplete. Thus, both structure and function remain to be elucidated.

Blood flow alteration is an early event in retinal diseases, such as diabetic and hypertensive retinopathies, which are the two major causes of blindness and visual impairment worldwide (Meyer-Rüsenberg et al., 2007). Thus, the function of arterial annuli, as presumptive sphincters, during blood

flow regulation and their impairment during retinopathy could be of interest in order to understand the physiopathology of vascular retinopathy.

Therefore, the main goals of this work have been:

1. To morphologically and molecularly characterize the cellular components of arteriolar annuli in the mouse retina.
2. To analyze the role of arteriolar annuli in blood flow regulation.
3. To study the alterations of arteriolar annuli during retinopathy using animal models of diabetic retinopathy (db/db mice) and hypertensive retinopathy (KAP transgenic mice).
4. To ascertain if human retinal vasculature presents arterial annuli

# *INTRODUCTION*

# A. THE RETINA AND ITS VASCULAR SYSTEM

The eye, the visual organ, is placed in the orbit surrounded and maintained by soft and bony tissue. In the mouse, the eye is relatively small and is characterized by adaptations to nocturnal vision (Leamey et al., 2008).

The eye is formed by the eyeball and the accessory organs, including the bulbar muscles, the orbital fasciae, the eyelids, the conjunctiva and the lacrimal apparatus.

## 1. LOCALIZATION OF THE RETINA IN THE EYEBALL

The eyeball (*Bulbus oculi*) consists of three coats: the fibrous coat of the eyeball (*Tunica fibrosa bulbi*), forming the outer wall of the eyeball; the vascular tunic of the eyeball (*Tunica vasculosa bulbi*), that is a highly vascularized and pigmented medial layer; and the internal lining of the eyeball (*Tunica interna bulbi*), consisting of the retina with its pigmented epithelium and the retinal blood vessels (*Vasa sanguina retinae*) (Schaller, 1992; Smith et al., 2002).

The **fibrous coat of the eyeball** is formed by the sclera (*Sclera*) and the cornea (*Cornea*) (Fig. 1). The sclera, the white protective layer covering the posterior portion of the eye, consists of dense fibrous connective tissue. The cornea forms the translucent anterior wall of the eyeball. This structure is avascular and highly innervated.

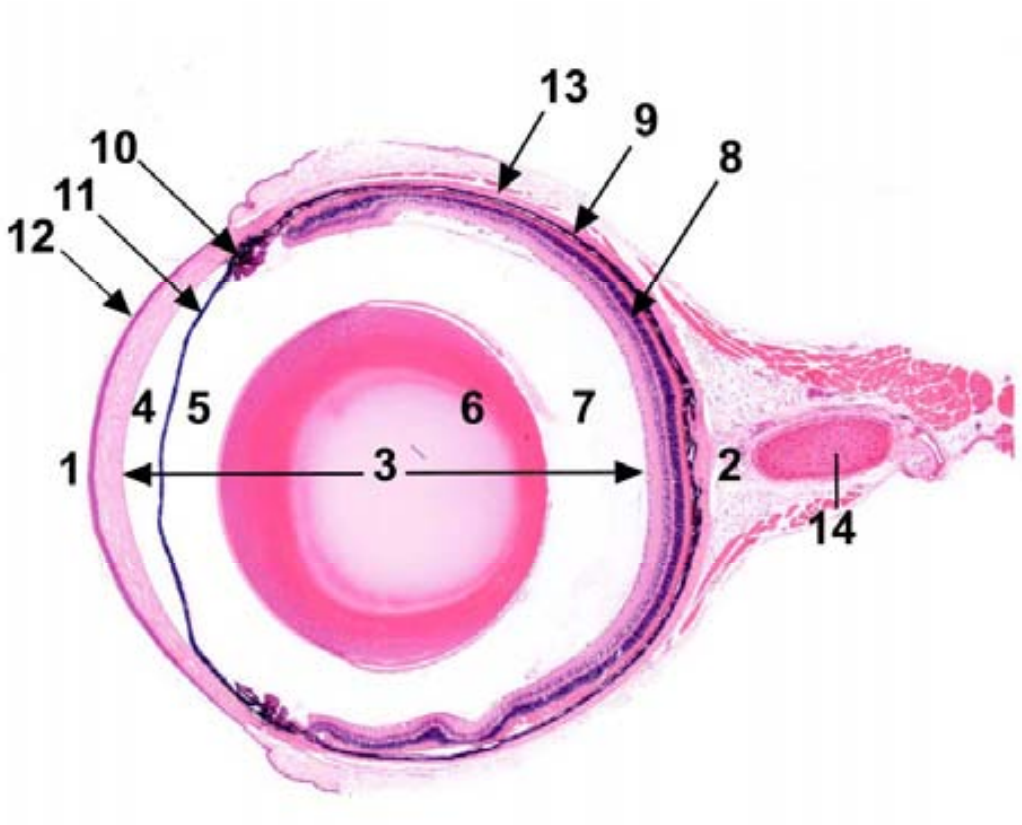


**Figure 1: The eyeball.** 1. Anterior pole; Posterior pole; 3: Internal axis of the eyeball; 4: Anterior chamber of the eyeball; 5: Posterior chamber of the eyeball; 6: Lens; 7: Vitreous chamber of the eyeball; 8: Retina; 9: Choroid; 10: Ciliary body; 11: Iris; 12: Cornea; 13: Sclera; 14: Optic nerve. Magnification: 20x.

The **vascular tunic of the eyeball**, also named uvea, comprises the choroid (*Choroidea*), the ciliary body (*Corpus ciliare*) and the iris (*Iris*) (Fig. 1). The choroid forms the posterior portion of the vascular tunic of the eye. This structure consists of a highly vascularized tissue whose principal function is to serve the metabolic needs of the outer retina. The choroid is loosely attached to the sclera and separated of the retina by the Bruch's membrane. The anterior portion of the vascular tunic consists of the ciliary body and the iris. The ciliary body is a thick annular structure located between iris and the vitreous chamber (*Camera vitrea bulbi*), that projects towards the lens (*Lens*). The main function

of this structure is to produce eye humors, which are secreted by the ciliary processes (*Processus ciliares*). Ciliary body is also the source of the suspensory apparatus that support the lens: the *zonula ciliaris*. The *Zonula ciliaris* consists of many fibers extending from the cilliary processes to the lens capsule at the equator. The iris is the most anterior part of the uvea and separates the anterior and posterior chambers of the eyeball (*Camera anterior and posterior bulbi*). This structure consists of a contractile diaphragm with a central opening (pupil). The iris regulates the amount of light admitted into the fundus of the eye.

The **lens** is a transparent, biconvex structure which focuses the light on the retina (Fig. 1). The lens plays a key role in the accommodation mechanism by providing the eye the ability to change the focus. The lens is composed of three main components: the lens capsule (*Capsula lentis*), a highly elastic covering of the lens; the lens epithelium (*Epithelium lentis*), formed by a single layer of cuboidal cells; and the lens fibers (*Fibrae lentis*), transparent fibers with a semiliquid content that constitute the substance of the lens. Epithelial cells of equatorial germinative zone produce the lens fibers and synthesize specialized lens proteins, the crystallins. Crystalins increase the refractive index of lens fibers. In comparison to the human eye, the mouse lens is relatively large and rounded, occupying more than the 60% of the intraocular space.

The **internal lining of the eyeball** (*Tunica interna bulbi*) consists of the retina with its pigmented epithelium (Fig. 1). The retina develops from the optic cup, an outpost of the diencephalon. The optic cup is composed of two neuroepithelial layers: the inner layer, that forms the neural retina after a

complex process of proliferation and differentiation; and the outer layer, that becomes the retinal pigment epithelium.

## 2. RETINAL ORGANIZATION AND FUNCTION

The retina, the most complex substructure of the eye, has been thoroughly studied anatomically by several methods. This structure is composed of several layers that, from the outermost (close to the choroid) to the innermost (adjacent to vitreous chamber), are (Fig. 2):

1. Retinal pigment epithelium (*Stratum pigmentosum*): is the pigmented external layer of the retina. This epithelium consists of a monolayer of cells containing numerous melanosomes.

2. Neuroepithelial layer (*Stratum neuroepitheliale*): is formed by two photoreceptor cell types: rods and cones. Photoreceptors have four primary structural and functional regions: the outer segment, containing visual pigments; the inner segment, endowed with the machinery needed to meet the high metabolic demand associated to phototransduction; the cell body, with very little perinuclear cytoplasm; and the synaptic terminal, responsible for light signal transmission. Photereceptor bodies are separated from inner and outer segments by the external limiting membrane, remaining the outer segments surrounded by cells of retinal pigment epithelium. As is characteristic of nocturnal mammals, rods

account for almost the 95% of photoreceptors in the mouse retina. Thus, mouse retina is more sensitive to changes in dim light intensity.

3. External limiting membrane (*Stratum limitans externum*): is not a membrane itself but the apical processes of Müller cells.

4. Outer nuclear layer (*Stratum nucleare externum*): this layer is mainly occupied by rod and cone nuclei.

5. Outer plexiform layer (*Stratum plexiforme externum*): consists of a thin layer of synapses between photoreceptor axons and dendrites of neural cells located in the inner nuclear layer: bipolar and horizontal cells.

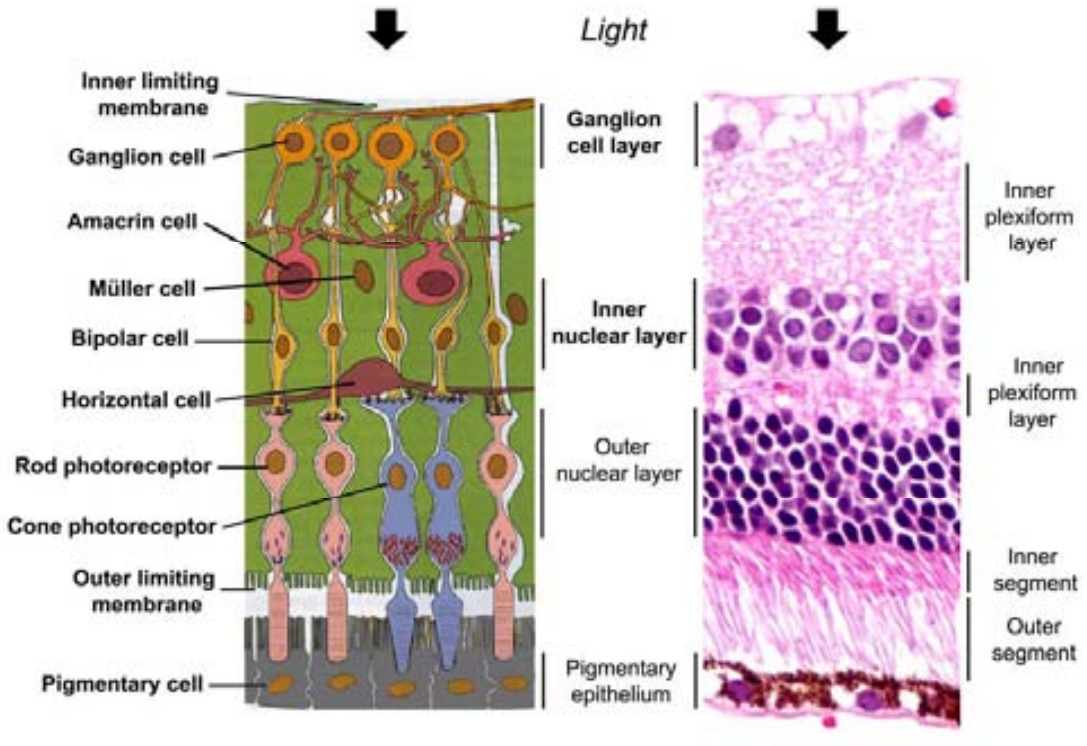


**Figure 2: Structure of the retina.** Schematic draw (left) and haematoxylin/eosin stained paraffin section (right) showing the different layers and cells of the retina.

6. Inner nuclear layer (*Stratum nucleare internum*): includes the nuclei of bipolar, horizontal, amacrine and Müller cells. Bipolar cells, the most abundant cells in this layer, connect photoreceptors to ganglion cells. Horizontal and amacrine cells are responsible for lateral integration of neurons. In this regard, each horizontal cell is connected to many photoreceptors and bipolar cells while amacrine cells establish synapses with bipolar and ganglion cells. Müller cells extend from vitreous chamber to external limiting membrane, filling all retinal space unoccupied by neurons. Thus, these cells help to maintain retinal structural integrity.

7. Inner plexiform layer (*Stratum plexiforme internum*): in this layer occur synapses between ganglion, bipolar and amacrine cells. Although usually free of nuclei, sporadic astrocyte or displaced cells from adjacent layers can also be found.

8. Ganglion cell layer (*Stratum ganglionare*): this layer is occupied by retinal ganglion cells, characterized by large vesicular nuclei with prominent nucleoli and abundant cytoplasm. Amacrine displaced cells have also been identified in this layer.

9. Nerve fiber layer (*Stratum neurofibrarum*): is composed of unmyelinated axons of ganglion cells as they extend towards the optic nerve. Cell processes of astrocytes and Müller cells are also found surrounding the axons.

10. Internal limiting membrane (*Stratum limitans internum*): directly internal to nerve fiber layer and adjacent to vitreous chamber, the internal limiting membrane is formed by the basal lamina of Müller cells.

The retina constitutes the sensory component of the eye. Thus, the main function of the retina is to transform light into an electrical signal, which is sent to the brain. Neural signals, generated by photereceptors, are transmitted by synaptic transmission along the vertical excitatory pathway to bipolar and ganglion cells (Maureen et al., 2008). In addition, lateral inhibitory pathways, mediated by horizontal and amacrine cells, modulate the nervous impulses (Maureen et al., 2008). Finally, axons of ganglion cells conduct the visual information along the optic nerve to reach the visual cortex.

In addition to photoreceptors and neurons, two types of glial cells are found in the retina: macroglial cells, constituted by Müller cells and astrocytes, and microglial cells. Müller cells have their nuclei located in the inner nuclear layer and their cytoplasm spanning from the internal to the external limiting membranes. Among others, Müller cell functions include blood flow regulation, synthesis and recycling of neurotransmitters and regulation of extracellular ionic balance (Newman and Reichenbach, 1996; Gardner et al., 2002). By contrast, astrocytes location is restricted to the nerve fiber layer where their processes surround blood vessels and unmyelinated axons (Hollander et al., 1991; Gardner et al., 2002). Together, macroglial cells integrate vascular and

neuronal activity in the retina to maintain the strictly regulated retinal environment (Gardner et al., 2002).

Microglial cells are considered the resident macrophages of the retina and are located in the superficial layers of the retina. Normally, microglial cells remain quiescent, but under certain stimuli become activated contributing to the defence against microorganisms, phagocytosis, immunoregulation and tissue repair (Roitt et al., 2001; Chen et al., 2002; Gardner et al., 2002).

## 3. RETINAL VASCULAR SYSTEM

Retinal vascular system shows unique adaptations to supply oxygen and nutrients to a tissue whose translucency is essential for function (Funk, 1997; Puro, 2012). Intra-retinal blood vessels deflect incoming light, compromising visual function (Puro, 2012). Thus, retinal capillaries are sparse and small (Wangsa-Wirawan and Linsenmeier, 2003), representing only the 5% of retinal mass (Gartner and Hiat, 2002). However, this specific vascular distribution leaves little functional reserve for adjusting the relatively low blood flow (Alm and Bill, 1973) to meet the extremely active retinal metabolism (.Bristow et al., 2002; Wangsa-Wirawan and Linsenmeier, 2003). In addition, neuron cell function requires a tightly regulated environment (Pournaras et al., 2008). Hence, retinal vasculature must strictly couple blood flow to local needs while preventing the free pass of blood-borne molecules to retinal parenchyma (Funk, 1997; Delaey and van de Voorde, 2000; Pournaras et al., 2008).

Vertebrates show a wide variety of vascular retinal patterns (Wise, 1971), mainly due to the direct relation established between vascularisation and retinal thickness (Dreher et al., 1992). Most mammals, including mouse and man, have **holoangiotic** retinas. In these retinas, blood from the central retinal artery is distributed to the entire retina through a complex network of blood vessels, including arteries, veins and a capillary network (Germer et al., 1998).

In other species only part of the retina is supplied by blood vessels. Thereby, in **merangiotic** retinas, found in lagomorpha, blood vessels are restricted to a narrow band over the nerve fiber layer. In other species, such as guinea-pig, retinal vessels are restricted to a narrow rim around the optic disc (**paurangiotic** retinas). Finally, **anangiotic** retinas, found in some rodents, completely lack intra-retinal vessels (Wise, 1971).

### 3.1. Retinal vascular pattern

In higher mammals, including man and mouse, the retina has a dual circulation: the retinal vessels supply blood to the inner portion of the retina, from the nerve fiber layer to the external aspect of the inner nuclear layer. By contrast, the outer retinal layers depend on choroidal circulation (Smith et al., 2002).

In man and mouse, the internal carotid artery branches to form the ophthalmic artery (*A. ophtalmica*), which, in turn, gives rise to the central retinal artery (*A. centralis retinae*) (Fig. 5A and B) (Schaller, 1992; Smith et al., 2002;

Saint-Geniez and D'Amore, 2004). The central retinal artery enters the eye through the lamina cribosa (Kur et al., 2012).

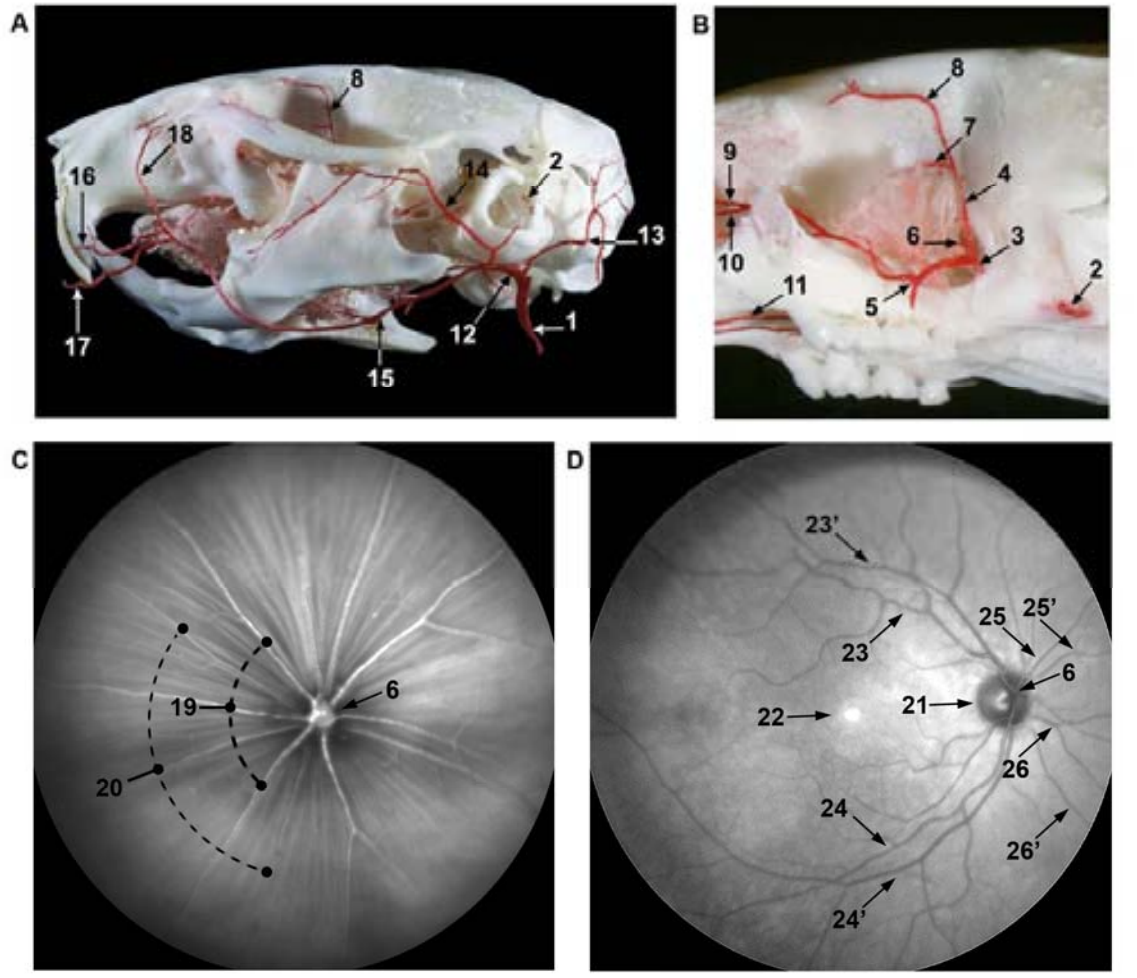


**Figure 3: Vascularization of the eye.** (A) and (B) show araldit injection of arteries followed by soft tissue digestion with pancreatin. (C) and (D) show fundus images of mouse and human eyes respectively. Images acquired with a Scan Laser Ophthalmoscope. 1: Common carotid artery; 2: Internal carotid artery; 3: Ophtalmic artery; 4: Dorsal branch; 5: Ventral branch; 6: Central retinal artery; 7: Ethmoid artery; 8: Frontal artery; 9: Infra-orbital artery; 10: Esphenopalatine artery; 12: External carotid artery; 13: Occipital artery; 14: Superficial temporal artery; 15: Facial artery; 16: Superior labial artery; 17: Inferior labial artery; 18: Angular artery; 19: Retinal arteries; 20: Retinal venules; 21: Optic disc; 22: Macula; 23: Superotemporal arteriole; 23': Superotemporal venule; 24: Inferotemporal arteriole; 24': Inferotemporal venule; 25: Superonasal arteriole; 25': Superonasal venule; 26: Inferonasal arteriole; 26': Inferonasal venule.

In the mouse, central retinal artery emerges at the optic disc where it branches into four to six arterioles (Fig. 3C and 4A). Retinal arterioles extend radially towards retinal periphery while dividing by both dichotomous and side-arm branching. As arterioles divide their lumen become narrower and their wall thinner giving rise to pre-capillary arterioles. Finally, pre-capillary arterioles drive blood to the capillary network (Figure 4B) (Wise, 1971).

The venous system originates at the *ora serrata*, where receives blood from enlarged capillary arcades (Wise, 1971). Post-capillary venules drain hypoxic blood from the capillary network into retinal venules. In the mouse, four to five retinal venules run parallel to arterial arrangement towards the optic disc (Fig 3C and 4A). As they approach the disc, venules increase in wall thickness and calibre (Wise, 1971). Finally, retinal venules join to form the central retinal vein that leaves the eye through the optic nerve, draining hypoxic blood into the cavernous sinus (Pournaras et al., 2008).

Distribution and topography of mouse retinal vasculature is similar to that of man (Fig. 3D). However, differences in vascularisation do exist between the two species. In example, human retinal vascular pattern displays few individual variations: from the optic disc emerge four main arterioles, namely superonasal and inferonasal arteries (*Arteriolae nasales superior et inferior retinae*) and superotemporal and inferotemporal arteries (*Arteriolae temporales superior et inferior retinae*) (Fig. 3D) (Sobotta and Becher, 1974). Venous drainage is also accomplished by four main venules, running parallel to arteriolar arrangement: superonasal and inferonasal venules (*V. nasales superior et inferior retinae*)

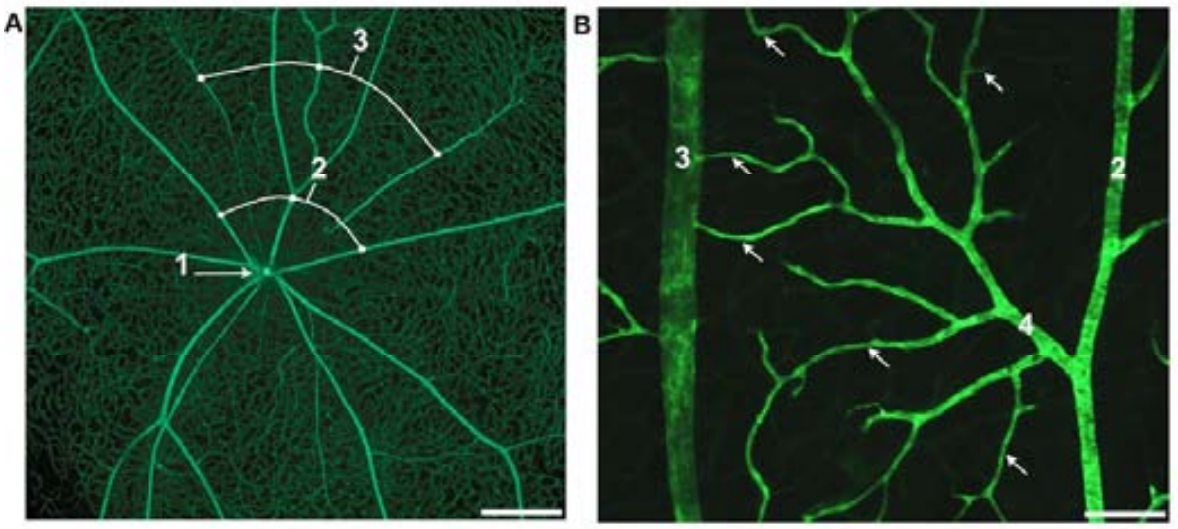


**Figure 4: Retinal vascular pattern:** (A) Fluorescein-isothyocyanate dextran retinal angiography. (B) Collagen IV immunohistiochemistry in whole mount retina. 1: Central retinal artery; 2: Retinal arterioles; 3: Retinal venules; 4: Precapillary arteriole; Arrows: Retinal capillaries. Scale bars: A = 362.8 μm; B = 89.1 μm.

and superotemporal and inferotemporal venules (*V. temporales superior et inferior retinae*) (Fig. 3D) (Sobotta and Becher, 1974).

In addition, human retina has an avascular area near the centre of the retina: the macula. In the macula resides the fovea (Fig. 3D), a depressed area of maximal visual acuity where retinal layers are displaced to avoid interfering light-path to photoreceptors (Gartner and Hiat, 2002). Mice lack macula and fovea, and in these animals the optic disc coincides with the central axis of the eye (Smith et al., 2002).

In the retina, blood vessels are placed forming three plexi: the superficial plexus, in the ganglion cell layer; the intermediate plexus, located in the inner

plexiform layer; and the deep plexus in the outer plexiform layer (Fig. 5) (Paques et al., 2003). No blood vessels are found in the outer nuclear layer (Fig. 5) (Wise, 1971). The superficial plexus consists of larger vessels, arterioles and venules, and a capillary network connecting them. Some arterioles from this plexus change its direction to drive blood towards the deeper plexi. The intermediate plexus is the less developed, and consists of short capillary segments that abruptly run towards the deep plexus. Thus, in many situations, it is difficult to identify. The deep vascular plexus is mainly formed by an anastomotic capillary meshwork. Hypoxic blood from this capillary network drains into transverse postcapillary venules that join major venules in the superficial plexus (Paques et al., 2003).

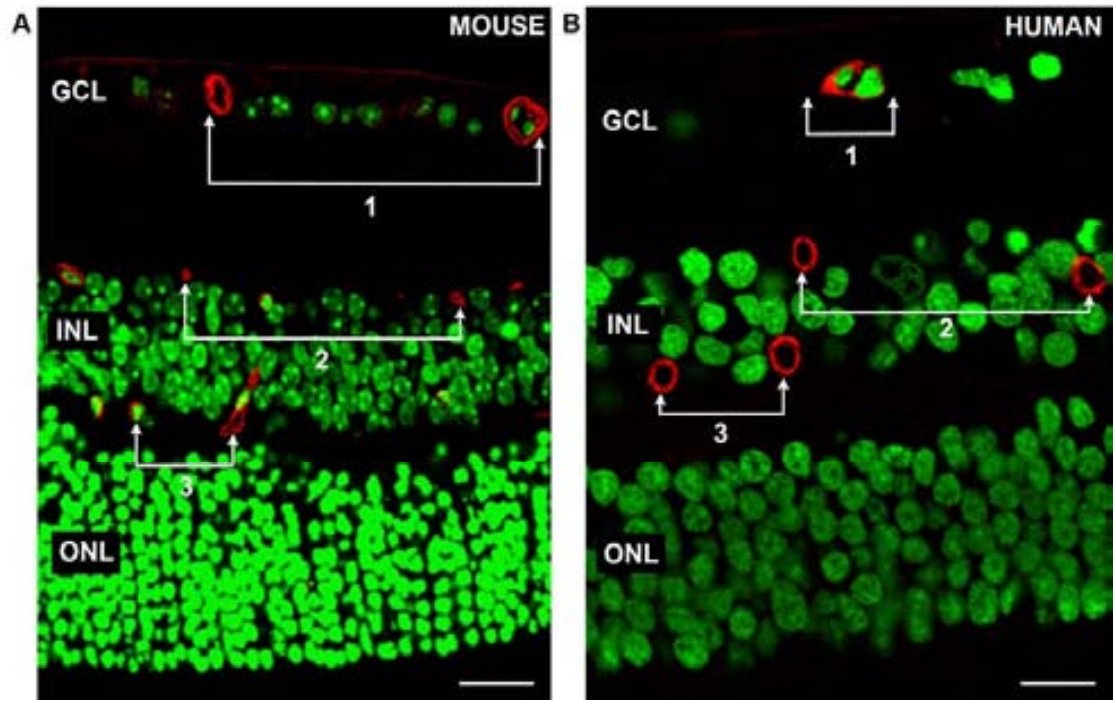


**Figure 5: Retinal vascular plexi.** Paraffin sections of mouse (A) and human (B) retinas immunohistochemically labelled with anti-collagen IV (red). Nuclei counterstain: sytox green. 1: Superficial plexus; 2: Intermediate plexus; 3: Deep plexus. GCL: Ganglion cell layer; INL: Inner nuclear layer; ONL: Outer nuclear layer. Scale bars: A = 16.92 μm; B = 13.73 μm.

Glial cells closely invest all retinal vessels, contributing to blood-retinal barrier (Wise, 1975; Holash and Stewart, 1993). Specifically, astrocyte end-feet ensheath blood vessels from the superficial plexus while Müller cell cytoplasmic processes surround blood vessels located in the intermediate and deep plexi (Wise et al., 1971; Holash and Stewart, 1993).

As previously detailed, the outer retina (photoreceptors) remains avascular and is nourished by the choroidal vasculature (Saint-Geniez et al., 2006) via diffusion processes through the retinal pigment epithelium. The choroid is a highly vascularized tissue that receives blood supply from the anterior and posterior ciliary arteries, branches of the ophthalmic artery. Externally in the choroid, are found the venules of the venous drainage system. The innermost vascular layer, the choriocapillaries (*Lamina choroidocapillaris*), is formed by heavily fenestrated blood vessels. Thus, choriocapillaries are very permeable to blood-borne proteins.

### 3.2. Fine structure of retinal vessels

In the retina, blood flows from arterioles to venules through a capillary network. As happens in other localizations of the body, the wall of retinal blood vessels can be divided into three layers or tunicae: the adventitia layer is the most external and consists of connective tissue; the media layer where can be found smooth muscle cells and/or pericytes, depending on vessel type; and the intima layer, formed by a monolayer of endothelial cells (Fig 6). However, since each vessel type must serve different functions, arterioles, venules and

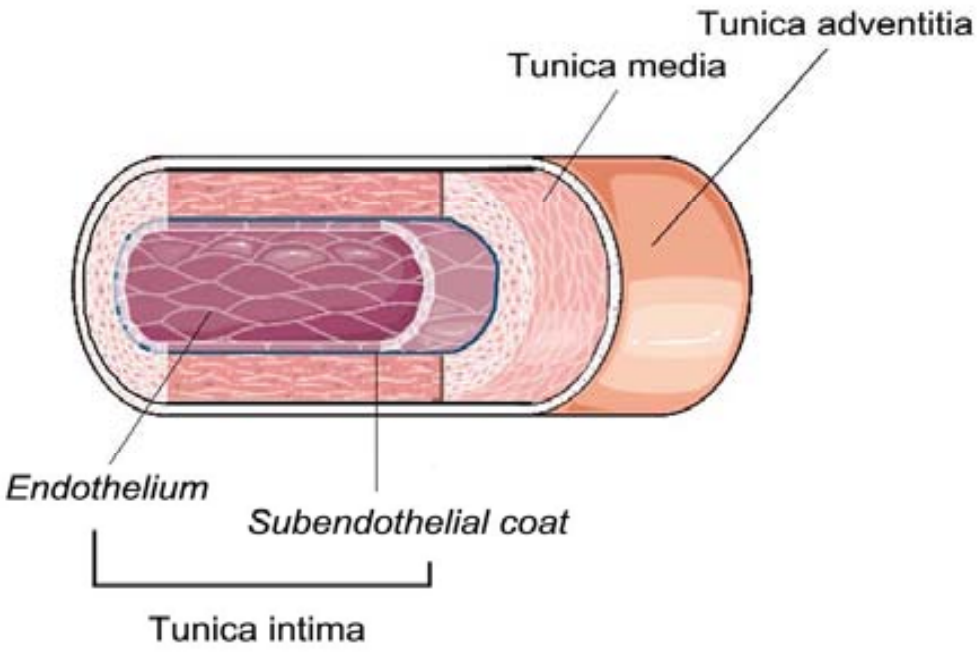


**Figure 6: Schematic draw of vascular wall layers in large vessels.**

capillaries are endowed with distinctive morphological features (Wise, 1971; Saint-Geniez and D'Amore, 2004).

**Arterioles:** retinal arterioles show a tunica intima consisting of a single layer of endothelial cells placed parallel to vessel axis. These cells are attached to a subendothelial layer consisting of connective tissue that is continuous to the basement membrane of the tunica media. Retinal arterioles have a well-developed tunica media, formed by one layer of circularly oriented smooth muscle cells. Smooth muscle cell number decreases as arterioles branch forming a discontinuous layer of sparse cells in pre-capillary arterioles. Finally,

the tunica adventitia, mainly formed by collagen IV, surrounds all the components of the arteriolar wall.

**Capillaries:** capillaries drive blood from pre-capillary arterioles to post-capillary venules and, according to blood flow direction, can be classified into three groups: pre-capillaries, mid-capillaries and post-capillaries (Nehls and Drenckhahn, 1991). The diameter of retinal capillaries vary from 3.5 to 6 μm, and their wall is formed by three elements: endothelial cells, pericytes and basement membrane (Wise, 1971).

**Venules:** retinal venules show, as arterioles do, three concentric layers: the tunica intima, the tunica media and the tunica adventitia. The intima is formed by a monolayer of endothelial cells lining the lumen. In the venules, subendothelial coat is thinner than that of retinal arteries. The tunica media of retinal venules greatly differ from that of arterioles. In this way, this layer contains widely spaced pericytes and smooth muscle cells are only found in larger venules, where they form a non-continous layer of sparse cells. The adventitia is mainly composed of loosely arranged, longitudinally oriented fibers of collagen IV.

Vascular wall components, endothelial cells, smooth muscle cells, pericytes and basement membrane, display distinctive molecular and structural features depending on blood vessel type, tissue under study, different regions of a certain vascular tree, and even between neighbouring cells of the same organ and vessel type (Nehls and Dreckhahn, 1991; Worth et al., 2001; Aird, 2012). Thus, each of these components will be studied in more detail.

### *3.2.1. Endothelial cells:*

The endothelium represents the inner cellular lining of the blood and lymphatic vessels (Aird, 2007). Developmentally, endothelial cells arise from mesoderm via the differentiation of hemangioblasts and/or angioblasts into arterial, venular or capillary endothelial cells (Coultas et al., 2005). However, other cell lineages, such as neural stem cells or adipose tissue, may transdifferentiate into endothelial cells (Planat-Bernard et al., 2004; Wurmser et al., 2004).

#### *3.2.1.1. Endothelial cell morphology*

Endothelial cells show a flat and elongated morphology with a cellular thickness varying from less than 0.1μm in capillaries and veins to 1μm in the aorta. Endothelial cells are thickest at the nucleus, thus bulging into the lumen at nuclear region; elsewhere, they consist of cytoplasmic prolongations encircling the vascular lumen (Fig 7). The luminal front of vascular endothelial cells displays a highly organized coat formed by proteins, glycoproteins,

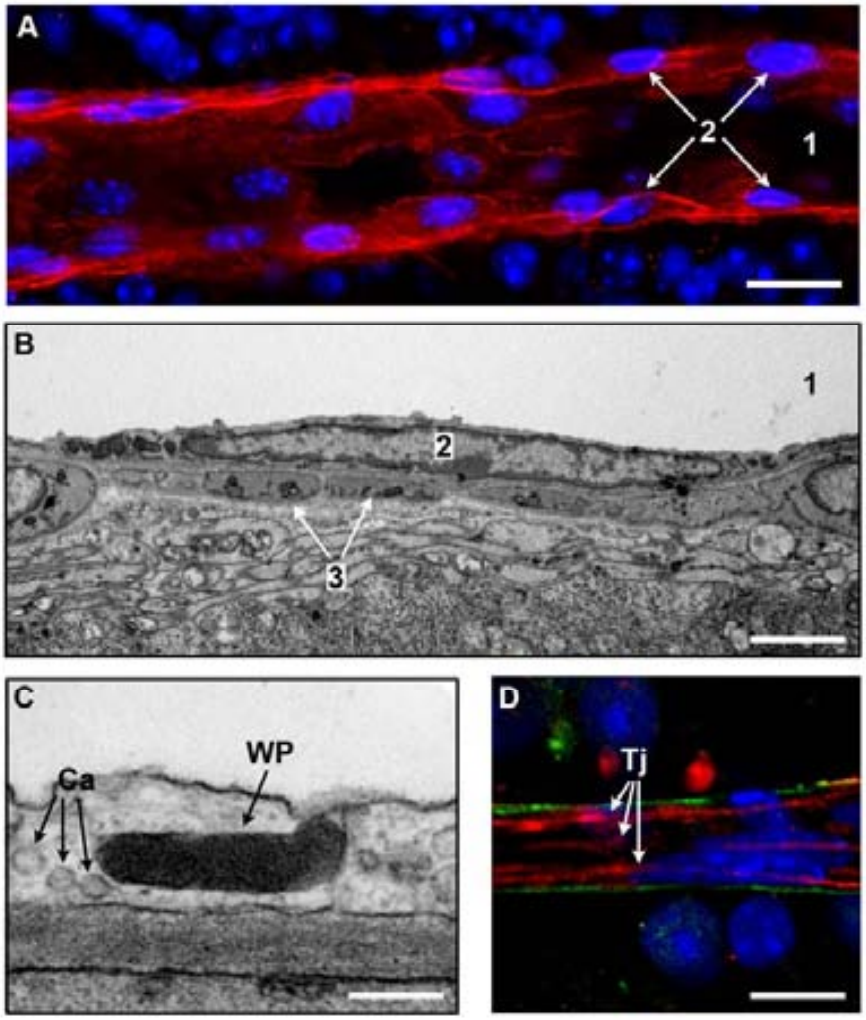


**Figure 7: Endothelial cells.** (A) Confocal microscopy image of a venule labelled with the lectin from *Lycopersicon sculentum* (red). (B) and (C) transmission electron microscopy micrographs. (D) Double immunohistochemistry anti-collagenIV (green) and anti-occludin (red). Nuclei counterstain: ToPro3. 1: Vascular lumen; 2: Endothelial cell; 3: Smooth muscle cell; WP: Weibel-Palade body; Ca: Caveolae; Tj: Tight junction. Scale bars: A = 4.34 μm; B = 2.05 μm; C = 174.54 nm; D = 10.06 μm.

sialoconjugates and proteoglycans: the glycocalix (Simionescu and Simionescu, 1986). Cells forming endothelium are oriented along the longitudinal axis of the vessel, as a response to hemodynamic shear stress (Wise, 1971; Aird, 2007).

Under transmission electron microscopy endothelial cells show irregularly contoured nuclei, with the chromatin mainly found as a slight concentration along the nuclear membrane; a nucleolus may also be prominent. Endoplasmic reticulum, free dense particles and relatively few small mitochondria are found scattered occupying the cytoplasm (Fig. 7B). Golgi apparatus appears near the nucleus (Ishikawa, 1963; Wise et al, 1971).

Tubular and vesicular components, mainly caveolae and Weibel-Palade bodies, are also found scattered throughout the cytoplasm (Fig. 7C). Caveolae are 70 nm membrane-bound, flask-shaped vesicles that usually open to luminal and abluminal sides of endothelial cells, but are also found free in the cytoplasm (Fig 7C). Caveolae system is related to transcytosis as well as to signalling integration (Anderson, 1998). Weibel-palade bodies, are highly organised cigar-shaped membrane-bound storage vesicles (Fig. 7C) (Weibel and Palade, 1964). These structures comprise a columnar rod delimited by a membrane that contains 4nm-thick tubules. Weibel-Palade bodies are a unique type of endothelial-cell specific inclusion, and the site of von Willebrand factor localization (Thorin and Shreeve, 1998).

However, endothelium displays a marked structural heterogeneity. In this way, endothelial cells of arteriolar straight segments are aligned with the blood flow but not at branch points, since shear stress triggers a structural remodelling. In the same way, these cells are elongated and spindle shaped in arterioles; irregularly shaped in capillaries; large and elliptical in post-capillary venules; and rounded in collecting venules (Aird, 2007).

More specifically, retinal endothelial cells display distinctive morphological features. In this way, retinal endothelial cells show tight junctional complexes along the opposing surfaces of adjacent cells (Fig 7D). Tight junctions are polymeric adhesion complexes with a transmembrane complex mainly formed of occluidn, claudins and junction adhesion molecules. This complex is linked to a cytoplasmic plaque containing zonula occludin protein and cingulin. Moreover, Weibel-Palade bodies are rarely found in brain (Miyagami and Katayana, 2005) and retinal capillaries (Frank et al., 1990). In addition, a highly developed caveolae system is recognizable in retinal endothelial cells (Wise, 1971), although other barriers, as blood-brain barrier, are associated with a low number of caveolae (Aird, 2007).

*3.2.1.2. Endothelial cell function:*

Endothelium has been considered a relatively inert cellular barrier until the late 1960s (Thorin and Shreeve, 1998). However, the development of the field has demonstrated that endothelial cells perform many functions. Thereby, endothelium participates in the regulation of vasomotor tone, regulates permeability and vascular structure, controls blood fluidity, and mediates both inflammatory and immunologic responses (Thorin and Shreeve, 1998; Aird, 2007). The synthesis of basement membrane components is also accomplished by endothelial cells (Félétou, 2011).

Most of endothelial functions are performed in a vascular bed and vessel type dependent manner (Aird, 2007). In this way, arteriolar endothelium is primarily responsible of vascular tone regulation while endothelial cells from post-capillary venules regulate leukocyte trafficking (Aird, 2006). Differences in basal permeability among the different vascular beds have also been reported, mainly due to differences in junctional properties and differential activity of transcytotic machinery. Optimal retinal function requires a thightly regulated environment, which is ascertained by the separation of functional compartments provided by blood-retinal barrier (Pournaras et al., 1998). Retinal endothelium is considered one main component of blood-retinal barrier mainly due to its elaborate network of tight junctions (Pournaras et al., 1998).

Hemostasis represents a finely tuned balance between procoagulant and anticoagulant forces to maintain blood in a fluid state while preventing blood loss from the closed circulation system (Aird, 2007). On the coagulant side, endothelial cells synthesize plasminogen activator inhibitor and von Willebrand factor, among others. On the anticoagulant side, endothelial cells express different factors, including nitric oxide, prostacyclin and heparan (Aird, 2007). Importantly, these endothelial-derived pro-coagulant and anti-coagulant molecules are unevenly expressed in the vasculature.

### *3.2.2. Smooth muscle cells:*

Vascular smooth muscle cells constitute the myogenic component of blood vessels (Hathaway et al., 1991). The majority of vascular smooth muscle cells are of mesodermal origin. However, it is still under discussion which embryonic cell populations are capable to follow the differentiation pathway of smooth muscle cells. (Hungerford et al., 1996; Lee et al., 1997)

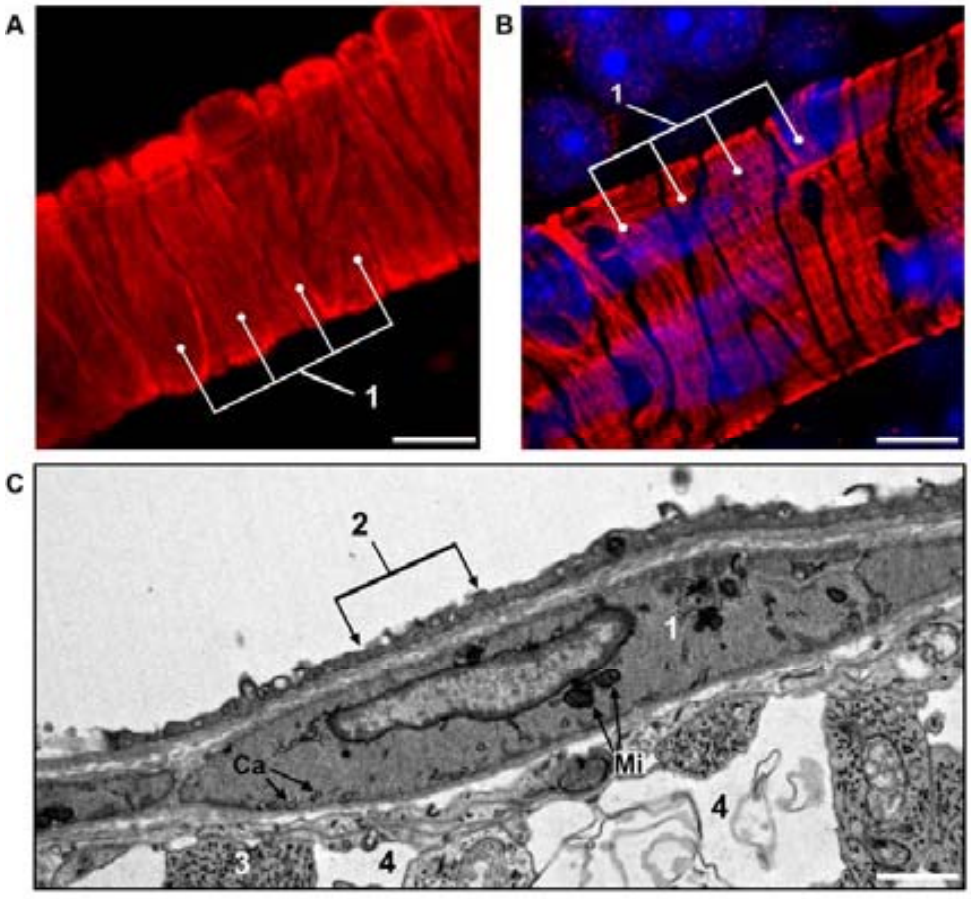


**Figure 8: Vascular smooth muscle cells.** (A) F-actin is stained with Phalloidin (red). (B) α-smooth muscle actin (red) evidenced by immunohistochemistry. (A) and (B) images have been acquired with from whole mount retinas with a confocal microscope. (C) Transmission electron micrograph. Nuclei counterstain: ToPro3. 1: Smooth muscle cell; 2: Endothelial cell; 3: Müller cell; 4: Astrocyte; Ca: Caveolae; Mi: mitochondria. Scale Bars: A = 7.69 μm; B = 8.51 μm; C = 0.55 μm.

*3.2.2.1. Vascular smooth muscle cell morphology*

Vascular smooth muscle cells display a spindle-shaped morphology which arrangement and size varies considerably in blood vessels. In retinal arterioles, smooth muscle cells appear forming a monolayer of circularly oriented cells (Fig. 8A and B).

The structure of retinal vascular smooth muscle cells is similar to that of muscular arteries elsewhere (Ishikawa, 1963). Ultrastructurally, the nucleus appears flat and elongated. Close to nuclear poles, there is an accumulation of mitochondria, Golgi apparatus and sarcoplasmic reticulum (Fig. 8C). Vesicles and caveolae are found along cell membranes in both sides of muscle cells (Fig.8C). Smooth muscle cells are also characterized by displaying a high cytoplasmic volume fraction of myofilaments, including thick filaments, actin filaments (Fig. 8A and B) and intermediate filaments.

However, smooth muscle cells are able to change its phenotype in response to local environmental signals (Owens et al., 2004). This vascular smooth muscle cell heterogeneity is mainly achieved by changes in the expression of cytoskeletal and contractile proteins (Worth et al., 2001).

*3.2.2.1. Vascular smooth muscle cell function*

Vascular smooth muscle cells are highly specialized cells whose principal function is contraction and thus, to regulate blood vessel tone, blood pressure and blood flow distribution (Owens et al., 2004). To serve this function, these cells express a unique repertoire of contractile proteins, mainly actin and myosin, together with several ion channels, and signalling molecules. Contractility of smooth muscle cells is highly dependent on free intracellular calcium (Nabika et al., 1985). In fact, membrane voltage changes and many vasoactive substances lead to smooth muscle contraction trough calcium mobilization from both intra- and extra-cellular calcium stores (Nabika et al., 1985; Puro, 2012; Kur et al., 2012). Then, the increased cytosolic calcium activates calcium-calmodulin-dependent myosin light chain kinase, which initiates the cascade of phosphorylations resulting in smooth muscle contraction (Nabika et al., 1985).

Smooth muscle cells are able to switch this highly specialized contractile phenotype to a more undifferentiated synthetic phenotype (Worth et al., 2001; Owens et al., 2004). These synthetic smooth muscle cells exhibit an increased capacity to synthesize large amounts of extracellular matrix, to participate in vascular repair, as well as to migrate and proliferate in response to growth factors and cytokines (Worth et al., 2001). At the same time, synthetic smooth muscle cells lose their ability to contract as a result of a decreased expression of contractile proteins (Worth et al., 2001).

### 3.2.3. Pericytes:

First described by Rouget (1873), pericytes constitute a contractile cell population embedded in the basement membrane and surrounding endothelial cells. Pericytes have been suggested to originate from mesenchymal cells that condense on the endothelial tube. However, tissue-dependent different developmental origins have been reported, including neural crest and mesothelium (Armulik et al., 2011).

Different types of pericytes have been distinguished according to morphology and location (Nehls and Drenckhahn, 1991). Due to its heterogeneity, these cells are usually defined using a mixture of location, morphological and protein expression pattern criteria (Armulik et al., 2011). Pericyte density varies between organs and vascular beds (Rucker et al., 2000), being the central nervous system and, more specifically, the retinal microcirculation the most pericyte-covered vasculature (Armulik et al., 2011; Lopes, 2012).

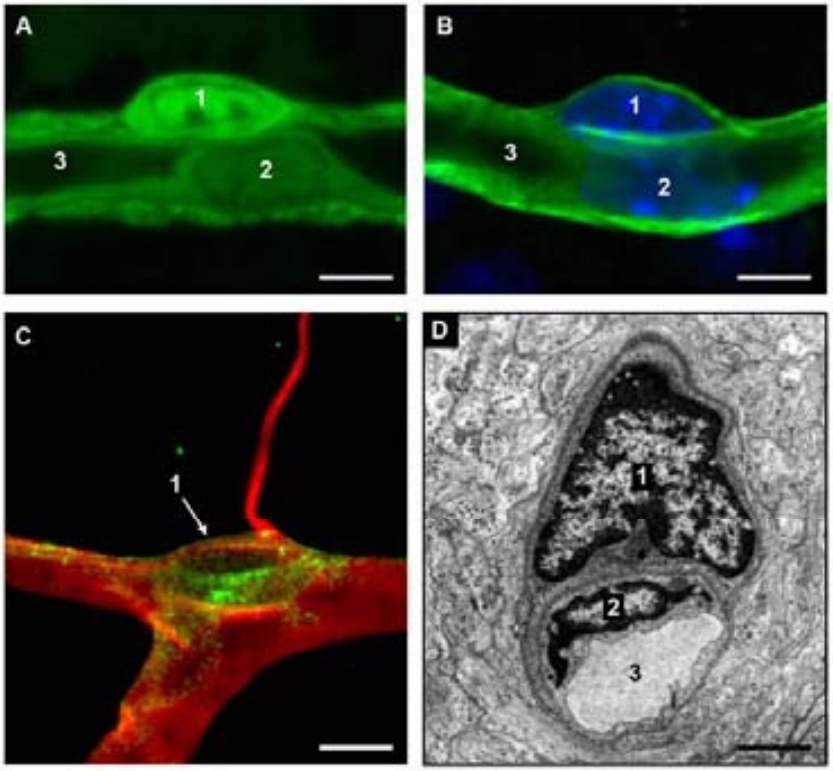


**Figure 9: Pericytes.** (A) Detection of EGFP in a capillary of a β-actin EGFP mouse. (B) Immunohistochemistry against collagen IV (green). Nuclei counterstain: ToPro3. (C) Double immunohistochemistry against collagen IV (red) and NG2 (green). (A), (B) and (C) micrographs have been performed in whole mount retinas with a confocal microscope. (D) Transmission electron micrograph. 1: Pericyte; 2: Endothelial cell; 3: vascular lumen. Scale bars: A = 3.2 μm; B = 3.2 μm; C = 5.31 μm; D = 1.4 μm.

### *3.2.3.1. Pericyte morphology*

As detailed above, pericytes display different morphological features in a location-dependent manner: in capillaries, pericytes have a nearly rounded cell body that gives rise to few primary cytoplasmic processes (Fig 9A, B and C). These primary processes extend along the abluminal surface of the endothelium in the length of the capillary (Fig. 9C). Primary processes give rise to thin secondary processes that extend perpendicularly to the vessel axis.

Thus, these secondary processes partially encircle the vessel. On post-capillary venules, by contrast, pericyte body flattens and extends many slender, branching processes.

Under transmission electron microscopy, pericytes appear enveloped by a basement membrane which is continous with endothelial basement membrane (Fig. 9). Pericytes show a discoid nucleus surrounded by a small amount of cytoplasm containing mitochondria and protein-producing organelles. Cytoplasmic processes contain different cytoskeletal filaments: microtubules are found in both primary and secondary processes. Intermediate filaments are mostly concentrated in primary proceses. Contractile filaments, including actin, myosin and tropomyosin, are concentrated forming dense bands close to the plasma membrane of luminal side. A number of caveolae can also be found in the cytoplasm, being more frequent on abluminal surface.

*3.2.3.1. Pericyte function:*

Pericytes serve many functional roles. The most supported functional property of pericytes is its ability to contract or dilate. Indeed, pericytes express a variety of both contractile proteins and receptors for vasoactive substances, enabling them to regulate blood flow. Thus, pericytes represent the myogenic mechanism for blood flow regulation at capillary level (Pfister et al., 2008; Pournaras et al., 2008).

Pericytes are also related to the regulation of endothelial proliferation and vascular development (Rucker et al., 2000). In this regard, pericytes are known to inhibit endothelial proliferation and thereby stabilize developing microvessels (Goupille et al., 2008). However, pericytes have also been shown to provide growth factors, such as VEGF, that promote proliferation of endothelia. Thus, pericytes are also involved in the process of angiogenesis and neovascularization (Rucker et al., 2000).

In adition, pericytes regulate vascular permeability (Pournaras et al., 2008; Armulik et al., 2011). In this regard, pericytes present a high number of caveolae, which are involved in transcellular transport. Moreover, these cells participate in permeability properties by secretion of matrix components (Pournaras et al., 2008). In fact, these cells play a critical role in the development and maintenance of both blood-brain and blood-retinal barriers (Herman and D'Amore, 1985; Nehls and Drenckhahn, 1991; Krueger and Bechman, 2010).

### 3.2.4. Basement membrane

Basement membrane forms a connective sheath around endothelial cells, pericytes and smooth muscle cells. In fact, these vascular cells synthesize and secrete the main constituents of basement membrane. Three layers can be distinguished in blood vessel basement membrane: *lamina lucida, lamina densa* and *pars fibroreticularis.* The lamina lucida, the inner and translucent layer, corresponds to the endothelial glycocalix. The lamina densa is the thickest

dense medial zone. This layer is mainly formed by type IV collagen as well as other glycoproteins, such as laminin (Timpl et al., 1983), fibronectin (Vaheri and Mosher, 1978), nidogen (Timpl et al., 1983) and heparan sulphate proteoglycan (Perlecan) (Hassell et al., 1985). Finally, the pars fibroreticularis makes up the transition between lamina densa and the underlying connective tissue.

Basement membrane has several functions. The most obvious function is that of support, acting as framework for vascular cells, as well as anchoring the blood vessel to the surrounding tissue. At the same time, basement membrane regulates endothelial cell proliferation and migration (Knott and Forrester, 2003) and act as an important selective barrier, regulating the pass of blood-borne molecules to retinal parenchyma (Pournaras et al., 2008).

### 3.2.5. Arteriolar annuli

Side-arm branching sites in retinal arterioles form singular structures constraining the vascular lumen, the arteriolar annuli. Although well-known by researchers working in retinal vasculature, both structure and function of arteriolar annuli remain to be elucidated. Moreover, the existence of these arteriolar structures has been poorly documented in recent years. Thus, the lack of modern technology has prevented rigorous morphological and functional studies.

Kuwabara and Cogan (1960) were first to describe arteriolar annuli in the retinal arterioles of cat and rat. However, the existence of specific structural

features in arteriolar branches had been previously reported. To note, Thuránszky (1957) published pictures of luminal constrictions at arteriolar branch points of cat retina and Loewenstein (1947) reported the presence of cell clusters occurring at retinal branching sites, what he called cushion cells. In accordance with Loewenstein studies (1947), arteriolar annuli have also been named intra-arterial cushions.

During the next decades, arteriolar annuli had been observed in the retinal vasculature of several species, including dog, monkey, pig (Henkind and De Oliveira, 1968), mice (Ikebe et al., 2001) and man (Lee, 1976; Ma, 1994). In addition, the presence of similar structures has been reported in arterioles of many different vascular beds, such as kidney, uterus, heart and brain (Moffat and Creasey, 1971; Kojimara and Ooneda, 1980; Casellas et al., 1982; Heidger et al., 1983; Whelan et al., 1996).

#### *3.2.5.1. Structure of arteriolar annuli*

The first evidence of the presence of arteriolar annuli is reported in PAS stained trypsin digested retinas (Kuwabara and Cogan, 1960). Here, annuli appeared as an increase in PAS-positive material in the side-arm branches of the main arterioles. According to these studies, arteriolar annuli are not associated with increased cellularity.

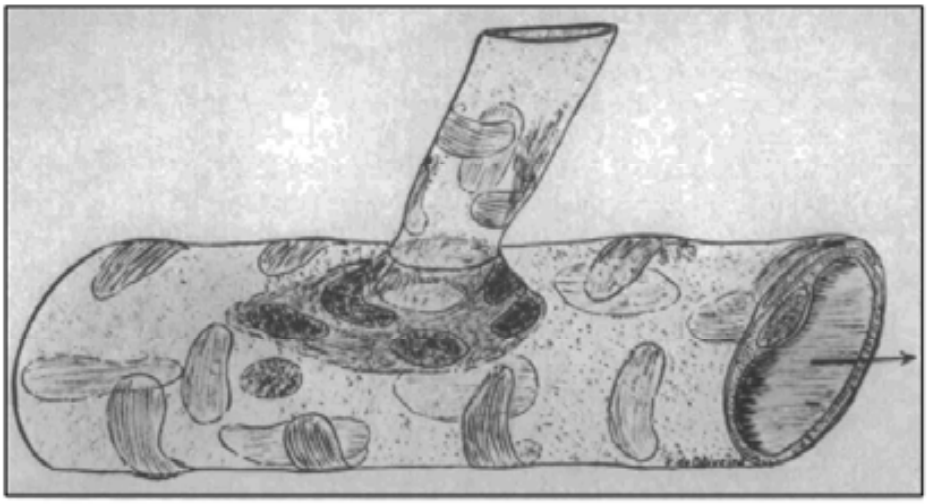

**Figure 10: Structure of arteriolar annuli.** Schematic draw from Henkind and De Oliveira (1968) representing the hypothetical structure of arteriolar annuli.

In 1968, Henkind and De Oliveira, analyzed the structure of arteriolar annuli using different techniques. According to these authors, arteriolar annuli adopt a conical appearance with the base lying within the wall of the larger vessel and small lip-like protrusions extending up the wall of the collateral arteriole (Fig.10). Related to the presence of arteriolar annuli they observe an increase in cell number (Fig. 10), which may correspond to the previously described cushion cells (Loewenstein, 1947). However, they conclude that this structure is mainly composed of basement membrane.

Arteriolar annuli have also been proposed to be composed of muscle tissue, adopting the structure of a sphincter. However, no clear evidence of a true sphincter structure at such level has been reported (Pannarale et al., 1996).

The use of vascular corrosion casts to analyze retinal vasculature evidenced the occurrence of oval depressions around the origin of arterioles (Pannarale et al., 1996; Ninomiya et al., 1999; Ninomiya et al., 2001). These reductions in vascular lumen have been related to the presence of arteriolar annuli.

*3.2.5.1. Function of arteriolar annuli*

It has been suggested that arteriolar annuli may regulate retinal blood flow by exerting a sphincter-like activity (Kuwabara and Cogan, 1960; Pannarale et al., 1996; Ninomiya and Inomata., 2005). This hypothesis is supported by previous studies demonstrating constrictions at arteriolar branch points (Thuránzsky, 1957; Friedman et al., 1964). Moreover, several in vivo studies of retinal vasculature have evidenced intermittencies in the blood flow of retinal capillaries (Friedman et al., 1964; Keith et al., 1967).

However, there is no general agreement about the function of arteriolar annuli. In this regard, Henkind and De Oliveira (1968) proposed that arteriolar annuli serve a structural function by ensuring the luminal opening and by preventing excessive dilations due to pressure alterations. A role of intra-arterial cushions in cell skimming has also been suggested. Since these structures project into the axial stream, they may favour the pass of blood cells into the branch (Fourman and Moffat, 1961).

## 3.3. Regulation of retinal blood flow

The rate of blood flow through most tissues is controlled in response to tissue metabolic needs. In turn, the regulation of the heart and circulation ensures the necessary cardiac output and arterial pressure to provide the needed blood flow to the tissue (Guyton and Hall, 2006). Blood flow control can be divided into two phases: acute control, achieved by local changes in arteriolar tone; and long-term control, resulting from kidney regulation of body fluids as well as from changes in number and size of blood vessels supplying the tissues (Guyton and Hall, 2006).

Acute blood flow regulation is achieved by three mechanisms: local control of blood flow, humoral regulation of the circulation, and nervous control of the circulation. Local control of blood flow, also called autoregulation, consists in the ability of each tissue to regulate its own blood flow in response to changes in perfusion pressure and/or metabolic rate. Humoral regulation of the circulation means control by substances secreted or absorved into the body fluids, including hormones and neurotransmitters such as norepinephrine, angiotensin II and vasopressin. Finally, autonomic nervous system regulates the circulation, mainly through the innervation of blood vessels by the sympathetic nervous system.

The retina has the highest metabolic demand in the body, together with conflicting requirements of sufficient blood supply and minimal interference with the light path (Kur et al., 2012). Thus, the ability to regulate blood flow is an essential feature of mammalian retina. In addition, the retina must maintain its

blood flow in spite of metabolic demands of non-retinal tissues (Puro, 2012). This functional independence is achieved by the retinal isolation from the effect of hormones (Laties, 1967; Delaey and van de Voorde, 2000) and the lack of sympathetic innervation in retinal vasculature (Laties, 1967; Funk, 1997). Thus, retinal flow regulation is only achieved through modifications in vascular resistance due to local autoregulatory mechanisms (Pournaras et al., 2008).

Recent functional studies suggest that mechanisms to regulate retinal blood flow are mainly controlled by arterioles, while capillaries contribute little to them (Lopes, 2012; Kur et al., 2012). However, whether arterioles or capillaries regulate blood flow remains to be elucidated. In fact, Puro (2012) has proposed a close functional relationship between capillaries and arterioles: the capillary network generates voltages that are transmitted to the arteriole via gap junction. There, voltage dependent calcium channels convert voltage signals into changes in intracellular calcium and, thereby, in mural cell contractility, lumen diameter and blood flow. Pre-capillary sphincters have also been proposed to play a role in blood flow regulation. However the presence of such structure in retinal vasculature remains controversial (Lopes, 2012).

### 3.3.1. Pressure regulation

Retinal blood flow remains largely unchanged until the mean ocular perfusion pressure is elevated by a 34-60% above baseline (Riva, 1981; Pournaras et al., 2008). This indicates the existence of compensatory mechanisms buffering most of the increase in blood pressure. These

mechanisms involve myogenic and metabolic components. An increase in transmural pressure elicits a myogenic response. This response is mainly related to smooth muscle cells, which transform the stretch into contraction through voltage-gated calcium channels (Pournaras et al., 2008; Puro, 2012; Kur et al., 2012). In addition, endothelial glycocalix act as a mechanotransducer triggering the release of endothelium-derived factors involved in the regulation of the arterial tone (Pournaras et al., 2008). Changes in the concentration of lactate, due to a decrease in perfusion pressure, also induce autoregulatory vasodilatation.

### 3.3.2 Metabolic regulation: functional hyperemia

In the retina, as happens in central nervous system, neuronal activity evokes changes in blood flow. This phenomenon, designated functional hyperemia, involves a coordinated interaction of neurones, glia and vascular cells (Metea and Newman, 2007; Kur et al., 2012). Due to the close relationship established between these cells, they are collectively called the neurovascular unit (Metea and Newman, 2007). However, mechanisms underlying functional hyperemia are still not fully understood, and metabolic feedback mechanisms have also been proposed (reviewed in Pournaras et al., 2008). The metabolic mechanism proposes that increased neuronal activity lowers O2 and glucose and produce vasoactive metabolites. These metabolites would cause vasodilation, and thus restore $O_2$ and glucose levels.

According to both mechanisms, increases in neuronal activity triggers the release of vasoactive substances by neurones, glial and/or endothelial cells. The main vasoactive molecules involved in retinal blood flow regulation are:

- **Nitric Oxide (NO):** is the main vasodilator agent in the organism. NO is a non-polar gas freely diffusible across membranes that is synthesized by the enzyme nitric oxide synthase (NOS) (Palmer et al., 1987; Ignarro, 1990; Venturini et al., 1991). There are three isoforms of this enzyme: neuronal NOS (NOS-1), which is present in ganglion, amacrine, horizontal, photoreceptors and glial cells; NOS-2, that generates large amounts of NO as a response to inflammatory and immunological stimuli; and endothelial NOS (NOS-3), mainly expressed by endothelial cells and pericytes. NO contributes to the regulation of retinal blood flow by reducing k+ conductance in smooth muscle cells and by modulating glial-to-vessel signalling (Kur et al., 2012).
- **Arachidonic acid metabolites:** metabolites from arachidonic acid regulate vessel tone through a complex mechanism involving both vasoconstriction and vasodilation. The release of vasodilating prostaglandins, such as $PGI_2$ and $PGE_2$, represents a possible mechanism to maintain the basal retinal arterial tone (Pournaras et al., 2008). Arachidonic acid metabolites are also related to glial blood flow regulation: synthesis of epoxyeicosatrienoic acid by glial cells

causes vasodilation, whereas glial-evoked vasoconstriction is mediated by 20-hydroxy-eicosatetraenoic acid (20-HETE) (Kur et al., 2012)

- **Endothelins (ETs):** there are three isoforms: ET-1, ET-2 and ET-3 (Inoue et al., 1989). Et-1, the most potent vasoconstrictor agent, is expressed by endothelial cells, neurons and astrocytes (Ripodas et al., 2001). In adition, two types of ET receptors have been described: $ET_A$ and $ET_B$. $ET_A$ receptor, expressed in pericytes and smooth muscle cells, shows high affinity to ET-1. The complex ET-1/$ET_A$ is highly related to the hemodynamic response during hyperoxia (Takagi et al., 1996). $ET_B$ receptor is expressed by pericytes and endothelial cells. There are two subtypes: $ET_{B1}$ and $ET_{B2}$. $ET_{B1}$ is expressed in endothelial cells and induces vasorelaxation through the release of NO (Hirata et al., 1993; D'Orleans-Juste et al., 1994). By contrast, $ET_{B2}$ binds ET-3 and mediates vasoconstriction (Sokolovsky et al., 1992).
- **Lactate:** in the retina, about the 90% of glucose is converted to lactate, indicating that retinal cells produce this metabolite rather than utilize it (Pournaras et al., 2008). Lactate has dual vasoactive capability, providing a mechanism to match metabolic needs: mediated by endothelium, lactate induces vasoconstriction in conditions of high energy supply. By contrast, under hypoxia, lactate causes relaxation of blood vessels.

- **Potassium:** Glial cells are able to capture potassium released by active neurons. This potassium influx is followed by an efflux at their distant endfeet, which are ensheating blood vessels. Modest increases in potassium levels cause vasodilation. Thus, this mechanism, called potassium siphoning, has been related to neurovascular coupling. In the retina, light stimulation triggers a rise in extracellular potassium coinciding with increased blood flow (Kur et al., 2012). However, studies of potassium siphoning in the retina, were Müller cells are highly permeable to potassium (Metea and Newman, 2007), have evidenced little effect of this mechanism in blood flow regulation (Metea et al., 2007).

Retinal blood flow is also modulated by blood gases. In this regard, hyperoxia induces vasoconstriction (Riva et al., 1986) and diminished blood flow (Luksch et al., 2002). By contrast, hypoxia triggers the release of NO by endothelial cells (Nagaoka et al., 2002) and the increase of retinal lactate (Winkler, 1995; Pournaras et al., 2008) driving to vasodilation.

### 3.3.3. Abnormal regulation of blood flow and retinopathy

The regulation of retinal blood flow is altered during the evolution of a number of eye disorders, including diabetic and hypertensive retinopathies.

*3.3.3.1. Diabetic retinopathy*

Diabetic retinopathy, a specific microvascular complication of diabetes, is the leading cause of blindness in working-aged people (Cheung et al., 2010). Although neuroretinal cells are also affected, most of the clinical signs in diabetic retinopathy are linked to disturbances in the vascular system. These vascular degenerative lesions include thickening of capillary basement membrane, smooth muscle cell and pericyte dropout, capillary occlusion and formation of microaneurysms (Gardiner et al., 2007). Then, vascular alterations drive to a retinal ischemia that, in turn, triggers neovascularization.

Several studies have demonstrated that vascular wall damage together with the altered blood rheological properties, may affect the ability of the retina to regulate its blood flow during diabetes (Reviewed in Pournaras et al. 2008). Importantly, the reduction in the regulatory response is observed before the appearance of overt clinical retinopathy (Kur et al., 2012). These retinal circulatory modifications include changes in basal blood flow and a reduction in the autoregulatory responses. Changes in the basal blood flow are characterized by a hypoperfusion during early diabetic retinopathy. As retinopathy progresses a switch to hyperperfusion occurs. In addition, a reduction in light evoked response has been reported. Thus, indicating a reduction in the functional hyperemia. The ability to respond to changes in blood gases is also impaired in diabetic retinas.

*3.3.3.2. Hypertensive retinopathy*

The 3-4% of adult individuals aged over 40 years show signs of hypertensive retinopathy (Wong et al., 2005). Thus, hypertensive retinopathy is the second most common type of retinopathy (Meyer-Rüsenberg, 2006). As diabetic retinopathy, hypertensive retinopathy is characterized by vascular alterations. Depending on vascular signs, hypertensive retinopathy is classified as (Wong et al., 2005):

- Grade 1: mild generalized arteriolar narrowing.
- Grade 2: severe generalized narrowing, local areas of arteriolar narrowing and arteriovenous nicking.
- Grade 3: lesions of previous grades plus retinal haemorrhages, mycronaurisms, hard exudates and cotton-wool spots.
- Grade 4: signs of preceding grades plus optic disk swelling and macular oedema. This grade is also known as malignant or accelerated hypertensive retinopathy.

Retinal autoregulation is effective over a wide range of systemic arterial pressures, but at the extremes fails. The first event as the pressure rises is a general constriction of retinal arterioles. However, due to focal lesions in vasculature, autoregulation fails and arterioles dilate. As arterioles dilate, the tension increases in the vessel wall of distal arterioles. Finally, microvessels become damaged when exposed to the full force of hypertension (Garner, 1975).

# B. INTERSTITIAL CAJAL CELLS

Multipolar cells with processes were first described in 1892 by Ramon y Cajal as a subset of nerve-like cells in the intestinal wall. A century later, Thuneberg (1982) named these cells interstitial cells of Cajal and proposed a key role of these cells in gastrointestinal motility. In the last years, the interest in ICCs has increased tremendously: according to the medline database, about 300 new papers from 2000 to 2004, in comparison with the 500 that had been published before 2000. However, there are still controversies concerning their location in organs, embryologic origin and possible functions.

In the gut, ICCs form a network, the accessory plexus, that runs whithin the muscle layers together with nerve processes coming from the Auerbach plexus (Fig 11).

## 1. Identification of interstitial Cajal cells

ICCs display different morphology depending on their location in different tissue layers and different portions of the gastrointestinal tract. In addition, ICCs also show different morphological features in different organs and species. This

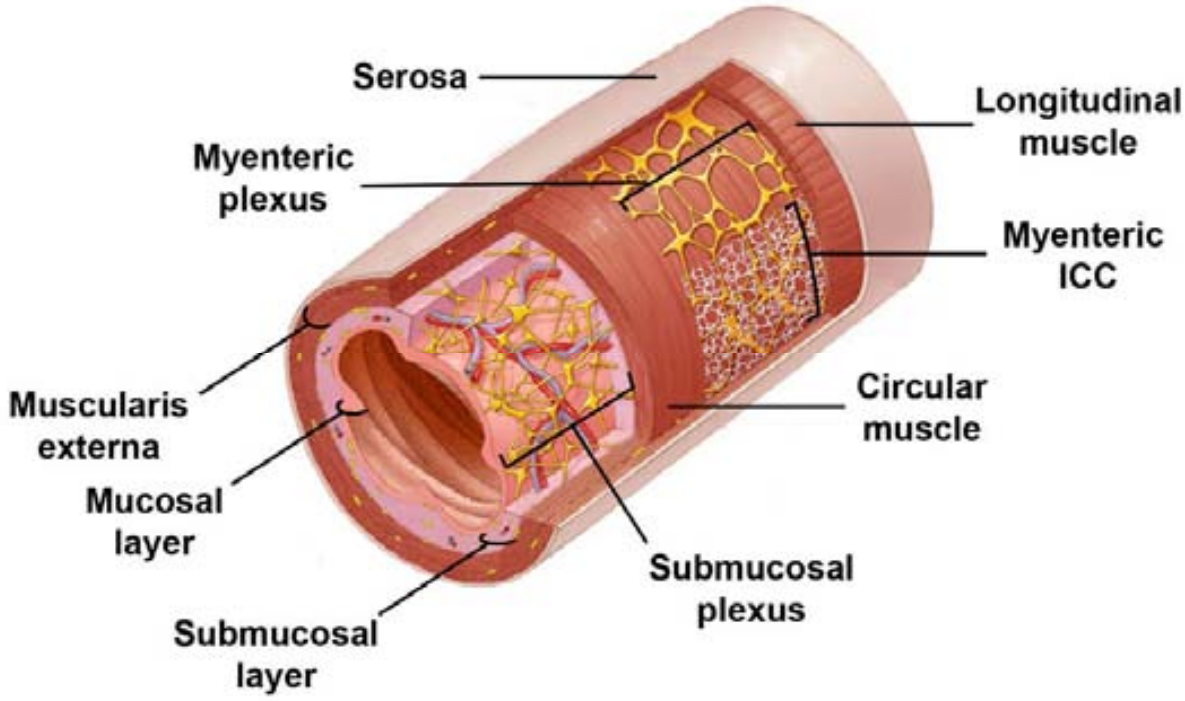


**Figure 11: Localization of ICCs in the small intestine.** ICCs form networks located within the muscularis externa, in close apposition with smooth muscle cells and neurons of the myenteric plexus. Schematic draw adapted from Ordog (2012).

fact results in a variety of cells which difficult their proper identification. In the view of these problems, an algorithm of morphological, ultrastructural and immunohistochemical criteria for ICCs identification has been proposed (Huizinga et al., 1997; Faussone-Pellegrini et al., 1999; Popescu et al., 2005):

- *Light transmission criteria:* ICCs are characterized by a multiopolar and elongated irregular body shape as well as by the presence of two or more long, thin cytoplasmic processes (Huizinga and Faussone-Pellegrini, 2005).
- *Ultrastructural criteria:* ICCs show multilobular nuclei. The cytoplasm of ICCs contains numerous, large and often elongated mitochondria,

bundles of intermediate filaments and well-developed smooth endoplasmic reticulum. A number of caveolae can also be identified in the membrane of these cells. ICCs are also characterized by establishing close appositions or gap junctional complexes with smooth muscle cells, as well as contacts with nerve bundles. ICCs present a basal lamina, although it is often discontinuous (Pucovský et al., 2003; Huizinga and Faussone-Pellegrini, 2005; Popescu et al., 2005).

- *Immunohistochemical criteria:* the presence of c-kit positive cells is considered the main indication of the presence of ICCs in certain location. However, c-kit positivity is not an essential criterion since it has been demonstrated that many ICCs do not express this protein. Thus, many other markers have been reported (Gomez-Pinilla et al., 2009).

## 2. Roles of interstitial Cajal cells

ICCs have been reported to serve three main functions in the gastrointestinal tract: (1) to pace slow waves and regulate slow wave propagation. (2) To mediate enteric neural signal to the smooth muscle cells. (3) To act as mechanosensors (Yin and Chen, 2008).

*(1) Pacemaker activity:* this is the most accepted and understood function of ICCs in the gastrointestinal tract (Popescu et al., 2005). ICCs generate a periodic depolarization called slow wave. The generation of the slow wave

involves rhythmic oscillations of intracellular calcium and the activation of several membrane channels, including non-selective cation channels, calcium-activated chloride channels and sodium channels. These rhythmic depolarizations propagate into the intestinal muscle layers resulting in periods of low and high excitability of the smooth muscle cells at the pacemaker frequency (Huang et al., 2009; Huizinga et al., 2009).

*(2) Neuromodulation:* Excitation and inhibition of gastrointestinal muscle are achieved via the cholinergic and nitrergic inputs from neural enteric system (Yin and Chen, 2008). Since ICCs establish close synaptic-like contacts with enteric neurons and make gap-junctional connections with neighbouring smooth muscle cells, it has been proposed a key role of ICCs mediating neural inputs.

*(3) Mechanosensor activity:* Location of ICCs allows these cells to monitor the contractile state of the gut musculature and to transmit this to the enteric nervous system (Huizinga et al., 2009). Moreover, it has been reported that mechanical distortion of ICCs increases pacemaker frequency of ICCs through the activation of sodium channels (Strege et al., 2003).

## 3. Interstitial Cajal cells in the vasculature

The location of ICCs has been restricted to the gastrointestinal tract for many years. However, several authors have recently reported the presence of these cells in many different organs outside the digestive tract (Pezzone et al., 2003; Gherghiceanu et al., 2005; Popescu et al., 2005 and 2007; Hinescu et al.,

2005, 2007 and 2008; Sergeant et al., 2006; Suciu et al., 2007 and 2009), mostly based on transmission electron microscopy studies (Ciontea et al., 2005). In fact, it has been proposed that ICCs accompany smooth muscle cells throughout the body (Pucovský et al., 2003).

The presence of ICCs in the blood vessel wall has been under discussion since 1953, when Meyling described a subset of cells in the vasculature which called “autonomic interstitial cells”. Years later, Dahl and Nelson (1964) found cells with irregular nuclei and multipolar processes in several arteries located in the central nervous system. Recently, cells resembling ICCs have been described in the wall of a number of blood vessels, such as rabbit portal vein (Povstyan et al., 2003), guinea pig and rat mesenteric arteries (Pucovský et al., 2003; Formey et al., 2011), human aorta and carotid artery (Bovryshev et al., 2005), rat middle cerebral artery (Harhun 2008) and human pulmonary veins (Morel et al., 2008).

## 4. Role of interstitial Cajal cells in disease

Alterations in the number of ICCs and/or disruption of ICCs networks have been related to almost every gastrointestinal motility disorder from the oesophagus to the rectum (reviewed in Farrugia, 2008; Huizinga et al., 2009). Such motor dysfunctions include pseudo-obstruction, irritable bowel syndrome, slow transit constipation, Crohn’s disease and diabetic gastropathy among others (Sanders et al., 2002; Soto Abádenas et al., 2008; Huizinga et al., 2009).

Although it still unclear if ICC damage is primary or secondary to the disease, resolution of motility disorders has been reported to result in repopulation of ICC networks (Huizinga et al., 2009).

# *MATERIAL and METHODS*

# A. MATERIAL

## 1. MICE

CD1 (ICR) wild type mice, β-actin-EGFP transgenic mice (Green mouse), nestin-GFP transgenic mice, BKS.Cg-*m* +/+ *Lepr*$^{db}$/J mutant mice (db/db mice) and Kidney Androgen-regulated Protein (KAP) transgenic mice were used.

Animal facility center of the Center of Animal Biotechnology and Gene Therapy (SER-CBATEG) supplied CD1 (ICR) wild type mice and β-actin-EGFP transgenic mice.

In 1997, Okabe et al. reported the first green transgenic mouse strain. These mice express enhanced green fluorescent protein (EGFP) under the control of chicken β-actin promoter and the cytomegalovirus enhancer (CAG). As a result, most of the tissues express very intense green fluorescence when studied under 488 nm excitation light (Okabe et al., 1997). We exploited this model to study β-actin expression in the different cell populations of the retinal vasculature.

Nestin-GFP transgenic mice were yielded by Dr. Méndez-Ferrer, Junior Group Leader in the CNIC (Madrid, Spain). In these mice, a cDNA of the enhanced version of the GFP was placed between the promoter and the second intron sequences of the nestin gene, thus matching the arrangement of the

regulatory sequences in the nestin gene (Mignone et al., 2004). This animal model allowed the analysis of the different cell populations expressing nestin in mouse retina.

db/db mice were provided by Dr. Assumpció Bosch, associate professor of U.A.B. and group leader in research of strategies for gene therapy for neuropathies in Center of Animal Biotechnology and Gene Therapy. Genetically diabetic db/db mouse have a mutation in the leptin gene which results in hyperglycemia, insulin resistance and hyperinsulinemia. Thus, these mice are widely used as a model of insulin resistant type 2 diabetes (De Angelis et al., 2008). To analyse retinal vascular alterations during type 2 diabetes, homozygous db/db mice were used. Littermate Lean mice were used as control animals.

Dr. Anna Meseguer, principal investigator in renal physiopathology group of CIBBIM, yielded KAP transgenic mice used in this study. These mice show an overexpression of kidney androgen-regulated protein driven by its own promoter (pKAP2-KAP). Thus, maintaining KAP complex regulation in kidney to produce an androgen-inducible overexpression of this protein in proximal tubule cells. KAP transgenic mice show hypertension apparently caused by increased oxidative stress and increased 20-HETE production (Tornavaca et al., 2009). This model was used to study morphological alterations that appear in retinal blood vessels during hypertension.

Mice were fed *ad libitum* with a Standard diet (2018S TEKLAD Global, Harlan Teklad, Madison, Wisconsin, USA) and maintained under conditions of controlled temperature and light (12-hour light/dark cicles, lights on at 8:00 A.M.). Transgenic animals were identified by Southern Blot of tail genòmic DNA.

Animals were euthanized by means of inhalational anesthetics (Fluothane®, AstraZeneca Farmacéutica Spain S.A., Madrid). Animal care and experimental procedures were approved by the ethics committee in animal and human experimentation of the Autonomous University of Barcelona.

## 2. HUMAN EYES

Human eyes were supplied by Dr. Alfonso Rodríguez, professor of Department of Morphological Sciences of the Medicine School in the Autonomous University of Barcelona (U.A.B.).

Eyes were obtained from two different donors:

- Donor 1: 39 years old woman, death from cardiorespiratory arrest. 7 hours elapsed between death and fixation of the eye.

- Donor 2: 89 years old diabetic woman, death from cardiorespiratory arrest. 5.5 hours elapsed from death to the fixation of the sample.

## 3. INTRUMENTAL AND EQUIPMENT

Material used in this work belongs to the Anatomy and Embriology Unit of Veterinary School, the Morphology Unit in the Centre of Animal Biotechnology and Gene Therapy (CBATEG) and the UAB Microscopy Service. All of them belong to the Universitat Autònoma de Barcelona.

Following equipment was used:

- Optical microscope with epiflourescence: Nikon Eclipse E-800 (Nikon Corp., Tokyo, Japan).
- Stereoscopic microscopes:
    - Nikon SMZ-800 (Nikon Corp.)
    - Nikon SMZ-1000 (Nikon Corp.)
- Confocal laser microscopes:
    - Leica TCS-SP2 AOBS (Leica Microsystems GmbH, Heidelberg, Germany).
    - Leica TCS-SP5 X confocal microscope (Leica Micorsystems GmbH)
- Transmission electron microscope: Jeol 1400 (Jeol Ltd., Tokyo, Japan).

- Scanning electron microscope: Hitachi S-570 (Hitachi Ltd.)

- Digital cameras:

    - Nikon digital camera DXM 1200F (Nikon Corp.)

    - Soft Imaging System CC-12 (Olympus Soft Imaging Solutions Gmbh, Münster, Germany).

- General laboratory equipment:

    - Centrifuge 5702R (Eppendorf, Hamburg, Germany).

    - Shaker UNIMAX -1010, incubator INKUBATOR-1000 and vortex REAX-top (Heidolph instruments, Schwabach, Germany).

    - Microtome Shandon Retraction AS325 (Rankin Biomedical Corporation, Holly, MI).

    - Modular inclusion center AP280: cryo-console AP280-1 and dispensing console AP280-2 (Especialidades médicas Myr SL, Tarragona)

    - pH meter PHM210 Standard (Radiometer analytical SAS, Villeurbanne Cedex, France).

    - Ultramicrotome Leica EM UC6 (Leica Microsystems).

# B. METHODS

Studies of this thesis have been divided into three groups: Morfological studies, functional studies and morfometrical studies.

## 1. MORFOLOGICAL STUDIES

Within morphological studies, different techniques are pooled: inmunohistochemical and cytochemical techniques performed on paraffin embedded and on *in toto* retinas, transmission electron microscopy analysis of retinas, scan electron microscopy of retinal vascular casts, optical microscopy analysis of digested retinas and angiographies.

### 1.1. INITIAL PROCESSING

Samples analysed were processed on a different way depending on whether samples were obtained from a mouse or a human donor.

### 1.1.1. Mouse samples:

Different protocols were used according to the technique needed to analyse the sample: paraffin embedding, *in toto* analysis or transmission electron microscopy studies.

#### *1.1.1.1. Paraffin embedding*

Samples followed the next process:

1. *Fixation:* enucleated eyeballs from euthanized mice were fixed for 24 hours at room temperature in a 10% formalin solution: neutral buffer formalin (NBF)[1].

2. *Washes:* fixative solution was removed by 4 washes in phosphate buffer solution (PBS)[2], every wash lasting 15-20 minutes. During rinses samples were maintained under constant agitation in a shaker system (UNIMAX-1010).

---

[1]**NBF:** 100 ml of 37% paraformaldhyde in 900 ml of distilled water + 4 g $NaH_2PO_4 \cdot H_2O$ + 6.5 g $NaH_2PO_4$.

[2]**PBS:** 1.5 g Na2HPO4·2H2O + 0.28 g NaH2PO4·H2O + 8.1 g NaCl + 900 ml distilled water.

3. *Dehydration:* samples were dehydrated through a series of graded ethanol baths to displace the water:

    - 70% ethanol, two changes, 1 hour each.
    - 80% ethanol, two changes, 1 hour each.
    - 95% ethanol, two changes, 1 hour each.
    - 100% ethanol, two changes, 1 hour each.

    Finally, samples were transparented in xylene for one hour.

4. *Paraffin embedding:* to achieve a correct paraffin infiltration within the tissue, samples were placed in a paraffin bath for 24 hours at 57ºC. Paraffin wax was changed once during this period. Then, samples were embedded into paraffin blocks.

5. *Sectioning:* samples were sectioned using a microtome. 3 to 4 μm thick sagittal sections of the eye were made. Sections were mounted in glass slides previously covered with silane (Sigma-Aldrich, St. Louise, Missouri, USA).

#### *1.1.1.2. Whole mount mouse samples*

Mouse retinas intended to be studied *in toto* were processed as follows:

1. *Extraction of retinas:* retinas were dissected in cold PBS on a dissection plate with a latex pad. Eyeballs were anchored to the latex pad by two insect pins: one of them fixed in the cornea and the other one in the posterior pole of the eyeball. An incision was made along the scleral groove to get access to the anterior chamber of the eye. Then, two cuts in the iris permitted an enlargement of the aperture of the pupil to extract lens through it. Once in the vitreous, retina was separated from the choroid and isolated by cutting the optic nerve. Usually, retinal pigment epithelium remained adhered to the choroid.

2. Retinas were then flattened and fixed with 10% NBF for 2 hours at room temperature.

3. *Washes:* retinas were rinsed 5 times, each of 10 minutes, in phosphate buffer igepal (PBI)[3] to remove the fixative solution.

---

[3]**PBI:** 1000 μl Igepal + 1000 ml PBS

#### *1.1.1.3. Transmission electron microscopy*

Mice were treated with an intraperitoneal injection of 10 units of 5% heparin (Hospira Productos Farmacéuticos y Hospitalarios S.L., Alcobendas, Madrid). Ten minutes later, animals were euthanized and chest cavity was opened. Mice were perfused through an intraaortic catheter with 1 ml. of freshly prepared PBS and 1 ml. of a fixative solution made of 2,5% glutaraldehye and 2% paraformaldehyde in miliQ water. Then, eyes were enucleated and retinas dissected as in the *in toto* initial processing. Retinal areas of 1mm$^2$ were cut to be processed according to the next protocol (all protocol was performed at 4ºC and under constant agitation):

1. *Fixation:*

    - Samples were fixed in a solution containing 2,5% glutaraldehyde and 2% paraformaldehyde for 2 hours.

    - Retinal pieces were rinsed in PBI and post-fixed for 2 hours with 1% osmium tetraoxide. Then, samples were washed in distilled water.

2. *Dehydration and infiltration:* retinal pieces were immersed in a series of increasing acetone solutions. Resin was also added gradually as follows:

    - 70% acetone, over night

- 80% acetone, 2 changes, 10 minutes each
- 90% acetone, 2 changes, 10 minutes each
- 96% acetone, 3 changes, 10 minutes each
- 100% acetone, 3 changes, 10 minutes each
- Acetone-Spurr resin 3:1, over night
- Acetone-Spurr resin 3:2, 5 hours
- Acetone-Spurr resin 1:1, over night
- Acetone-Spurr resin 2:3, 5 hours
- Acetone-Spurr resin 1:3, over night
- 100% Spurr resin for 2 days

3. *Polymerization:* Spurr resin blocks were performed. Then, semithin (1 μm) and ultrathin (60-80 nm) sections were made.

- Semithin sections were stained with 1% toluidine blue (Panreac Química S.A., Barcelona, Spain). Semithin sections were used to choose regions of the sample to be ultrathin sectioned.

- Ultrathin sections were contrasted with lead citrate[4] and 2% aqueous uranyl acetate. Analysis was performed with electron transmission microscopy Jeol 1400 (Jeol Ltd., Tokyo, Japan).

### 1.1.2. Human samples

Eyes from human donors were processed as described below:

1. *Fixation:* enucleated eyes were quickly immersed on a fixative solution (4% paraformaldehyde and picric acid[5] in PBS) for 24 hours at 4ºC.

2. *Washes:* Fixative was removed by 4 rinses in PBS at 4ºC during 1-2 days.

---

[4]**Lead citrate:** 1.33 g $Pb(No_3)_2$ + 1.76 g $Na_3(C_6H_5O_7)\cdot 2H_2O$ + 30 ml of boiled water. Mix the solution for 30 minutes and ad 8 ml NaOH 1N. Then, ad 12 ml of boiled water to the solution.

[5]**Picric acid:** 150 ml of picric acid saturated solution + 1000 ml PBS

3. *Partial dehydration:* samples were partially dehydrated through a series of gradient ethanol baths, from 30% to 70% ethanol. Samples were stored for several weeks at 4ºC in a 70% ethanol bath.

4. 3 $mm^2$ portions were cut from the retina and washed in 5 PBI baths during one hour to remove ethanol.

### 1.2 RETINAL DIGESTION

To isolate mouse retinal blood vessels from the rest of retinal tissue, trypsin/pepsin digestion technique was used. Some modifications were made to the method described by Kuwabara and Cogan (Kuwabara and Cogan, 1960) and Hammes et al. (Hammes et al., 1991). Tripsin and pepsin have low effect on blood vessel basement membrane. Thus, vascular architecture is preserved.

After retinas were initially processed as described in **a.2**, they were subject to the following protocol:

1. Retinas were digested for 15 minutes at 37ºC with 5% pepsin/0.2% HCl in PBS.

2. Then, retinas were subjected to a tripsin digestion (5% tripsin in PBS) for 4 hours at 37ºC.

Digested retinas followed different protocols depending on which methodology was needed to analyse the sample:

**a. Optical microscopy observation:**

Retinal blood vessels were stained with haematoxilin and periodic acid schiff (PAS) stain to evidence carbohydrates (Presnell and Schreibman, 1997). Next protocol was followed:

1. Samples were rinsed in running water for 5 minutes.
2. Incubation in 5% periodic acid for 10 minutes.
3. Wash in running water for 5 minutes.
4. Incubation in Schiff reactive (Merck, KGaA, Darmstadt, Germany) over night at 4ºC.
5. Samples were stained with Harris' haematoxylin (Merck) for 5 minutes.
6. Rinse in running water for 5 minutes.
7. Dehydration: samples were dried for 10 minutes at 60ºC.

After this protocol, samples were mounted on a glass slide with Entellan® (Merck) and protected with a coverslip. Images were taken with an optical microscope with epiflourescence (Nikon Eclipse E-800).

**b. Scan electron microscopy (SEM) analysis**

1. *Dehydration:* isolated retinal blood vessels were immersed in a series of ethanol baths, from 50% ethanol to 100% ethanol through 70, 80 and 90% ethanol baths.

2. Ethanol content of the sample was replaced by carbon dioxide following the process of critical point drying. This process was carried out by Microscopy Service of U.A.B.

Samples were mounted on SEM specimen mount stubs (Electron Microscopy Sciences, Hatfield, Pennsylvania, USA). Then, samples were sputter-coated with a layer of gold-palladium for 4 minutes. SEM images were then recorded with a scanning electron microscope (Hitachi S-570, Hitachi Ltd.) at a voltage of 20 kV.

### 1.3. IMMUNOHISTOCHEMISTRY

Immunohystochemistry is the process for detecting proteins within a tissue by exploiting the ability of antibodies to bind specifically its antigen (Presnell and Schreibman, 1997). The site of antigen-antibody binding is then visualized with an appropriate chromogen marker labelled to a secondary antibody directed against the primary antibody.

Often, to analyse structural relations between two proteins or to identify two different cells or structures together, double immunohystochemistry technique was used. In this way, two antibodies were used on the same sample, revealing each of them with a different chromogen.

#### 1.3.1. IMMUNOHISTOCHEMISTRY OVER *IN TOTO* RETINAS

In this study, most of the immunohystochemical studies were performed over *in toto* retinas. Negative controls of the technique were always carried out by omitting the primary antibody. Thus, allowing for differentiating specific positive staining from nonspecific background staining on the specimens under investigation.

The specification of the antibodies, as well as its reactivity and supplier are summarized in table 1.

| Antibody | Specificity | Commercial supplier |
|---|---|---|
| **Rabbit anti-collagen IV** | Blood vessel basement membrane | MILLIPORE |
| **Goat anti-collagen IV** | Blood vessel basement membrane | MILLIPORE |
| **Mouse anti-Von Willebrand factor** | Endothelial cells | Dako Cytomation |
| **Rabbit anti-αSMA** | Smooth muscle cells | Abcam |
| **Rabbit anti-Ckit** | Interstitial cajal cells, mesenchimal stem cells | Abcam |
| **Rat anti-CD44** | Adhesion molecules of hematopoietic cells | Abcam |
| **Rat anti-CD31** | Adhesion molecules of endothelial cells | BD Pharmingen |
| **Rat anti-CD34** | Endothelial cells | Biolegend |
| **Rabbit anti-vimentin** | Intermediate filaments of mesenchimal cells | Abcam |
| **Rabbit anti-desmin** | Intermediate filaments | Sigma |
| **Rabbit anti-connexin 43** | GAP junctions | ZYMED Laboratories Inc. |
| **Rabbit anti-Ano1** | Calcium activated chloride channels | Abcam |
| **Rabbit anti-GS** | Müller cells | Sigma-Aldrich |
| **Rabbit anti-GFAP** | Neuroglial cells | Dako Cytomation |
| **Rabbit anti-occludin** | Tight junctions | Zymed Laboratories Inc. |
| **Rabbit anti-laminin** | Blood vessel basement membrane | Dako Cytomation |
| **Rabbit anti-fibronectin** | Blood vessel basement membrane | BD Pahrmingen |
| **Rabbit anti-NG2** | Pericytes | MILLIPORE |
| **Rabbit anti-PDGF Rβ** | Tyrosine kinase receptor | Abcam |

**Table 1:** antibodies used to perform immunohistochemistry over *in toto* retinas, together with its specificity and commercial supplier.

Retinas, both coming from mouse and human, were initially processed as detailed in **1.1.1.2** and **1.1.2** respectively. Mouse retinas intended to be analyzed by anti-Ano 1 and anti-CKit inmunohistochemistries were initially processed as follows:

1. Once retinas were dissected and isolated as described in *in toto* mouse retinas initial processing, they were flattened and fixed with 100% cold acetone (Panreac Química S.L.U., Castellar del Vallés, Barcelona) for 15 minutes.

2. Washes: retinas were rinsed 5 times, each of them lasting 10 minutes, in PBI to remove the fixative solution.

Once fixed and washed, samples followed the protocol described below. All protocol, excepting those protocol steps performed at 4ºC, were carried out under constant agitation (UNIMAX-1010):

1. *Permeabilization:* to achieve a correct penetration of antibodies within the tissue, retinas were permeabilized before incubation of any antibody. To do so, next methodology was followed:

    - Retinas were immersed in a permeabilizing solution made of 0,1% triton-X-100 (Sigma-Aldrich) in PBS. Samples were maintained in this solution for 2 hours at room temperature or over night at 4ºC.

- Samples were then rinsed in PBI at room temperature. 3 changes of 10 minutes each of them were performed.

- Finally, two baths of 10 minutes in Wash Buffer[6] (WB) were performed.

2. *Incubation of primary antibodies:* Antibodies used in this study are summarized in table 2.

[6]**WB:** 1000 ml Igepal + 3 g bovine serum albumin (BSA) + 1000 ml PBS

| Antibody | Dilution | Incubation solution |
|---|---|---|
| Rabbit anti-collagen IV | 1:200 | |
| Goat anti-collagen IV | 1:20 | |
| Rabbit anti-Von Willebrand factor | 1:50 | |
| Rabbit anti-αSMA | 1:500 | |
| Rabbit anti-Ckit | 1:50 | |
| Rat anti-CD44 | 1:100 | WB + |
| Rat anti-CD34 | 1:50 | 10% Neutral Donkey Serum |
| Rabbit anti-vimentin | Not diluted | (NDS) |
| Rabbit anti-desmin | 1:20 | |
| Rabbit anti-connexin 43 | 1:100 | |
| Rabbit anti-Ano1 | 1:90 | |
| Rat anti-CD31 | 1:25 | |
| Rabbit anti-occludin | 1:1000 | |
| Rabbit anti-laminin | 1:200 | |
| Rabbit anti-fibronectin | 1:100 | |
| Rabbit anti-NG2 | 1:200 | |
| Rabbit anti-PDGF-Rβ | 1:100 | |

**Table 2:** antibodies used to perform immunohistochemistry over *in toto* retinas, together with its dilution and incubation solution.

Primary antibodies were always incubated for 30 minutes at room temperature plus over night at 4ºC. Except Anti-Von Willebrand factor that was incubated over night at room temperature.

3. *Wash* in PBI (3 changes of 10 minutes each) and in WB (2 changes of 10 minutes each).

4. *Incubation of secondary antibodies:* secondary antibodies were incubated under same temperature and time conditions as primary antibodies. These antibodies were always diluted in WB. A summary of secondary antibodies used in this study is found in table 3.

| Secondary antibody | Dilution |
|---|---|
| Anti-rat IgG Biotin | 1:100 |
| Anti-goat IgG Biotin | 1:100 |
| Anti-rabbit IgG alexa 568 | 1:100 |
| Anti-rabbit IgG alexa 488 | 1:100 |

**Table 3:** secondary antibodies used to perform immunohistochemistry over *in toto* retinas, together with its dilution.

5. Samples were rinsed in PBI: 5 changes of 10 minutes each.

6. In order to detect immunocomplex, when secondary antibodies were not labelled to cromophers, two different fluorochromes were used: Streptavidin Alexa Fluor 488 and Streptavidin Alexa

Fluor 568, both of them diluted 1:100 in PBS. Incubation of fluorophores was performed in the same time and temperature conditions as antibodies.

7. Then samples were washed in PBI: 5 changes of 10 minutes each.

8. *Counterstain:* two different nuclei markers were used

   Hoescht: diluted in PBS 1:100.

   ToPro 3: diluted in PBS 1:100.

   Both markers were incubated for 10 minutes at room temperature.

9. *Mounting samples*: retinas were rinsed in PBI for 1 hour (changing PBI 5 times). Samples were then flattened over a slide with retinal internal aspect facing the coverslip. Some drops of Fluoromount ® (Sigma-Aldrich) were used as mounting media. Finally, slides were sealed with nail lacquer.

10. Images were taken with a Leica TCS SP2 AOBS confocal microscope (Leica Microsystems).

### 1.3.2. IMMUNOHISTOCHEMISTRY IN PARAFFIN SECTIONS

After retinas were processed as detailed in section **1.1.1.1,** next protocol was performed:

1. *Deparaffinization and rehydration:*

   - Xylane: 2 washes of 5 minutes each.
   - 100% ethanol: 2 washes of 5 minutes each.
   - 96% ethanol: 2 washes of 5 minutes each.
   - 80% ethanol: 5 minutes
   - 70% ethanol: 5 minutes.
   - Distilled water: 5 minutes

2. Slides were then washed in WB for 5 minutes.

3. *Incubation of primary antibody:* Antibodies used in paraffin embedded retinal sections are summarized in table 4.

| Antibody | Dilution | Specificity | Commercial supplier |
|---|---|---|---|
| **Goat anti-collagen IV** | 1:20 | Blood vessel basement membrane | MILLIPORE |
| **Rabbit anti-αSMA** | 1:500 | Smooth muscle cells | Abcam |
| **Chicken anti-GFP** | 1:200 | GFP-tagged proteins | Abcam |
| **Rabbit anti-GS** | 1:500 | Müller cells | Sigma-Aldrich |
| **Rabbit anti-GFAP** | 1:1000 | Neuroglial cells | Dako Cytomation |

**Table 4:** antibodies used to perform immunohistochemistry on paraffin embedded retinal sections, together with its dilution, specificity and commercial supplier.

Primary antibodies were always diluted in a WB solution containing 10% of NDS and incubated over night at 4ºC.

4. Samples were washed in PBI three times, each wash lasting 5 minutes. An additional wash in WB was performed during 5 minutes.

5. *Incubation of secondary antibodies:* secondary antibodies were incubated in a WB solution for 3 hours at room temperature. Table 5 summarizes secondary antibodies used to perform this study as well as its dilutions.

| Secondary antibody | Dilution |
|---|---|
| Anti-chicken FITC | 1:100 |
| Anti-goat IgG Biotin | 1:100 |
| Anti-rabbit IgG alexa 568 | 1:100 |

**Table 5:** secondary antibodies used to perform immunohistochemistry over retinal paraffin sections, together with its dilution.

6. *Washes:* samples were rinsed three times in PBI. Every wash lasted 5 minutes

7. *Fluorochrome incubation:* to evidence immunolabeling Streptavidin Alexa Fluor 488 was used, diluted 1:100 in PBS. In the triple immunohistochemistry the fluorochrome Streptavidin Cy5, diluted 1:500, was used. Incubation of fluorophores was performed in the same conditions as detailed for the incubation of secondary antibodies.

8. Sections were placed on three baths of PBI, each of them lasting 5 minutes.

7. *Counterstain:* retinal sections were counterstained with a Hoescht solution diluted in PBS 1:100. Samples were incubated in this solution at room temperature for 5 minutes.

8. Retinal sections were then rinsed three times in PBI, each wash lasted 5 minutes.

9. Samples were mounted in some drops of Fluoromount ® (Sigma-Aldrich) and covered with a coverslip. Finally, slides were sealed with nail lacquer.

10. Images were taken by a Leica TCS SP2 AOBS confocal microscope (Leica Microsystems).

## 1.4. HISTOCHEMISTRY

Different histochemical techniques were performed in this work.

### 1.4.1 Haematoxilin/Eosin stain

Histological stain with hematoxilin/eosin was performed as follows:

1. Desparaffinization and rehydration as detailed in section **1.3.2**

2. Samples were washed in running water for 5 minutes.

3. Harris haematoxilin (Sigma-Aldrich): 5-10 minutes.

4. Wash in running water for 5 minutes.

5. Quick bath in a solution of 0.25% hydrochloric acid diluted in 70º ethanol.

6. Eosin (Merck): from 30 seconds to 1minute.

7. Quick dehydration by two quick baths in 96º ethanol and one quick bath in 100º ethanol.

8. Transparentation: samples were transparented by means of two baths in xylane (Panreac), each of them lasting 5 minutes.

9. Mounting: Samples were mounted with Entellan ® (Merck) and covered with a coverslip.

10. Samples were analyzed in an optical microscope (Nikon Eclipse E- 800) and images were acquired by a digital camera (Nikon DXM 1200F).

**1.4.2. Phalloidin**

Phalloidin is a toxin from *Amanita phalloides* that shows high affinity in F-actin binding (Cooper, 1987). Thus, fluorescent derivatives of phalloidin have

been extremely useful for localizing actin filaments in cells and tissues (Faulstich et al., 1988).

Methodology used to evidence F-actin binding by phalloidin was almost the same as the one described to perform *in toto* inmunohystochemistries. Some variations added to that protocol are described below:

1. Perform steps described in section about *in toto* inmunohystochemical techniques from first step to eighth.

2. Rinse samples several times in PBI, each of them lasting 15 minutes.

3. Incubation of Phalloidin-TRITC (Sigma-Aldrich):

   - Concentration: 5 μg/ml diluted in PBS.

   - Samples were incubated in this solution for 1 hour at room temperature.

4. Samples were then washed several times in PBI.

5. Mounting and analysis as described in methodology for inmunohistochemistry.

### 1.4.3. Lectins:

Lectins are non-inmune sugar-binding proteins from vegetal origin, mostly from *Labitae* and *Leguminosae* families. Specific carbohydrate-binding properties shown by lectins make them key tools in the detection and isolation of certain carbohydrates (Henry and DeFouw, 1995).

Lectins used in this study are listed in the table 6, together with its supplier, carbohydrate specificity and inhibitory sugar (according to Sharon and Lis, 1990; Debray et al., 1981):

| *Lectin* | *Specificity* | *Inhibitory sugar* | *Supplier* |
|---|---|---|---|
| ***Ricinus communis*** | galactose/N-acetylgalactosamine | Galactose | Vector Laboratories |
| ***Griffonia simplicifolia*** | galactose/N-acetylgalactosamine N-acetilglucosamine | Galactose | |
| ***Wisteria floribunda*** | galactose/N-acetylgalactosamine | N-acetylgalactosmine | |
| ***Triticum vulgaris*** | N-acetylglucosamine / sialic acid | N-acetylglucosamine | |
| ***Arachis hypogaea*** | Galactose / N-actylgalctosamine | Galactose | |
| ***Lycopersicon escolentum*** | N-acetylglucosamine | N-acetylglucosamine | |
| ***Sambucus nigra*** | Sialic acid / Galactose | a-(2-6)-sialyllactose | |
| ***Glycine max*** | galactose/N-acetilgalcatosamine | N-acetylgalctosamine | |

**Table 6:** lectins used to analyze carbohydrates, together with its specificity, inhibitory sugar and commercial supplier.

Methodology explained below was followed to perform this histochemical technique:

1. Perform steps described in section about immunohistochemistry over *in toto* retinas from first to eighth steps.

2. Several washes in PBI were performed, each of them lasting 15 minutes.

3. *Incubation of lectins* was performed over night at 4ºC. Incubation solutions are described in table 7.

| *Lectin* | *Concentration* | *Triton -X- 100* | *Diluent* |
|---|---|---|---|
| **RCA** | 20 μg/ml | 0,10% | PBS cations |
| **GSA** | 20 μg/ml | 0,50% | |
| **WFA** | 10 μg/ml | 0,10% | |
| **WGA** | 20 μg/ml | 0.10% | |
| **PNA** | 25 μg/ml | 0.10% | |
| **LEA** | 20 μg/ml | 0.10% | |
| **SNA** | 40 μg/ml | 0.10% | |
| **SBA** | 20 μg/ml | 0,10% | |

**Table 7:** Working concentration and incubation solution of lectins used im this work.

4. Several washes in PBI were performed.

5. *Flourochrome incubation*: to amplify lectin signal Streptavidin Alexa 488 was used at 1:100 dilution in PBS. Samples were incubated in this solution over night at 4ºC.

6. Samples were rinsed in PBI several times.

7. Mounting and analysis as described in methodology for immunohistochemistry on *in toto* retinas.

### 1.4.4. NADPH diaphorase

NADPH diaphorase histochemical technique is based on the presence of an enzyme capable of catalysing the NADPH-dependent conversion of the soluble tetrazolium salt to the insoluble, visible formazan (Hope et al., 1991).

Several studies demonstrate that NADPH diaphorase is a nitric oxide synthase, an enzyme involved in nitric oxide (NO) synthesis (Dawson et al., 1991; Hope et al., 1991). Thus, NADPH diaphorase histochemistry was used as specific marker for cells producing NO (Hope et al., 1991).

Once retinas from control mice were dissected as described on section of initial processing of *in toto* techniques, following protocol was performed:

1. Retinas were fixed in NBF 10% for 2 hours at room temperature.

2. Several washes in PBI were done.

3. Then, retinas were washed several times in TRIS HCl Buffer 0.1 M pH: 8[7].

4. Samples were incubated for 90-120 minutes at 37ºC in a reaction solution containing 15 mM malic acid, 1mM $MnCl_2$, 1 mM NADP, 0.2 mM Nitro Blue Tetrazolium and 0.2% triton X-100 in TRIS HCl Buffer.

5. Retinas were then washed several times in TRIS HCl Buffer 0.1 M pH:8.

6. Samples were mounted in buffered glycerol and analyzed in an optical microscope (Nikon Eclipse E- 800) and images were acquired by a digital camera (Nikon DXM 1200F).

7. Samples were analyzed with an optical microscope (Nikon Eclipse E-800) and images were acquired with a digital camera (Nikon digital camera DXM 1200F).

### 1.4.5. Salivary amylase digestion

Salivary amylase hydrolyzes glycogen (Walker and Whelan, 1960). To evidence glycogen content in cells of arteriolar annuli, next protocol was followed:

1. Retinas were digested according to the method described in section **1.2**.

2. Samples were rinsed in running water for 5 minutes.

3. Incubation in salivary amylase for 30 minutes at 37ºC. Salivary amylase was renewed every 10 minutes.

4. Samples were rinsed in running water for 5 minutes.

Amylase digested retinas followed different protocols depending on which methodology was needed to analyse the sample:

**a. PAS stain:**

1. Incubation in 5% periodic acid for 10 minutes.
2. Wash in running water for 5 minutes.
3. Incubation in Schiff reactive (Merck) over night at 4ºC.
4. Samples were stained with Harris' haematoxylin (Merck) for 5 minutes.
5. Rinse in running water for 5 minutes.
6. Dehydration: samples were dried for 10 minutes at 60ºC and then mounted on a glass slide with Entellan® (Merck) and protected with a coverslip.
7. Samples were analyzed with an optical microscope (Nikon Eclipse E-800) and images were acquired with a digital camera (Nikon digital camera DXM 1200F).

**b. *Griffonia simplicifolia* cytochemistry together with anti-collagen IV immunohistochemistry:**

1. Digested retinas were washed in PBI for 15 minutes. PBI was changed three times during this period of time.

2. *Incubation of primary antibody:* samples were incubated for 2 hours at room temperature in a solution containing rabbit anti-collagen IV (diluted 1:200) and 10% of neutral goat serum in WB.

3. Retinas were rinsed in PBI 3 times. Each wash lasted 5 minutes.

4. *Lectin incubation:* samples were incubated over night at 4ºC in a solution containing 20mg/ml of the lectin *Griffonia simplicifolia* in PBS cations with 0.5% of triton-X-100.

5. Wash the sample in PBI 3 times, each wash lasting 5 minutes.

6. *Incubation of secondary antibody and fluorochrome:* retinas were incubated in a WB solution containing Alexa-fluor 488 goat anti-rabbit (diluted 1:200) and Streptavidin Alexa-fluor 568 (diluted 1:100).

7. Samples were washed 3 times in PBI, lasting 5 minutes every wash

8. *Counterstain:* nuclei were stained with Hoescht diluted in PBS 1:100. Samples were incubated in this solution for 10 minutes at room temperature.

9. Mounting as described in methodology for inmunohistochemistry.

10. Sample analyses and image acquisition were performed with a Leica TCS SP2 AOBS confocal microscope.

### .1.5. FLUORESCEIN ISOTHIOCYANATE-DEXTRAN ANGIOGRAPHY

High-molecular-weight fluorescein (FITC)-dextran cannot leak through vascular walls. Thus, FITC-Dextran intravascular injection is a successful approach for studying vascular lumen in mouse retina (Li et al., 2011).

In our laboratory, “ex vivo” injection of fluorescein isothiocyanate-dextran (Sigma-Aldrich) has been successfully performed as follows:

1. Animals were Intraperitoneally injected with 0.1 ml of 5% sodium heparin. 10 minutes after injection mice were euthanized with a fluothane overdose.

2. Mice were dissected to access to thoracic cavity. Then thoracic aorta was cranially cannulated with a 25G catheter to inject 1 ml of a 50 mg/ml FITC-dextran solution.

3. Retinas were then removed from the eyeball and fixed in a 10% NBF bath for 2 hours at 4ºC.

4. 5 washes of 10 minutes each in a PBI bath were performed.

5. Nuclei were counterstained with ToPro-3.

6. After several washes in PBI samples were mounted in a slide with some drops of Fluoromount® (Sigma-Aldrich).

7. Angiography analyses and image acquisition were performed with a TCS SP2 AOBS confocal microscope.

. **1.6. INDIAN INK ANGIOGRAPHY**

Indian ink *ex vivo* injected retinas allowed the analysis of vascular lumen in arteriolar annuli. To perform the angiography next protocol was followed:

1. *Injection:* 1 ml of a solution containing 1 ml Indian ink + 9 ml of distilled water + 0.5 g of DQ gelatin from pig skin (Molecular Probes)

was injected as described in fluorescein isothiocyanate-dextran angiography protocol.

2. Retinas were then removed from the eyeball and fixed in a 10% NBF bath for 2 hours at 4ºC.

3. After several washes in PBI samples were mounted in a slide with some drops of Fluoromount® (Sigma-Aldrich).

4. Angiography analyses and image acquisition were performed with a TCS SP2 AOBS confocal microscope (Leica Microsystems).

## 2. FUNCTIONAL STUDIES

### 2.1. BLOOD RETINAL BARRIER ANALYSIS

Horseradish peroxidase (HRP) has been widely used as a tracer to demonstrate blood-retinal barrier breakdown (Vinores, 1995). To assess integrity of the barrier in arteriolar annuli next protocol was performed:

1. HRP injection: 1 ml of a solution of 15 mg/ml of HRP (Sigma-Aldrich) diluted in saline solution was injected in tail vein.

2. 6 hours after injection mice were euthanized and retinas were dissected according to methods described above.

3 The presence of HRP was ascertained by its revelation with 3,3'-diaminobenzidine tetrahydrochloride (DAB) (Sigma-Aldrich).

4. Samples were mounted in buffered glycerol.

5. Retinas were analyzed with an optical microscope (Nikon Eclipse E-800) and images were acquired with a digital camera (Nikon digital camera DXM 1200F).

### 2.2. EVALUATION OF SPONTANEOUS CONTRACTILE ACTIVITY

Dissection and perfusion procedures were identical to those previously reported in section **1.6**. Once retinas were dissected, were gently transferred to a plate containing culture medium: Dulbecco modified Eagle's Medium (DMEM) supplemented with 10% phoetal calf serum, 1% penicillin/streptomycin and 2mM glutamine. Retinas were oriented with inner limiting membrane facing down and flattened with a coverslip to allow well-focused images of retinal vasculature.

Images were taken every 2 seconds by a Leica TCS SP2 AOBS confocal microscope (Leica Microsystems) and processed with the Leica LAS AF Lite

imaging software (Leica Microsystems). During image acquisition, retinas were maintained under controlled temperature and $CO_2$ conditions of 37ºC and 5% respectively.

### 2.3. ANALYSIS OF TISSULAR HYPOXIA

Retinal oxygenation was analysed using Hypoxiprobe$^{TM}$-1 commercial kit (Chemicon Int.). In order to assess if certain retinal regions were less susceptible to lack of oxygen, partial hypoxia was induced in mice retinas by partially clamping common carotid arteries. Then animals were injected with Pimonidazole. This marker specifically binds certain proteins in hypoxic cells (Ruberte et al., 2011). Inmunohistochemistry against pimonidazole allows the detection of these pimonidazole binded proteins.

Working protocol to perform this study is described below:

1. Mice were intravenously injected with 60 mg pimonidazole/kg body weight in phosphate-buffered saline.

2. 30 minutes post-injection animals were anesthetized with an intraperitoneal injection of a 100 mg/kg ketamine (Imalgène 500, Merial Laboratorios S.A., Barcelona, Spain) and 10 mg/kg xylacine (Rompun®, Bayer, Kiel, Germany) solution.

3. Ventral aspect of mice's neck was dissected to exhibit common carotid arteries, which were clamped for 10 minutes.

4. Retinas were removed from the eyeball and then fixed over night at 4ºC with 10% NBF.

5. After several washes in PBI to remove the fixative solution, samples were permeabilized in a 0.1% triton-X-100 solution.

6. As Pimonidazole is a monoclonal antibody produced in mouse, the use of the blocking MOM commercial kit was necessary (Kit MOM™, Vector Laboratories, Inc.; Burlingane, CA, USA). Thus, after permeabilization, samples were incubated in a solution of 36 μl/ml *Blocking IgG Reagent* (Kit MOM component) in PBS for 1 hour at room temperature.

7. Samples were washed 5 times in PBI, each wash lasting 10 minutes.

8. Retinas were then incubated for 30 minutes at room temperature with the *MOM diluent*: 80 μl of *protein concentrate* (Kit MOM component) in 1 ml of PBS.

9. Primary antibodies diluted in a solution containing MOM diluent with 10% neutral goat serum were then incubated over night at 4 ºC. Primary antibodies and its dilutions were:

* Rabbit anti-collagen IV diluted 1:200

* Mouse anti-pimonidazole diluted 1:50

10. Samples were washed in PBI 5 times, each wash lasted 10 minutes.

11. Secondary antibodies were also diluted in MOM diluent and incubated over night at 4ºC. Secondary antibodies used and its dilutions were:

* Antimouse Biotin (Kit MOM component) diluted 1:250

* Donkey anti-rabbit 568 diluted 1:100

12. Several washes of 10 minutes each were performed to the retinas.

13. Streptavidin Alexa 488 diluted 1:100 in PBS was incubated over night at 4ºC.

14. Retinas were washed several times in PBI.

15. Nuclei were counterstained with ToPro 3 diluted 1:100 in PBS. Retinas were incubated in this solution for 10 minutes at room temperature.

16. After several washes in PBI retinas were mounted on slides with some drops of anti-fading mounting media (Fluoromount®) and

analyzed with a Leica TCS SP2 AOBS confocal microscope (Leica Microsystems).

## 2.4. IN VIVO CALCIUM IMAGING

Calcium is an intracellular messenger that controls a wide range of cellular processes (Thomas et al., 2000). The use of fluorescent compounds that undergo large fluorescent enhancements upon binding Ca2+ has made possible the observation of calcium signalling (Gee et al., 2000; Thomas et al., 2000).

Fluo-4 is a fluorescent dye that responds to calcium binding with an increase of fluorescence intensity. This compound has higher absorptivity of 488 nm excitation light and less cytotoxicity than other calcium-binding dyes. Thus, Fluo-4 can be used effectively to detect and quantify calcium changes in both whole cells or in subcellular regions of interest (Gee et al., 2000).

In order to detect calcium events in different retinal cell populations protocol described below was followed:

**a) Retinal preparation**

1. Mice were euthanized with a fluothane overdose.

2. Enucleation and retinal dissection was performed in sterile PBS

3. Retinas were transferred to a plate containing culture medium: Dulbecco modified Eagle's Medium (DMEM) supplemented with 10% phoetal calf serum, 1% penicillin/streptomycin and 2mM glutamine. Retinas were maintained under controlled temperature and $CO_2$ conditions of 37ºC and 5% respectively.

**b) Dye loading**

1. Samples were washed in Hanks balanced salt solution (HBSS) (Life Technologies Corporation, Carlsbad, CA, USA).

2. Dye incubation: retinas were incubated in a solution containing 10 μM Fluo-4 (Life Technologies Corporation) and 0.3% of 20% pluronic acid. Samples were incubated in this solution for 1 hour at 37ºC.

3. Retinas were washed in HBSS and maintained at 37ºC in new culture medium.

**c) Image acquisition and analysis**

Loaded retinas were disposed in a plate with inner limiting membrane facing down. To allow optimal focus of arteriolar annuli, retinas were gently flattened and maintained under a metal grid.

Functional imaging was performed on a Leica TCS SP5 confocal microscope using Leica oil immersion lenses (63x, Leica, Germany). The Fluo-4 indicator was excited at 488 nm and image sequences were captured every 2 seconds. Fluo-4 AM fluorescence intensity was measured on image sequences with the Leica LAS AF Lite imaging software (Leica, Germany).

**d) Drug application**

Retinas were maintained unstimulated for 30 seconds to obtain calcium images under basal conditions. Then, culture medium containing 150 μM of histamine was carefully applied to the retina through the metal grid.

## 3. MORPHOMETRICAL STUDIES

### 3.1. DISTRIBUTION AND TOPOGRAPHY OF ARTERIOLAR ANNULI

To determine topography and distribution of arteriolar annuli, all arteriolar branches of whole mount retinas double stained with anti-collagen IV antibody and *Griffonia simplicifolia* were analyzed (n = 5). Within each retina three different areas were considered:

1. Central retina: from the optic disc to the midpoint of the retinal radius.

2. Peripheral retina: from the midpoint of retinal radius to the retinal outer edge.

3. Arterio-arteriolar shunts: specific retinal areas where arterioles communicate directly to each other by a capillary network.

Results are expressed as percentage of arteriolar branches occupied by arteriolar annuli in each area.

### 3.2. PROTEIN AND CARBOHYDRATE QUANTIFICATION

Although several methods to quantify proteins in a tissue have been developed over the years, fluorescence molecular imaging has provided to

researchers a method that is both sensitive and specific (Gustashaw et al., 2010).

Mean fluorescence intensity was measured with Leica LAS AF Lite imaging software (Leica, Germany) according to the equation:

$$\mathbf{AFP} = \frac{\sum i(p)}{n(p)} \text{ (intensity units/pixel)}$$

Where i(p) is the intensity of a pixel within the confocal plane of the cell, and n(p) is the total number of pixels of the plane. Results are reported in arbitrary intensity units, such as grays.

**a. Hemostatic function:**

To evidence differences in hemostatic function of arteriolar annuli, whole mount retinas were double immunolabeled with antibodies against Von Willebrand factor and collagen IV. Then samples were analyzed using a TCS SP2 confocal microscope. Von Willebrand factor intensity was determined in 643.04 $\mu m^2$ regions of interest of 6 arteriolar annuli and its correspondent adjacent vessel wall.

**b. Basement membrane:**

To test whether the presence of arteriolar annuli induced changes in the basement membrane, retinas were immunolabeled with antibodies against collagen IV, laminin and fibronectin. Mean fluorescence intensity of fibronectin was determined in 8 arteriolar annuli and its correspondent adjacent blood vessel wall; collagen VI was expression was ascertained in 6 arteriolar annuli and 6 regular arterioles; and finally, laminin was analyzed in 11 arteriolar annuli and its correspondent regular arteriole. Images were obtained with a TCS SP2 confocal microscope.

**c. Diabetic retinopathy:**

Retinas from db/db mice were labeled with *Griffonia simplicifolia* to study alterations of arteriolar annuli during type 2 diabetes. Mean fluorescence emission of *Griffonia simplicifolia* was measured in 4 arteriolar annuli per retina. Retinas from 2 db/db mice were compared with retinas from 2 Lean control age-matched mice. Images were acquired under same conditions in all animals with a TCS SP2 AOBS confocal microscope.

**d. Hypertensive retinopathy**

To analyze alterations of arteriolar annuli during hypertension, retinas from KAP transgenic mice were double labeled with anti-Ano1 and anti-collagen IV antibodies. Ano1 mean fluorescence intensity was determined in 5 to 10 arteriolar annuli per retina. Retinas from 5 KAP transgenic mice and 5 control littermate mice were analyzed. Images were obtained under same conditions in all animals with a TCS SP2 AOBS confocal microscope.

## 3.3. EVALUATION OF WALL THICKNESS DURING HYPERTENSIVE RETINOPATHY

To establish arteriolar wall thickness during hypertensive retinopathy $\alpha$-SMA immunolabeled paraffin embedded retinal sections were analyzed. 2 measures were stablished:

**1** = Transversal diameter of arteriole

**2** = Transversal diameter of arteriolar lumen

From these measures, wall thickness was estimated as follows: WALL THICKNESS = 1 – 2.

To avoid bias errors, each measure was determined 3 times per arteriole in 5 arterioles per retina. Retinas from 4 KAP transgenic mice and 4 littermate control mice were analyzed.

### 3.4. COLOCALIZATION ANALYSIS

Spatial colocalization between two fluorescently labeled proteins was determined by the Leica LAS AF Lite imaging software (Leica Microsystems) under the following calculations:

- Overlap coefficient:

$$r_O = \frac{\sum(R_i \; G_i)}{\sqrt{\sum R_i^2 \sum G_i^2}}$$

Where $R_i$ and $G_i$ correspond to signal intensity of pixels in red and green channels respectively (Manders et al., 1993).

- Colocalization Rate (%) = Colocalization area / area forground, and area foreground = area image – area background (Bratic et al., 2011).

Arteriolar annuli and regular adjacent arteriolar wall areas were selected using the “region of interest” tool in 8 – 10 side-arm branches of collagen IV and

laminin double immunolabeled whole mount retinas from 3 different control mice.

**C. STATISTICAL ANALYSIS**

Results are shown as the mean ± SEM. Statistical analyses were performed by paired t test when regions of interest in the same image were compared. Otherwise, as happened when comparing regions of interest from different mice, unpaired t test analysis was performed. Significance was accepted at $p \leq 0.05$.

# *RESULTS and DISCUSSION*

# A. ARTERIOLAR ANNULI IN THE MOUSE RETINA

## A.1 Localization and distribution

### A.1.1 identification of arteriolar annuli

Arteriolar annuli are evident in mouse pepsin/trypsin digested retinas stained with PAS and hematoxylin, according to the method described by Kuwabara and Cogan (1960). This result contradicts previous studies from these authors, who were not able to found these structures in the retinal vasculature of the mouse.

As previously described (Kuwabara and Cogan, 1960; Henkind and De Oliveira, 1968; Agrawal et al., 1968; Rootman, 1971), arteriolar annuli in mouse retina appeared as a collar of more intensely PAS stained material at the site of branching of retinal arterioles (Fig. 12). Retinal arterioles give rise to precapillary arterioles following two different patterns: side-arm and dichotomous branching (Anderson and McIntosh, 1967; Kuwabara and Cogan, 1960; Pannarale, 1996). The side-arm branching shows precapillary arterioles coming off from the main arteriole, usually at a right angle, with a reduction of the caliber (Fig. 12A); while dichotomous branching forms Y-shaped branches with arms of equal diameter (Fig. 12B). Arteriolar annuli occurred in the majority of side-arm branching sites of mouse retinal arterioles, but were never present at arterioles branched following a dichotomous pattern. Nor arteriolar annuli were seen at the venular side of the mouse retinal vasculature. These results are in accordance with those previously observed in the retinal

vasculature of different species, such as cat, rat, pig, dog, rabbit, goat and owl monkey (Kuwabara and Cogan, 1960; Henkind and De Oliveira, 1968; Agrawal et al., 1968; Rootman, 1971).

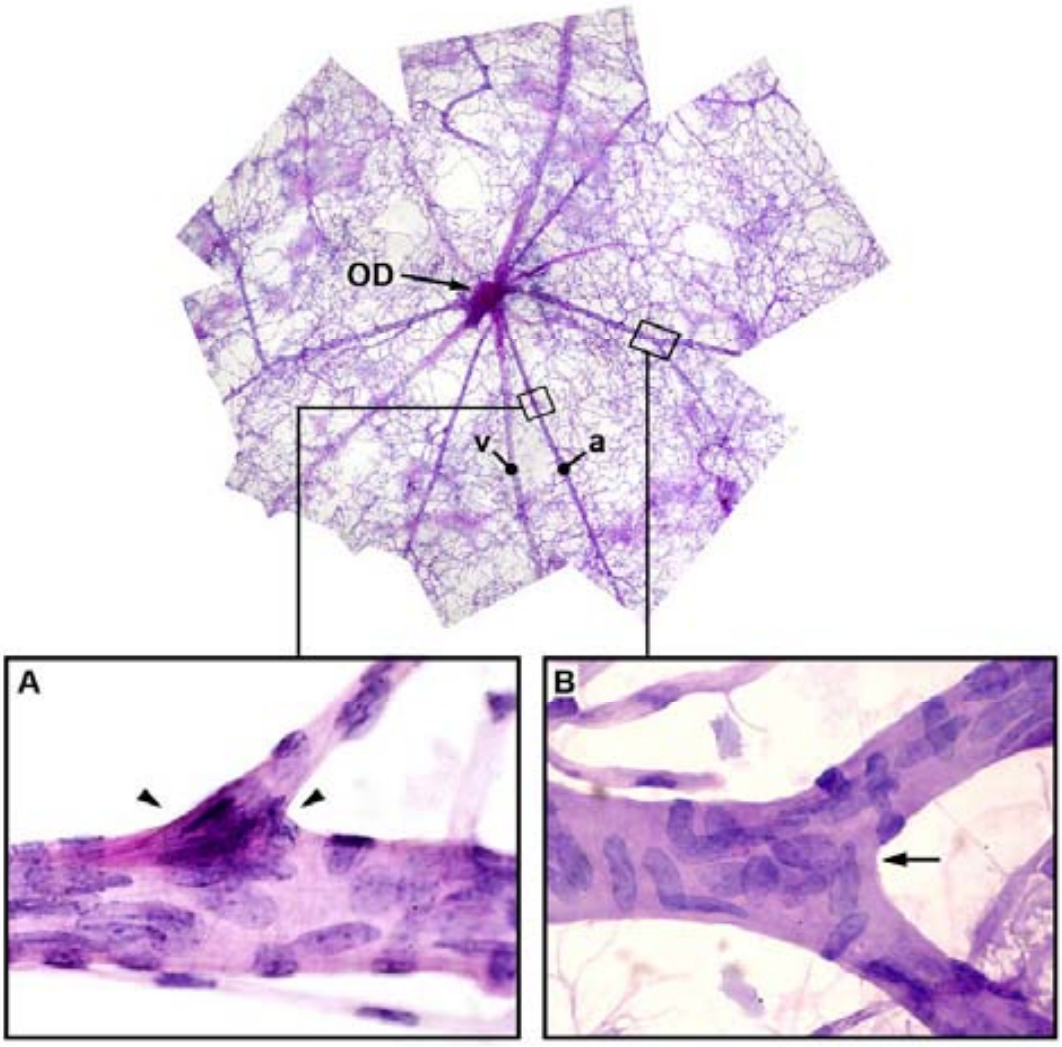


**Figure 12: Identification of arteriolar annuli in the mouse retina.** PAS stain of pepsin/trypsin digested retinas evidenced the presence of arteriolar annuli in side-arm arteriolar branches (A) but not in dichotomous branching sites (B). Nuclei counterstain: haematoxilin. Arrowhead: arteriolar annuli. OD: optic disc. a: arteriole. v: venule. Magnification: 1000x.

Arteriolar annuli found in mouse retinal arterioles showed a conical appearance with increased cellularity. Most of these cells present in the arteriolar annuli were different from those found in the neighboring vessel, since their nuclei were more intensely stained with hematoxylin (Fig. 12A). This observation supports the results reported by Henkind and De Oliveira (1968), who observed hypercellularity in arteriolar annuli of several species.

### A.1.2. Analysis of carbohydrate expression

The increased PAS stain seen at arteriolar annuli (Fig. 12) can indicate a high carbohydrate expression, since Schiff reagent specifically binds with polysaccharides including some components of the blood vessel basement membrane, glycogen, glycoproteins and mucoproteins (Presnell and Schreibman, 1997)

In order to analyze which carbohydrates are expressed in the arteriolar annuli, a study of the specific binding of a battery of eight lectins was performed (Table 1). Lectins are specific carbohydrate-binding non-immune proteins which have been widely used to detect glycoconjugates on animal tissues (Henry and DeFouw, 1995).

An increased expression of $\alpha$- and $\beta$-galactose as well as N-acetylgalactosamine carbohydrates in mouse arteriolar annuli was demonstrated by the specific increased binding of lectins from *Griffonia simplicifolia* (Fig. 13A), *Wisteria floribunda* (Fig. 13B), *Glycine max* (Fig. 13C)

and *Ricinus communis* (Fig. 13D). In contrast, N-acetylglucosamine and sialic acid carbohydrates were not expressed in arteriolar annuli, as specific binding of *Triticum vulgaris, Arachis hypogaea, Lycopersicon esculentum and Sambucus nigra* lectins was not found (Table 1).

| Acronym | carbohydrate specificty | IN Annuli | OUT Annuli |
|---|---|---|---|
| GSA-I | α-Gal | ++ | + |
| WFA | α/β-GalNac | ++ | + |
| SBA | α/β-GalNac, Gal | + | - |
| RCA-I | β-Gal, α-Gal, GalNac | ++ | + |
| WGA | GLcNac, NeuAc | - | - |
| PNA | β-Gal, GalNac | - | - |
| LEA | GLcNac | - | - |
| SNA | NeuAc (2-6), Gal | - | - |

**Table 1:** Carbohydrate expression in arteriolar annuli shown by specific lectin binding.

In the vasculature, carbohydrates are mainly found as components of cell glycocalix, a coat composed of glycoproteins, proteoglycans, sialoconjugates and glycosaminoglycans (Simionescu and Simionescu, 1986; Pournaras et al., 2008). Glycoproteins from the glycocalix contain several types of carbohydrates including those overexpressed in arteriolar annuli: galactose and N-acetylgalactosamine (Henry and DeFouw, 1995). The major functions of the glycocalix are to act as a charge-selective barrier; to attenuate the effects of bloodstream shear stress (Pournaras et al., 2008). Glycocalix is also an important determinant of other membrane properties, including cell adhesion

(Gerrity et al.,1977). Since most of the components of the glycocalix are synthetized by endothelial cells (Simionescu and Simionescu, 1986), our results in lectin binding could indicate the existence of a distinct subpopulation of endothelial cells with specific properties and functions in arteriolar annuli.

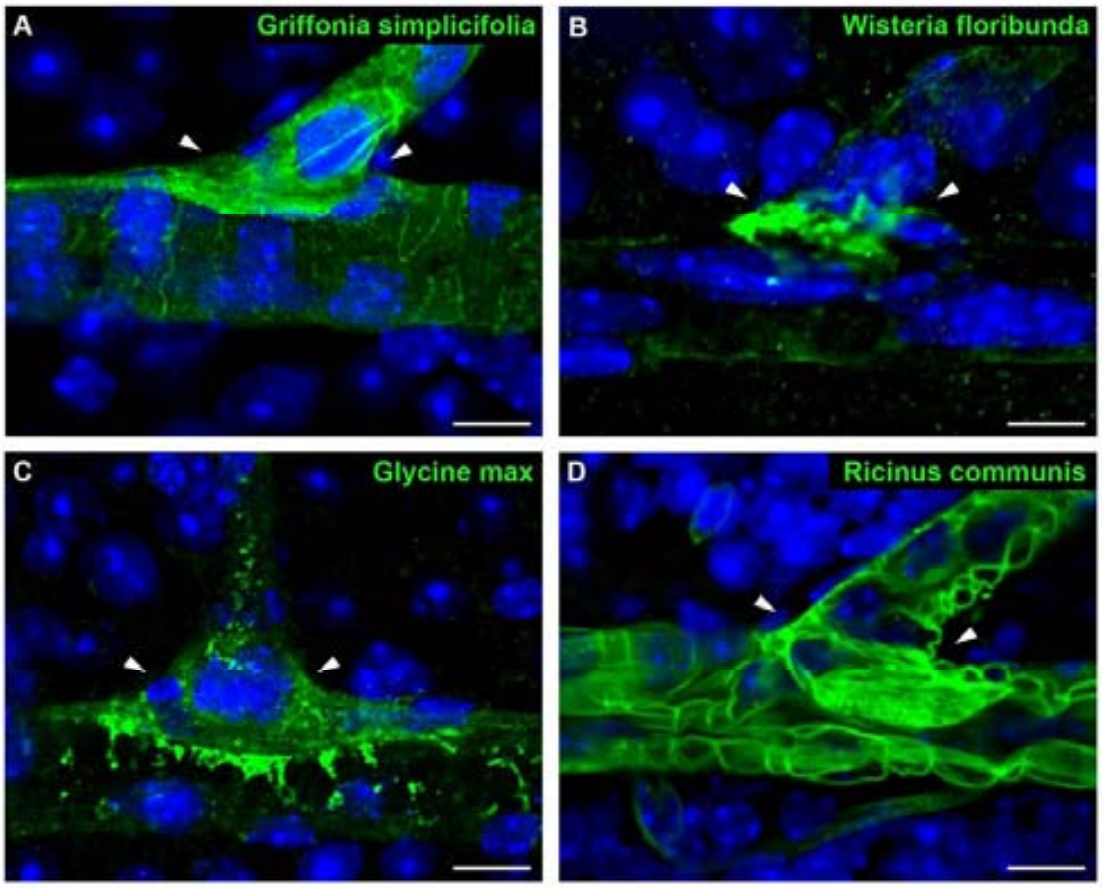


**Figure 13: Analysis of carbohydrate expression in arteriolar annuli.** Confocal images of whole mount retinas labeled with lectins from *Griffonia simplicifolia* (A), *Wisteria floribunda* (B), *Glycine max* (C) and *Ricinus communis* (D) evidenced increased expression of carbohydrates in arteriolar annuli. Nuclei counterstain: ToPro-3. Arrowhead: arteriolar annuli. Scale bars: A = 11.02 μm; B = 7.72 μm; C = 11.57 μm; D = 9.52 μm.

In addition to glycocalix, carbohydrates can also be found forming part of blood vessel basement membrane. In this regard, the specific increase of lectin binding could indicate an accumulation of basement membrane as pointed by Henkind and De Oliveira (1968). In this way, the accumulation of basement membrane may indicate a key role of arteriolar annuli in the blood flow maintenance by ensuing the luminal opening at the side-arm branching sites (Henkind and De Oliveira, 1968).

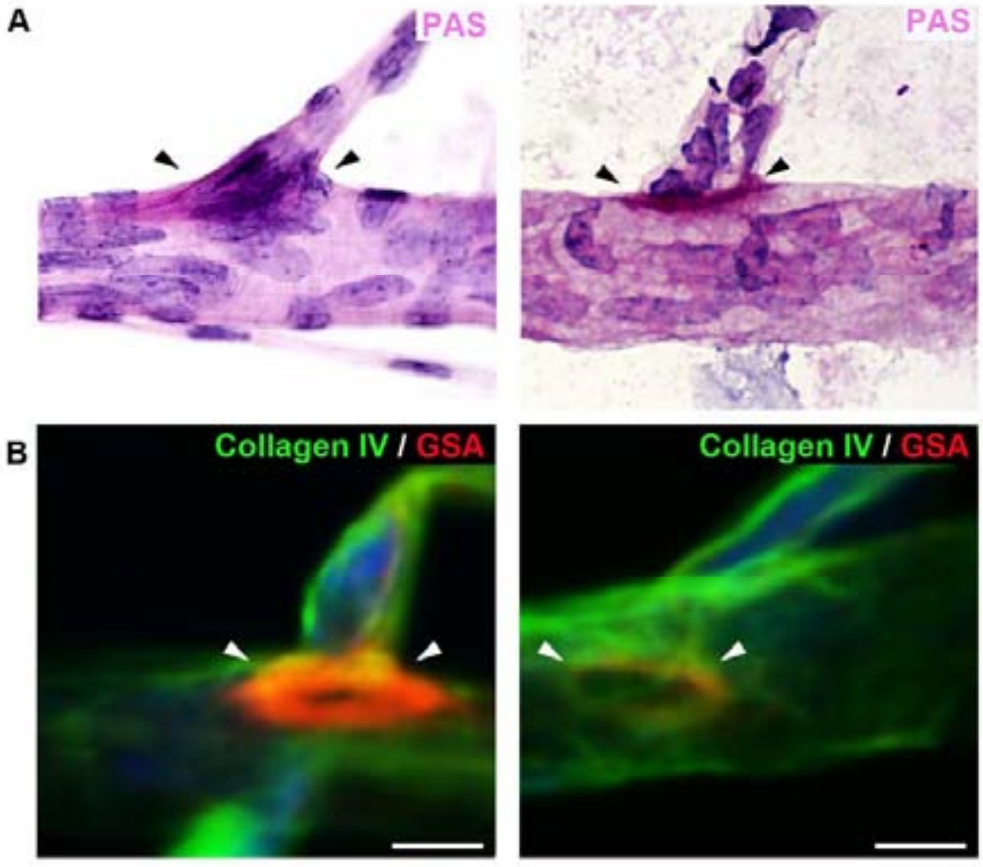


**Figure 14: Analysis of glycogen in arteriolar annuli.** Increased content of glycogen in arteriolar annuli was evidenced by the decreased PAS stain (A) and *Griffonia simplicifolia* binding (B) after salivary amylase specific digestion of glycogen in pepsin/trypsin digested retinas. (B) Retinal vasculture was evidenced by collagen IV immunohistochemistry (green). Nuclei counterstain: Hoescht. Arrowhead: arteriolar annuli. GSA: *Griffonia simplicifolia* agglutinin. Magnification A = 1000x ; Scale bars: B (left micrograph) = 4.7 μm; B (right micrograph) = 5.7 μm.

PAS stain and *Griffonia simplicifolia* lectin binding have also been used to evidence glycogen in many cell types and tissues (Hennigar et al., 1986; Hennigar et al., 1987; Presnell and Schreibman, 1997). Cytoplasmic PAS stain and lectin binding has been observed in arteriolar annuli cells (Fig. 12A and 13A), suggesting that this glucose polymer is present at branching points. In order to verify this finding, whole mount retinas were incubated with salivary amylase, an enzyme that hydrolyzes glycogen (Walker and Whelan, 1960). A decrease in PAS and *Griffonia simplicifolia* cytoplasmic was observed, indicating increased glycogen content in cells of arteriolar annuli (Fig. 14).

### A.1.3 Topography and distribution

As seen in figure 13A, the lectin *Griffonia smplicifolia* showed high sensitivity and specificity in binding arteriolar annuli, allowing an easy differentiation of this structure from the rest of the vessel. In this regard, *Griffonia smplicifolia* will be considered as a reliable specific marker of arteriolar annuli in the mouse arterial vasculature.

Double stain of *in toto* mouse retinas was performed with an antibody against collagen IV, to evidence blood vessel basement membranes, and the lectin *Griffonia smplicifolia* to specifically stain arteriolar annuli (Fig. 15A). This technique allowed a morphometrical analysis of both topography and distribution of arteriolar annuli within the mouse retina.

As expected, arteriolar annuli appeared as an increased binding of the lectin *Griffonia smplicifolia* at side-arm branching sites of retinal arterioles. These structures were never seen at arteriolar dichotomous branching sites or in the venous side of vasculature (Fig. 15A). In this regard, the 55.36 % of arteriolar branches of mouse retinal vasculature showed the presence of arteriolar annuli.

To better analyze the distribution of arteriolar annuli within retinal vasculature, two different areas were considered: the first, named central retina, occupied the area located between the optic disc and the midpoint of the radius of the retinal tissue. The peripheral retina, located between the midpoint of the radius and the outer edge of the retina, was the second area analyzed (Fig. 15B). Interestingly, the presence of arteriolar annuli varied depending on the considered area: arteriolar annuli were found in a 62.36 $\pm$ 2.831% of the arteriolar branching sites in the central retina while, in the peripheral retina, the presence of arteriolar annuli at branching sites decreased to account just for 43.51 $\pm$ 3.47%. This difference was statistically significant when compared by means of a T-Student analysis ($p = 0.0136$) (Fig. 15B). Also Henkind and De Oliveira (1968) found differences between arteriolar branches located in the central retina and those located in the periphery, since PAS stain was more intense at those side-arm branches found closer to the optic disc.

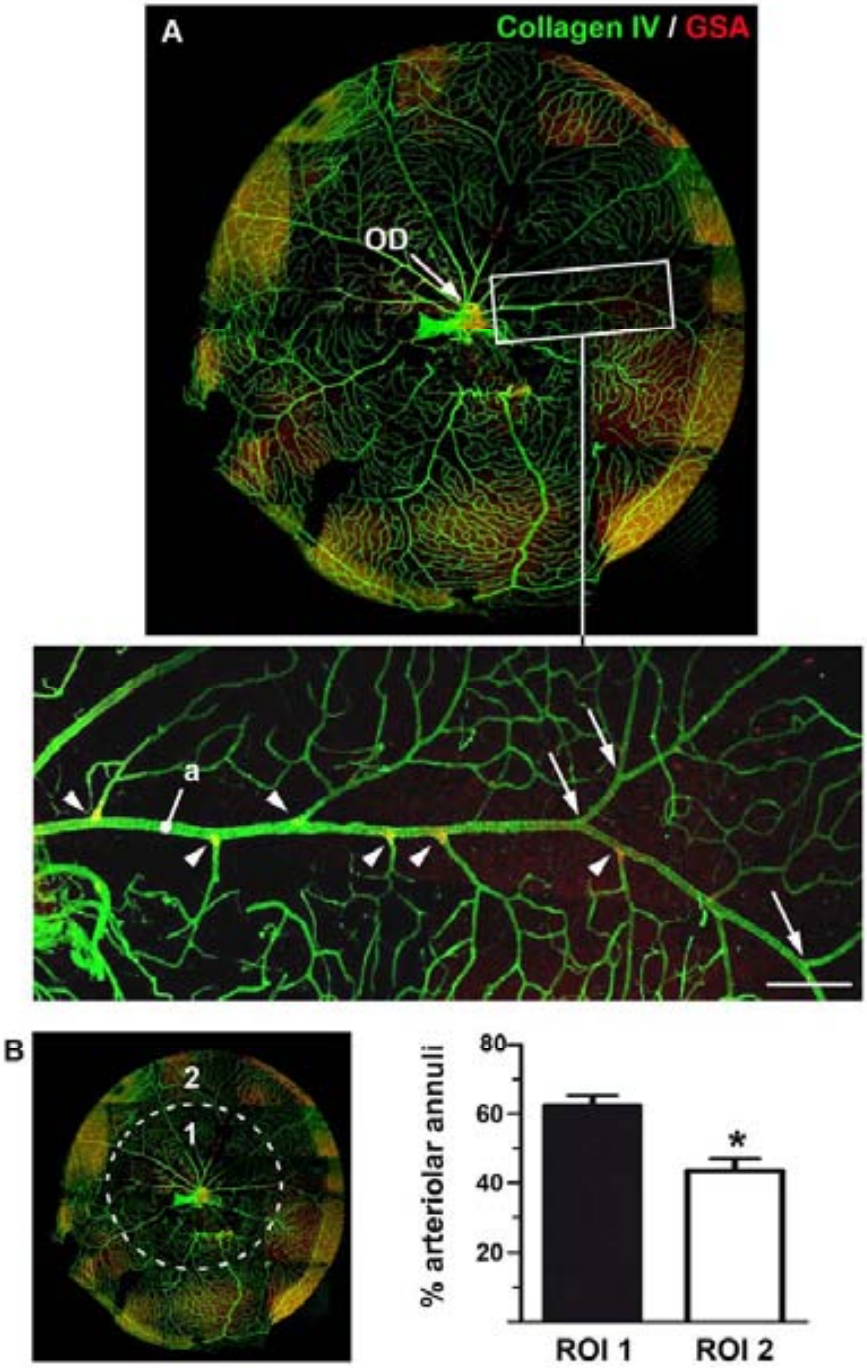


**Figure 15: Topography and distribution of arteriolar annuli.** (A) Whole mount retinas labeled with the lectin from *Griffonia simplicifolia* (red) and the antibody anti-collagen IV (green) evidenced the presence of arteriolar annuli in side-arm branches of retinal arterioles. Image of the entire retina correspond to a composition of several confocal images. (B) Arteriolar annuli occurred more frequently in the central retina. As bar-graphs show, differences of distribution were statistically significant. GSA: *Griffonia simplicifolia* agglutinin. OD: Optic disc; a: arteriole; 1: central retina; 2: peripheral retina; Arrow: dichotomous branching; Arrowhead: side-arm branching; Asterisk: $p < 0.05$. Scale bar: A = 225.70 μm.

### A.2. Characteristics of the vascular lumen

Several techniques have been used to analyze whether arteriolar annuli modified the vascular lumen of mouse retinas at branching sites. Indian ink injection (Fig. 16B), vascular corrosion casts (Fig. 16B) and fluorescein-dextran angiography (Fig. 16C) evidenced a vascular constriction at the origin of collateral arterioles arising at side-arm branching. Both vascular corrosion casts (Fig. 16C) and fluorescein angiography (Fig. 16D) also showed an oval depression in the lumen of the parent vessel surrounding the origin of the collateral arteriole. This constriction of the vascular lumen has been found in many different species and vascular beds (Moffat and Creasey, 1971; Whelan et al., 1996; May and Lütjen-Drecoll, 2002), and more specifically, has been found in retinal arteriolar side-arm branchings of cat (Risco and Nopanitaya, 1980), rat (Pannarale et al., 1996; Ninomiya and Kuno, 2001), hamster (Ninomiya and Inomata, 2005) and miniature pig (Simoens et al., 1992).

Analyses of vascular lumen of Indian ink injected retinas (Fig. 16A) and retinal fluorescein angiographies (Fig. 16C) under light microscopy and confocal laser microscopy respectively, showed a population of cells bulging into the vascular lumen. These cells presented a different appearance from the other intimal cells. Such cells, compatible with those described by Loewenstein in 1947 as cushion cells (Loewenstein, 1947), may be responsible of either vascular constriction and oval depression found in vascular casts (Fig. 16B). In this regard, many different authors have described intra-arterial cushions in

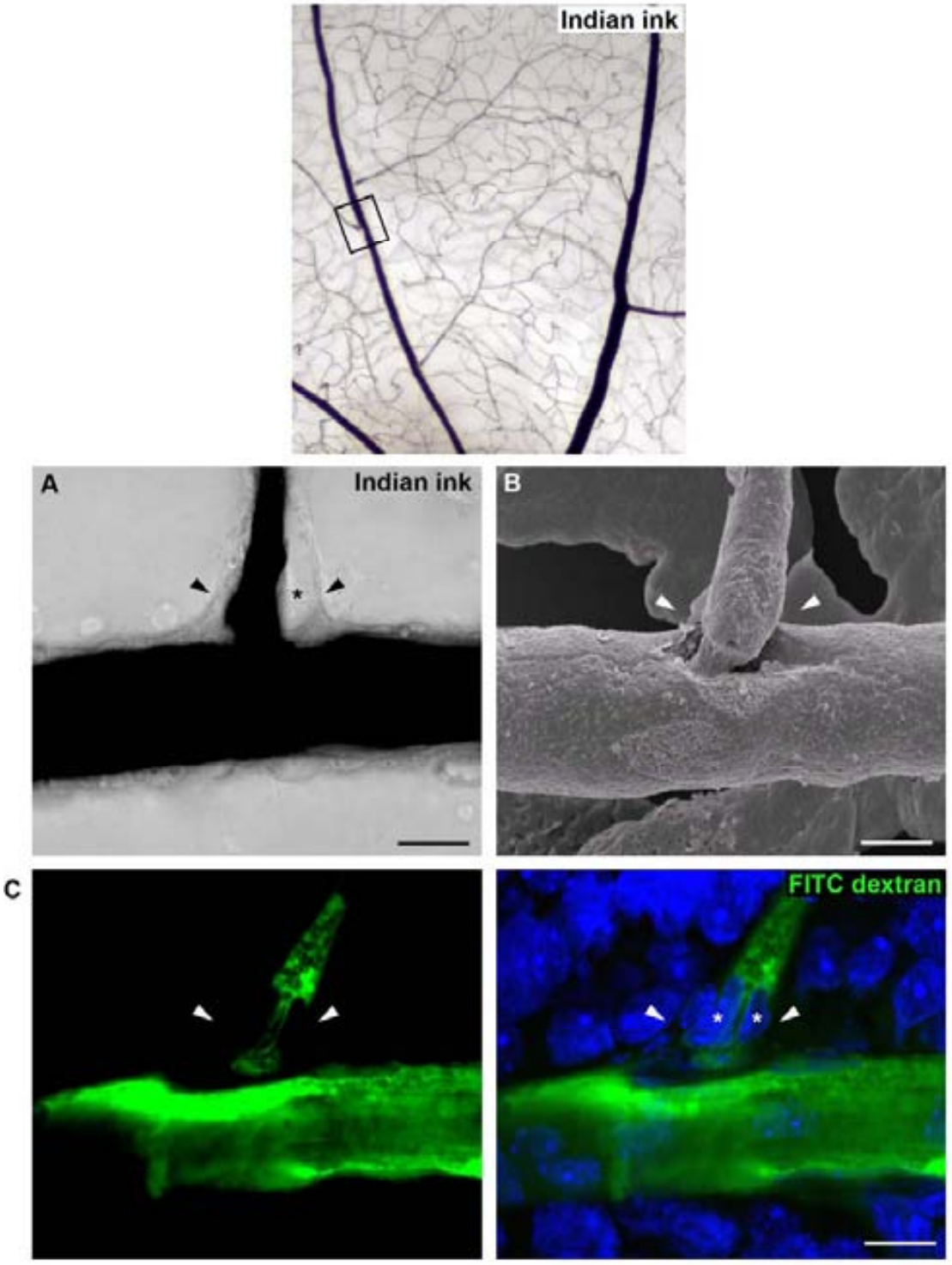


**Figure 16: Analysis of vascular lumen.** Arteriolar annuli caused a constriction of the vascular lumen, as evidenced by Indian ink angiography (A), scan laser microscopy analysis of vascular corrosion casts (B), and confocal images of fluorescein-isthyocyanate dextran angiography (C). Increased cellularity related to arteriolar annuli (asterisk) was evident on Indian ink (A) and fluorescein-isthyocyanate dextran (B) angiographies. Nuclei counterstain: ToPro3. Arrowhead: arteriolar annuli. Scale bars: A = 12.87 μm; B = 13.39 μm; C = 12.44 μm.

other body localizations (Moffat and Creasy, 1971; Matsuura and Yamamoto, 1988; Ninomiya and Kuno, 2001; Ninomiya and Inomata, 2005).

### A.3. Morphological analysis of the vascular wall

In order to analyze the fine structure of arteriolar annuli, side-arm branching sites of mouse retinal arterioles where studied under transmission electron microscopy (Fig. 17). As can be seen on the micrographs, the opening of the side-arm branching is enclosed by a ridge of tissue which projects into the lumen, this in accordance with the existence of an intra-arterial cushion in the arteriolar annuli.

Surprisingly, three distinct cellular types could be distinguished in the arteriolar annuli (Fig. 17). Only two cellular types, endothelial and smooth muscle cells, will be expected in the wall of a regular arteriole (Saint-Geniez and D'Amore, 2004; Cross and Mercer, 1993).

Endothelial cells were observed covering the luminal surface of arteriolar annuli, where they formed a continuous layer which greatly varied in thickness and shape. Vascular smooth muscle cells could also be seen in the arteriolar annuli occupying the tunica media of the vascular wall. Interestingly, a population of morphologically distinct cells was observed in the arteriolar annuli. These cells were embedded in a loose extracellular matrix located in the vascular wall between endothelial and smooth muscle cells. Because of this particular location, we have called them interstitial cells. These interstitial cells

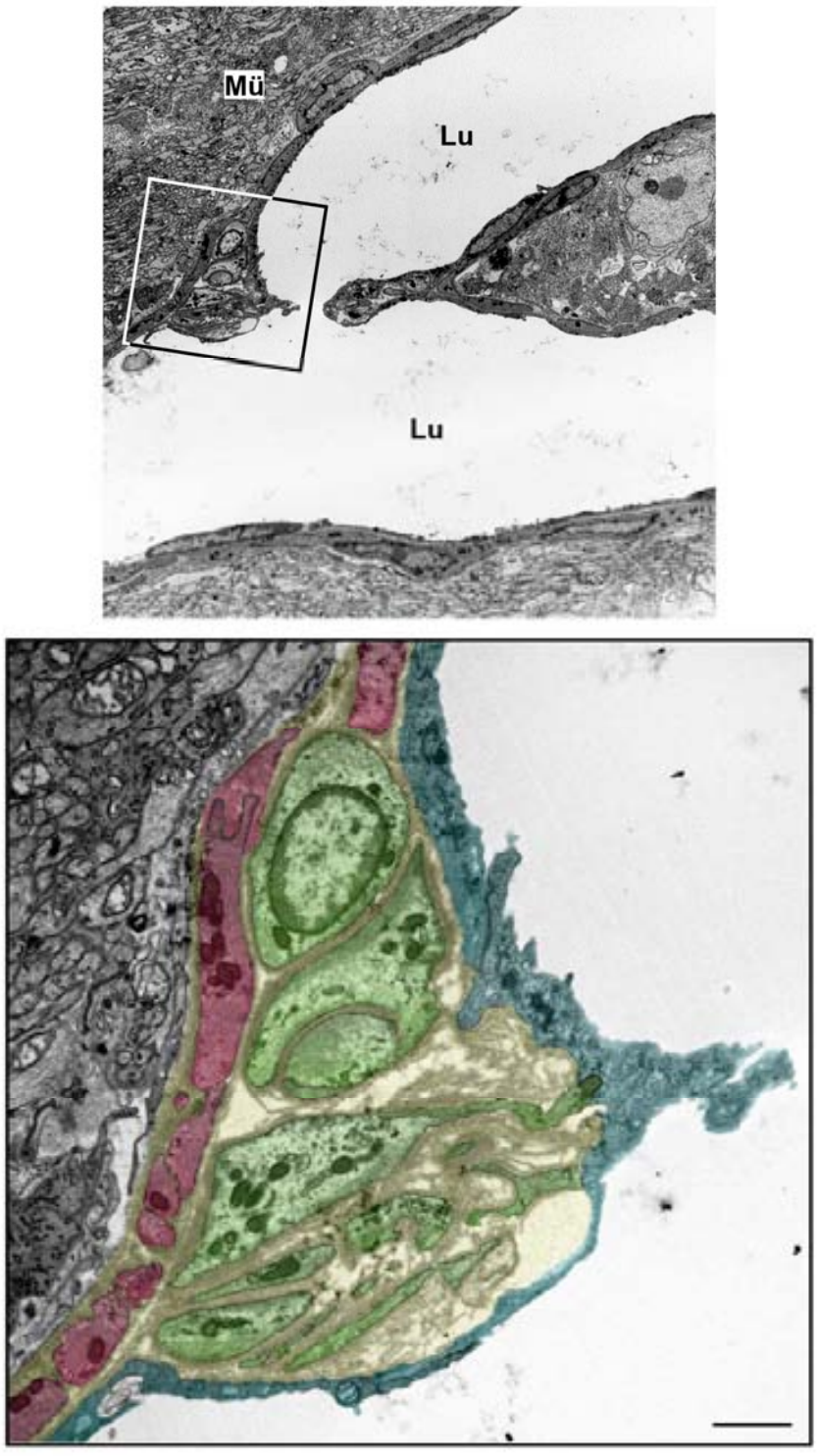


**Figure 17: Ultrastructure of arteriolar annuli.** Digitally colored transmission electron micrograph evidences the different components of arteriolar annuli vascular wall. A new cell population, named interstitial cells (green), was evident between endothelium (blue) and smooth muscle cells (red). Yellow: basement membrane. Scale Bar: 1.10 μm.

may explain the increased cellularity seen in the Indian ink and FITC-dextran angiographies (Figs. 16A and 16C) as well as in pepsin/trypsin digested retinas stained with PAS and hematoxylin (Fig. 12).

### A.3.1. Endothelial cells

In order to characterize endothelial cells in the arteriolar annuli, inmunohistochemical and histochemical techniques, as well as transmission electron microscopy were performed.

#### *A.3.1.1 Molecular characterization*

Three specific markers have been used to identify vascular endothelial cells in the mouse retina: CD34 (Fig. 18A), CD31 (Fig. 18B) and NADPH diaphorase (Fig. 18C).

CD34 is a highly glycosylated transmembrane cell surface glycoprotein expressed by endothelial cells (Siemerink et al., 2012) which has been widely used as an specific marker for monitoring such cells in mouse retinal vasculature (Mendes-Jorge et al., 2012). As expected, CD34 binding in the arteriolar annuli allowed the observation of a continuous layer of endothelial cells lining the lumen at these sites (Fig. 18A).

CD31 expression was observed on the cell surface of endothelial cells of both the main arteriole and the side-arm branch (Fig. 18B). But a very low expression of this marker was observed in the endothelial cells covering arteriolar annuli. CD31, also known as PECAM-1, is an integral membrane glycoprotein which has been shown to be involved in the processes of cell-cell adhesion such as leukocyte-endothelial adhesion (Calabrese et al., 1998). In this regard, the lack of CD31 antigen expression would possibly difficult the cellular adhesion at these sites and thus, prevent the luminal closure by the adhesion of blood cells under certain conditions.

NADPH diaphorase is an enzyme involved in NO synthesis (Funk, 1997) and reflects nitric oxide synthase (NOS) activity (Vincent and Hope, 1992; Amir et al., 1997; Hardy et al., 2000). eNOS is the enzyme that catalyzes nitric oxide (NO) formation by endothelial cells acting as a potent signaling molecule on the underlying smooth muscle cells causing vasodilatation (Haefliger et al., 1994; Shah et al., 1997; Ando et al., 2002; Pournaras et al., 2008; Chakravarty et al., 1995). As previously described (Hardy et al., 2000; Al-Shabrawey et al., 2003), NADPH diaphorase activity stains vascular endothelial cells in mouse retina (Fig. 18C). At the level of arteriolar annuli a large increase in NADPH diaphorase expression could be observed, when compared with the rest of the vessel (Fig. 18C), supporting the results reported by Funk (1997) in his studies of retinal vascularization. This result suggests an increased machinery to synthesize NO and perhaps the establishment of a localized vasodilatation at the level of the arteriolar annuli. The increased expression of NOS may be due

to the special characteristics of blood flow at the branching points, where increased shear stress (Zarins et al., 1983) could act as promoter of both NOS mRNA and protein expression (Hardy et al., 2000).

NO can also affect the vascular system through its capacity to inhibit platelet aggregation and adhesion (Hardy et al., 2000). This fact supports the low expression of CD31 observed in arterial annuli (Fig. 18B).

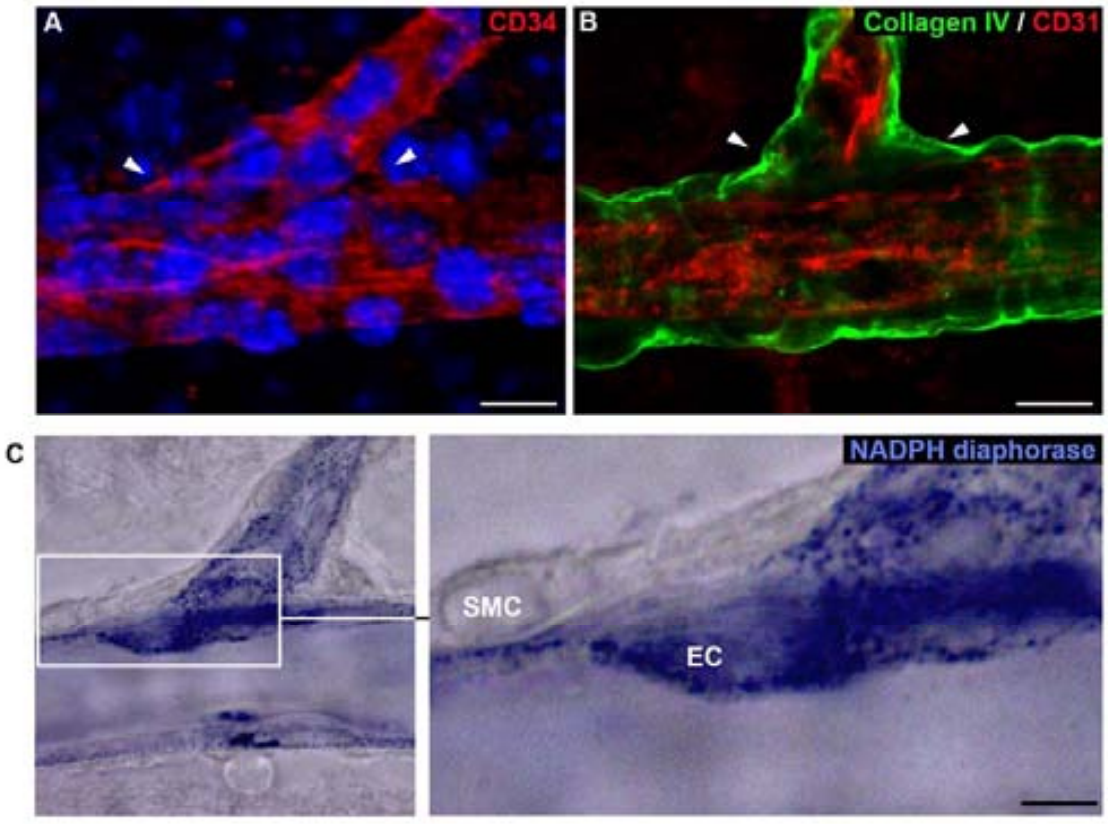


**Figure 18: Molecular analysis of annuli endothelial cells.** (A) Immunohistochemical labeling of CD34 showed the presence of endothelial cells lining the luminal surface of arteriolar annuli wall. (B) CD31 expression was diminished in annuli endothelial cells, evidenced by double immunohistochemistry against collagen IV (green) and CD31 (red). (A) and (B) correspond to maximum projections of confocal microscopy optical sections. (C) NADPH diaphorase activity was increased in arteriolar annuli. Arrowhead: Arteriolar annuli; SMC: Smooth muscle cell; EC: Endothelial cell. Scale Bars: A = 10.37 μm; B = 9.25 μm; C = 4.26 μm.

All those results indicate that endothelial cells of arteriolar annuli show important molecular characteristics which confer distinctive functional features to arteriolar annuli. This has also been recently reported by several authors who observed that Msx1 gene (Goupille et al., 2008; Lopes et al., 2012) as well as Jag1 Notch ligand (Hoffman et al., 2007) are increased in endothelial cells of retinal arteriolar branching sites. This phenomenon is known as “endothelial cell heterogeneity” (Page et al., 1992; Cines et al., 1998; Aird, 2007).

### *A.3.1.2 Transmission electron microscopy analysis*

In order to analyze whether endothelial cells of arteriolar annuli show structural heterogeneity in addition to the molecular heterogeneity demonstrated above, arteriolar annuli were studied under transmission electron microscopy.

Ultrastructural analysis of arteriolar annuli showed two subtypes of endothelial cells (Fig. 19A and 19B), subtypes I and II, morphologically distinguishable from the rest of endothelial cells existing within the vascular wall adjacent to the arteriolar annuli (Fig. 19C). Endothelial cells of retinal arterioles, as can be seen in figure 19C, presented a flat and elongated shape. Although nucleus was also elongated, endothelial cells were slightly thicker at this area protruding into the lumen. Many caveolae could be seen in both luminal and abluminal surfaces of these cells. Cytoplasm appeared thin, with few organelles.

Figure 19A shows subtype I endothelial cell population. We have classified these cells as a subset of activated endothelial cells. These cells exhibited enlarged nuclei with the chromatin condensed on the periphery. Their perinuclear space appeared swollen. These cells also presented an increased number of vesicles and caveolae, the later specially found at abluminal surface. Caveolae were first defined by Yamada in 1955 as “small pockets, vesicles, caves or recesses communicating with the outside of the cell”. Some years later, Palade described the sequence of events in the fate of caveolae (Palade and Bruns, 1968). Such sequence implies the closure of caveolae to form a vesicle which will move across the cell to fuse with the cell membrane of the opposite front. In this regard, one of the first functions attributed to caveolae was transcytosis (Frank et al., 2009). The fact that both biogenesis and maintenance of caveolae involve endoplasmic reticulum activity (Anderson, 1998) could explain the appearance of a swollen perinuclear space in the activated endothelial arteriolar annuli cells, since the outer membrane of the nuclear envelope is continuous with the endoplasmic reticulum (Cross and Mercer, 1993).

Caveolae have been found to be rich in cell-signalling molecules (Anderson, 1998). As caveolae contain many different signaling molecules in one location, these are sites where can take place signal integration (Anderson, 1998). Such molecules include $Ca^{2+}$ (Anderson, 1998) and NO (Minshall et al., 2003). In fact, caveolae have been suggested to be the sites of NO production (Anderson, 1998), since eNOS is a resident protein of these structures (Isshiki

el al., 2002). This fact, together with our results suggesting that eNOS is expressed at high amounts at the endothelial cells of arterial annuli (Fig. 7C), could indicate that this population of endothelial cells is endowed with a system of NO signaling pathway usable under demand.

Endothelial cells shown in figure 19B, the subtype II, were thicker than the rest of endothelial cells of mouse retinal arterioles. Nuclei were bilobulated as a difference of other arteriolar endothelial cells (Fig. 19C). Within their cytoplasm, those cells presented a well-developed endoplasmatic reticulum and an increased number of cytoplasmic vesicles. This endothelial cell subpopulation also exhibited a large increase in the number of mitochondria. All those features identically match all the morphological characteristics shown by endothelial cells under increased shear stress (Masuda et al., 2003). Since these cells appeared in a specific site of the branching structures exposed to a very high shear stress (Zarins et al., 1983), this increased shear stress seems to be the most plausible reason for the morphological features exhibited by this endothelial cell subpopulation. Also Porat et al. (2004) found adaptations to disturbed flow in these endothelial cells residing just downstream of the branching site, since these cells exhibited an upregulation of Tie1 promoter activity.

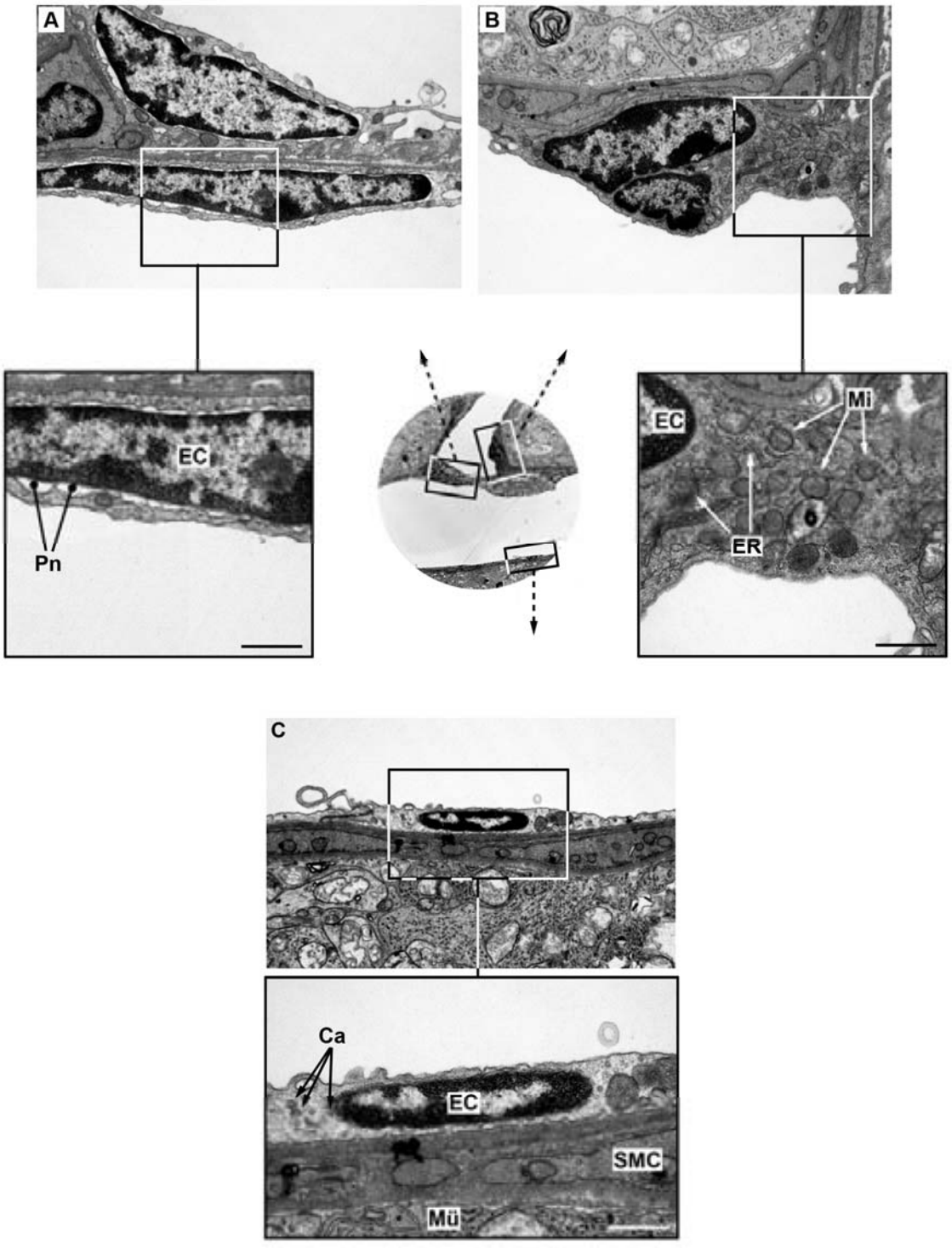


**Figure 19: Ultrastructural analysis of annuli endothelial cells.** Transmission electron microscopy analysis evidenced the presence of three morphologically distinct endothelial cell populations in arteriolar annuli: activated endothelial cells (A), shear stress-adapted endothelial cells (B), and regular retinal endothelial cells (C). Pn: Perinuclear space, Ec: Endothelial cell; Mi: Mitochondria; ER: Endoplasmic reticulum; Ca: Caveolae; SMC: Smooth muscle cell; Mü: Müller cell. Scale Bars: A = 0.6 μm; B = 0.58 μm; C = 0.53 μm.

### *A.3.1.3 Hemostatic function*

Both molecular and structural modifications shown by endothelial cells in the arterial annuli led to further analyze whether these cells also displayed distinctive functional characteristics.

Among others, endothelial cell functions include the hemostatic balance (Wu and Thiagarajan, 1996; Hoffman and Monroe, 2001). Hemostasis, the ability to prevent blood loss by promoting platelet aggregation and clot formation in a damaged vasculature (Guyton and Hall, 2006), is a common function of endothelial cells (Aird, 2007). To carry out this function, endothelial cells express both anticoagulant and procoagulant molecules. Interestingly, anticoagulant and procoagulant molecules are not equally distributed throughout the vasculature (Aird, 2007).

von Willebrand factor is a glycoprotein synthetized and released into circulation by endothelial cells (Vischer, 2006). This protein plays an essential role in hemostasis, by mediating platelet adhesion and aggregation as well as acting as a carrier for factor VIII (van Mourik et al., 2002; Vischer, 2006). In order to investigate if arteriolar annuli display a specific expression of von Willebrand factor immunohistochemistry was used. As figure 20A unequivocally shows, the expression of von Willebrand factor was increased at arteriolar side-arm branching sites when compared with the adjacent vessel wall. When the fluorescence intensity emitted was quantified by confocal laser microscopy, it was ascertained that differences in emitted fluorescence were statistically significant (87.49 $\pm$ 13.49 intensity units in arteriolar annuli VS 42.71 $\pm$ 4.34

intensity units in the adjacent vessel wall; p = 0.0195) (Fig. 20B). This result suggested a specific role in hemostatic function of endothelial cells at arteriolar annuli. Interestingly, in another branching arterial point, the origin of intercostal arteries, Senis and colleagues (1996) found groups of intensely von Willebrand stained endothelial cells, and these authors suggested shear-stress as a possible factor in the regulation of von Willebrand factor expression by endothelial cells.

Pre-pro-von Willebrand factor is synthesized at the endoplasmic reticulum and then transported to the Golgi apparatus. Once processed, leaves the trans-Golgi network and is either constitutively secreted or is stored in newly formed Weibel-Palade bodies (Michaux and Cutler, 2004). Weibel-Palade bodies are highly organised storage organelles of endothelial cells which release their content by regulated exocytosis (van Mourik, 2002; Michaux and Cutler, 2004). In this way, von Willebrand factor stored in Weibel-Palade bodies is released at sites of injury in a regulated fashion (Michaux and Cutler, 2004). Transmission electron microscopy analysis of arterial annuli showed a high presence of Weibel-Palade bodies in the cytoplasm of its endothelial cells (Fig. 20C). Thus, these results suggest that these cells release this procoagulant molecule mainly in a regulated manner.

Several studies have demonstrated the existence of both activators and inhibitors of von Willebrand factor exocytosis (reviewed in Vischer, 2006). NO has been shown to inhibit exocytosis of Weibel-Palade bodies (Santhaman et al., 2011) and von Willebrand factor secretion (Vischer, 2006). Our previous

results demonstrating an increased eNOS activity in arteriolar annuli could indicate that release of von Willebrand factor is inhibited at these sites of the

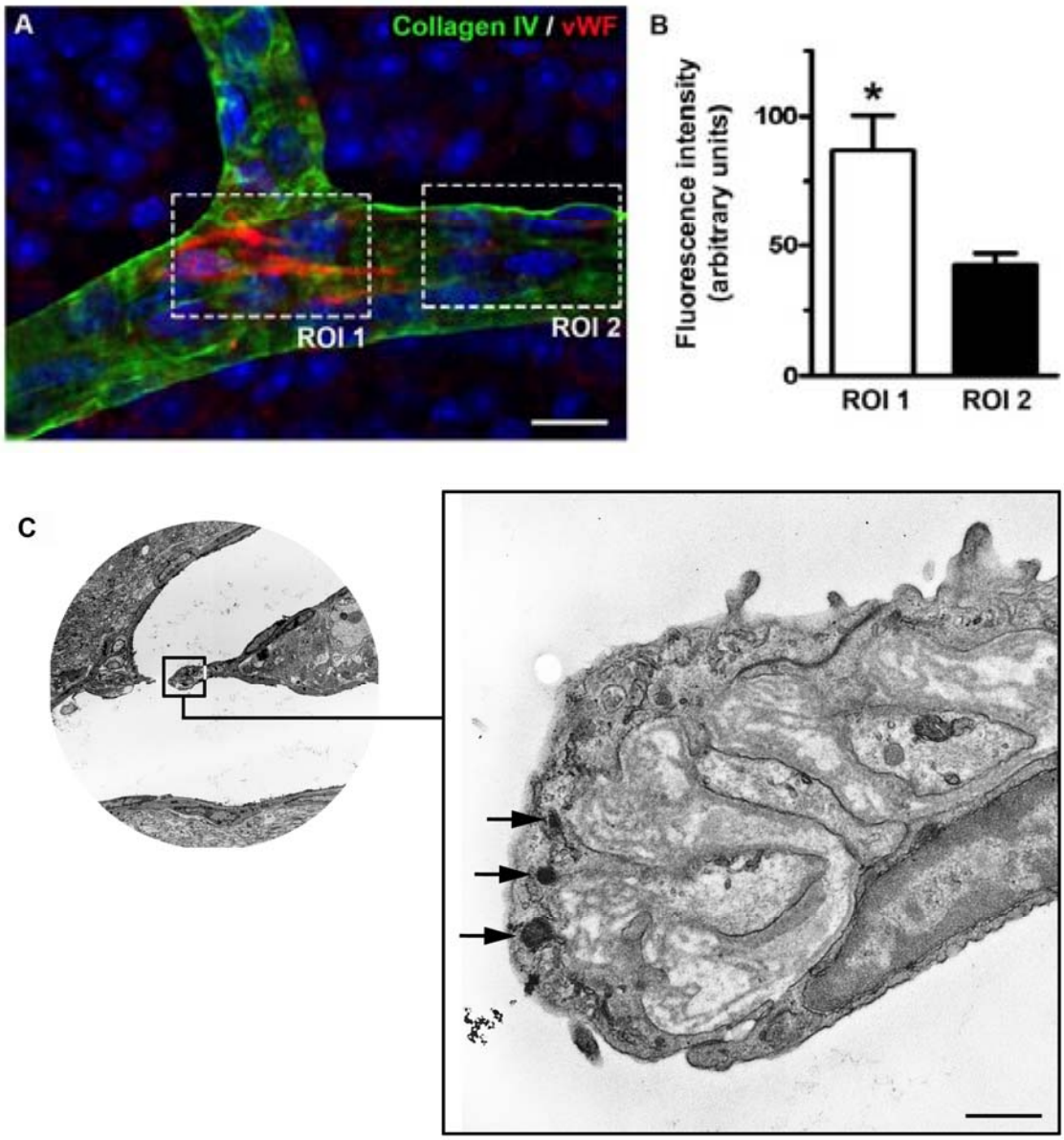


**Figure 20: Hemostatic function of annuli endothelial cells.** (A) Confocal microscopy analysis of double immunohistochemical labeling against collagen IV (green) and von Willebrand factor (red) showed increased expression of von Willebrand factor in arteriolar annuli. (B) Quantification of fluorescence intensity evidenced statistically significant differences in the expression of this protein between annuli endothelial cells and regular arteriolar endothelial cells. (C) Transmission electron microscopy evidenced the presence of Weibel-Palade bodies in annuli endothelial cells. ROI 1: Arteriolar annuli; ROI 2: Regular retinal arteriole; Arrow: Weibel-Palade bodies; Asterisk: $p < 0.05$. Scale bars: A = 13.59 μm; C = 0.54 μm.

vasculature, remaining stored in Weibel-Palade bodies. Altogether, these observations suggest that endothelial cells are able to maintain an antithrombotic milieu at arterial annuli.

#### *A.3.1.4. Blood retinal barrier function*

Another important feature of retinal endothelial cells is the presence of tight junctions, which represent the main component of the inner blood-retinal barrier (Cunha-Vaz, 1976; Pournaras et al., 2008; Kur et al 2012). Since the structure of endothelial tight junctions has been shown to vary along the vascular tree (Simionescu et al., 1975; Schneeberger and Lynch, 1984), a transmission electron microscopy analysis of arteriolar branching sites of the mouse retina was performed to study these junctional complexes in arteriolar annuli. Ultrastructural analysis allowed the observation of tight junctions between endothelial cells located at arterial annuli (Fig. 21A). Their morphology is similar to that observed outside de arterial annuli (Fig. 21A).

Occludin is one of the main integral membrane proteins of endothelial tight junctions (Gardner et al., 1999; Morcos et al., 2001) and contributes to both its formation and properties (Furuse et al., 1996; Hirase et al., 1997). Immunohistochemistry was performed on flat mounted whole retinas to analyze occludin expression at arterial annuli (Figure 21B). No differences in the distribution of occludin could be seen among endothelial cells inside and outside the arterial annuli (Fig. 21B).

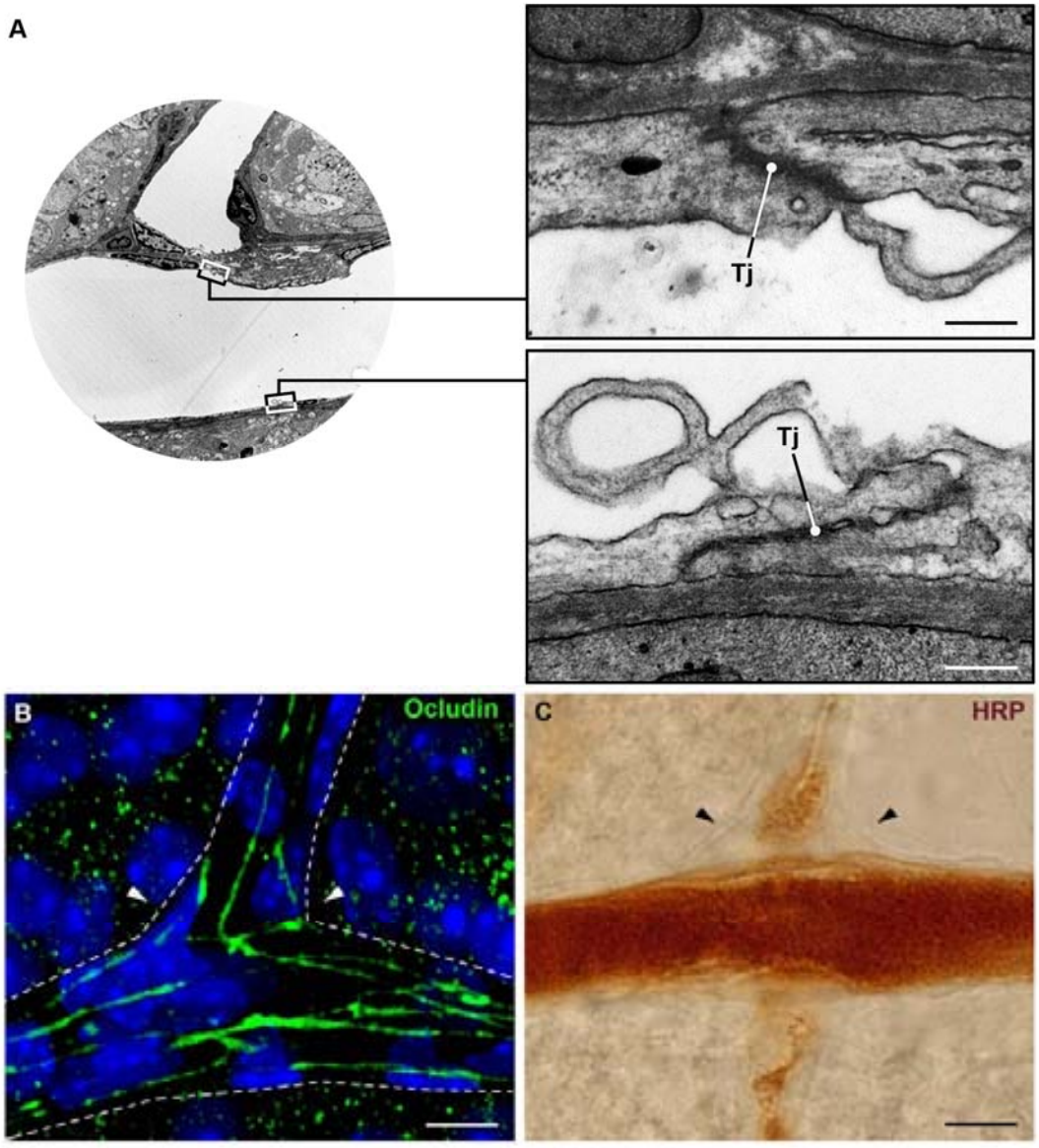


**Figure 21: Blood-retinal barrier in arteriolar annuli.** (A) Transmission electron microscopy evidenced that integrity of tight junctions was maintained in arteriolar annuli. (B) Confocal microscopy analysis of immunohistochemically labeled whole mount retinas showed no differences in the expression of occludin (green) in arteriolar annuli. (C) No leakage through blood-retinal barrier appeared after horseradish peroxidase injection, thus indicating that barrier integrity was maintained. Nuclei counterstain: ToPro3. Tj: Tight junction; HRP: Horseradish peroxidase. Scale bars: A = 0.24 μm; B = 8.96 μm; C = 8.43 μm.

The main function of blood-retinal barrier is to maintain an appropriate retinal environment by preventing the free pass of blood-borne molecules to the retinal tissue (Pournaras et al., 2008). In this regard, several molecules, including horseradish peroxidase, have been widely used as tracers to assess the blood-retinal barrier integrity (Tso and Shih, 1976), since leakage of such molecules indicates areas of increased permeability. As expected, intravascular injection of horseradish peroxidase demonstrated that leakage did not occur at arteriolar annuli (Fig. 21C). Altogether, these results demonstrated that both structural characteristics and function of blood-retinal barrier are preserved at arteriolar annuli.

Taken together, all these results suggest that endothelium of arteriolar annuli is formed by a subset of endothelial cells endowed with distinctive structural and molecular properties (Table 2) which allow them to play a key role in the maintenance and regulation of retinal blood flow. At the arteriolar annuli blood flow seems to be ensued by two mechanisms:

(**1**) Establishment of an antithrombotic milieu. Down-regulation of CD31 and NO synthesis difficult cell adhesion of platelets and leucocytes to the arteriolar annuli. Moreover, NO inhibit the release of von Willebrand factor by preventing exocytosis of Weibel-Palade bodies.

(**2**) Vasodilatation of arteriolar annuli. Increased synthesis of NO could produce vasodilation at arteriolar annuli by its paracrine action on smooth

muscle cells. The increased number of caveolae and vesicles would also suggest that endothelial cells are endowed with machinery to prompt release vasoactive molecules, as NO, in response to certain stimuli.

| Molecule | Endothelial cells IN annuli | Endothelial cells OUT annuli |
|---|---|---|
| CD 34 | + | + |
| CD31 | - | + |
| NADPH diaphorase | ++ | + |
| vWF | ++ | +/- |
| Occludin | + | + |

**Table 2:** Comparative table of molecular phenotype between endothelial cells found in the arteriolar annuli and in the adjacent vascular wall

### A.3.2 Interstitial cells

As previously described, a new cell population has been found within the vascular wall in the arteriolar annuli: the interstitial cells (Fig. 17). In order to characterize these cells, different approaches were performed.

#### *A.3.2.1 Transmission electron microscopy analysis*

Ultrastructural analysis of arteriolar annuli evidenced the presence of a cell population with irregular body shape and multiple long thin processes

located between endothelial and smooth muscle cells (Fig. 22A). As micrographs showed, these cells were surrounded by a well-developed basal membrane (Fig. 22B). The cytoplasm contained numerous large and often elongated mitochondria as well as many cisternae of smooth and rough endoplasmic reticulum (Fig. 22B). Numerous caveolae could also be found both in the nucleated region of the cell and in the processes (Fig. 22B). Nuclei often showed more than one lobe. These morphological features matched most of the ultrastructural criteria described by Huizinga et al. (1997) as “gold standard” to define the interstitial Cajal cells (ICCs) in transmission electron microscopy.

ICCs found within the arteriolar annuli showed cell contacts with smooth muscle and endothelial cells (Figs. 23A and 23B). These cell-to-cell contacts presented ultrastructual morphology compatible with gap junctions. Although many authors have demonstrated an abundant presence of cell-to-cell junctions between ICCs as well as between ICCs and smooth muscle cells (Huizinga et al., 1997; Sanders et al., 2002; Iino et al., 2008; Huang et al., 2009), there is still controversy about the nature of these junctions. To confirm the presence of gap junctions between ICCs and neighboring vascular cells, the expression of connexin 43 was analyzed by immunohistochemistry.

---

**Figure 22: Ultrastructural analysis of interstitial cells.** (A) Transmission electron microscopy evidenced the presence of a cell population with irregular body shape and multiple processes located between endothelial and smooth muscle cells: the interstitial cells (green). (B) Higher magnification showed the presence of many mitochondria, caveolae and vesicles from the endoplasmic reticulum in the cytoplasm of interstitial cells. Mi: Mitochondria; BM: Basement membrane; Ca: Caveolae. Scale bar = 142.38 nm.

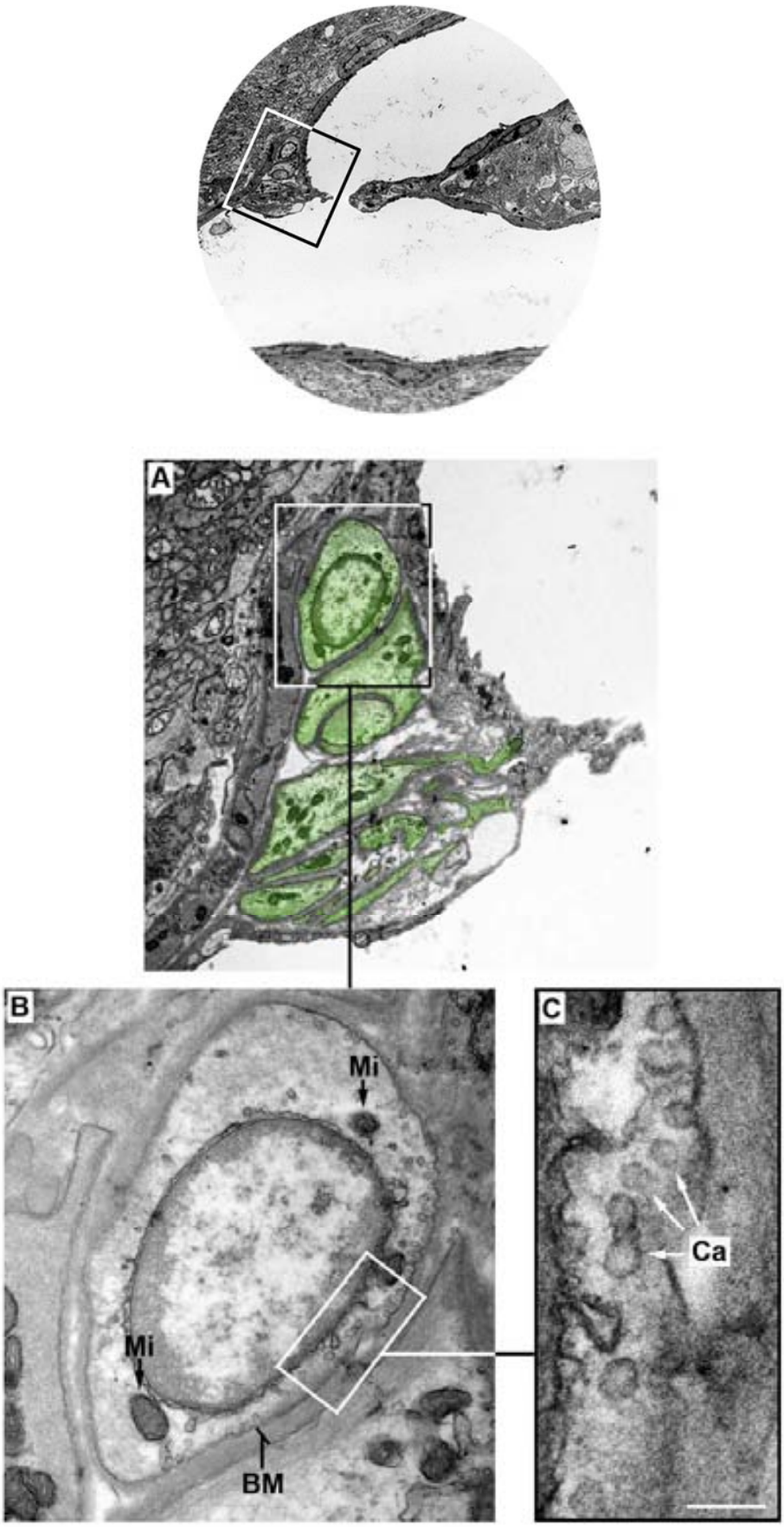
A
B
Mi
Mi
BM
C
Ca

Connexins are a family of transmembrane proteins that assemble to form gap junctions (Evans and Martin, 2002). More specifically, Connexin 43 (Cx43) is the most widely expressed and best-studied protein found in gap junction channels (Giepmans, 2003). Analysis by confocal laser microscopy of arteriolar annuli, evidenced by *Griffonia simplicifolia* lectin histochemistry, showed the expression of Cx43 within this structure (Fig. 23C), confirming that cells of arteriolar annuli communicate with each other by means of gap junctions. Although the absence of gap junctions between ICCs has been reported in other locations (reviewed in Daniel, 2004), our results are in accordance with many authors demonstrating an abundant presence of gap junctions between ICCs as well as between ICCs and smooth muscle cells (Huizinga et al., 1997; Sanders et al., 2002; Iino et al., 2008; Huang et al., 2009).

Gap junctions allow the exchange of small molecules between cells (Holder et al., 1993). Therefore, gap junctions couple metabolically and/or electrically neighboring cells (Hoffmann et al., 2003). Thus, our results suggest that ICs may play a role in the transmission of chemical and/or electrical signals to endothelial and smooth muscle cells in the arteriolar annuli.

---

**Figure 23: Analysis of cell-to-cell contacts.** Transmission electron microscopy evidenced that interstitial cells formed close contacts with smooth muscle cells (A), as well as with endothelial cells (B). The ultrastructure of these cell-to-cell junctions was compatible with gap junctions. (C) Confocal microscopy analysis of whole mount retinas labeled with *Griffonia simplicifolia* and anti-conexin 43 demonstrated the establishment of gap junctions between cells of arteriolar annuli. Nuclei caounterstain: ToPro3. EC: Endothelial cell; IC: Interstitial cell; SMC: Smooth muscle cell; Arrowhead: gap junctions. Scale bars: A = 393.6 nm; B = 433.2 nm; C = 9.38 μm.

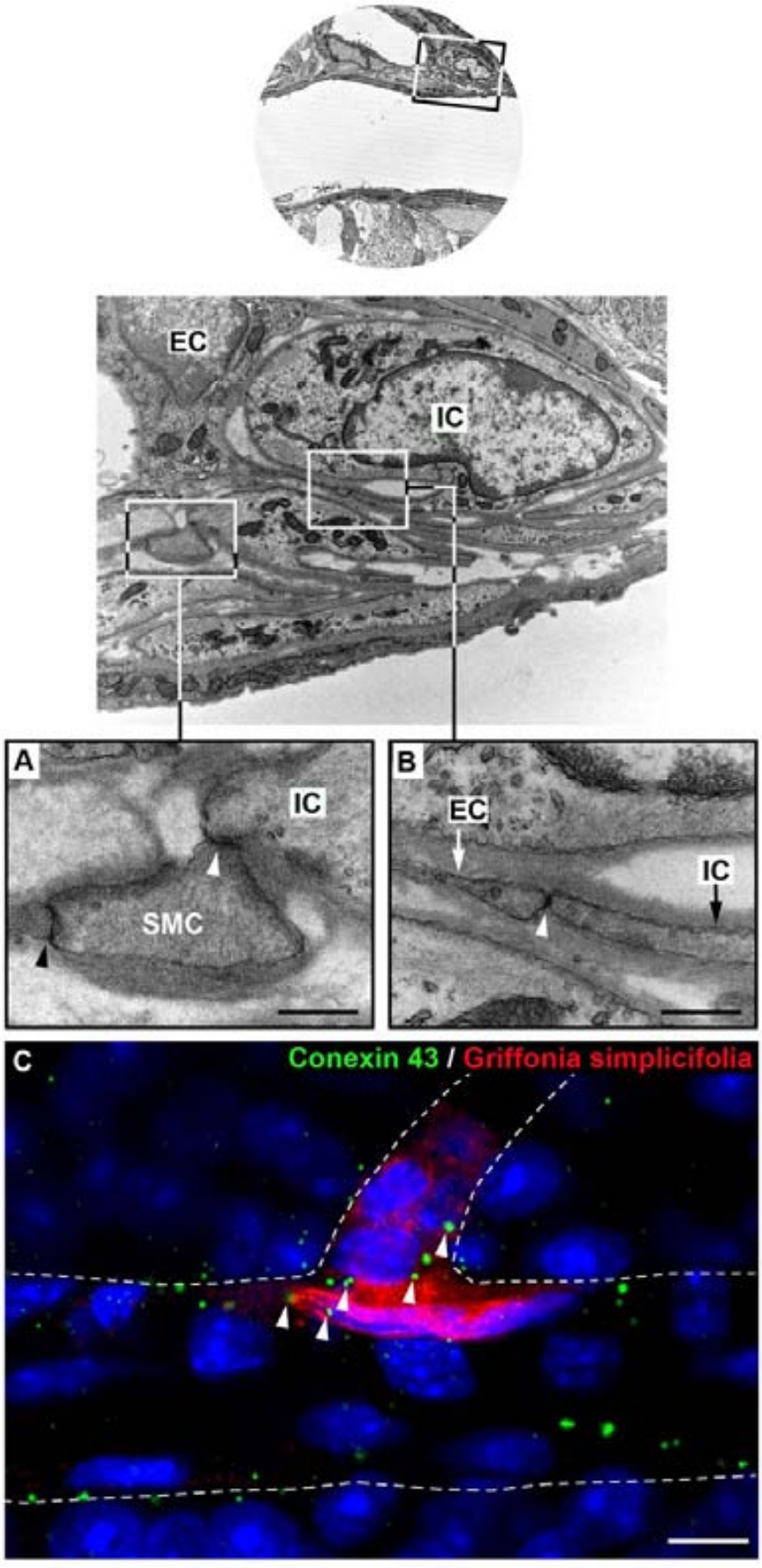
EC
IC
A
IC
SMC
B
EC
IC
C
Conexin 43 / Griffonia simplicifolia

### *A.3.2.2 Molecular characterization*

For many years ICCs have only been identified by non-specific histological stains and electron microscopy (Sanders and Ward, 2006). Recently, several specific markers have been proposed to identify these cells in the gastrointestinal tract as well as in other locations.

c-kit is a proto-oncogen that encodes a transmembrane tyrosine kinase receptor (Huizinga et al., 2000; Yu et al., 2008). Since Maeda and coworkers (1992) discovered the specific expression of c-kit by ICCs in gastrointestinal tract, this marker has become a powerful tool to identify ICCs in many locations throughout the body. For this reason, immunohistochemical analysis of c-kit expression was performed in whole mount retinas. No evidence of c-kit positive cells was observed within the arteriolar annuli (Fig. 24A). Although it is generally accepted that the discovery of c-kit positive cells is the first indication that a tissue contains ICCs, c-kit negative ICCs have been found in urethra (Sergeant et al., 2000), uterus (Duquette et al., 2005) and gastrointestinal tract (Torihashi et al., 1999). Moreover, studies about the presence of ICCs in the vasculature have shown that these cells can be both c-kit positive (Harhun et al., 2005; Fourmey et al., 2011) and negative (Pucovský et al., 2003; Bovryshev, 2005; Harhun et al., 2008) depending on arteries and/or species under study.

The protein Ano1 has been identified as a highly selective molecular marker for ICCs (Gomez-Pinilla et al., 2009). To analyze the expression of this protein in arteriolar annuli, double immunohistochemistry for Ano1 and collagen IV was performed. As figure 24B clearly shows, Ano1 was specifically

expressed at arteriolar annuli. Ano1 expression has been observed in retinal isolated smooth muscle cells (McGabon et al., 2009). However, our results are in accordance with other authors who showed that Ano1 is excusively expressed in ICCs (Gomez-Pinilla 2009; Huang et al., 2009).

Ano1 protein, also named TMEM16A, is a subunit of a calcium activated chloride channel, which have been implicated in the pacemaker activity of ICCs (Huang et al., 2009). These results have been reinforced by studies showing a reduction of gastrointestinal motility in Ano1 knockout mice (Huang et al., 2009). Since these mice displayed normally organized gastrointestinal smooth muscle layers as well as normal c-kit positive ICCs, the alterations in gastrointestinal motility were probably due to the absence of Ano1 (Huang et al., 2009).

In addition to c-kit and Ano1, the transmembrane glycoprotein CD44 can be used as a marker to identify ICCs in murine digestive tract (Yu et al., 2008). Double immunohistochemistry for CD44 and collagen IV demonstrated the presence of cells strongly positive for this protein within the wall of arteriolar annuli in the mouse retina (Fig. 24C). CD44 expression has been implicated in the adhesion of cells to the basement proteins fibronectin and laminin (Underhill, 1992).

In addition to ICs, some CD44-positive cells were found within the vascular lumen of retinal vasculature (Fig. 24C). These cells may correspond to the white blood cell lineage, since many authors have demonstrated that expression of this glycoprotein is implicated in leukocyte homing (Haynes et al., 1989; Underhill, 1992).

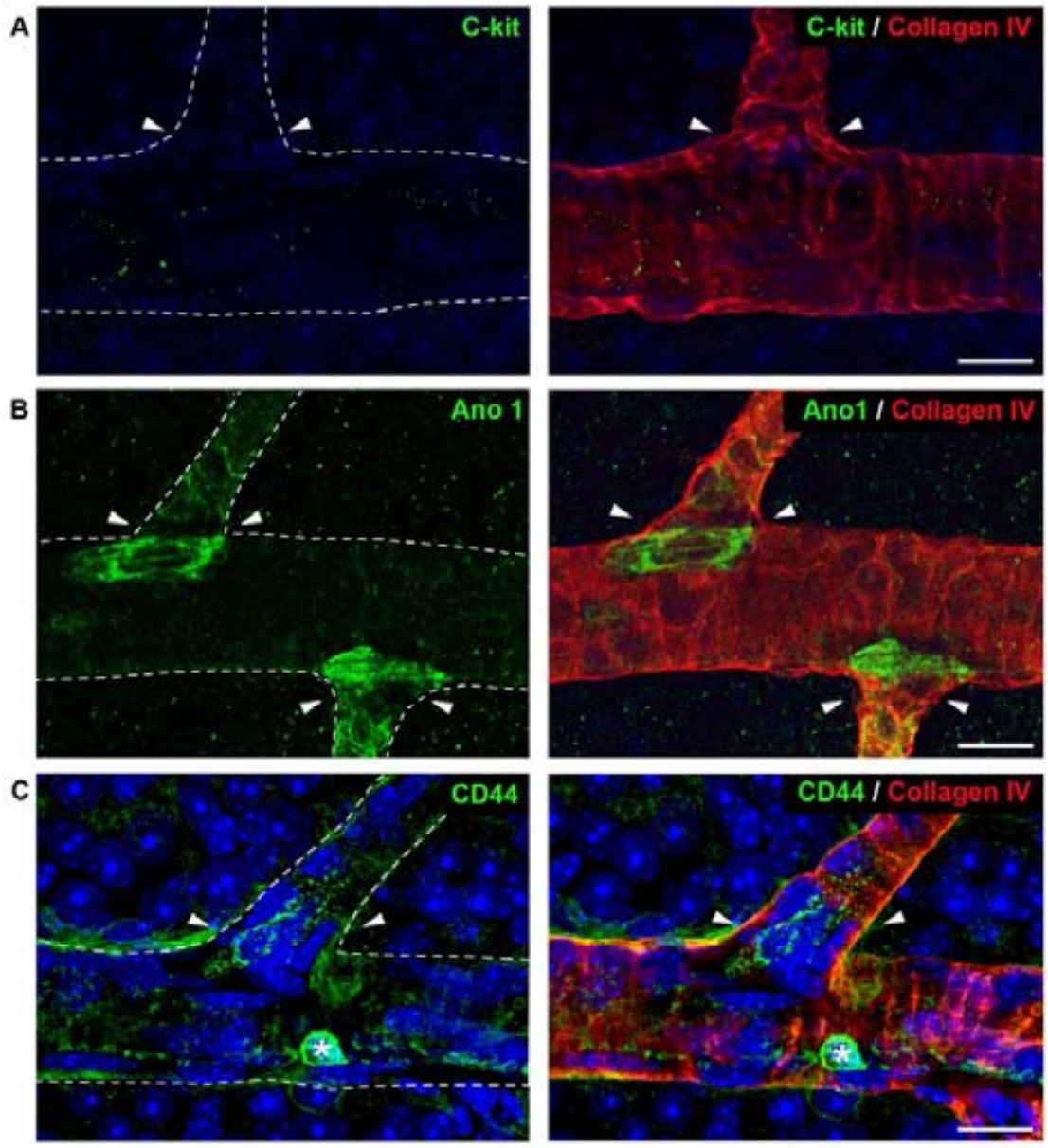


**Figure 24: Annuli interstitial cells express specific markers of interstitial Cajal cells.** (A) No evidence of c-kit positive cells was observed in arteriolar annuli during confocal microscopy analysis of whole mount retinas double immunolabelled against c-kit (green) and collagen IV (red). (B) Maximum projection of confocal microscopy optical sections of the whole arteriole width evidenced a strong and specific expression of Ano 1 in arteriolar annuli. Retinas were double immunolabeled with antobodies anti-Ano 1 (green) and anti-collagen IV (red). Annuli IC express CD44 as evidenced confocal microspcopy analysis of whole mount retinas double immunostained with antibodies against CD44 (green) and collagen IV (red). Nuclei counterstain: Hoescht. Arrowheads: arteriolar annuli. Asterisk: leukocyte. Scale bars: A = 13.55 μm; B = 15.99 μm; C = 14.36 μm.

Our study showed the expression of three unexpected molecular markers in annuli ICs: platelet derived growth factor receptor β (PDGF-Rβ), Neuron-glial 2 (NG2) chondroitin-sulphate proteoglycan and NADPH diaphorase.

PDGF-Rβ has been widely used as a surface marker to identify pericytes in many tissues, including mouse retinal vasculature (Ramos et al., 2013). Immunohistochemical analysis of retinal vasculature double stained with antibodies anti-collagen IV and anti-PDGF-Rβ showed that, in addition to pericytes, ICs of arteriolar annuli were positive to PDGF-Rβ (Fig. 25A). PDGF-Rβ is a member of the type III tyrosine-kinase receptor subfamily which includes the c-kit tyrosine-kinase receptor (Huizinga et al., 2000). In fact, PDGF and kit receptors are structurally and functionally similar (Camborová et al., 2003). In this regard, our results could suggest that PDGF-Rβ might be conducting the tyrosine-kinase activity in the c-kit negative ICs.

NG2 is a surface marker of pericytes (Bergers and Song, 2005; Ramos et al., 2013). In addition to pericytes, NG2 signal was observed in annuli ICs (Fig.25B). Retinal arterial smooth muscle cells were also positive to the NG2 immunostaining, but the expression of this marker was noticeably weaker than in ICCs (Fig. 25B). Although our results disagree with those reported by other authors indicating that ICCs are negative to NG2 (Harhun et al., 2009; Pucovský, 2010), Lopes and coworkers (2012) have also reported an increased expression of NG2 at arteriolar branching sites of mouse retina.

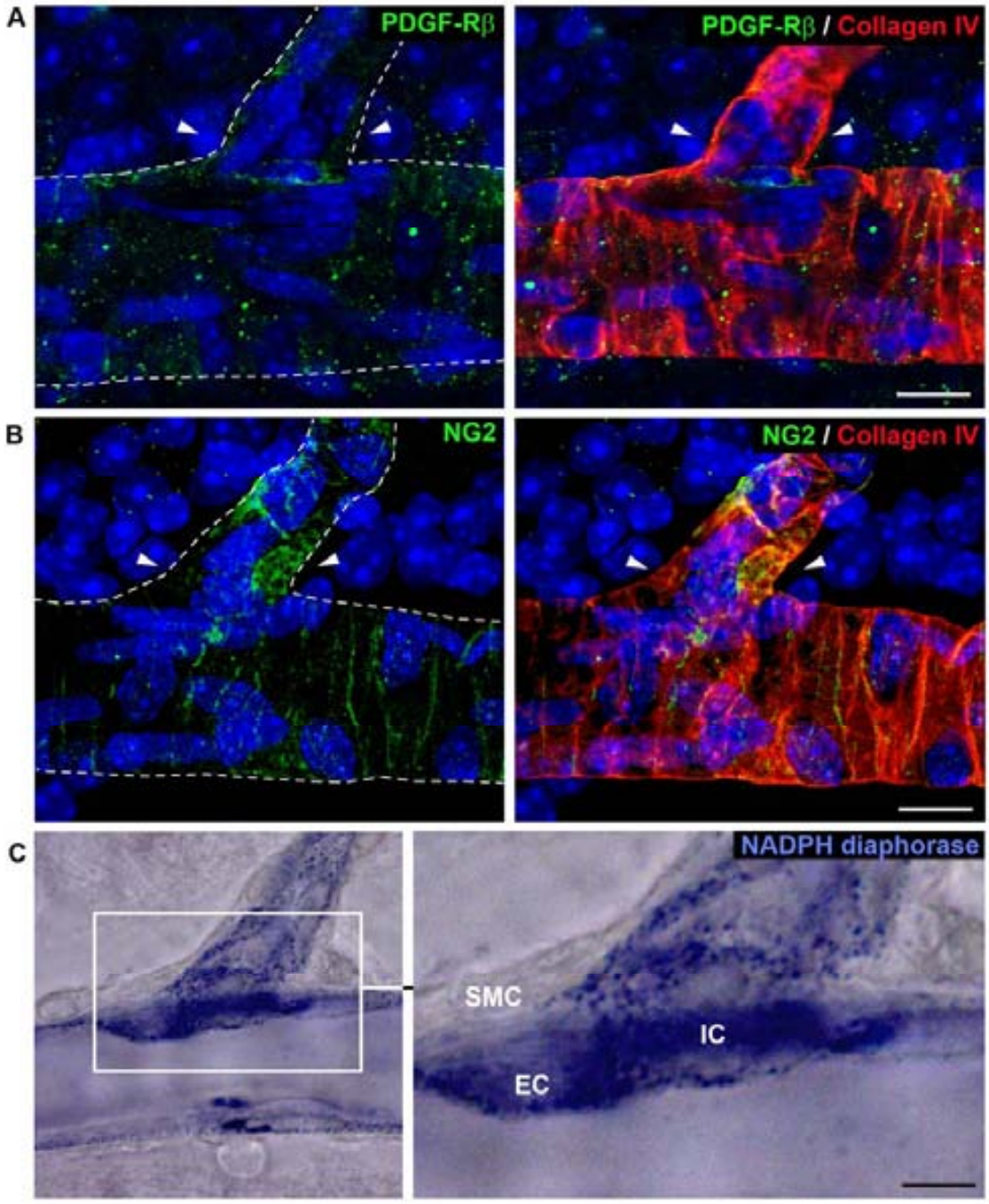


**Figure 25: Molecular characterization of annuli interstitial cells.** Whole mount retinas were immunolabeled to evidence PDGF-Rβ (A) and NG2 (B). Basement membrane was also evidenced by immunohistochemistry against collagen IV (red) (A) and (B). Confocal analysis of these retinas evidenced a high expression of both PDGF-Rβ (A) and NG2 (B) in annuli interstitial cells. (C) NADPH diaphorase expression was increased in annuli interstitial cells as well as in endothelial cells. Arrowhead: Arteriolar annuli; SMC: Smooth muscle cell; EC: Endothelial cell; IC: Interstitial cell. Scale bars: A = 12.39 μm; B = 10.58 μm; C = 6.25 μm.

NADPH diaphorase histochemistry demonstrated a highly increased expression of this enzyme in annuli ICs (Fig. 25C), together with the previously observed overexpression in annuli endothelial cells (Fig 7C). Since NADPH diaphorase is involved in NO synthesis (Funk, 1997), our results suggest an increased machinery for NO signaling in annuli ICs. This result is accordance with previous studies evidencing increased expression of proteins involved in NO signaling in ICCs of guinea pig gastrointestinal tract (Iino et al., 2008).

### *A.3.2.3 Analysis of cytoskeleton*

Cytoskeleton is a complex network that plays many important functions in the cell, including the maintenance of shape and internal organization, the intracellular transport, intracellular responses and modulation of anchoring system to basement membranes (Kivelä and Uusitalo, 1998). Cytoskeleton is formed different filamentous proteins that are classified, according to size, into three groups: actin filaments, intermediate filaments and microtubules (Fuchs and Cleveland, 1998; Alberts et al., 2002). Cytoskeletal filaments are expressed in a cell and tissue specific manner. Thus, these differences are related to specific cell functions (Kivelä and Uusitalo, 1998).

Several authors have reported distinctive features for actin and intermediate filaments in the ICCs (Pukovský et al., 2007; Popescu et al., 2009). To analyze the expression of filaments of annuli ICs different approaches have been used.

*A.3.2.3.1 Actin filaments*

Actin can be found as monomeric globules (G-actin) or forming polymeric filaments (F-actin). Two types of filaments have been described: microfilaments, and thin filaments, which are one of the main components of contractile muscular apparatus (Bois, 1973).

Confocal microscopy imaging of whole mount retinas labeled with phalloidin, a toxin that specifically binds F-actin, showed a differential distribution of these filaments between ICs and smooth muscle cells in arteriolar annuli (Fig. 26A). In ICs F-actin appeared organized into stress fibers running in various directions. In contrast, in smooth muscle cells F-actin filaments appeared organized into thin filaments. These filaments occupied the whole cytoplasm. It was not possible to distinguish the individual fibers, leaving free space only for nucleus (Fig. 26A). F-actin filaments in ICs appeared located mainly in the periphery of the cell body as well as in the processes, appearing many gaps between the groups of fibers. (Fig. 26A). These results completely match the observations of Harhun and coworkers (2005) in their studies on arterial ICCs.

Six different actin isoforms have been described in mammals. The expression of actin isoforms has been found to be different depending on the cell type. $\alpha$-actins and some $\gamma$-actin are expressed in skeletal, cardiac and smooth muscle cells, including vascular smooth cells. In contrast, $\beta$-actin and

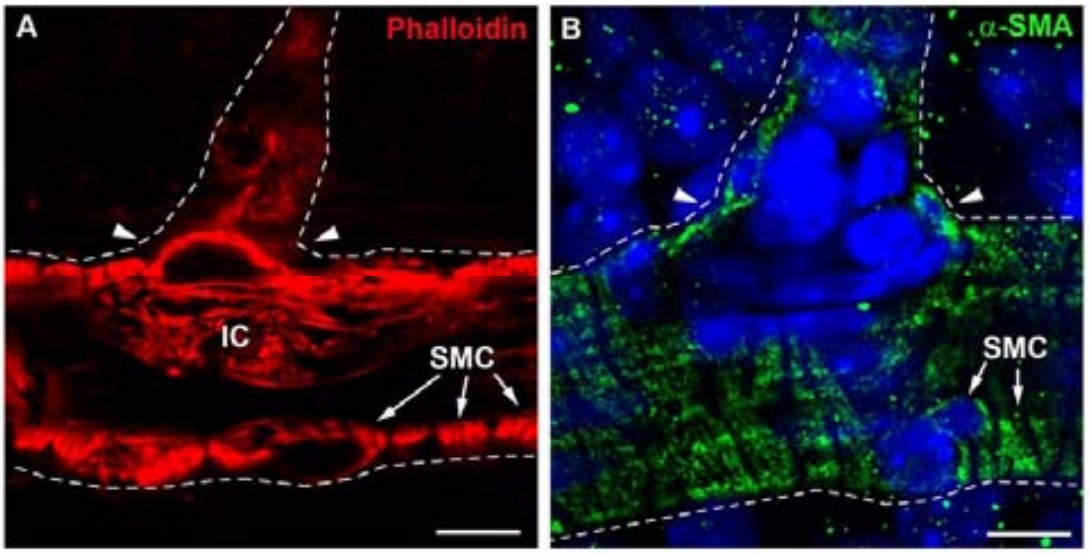


**Figure 26: Analysis of actin filaments in annuli interstitial cells.** (A) Phalloidin histochemistry was performed to analyze the expression and distribution of F-actin. F-actin appeared distinctly distributed in interstitial cells with respect to smooth muscle cells. (B) α-smooth muscle actin (SMA) appeared strongly expressed in vascular smooth muscle cells but not in annuli interstitial cells, as evidenced by immunohistochemistry. (A) and (B) correspond to confocal microscopy images of whole mount retinas. Arrowhead: Arteriolar annuli; IC: Interstitial cell; SMC: Smooth muscle cell. Scale bars: A = 7.92 μm; B = 5.78 μm.

γ1-actin are found in most muscle and non-muscle cells (Allen et al., 1996; Kivelä and Uusitalo, 1998).

Several studies have reported differences in actin isoforms between ICCs and smooth muscle cells in vasculature (Harhun et al., 2005 and 2009; Pucovský et al., 2007). ICCs do not show α-actin in contraposition with its higher expression found in smooth muscle cells (Ciontea et al., 2005). As expected annuli ICs do not show α-actin staining (Fig. 26B).

ICCs show higher expression of β-actin (Harhun et al., 2009). To further analyze the expression of β-actin in the arteriolar annuli, the β-actin/EGFP transgenic mouse was used.

In 1997, Okabe and coworkers generated a transgenic mouse expressing enhanced green fluourescent protein (EGFP) under the control of the chicken β-actin promoter as a source of green fluorescent cells.

Haematoxilin/eosin stained sections of paraffin embedded retinas from β-actin/EGFP mice did not show any morphological alteration, thus suggesting that retinal architecture is maintained in these mice although the EGFP transgene expression (Fig. 27A).

Despite data of Okabe and coworkers (1997), who reported that all cells except hair and eritrocytes expressed EGFP, green fluorescence was not homogeneously distributed through all retinal layers (Fig. 27B). The analysis under scan laser confocal microscopy showed an increased fluorescence in retinal blood vessels as well as in the inner limiting membrane and in the outer plexiform layer (Fig. 27B). An intense fluorescence emission was also observed in cytoplasm and inner segments of photoreceptors (Fig. 27B). Since EGFP fluorescence intensity is a quantitative reporter of differences in the tagged-gene expression (Soboleski et al., 2005), our results suggest that β-actin is not homogenously expressed by retinal cells.

To analyze the EGFP fluorescence in retinal blood vessels, whole mount retinas were cytochemically stained with phalloidin (Fig. 27C). EGFP fluorescence was not homogeneous along the vascular wall. Interestingly, two distinct cell types could be easily differentiated in the wall of retinal arterioles due to its brighter green fluorescence. The first cell type corresponded to elongated interstitial cells with a thin cell body and long cytoplasmic processes

running along the vessel axis (Fig. 27C). The second cell type showed a smooth muscle-like morphology with spindle-shaped body placed perpendicularly to vessel axis (Fig. 27C).

Smooth muscle cells change phenotype from an undifferentiated or synthetic phenotype to a mature contractile phenotype (Worth et al., 2001). In this regard, protein expression in these cells varies between synthetic and mature smooth muscle cells. Mature smooth muscle cells express contractile proteins, such as $\alpha$-SMA, smooth muscle-myosin heavy chain (SM-MHC) and calponin. In contrast, synthetic smooth muscle cells show an increased expression of cytoskeletal proteins, like $\beta$-actin, with a concomitant decrease in the expression of contractile proteins (Worth et al., 2001). Thus, our results suggest the presence of synthetic smooth muscle cells in mouse retinal arterioles. Synthetic smooth muscle cells have an increased capacity for motility, protein synthesis and proliferation (Worth et al., 2001).

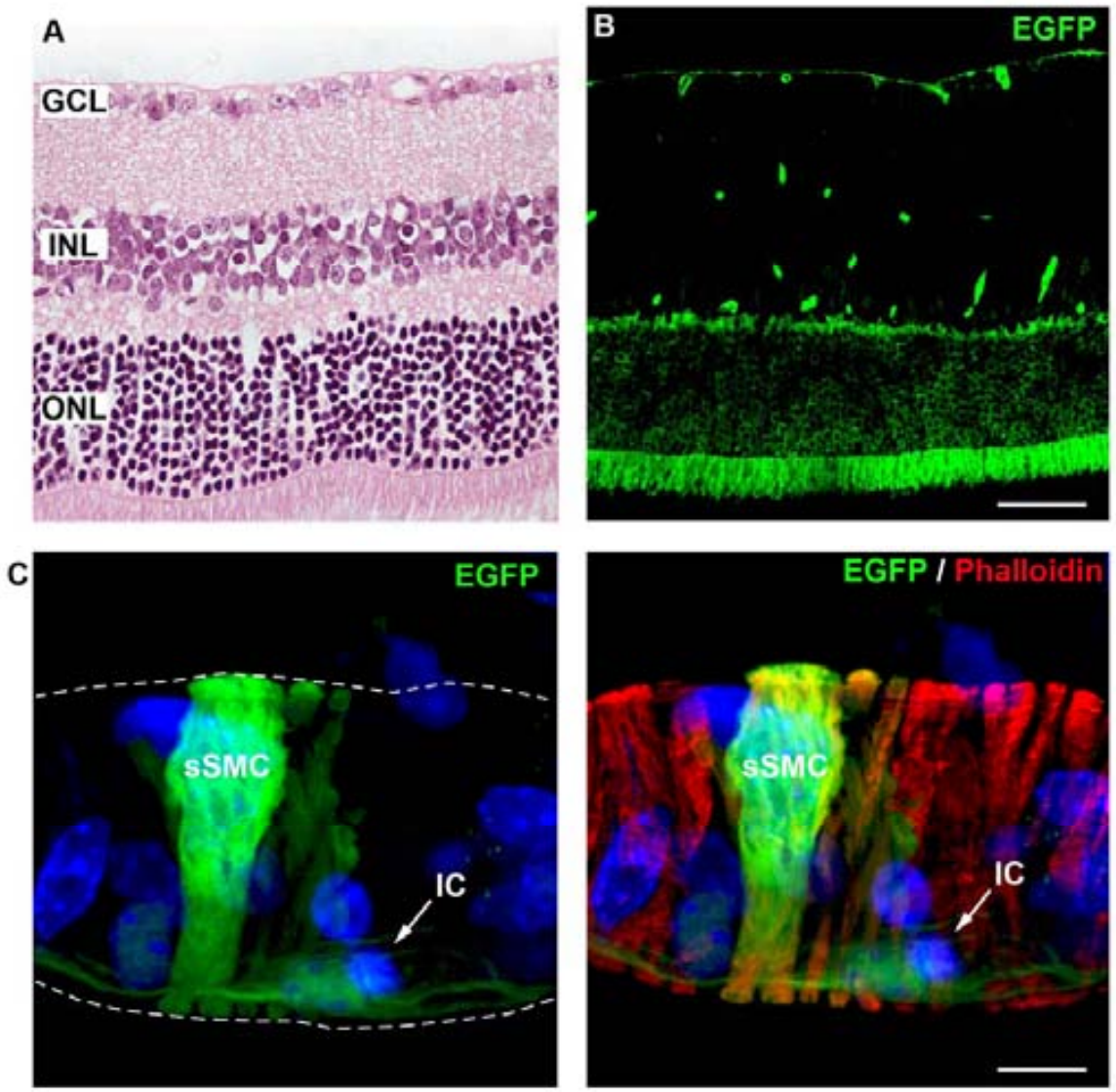


**Figure 27: Analysis of retina vasculature in β-actin EGFP mice.** (A) hematoxilin/eosin stained paraffin sections evidenced that retinal architecture was maintained in transgenic mice. (B) Confocal microscopy analysis of β-actin EGFP mice retinas evidenced a strong fluorescent emission in blood vessels as well as in the cytoplasm and the inner segments of photoreceptors. (C) Whole mount retinas from transgenic mice were labelled with phalloidin and analyzed under confocal microscopy. Two highly green fluorescent cell populations were observed within the vascular wall: interstitial cells and synthetic smooth muscle cells. GCL: Ganglion cell layer; INL: Inner nuclear layer; ONL: Outer nuclear layer; EGFP: Enhanced green fluorescent protein; sSMC: Synthetic smooth muscle cell; IC: Interstitial cell. A magnification: 400x; Scale bars: B = 59.3 μm; C = 8.60 μm.

The study of arteriolar annuli in phalloidin stained whole mount retinas from β-actin/EGFP mice evidenced the presence of strongly green fluorescence cells (Fig. 28). EGFP-positive cells also showed very low expression of f-actin, as evidenced by phalloidin stain. This result reinforce the presence of ICCs in arteriolar annuli, since this pattern of actin proteins expression match that previously described for ICCs found in other blood vessels (Harhun et al., 2005; Harhun et al., 2009).

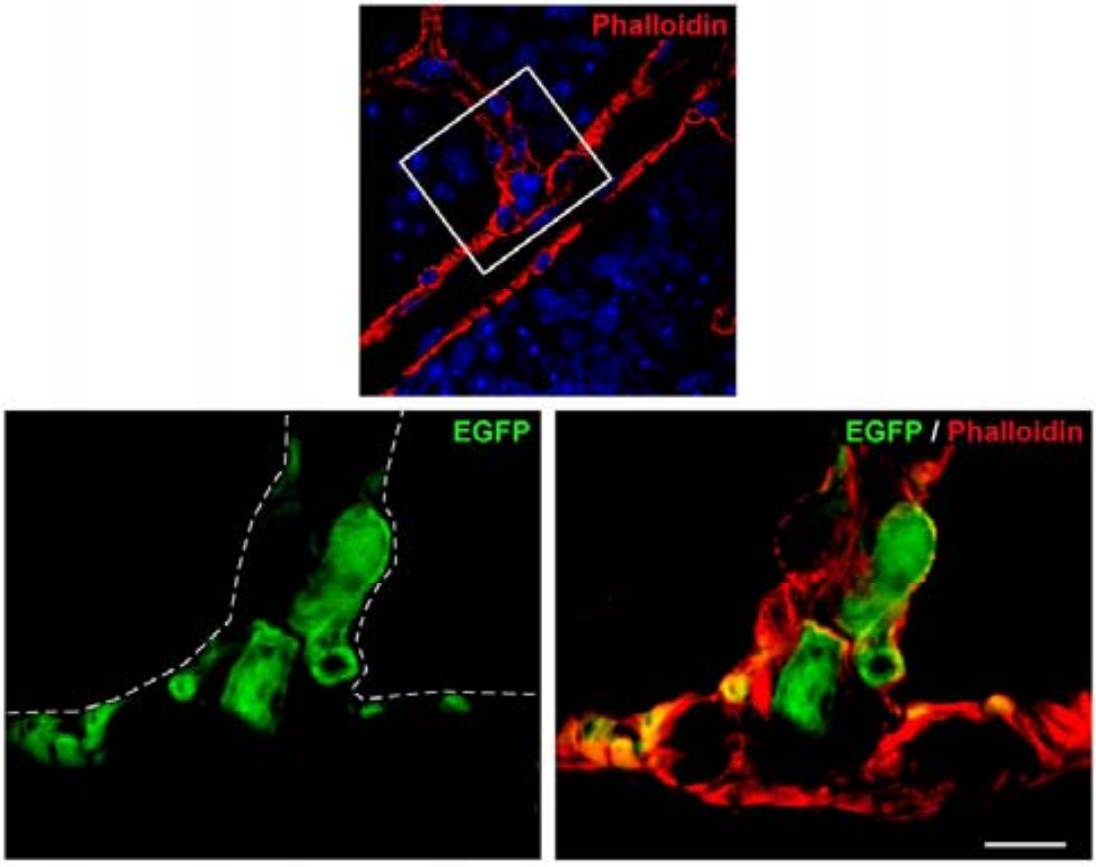


**Figure 28: Analysis of β-actin expression in annuli interstitial cells.** Retinas from β-actin EGFP transgenic mice were labelled with phalloidin and studied under confocal microscopy. As micrographs show, annuli interstitial cells were characterized by high expression of β-actin (green), whereas F-actin (red) appeared restricted to the periphery. EGFP: Enhanced green fluorescent protein. Scale bar: 6.75 μm.

Actin specific expression pattern observed in annuli ICs, showing up-regulated β-actin (Fig.28) together with down-regulated α-actin (Fig. 26B), indicates a lack of contractility of these cells. This result is in accordance with previous studies on isolated vascular ICCs demonstrating that this cell population does not contract in response to the administration of several vasoactive drugs (Povstyan et al., 2003).

*A.3.2.3.2 Intermediate filaments*

At least 65 different proteins have been reported to belong to the superfamily of intermediate filaments (Herrmann and Aebi, 2004). These proteins assemble into approximately 10nm wide filaments and provide a flexible scaffold to the cell in order to give resistance against to externally applied forces (Fuchs and Cleveland, 1998).

One ultrastructural criterion for the identification of ICCs is the presence of bundles of intermediate filaments (Popescu et al., 2005). As expected, transmission electron microscopy analysis of arteriolar annuli allowed the observation of intermediate filaments in the cytoplasm of annuli ICs (Fig. 29).

In order to study molecularly the intermediate filaments of ICs, the expression of four different proteins has been analyzed.

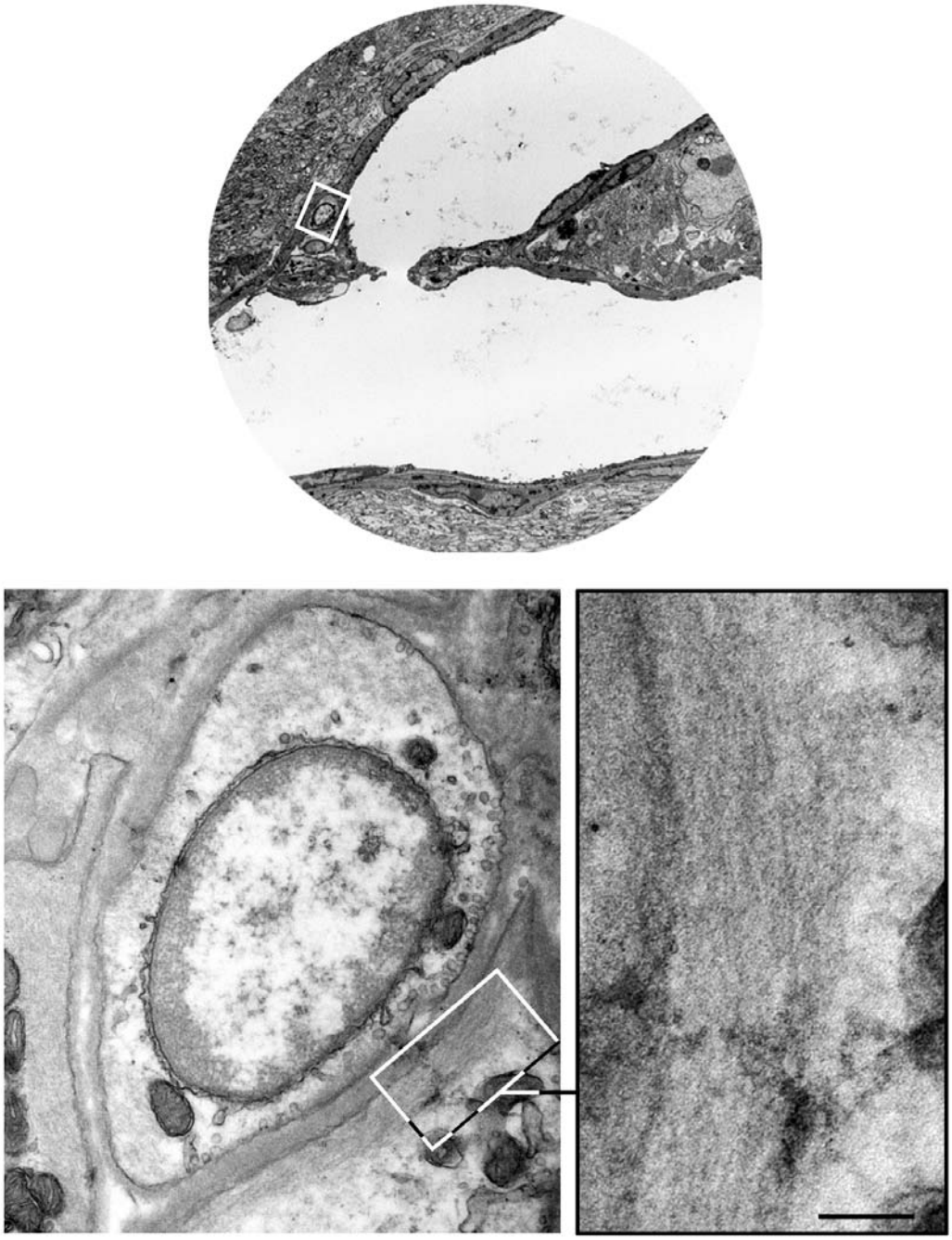

**Figure 29: Analysis of intermediate filaments.** Ultrastuctural analysis of annuli interstitial cells allowed the observation of bundles of intermediate filaments close to the cell membrane. Scale bar: 150 nm.

Nestin is an intermediate filament protein predominantly expressed in progenitor cells of nervous and myogenic systems, where regulates the remodeling of cell cytoskeleton during development. Although being down-regulated upon cell differentiation, nestin expression is reinduced during pathological situations, such as muscular regeneration or neuroglial scar formation (reviewed in Michalzick and Ziman, 2005). Interestingly, many authors have reported the expression of this protein in the ICCs of several tissues (Vanderwinden et al., 2002; Tsujimura et al., 2001; Popescu et al., 2005; Hinescu et al., 2007).

In 2004, Mignone and coworkers generated a mouse strain that expressed the EGFP under the control of the nestin gene regulatory elements. These mice serve as a highly sensitive reporter system for the detection of nestin-positive cells (Mignone et al., 2004) and we use them to analyze the presence of nestin in ICs.

Haematoxilin/eosin stained sections of paraffin embedded eyes from nestin-EGFP transgenic mice did not show any morphological alteration, indicating that EGFP transgene expression do not produce morphological defects in the retina of these mice (Fig. 30A).

EGFP fluorescence was more evident in a retinal population of cells with their nuclei located in the inner nuclear layer. Moreover, the cytoplasm of these cells extended from the inner to the outer limiting membranes (Fig. 30B). This disposition matched the morphology of Müller cells. In order to verify their nature, glutamine synthetase (GS), a specific marker for retinal Müller cells

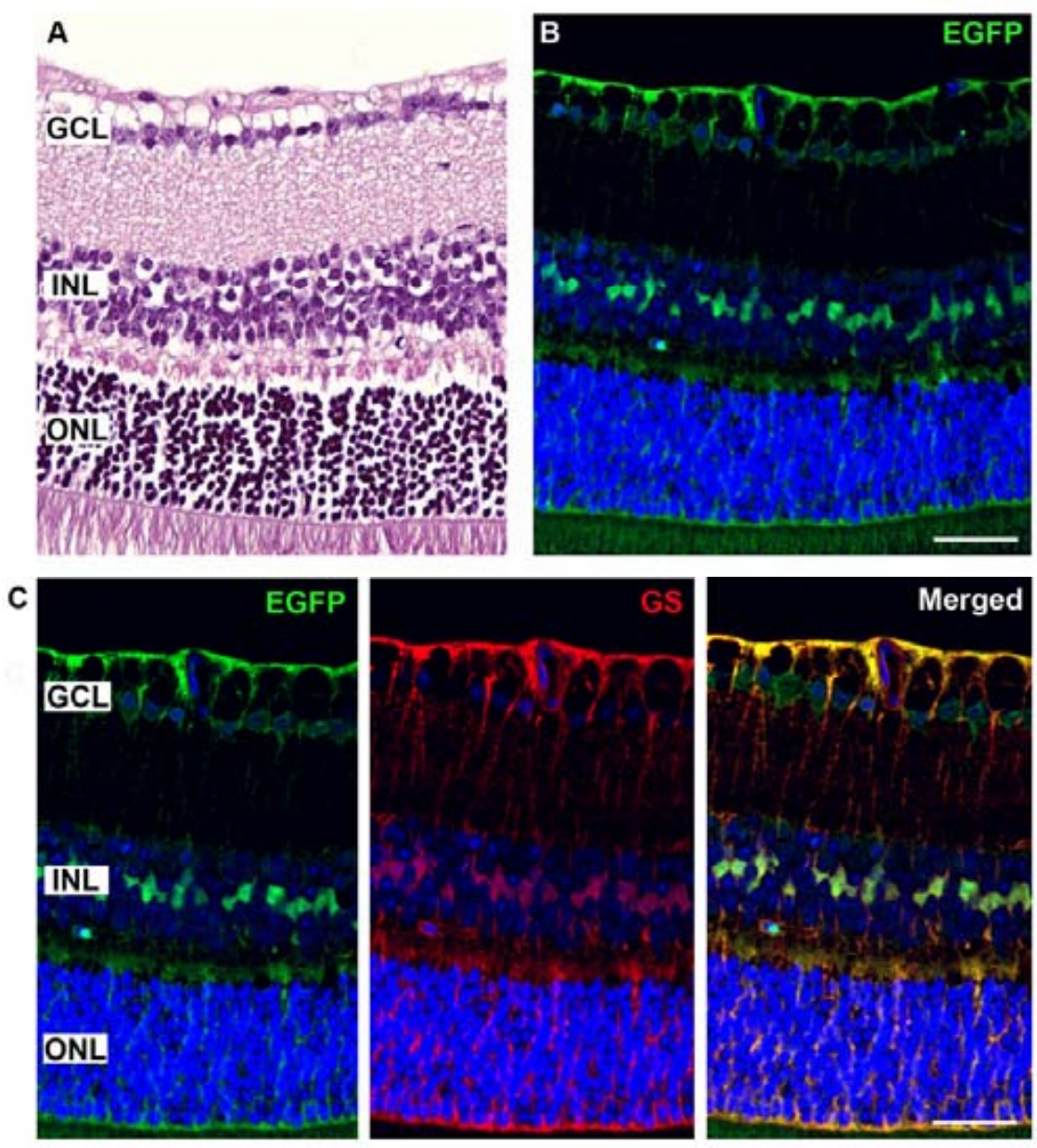


**Figure 30: Analysis of retinas from nestin-EGFP transgenic mice.** (A) Haematoxilin/eosin stain of retinal paraffin section showed that transgen expression did not cause morphological alterations in retinal vasculature. (B) Analysis of retinal sections under confocal microscopy showed specific green fluorescent emission in cells resembling Müller cells. (C) Confocal microscopy showed high colocalization (yellow) between GS immunlabeling (red) and EGFP emission (green), indicating that Müller cells expressed nestin. GCL: Ganglion cell layer; INL: Inner nuclear layer; ONL: Outer nuclear layer; EGFP: Enhanced green fluorescent protein; GS: Glutamine synthetase. Magnification A: 400x; Scale bars:; B = 38.64 μm; C = 34.57 μm.

(Hojo et al., 2000), was used. Confocal laser microscopy analysis confirmed that EGFP-positive cells were mainly Müller cells (Fig. 30C). Although several authors have reported the expression of nestin by reactive Müller cells (Xue et al., 2006; Luna et al., 2010; Xue et al., 2011; Lee et al., 2012), the nestin-EGFP transgenic mouse analysis suggested that nestin is expressed in Müller cells of healthy mature mouse retina.

In order to analyze the nestin expression in arteriolar annuli, nestin-EGFP whole mount retinas were immunostained with an anticollagen IV antibody (Fig. 31). Strongly fluorescent cells were found in ICs of arteriolar annuli (Fig. 31). The EGFP expression occupied both nucleus and cytoplasm of these cells revealing its elongated morphology. Thus, confirming that arteriolar annuli ICs express nestin in a differential manner. Previous studies have demonstrated a specific expression of this intermediate filament in ICCs of gastrointestinal tract (Tsujimura et al., 2001).

It has been reported that dynamic integration of the three distinct types of cytoskeletal filaments is needed for modulation of mechanical strength (Kanaya et al., 2005). Nestin possess a long carboxy-terminal which act as a linker among intermediate filaments, microfilaments and microtubules (Hermann and Aebi, 2000). Thus, nestin could play a role in coordinating cytoskeletal dynamics in arteriolar annul ICs.

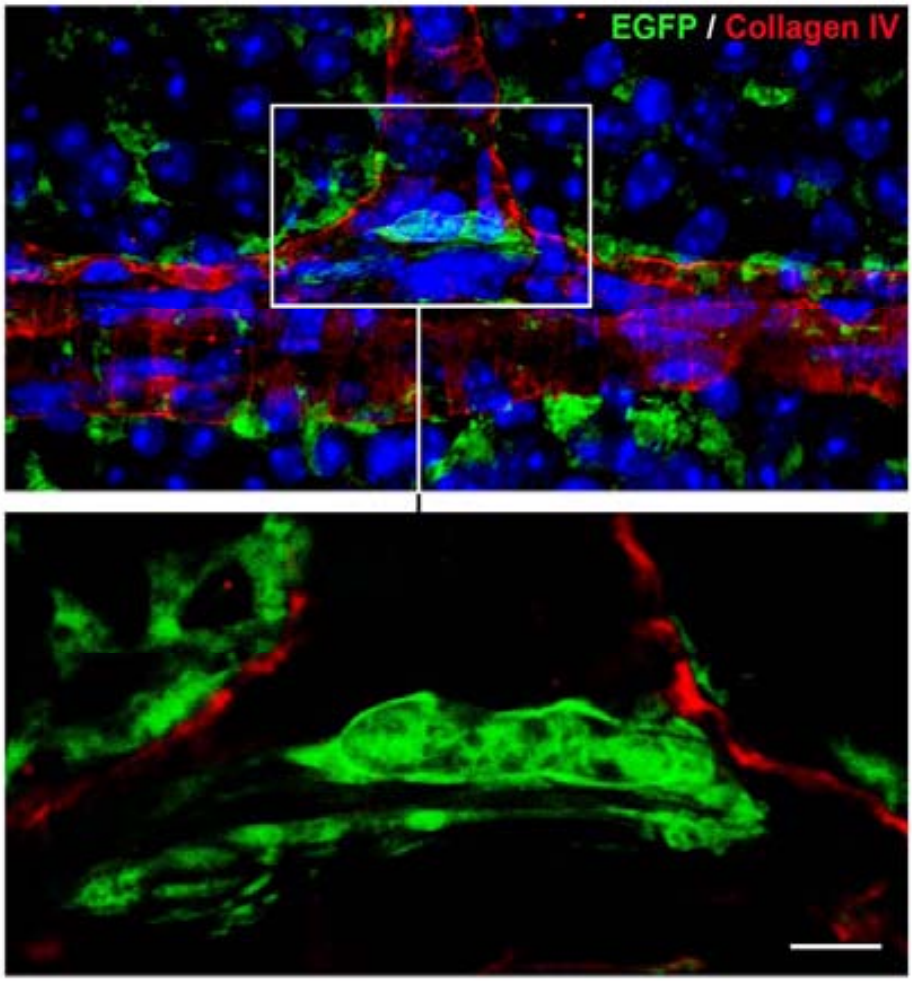


**Figure 31: Analysis of nestin expression in annuli interstitial cells.** Whole mount retinas from nestin-EGFP mice were immunostained with anti-collagen IV antibody (red) to evidence retinal vasculature. Confocal microscopy analysis evidenced high EGFP fluorescent emission (green) in annuli interstitial cells, indicating that nestin is expressed in these cells. Scale bar: 4.38 μm.

Vimentin forms intermediate filament and is commonly used as a marker for mesenchymal cells (Fraga et al., 1998; Schneider et al., 2010). High expression of vimentin in ICCs has been demonstrated by many authors in several tissues (Sircar et al., 1999; Popescu and Hinescu, 2005; Hinescu et al.,

2006). In order to ascertain if ICs of arteriolar annuli express vimentin, double immunohistochemistry for this protein and collagen IV was performed in whole

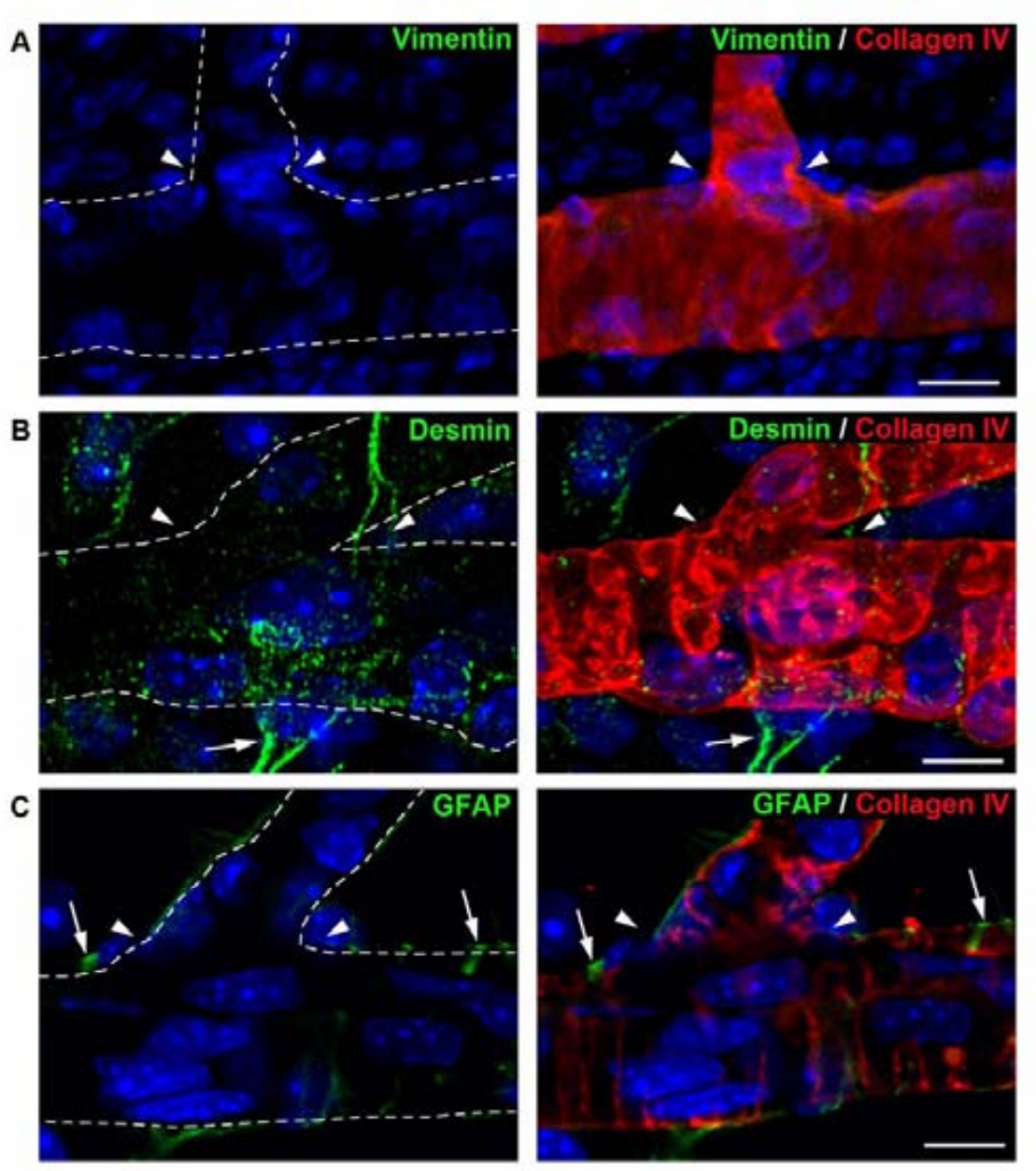


**Figure 32: Expression of intermediate filaments in arteriolar annuli.** Confocal maximum projections of optical sections of the whole arteriolar width showed no expression of vimentin (A), desmin (B) and GFAP (C) intermediate filaments in arteriolar annuli. Desmin (B) and GFAP (A) expression was restricted to glial cells. Retinas were double immunostained using specific antibodies against intermediate filaments together with anti-collagen IV antibody (red) to evidence retinal vasculature. Nuclei counterstain: Hoescht. Arowhead: Arteriolar annuli; Arrow: glial cell; GFAP: Glial fibrilary acidic protein. Scale bars: A = 13.78 μm; B = 7.86 μm; C = 10.31 μm.

mount retinas (Fig. 32A). In contraposition with previous results, laser confocal microscopy analysis demonstrated that vimentin was not expressed in annuli ICs (Fig. 32A).

The expression of intermediate filament proteins desmin and GFAP, which normally are exclusively expressed by neuroglial cells, was tested by immunohistochemistry in the arteriolar annuli. As expected, laser confocal analysis showed that desmin (Fig. 32B) and GFAP (Fig. 32C) immunoreactivity was restricted to glial cells.

### A.3.3 Smooth muscle cells

In order to characterize smooth muscle cells in the arteriolar annuli, transmission electron microscopy as well as inmunohistochemical and histochemical techniques were performed.

#### *A.3.3.1 transmission electron microscopy analysis*

Ultrastructual analysis of arteriolar annuli showed that smooth muscle cells formed exclusively a single layer surrounding the ICs (Fig. 33A). No morphological differences were observed in the smooth muscle cells found within arteriolar annuli when compared with the same cell type in the vessel wall adjacent to the branching site (Fig 33A).

The presence of a sphincter within arteriolar annuli has long been under discussion. While some authors have described a sphincter-like activity in the origin of retinal precapillary arterioles in several species (Thuránszky, 1947; Menschik and Dovi, 2005; Yi Yu et al., 2005), many others have reported the absence of such structure in arteriolar annuli (Friedman et al., 1964; Henkind and De Oliveira, 1968; Pannarale et al., 1996). True sphincters are defined as a multilayered circumferential arranged smooth muscle cells capable of closing the vessel lumen (Pannarale et al., 1996). However, we never observed this morphology during ultrastructural studies of arteriolar annuli. In fact, transmission electron microscopy analysis clearly showed that cells bulging into the lumen at arteriolar branching sites do not correspond to smooth muscle cells but to ICs (Fig. 22A).

In addition, ultrastructural analysis revealed the presence of peg-and-socket junctions interconnecting smooth muscle cells at the arteriolar annuli (Fig. 33B). Peg-and-socket junctions consist of a cell process, the so-called peg, getting into a tightly fitting invagination (socket) of a neighboring cell (Thuneberg and Peters, 2001). Several authors have reported the presence of this kind of junctions between smooth muscle cells in the small intestine (Thuneberg and Peters, 2001; Huizinga et al., 2010) as well as coupling pericytes and endothelial cells in human retinal capillaries (Carlson, 1989). Peg-and-socket junctions have also been described between ICCs and smooth muscle cells in mouse and human small intestine (Huizinga et al., 2010). However, our observations of mouse arteriolar annuli under transmission electron microscopy did not reveal the presence of peg-and-socket junctions between ICs and smooth muscle cells.

Thuneberg and Peters (2001) reported that peg-and-socket junctions may function as stretch sensors between smooth muscle cells. Smooth muscle cells contract in response to stretch (Thuneberg and Peters, 2001). When a smooth muscle cell contracts, its socket stretches the peg causing the contraction of the coupled cell, thus acting as a mechanical transmitter of contraction. In this regard, our results suggest that smooth muscle cell contraction at arteriolar annuli is coordinated by the peg-and-socket stretch-sensitive coupling.

### *A.3.3.2 Molecular characterization*

Smooth muscle cells have been studied by means of phalloidin histochemistry and α-SMA immunohistochemistry.

The use of confocal microscopy allowed scanning separate optical sections of the whole arteriole width. Then, digital three dimensional reconstructions of the optical sections were performed to study the arrangement of vascular smooth muscle cells at arteriolar annuli (Fig. 33C). Normally smooth muscle cells appeared orientated perpendicular to the main axis of the arteriole. However, arteriolar annul were characterized by a change in the orientation of smooth muscle cells, which became arranged in the direction of the collateral arteriole. In addition, some smooth muscle cells of main vessel got divided to embrace the origin of the stem vessel. Specific immunohistochemical labeling of smooth muscle cells with anti-α-SMA antibody showed the same characteristic disposition of these cells in arteriolar annuli (Fig. 33D). Our results

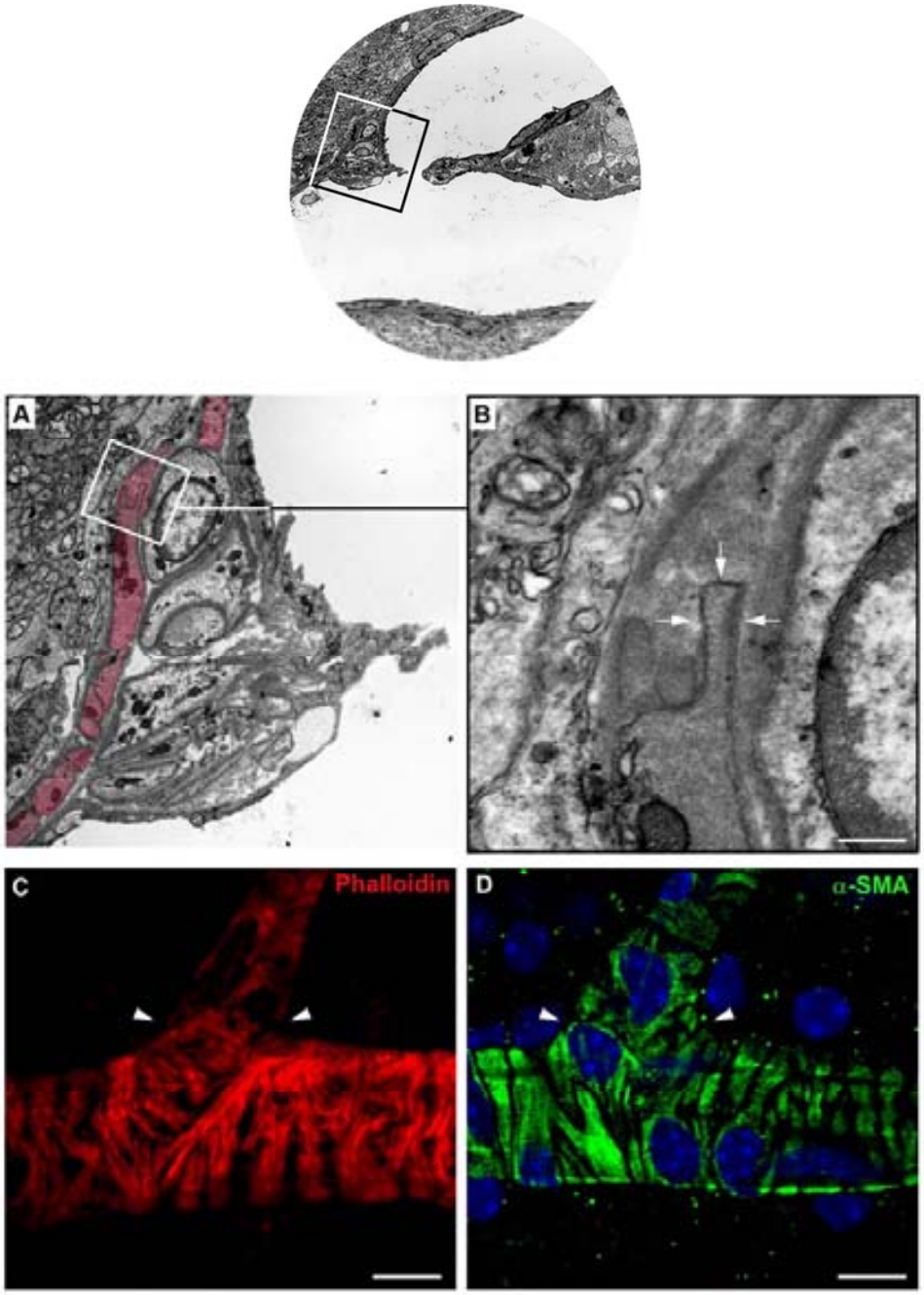


**Figure 33: Structural and molecular analysis of annuli smooth muscle cells.** (A) Transmission electron microscopy analysis showed a single layer of smooth muscle cells (digitally coloured in red) in the arteriolar annuli, indicating the absence of a true sphincter at such level. (B) Higher magnification evidenced the presence of peg-and-socket junctions coupling smooth muscle cells in arteriolar annuli. (C) The specific histochemical stain of F-actin (red) with phalloidin was analyzed under confocal microscopy. Maximum projection of optical sections allowed observing a change in the disposition of smooth muscle cells, which reoriented to embrace the origin of collateral arteriole. (D) immunohistochemical labelling of α-smooth muscle actin (-SMA) confirmed the results obtained by phalloidin stain. Nuclei counterstain: ToPro3. Arrow: Peg-and-socket junction; Arrowhead: Arteriolar annuli. Scale bars: A = 392.85 nm; B = 10.41 μm; C = 10.01 μm; D = 9.08 μm.

are in accordance with the observations of Pannarale and coworkers (1996), who reported similar changes in the disposition of smooth muscle cells found at arteriolar branches of semicorroed rat retinal vascular casts.

### A.3.4 Blood vessel basement membrane

Transmission electron microscopy and inmunohistochemical analyses were performed in order to ascertain morphology of basement membranes in arteriolar annuli.

#### A.3.4.1 Transmission electron microscopy analysis

Ultrastructutral analysis of arteriolar annuli evidenced a great thickening of the basement membranes in the arteriolar annuli (Fig. 34B) when compared with the arteriolar wall adjacent to the branching site (Fig. 34A). In addition, these studies showed a change in the aspect and texture of basement membranes (Figs. 34A and B). While basement membrane of arteriolar wall appeared with a uniform aspect, thin and closely associated with vascular cells (Fig 34A), arteriolar annuli showed basement membranes with irregular thickness and a loose multilayered disposition, leaving electronlucide spaces among the different layers (Fig 34B).

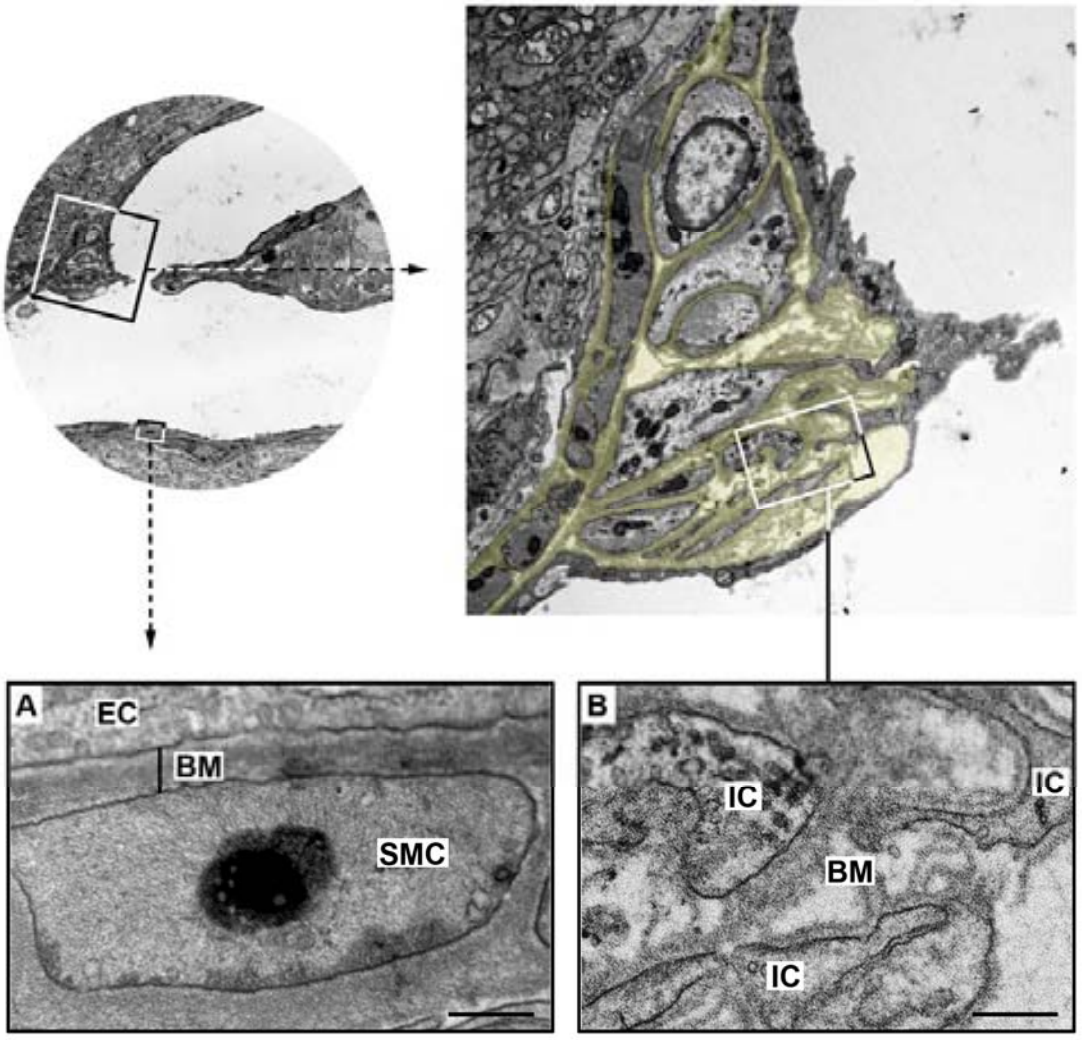


**Figure 34: Ultrastructure of basement membrane in arteriolar annuli.** Transmission electron microscopy evidenced differential structure and thickness of annuli basement membrane (digitally coloured yellow) when compared with that of regular arteriolar wall (A). (B) Annuli basement membrane showed irregular thickness and a loose multilayered disposition. SMC: Smooth muscle cell; BM: Basement membrane; EC: Endothelial cell; IC: Interstitial cell. Scale bars: A = 249.16 nm; B = 358 nm.

### A.3.4.2 Molecular characterization and organization

To analyze extracellular matrix modifications more deeply, three main components of blood vessel basement membrane were studied by immunohistochemistry in whole mount retinas.

Collagen IV is the most important structural protein of basement membrane (Gelse et al., 2003). Confocal microscopy examination of whole mount retinas immunolabeled with an anti-collagen IV antibody showed an increase of this protein at the arteriolar annuli (Fig. 35A). The quantification of fluorescence intensity evidenced that the increased collagen IV expression in arteriolar annuli was statistically significative (mean intensity in arteriolar annuli = 84.90 $\pm$ 8.48 VS mean intensity in adjacent vessel wall = 48.05 $\pm$ 8.81; p = 0.0002). Collagen IV acts as a scaffold of basement membrane network, giving rigidity to this structure (Timpl et al., 1979). Thus, our results suggest a reinforcement of the basement membrane at arteriolar annuli.

Laminin, the most abundant non-collagenic protein of vascular basement membrane (Dumortier et al., 1998), appeared also increased at arteriolar annuli (Fig. 35B). Confocal microscopy quantification of fluorescence intensity demonstrated that differences on laminin expression between arteriolar annuli (mean intensity = 59.03±9.91) and adjacent basement membrane (mean intensity = 36.60±6.13) were statistically significative (p = 0.0024). This result is in accordance with those previously reported by Lopes and coworkers (2012), showing a specific increased expression of laminin at arteriolar branching sites of mouse retinal vasculature.

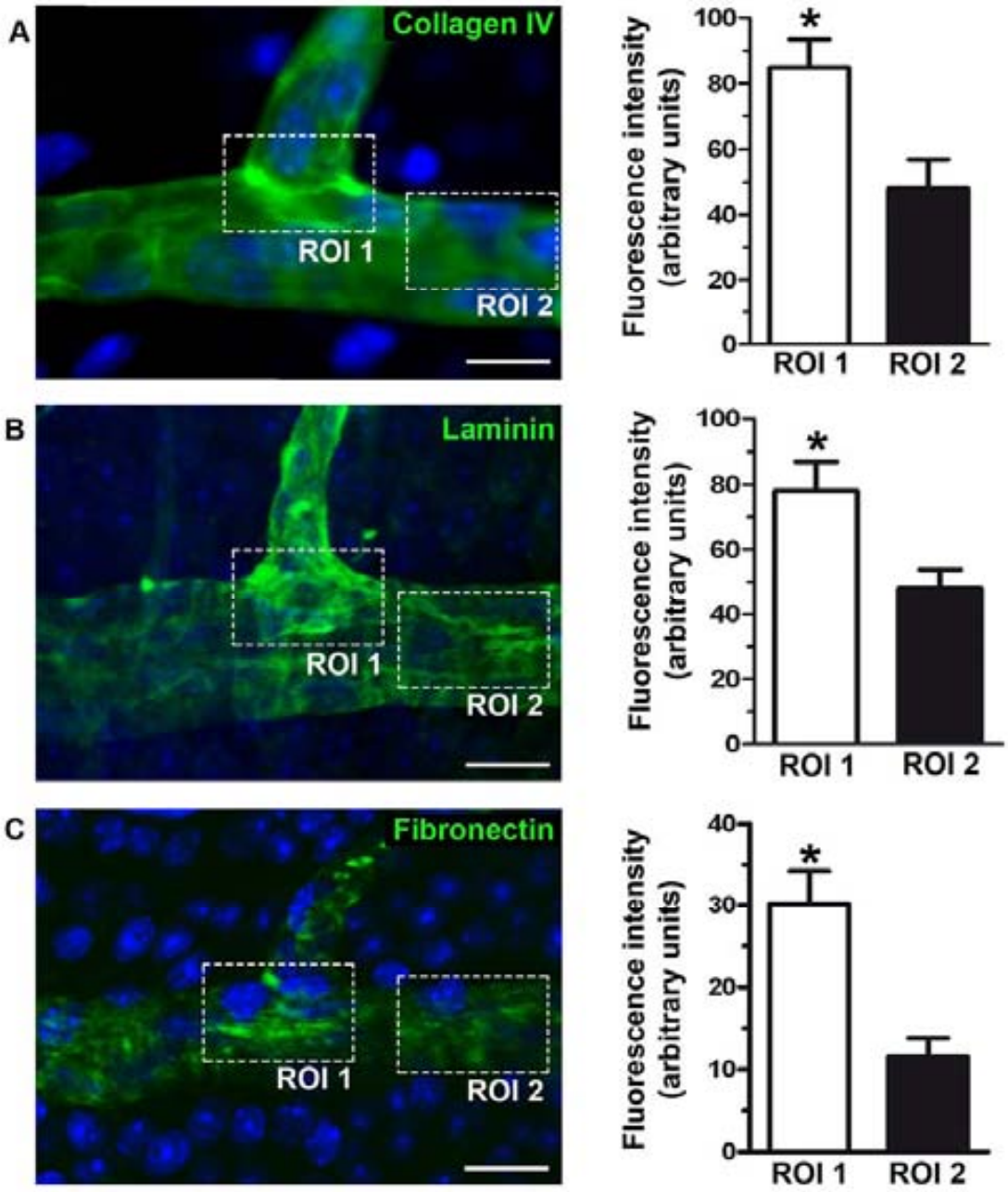


**Figure 35: Expression of basement membrane proteins in arteriolar annuli.** Whole mount retinas immunolabelled with antibodies against collagen IV (A), laminin (B) and fibronectin (C) were analyzed with a confocal microscope. To quantify proteins of the whole arteriolar wall, maximum projections of optical sections of the whole arteriole width were performed. The expression of collagen IV (A), laminin (B) and fibronectin (C) was increased. As bargrphs show, differences in protein expression were statistically significant. ROI 1: Arteriolar annuli; ROI 2: regular arteriolar wall; Asterisk: $p < 0.05$. Scale bars: A = 10.23 μm; B = 16.06 μm; C = 17.20 μm.

In addition to collagen IV and laminin, the expression of fibronectin, the main adhesion protein of connective tissue (Cooper and Hausman, 2010), was increased at arteriolar annuli (Fig 35C). The quantification of fluorescence intensity sowed that the increased expression of fibronectin at arteriolar annuli when compared with adjacent vessel wall (27.62 $\pm$ 13.31 VS 13.31 $\pm$ 2.517) was statistically significative ($p = 0.0170$).

Ultrastructural analysis showed morphological modifications in the organization of arteriolar annuli extracellular matrix (Fig. 34). To confirm this morphological fact, colocalization was analyzed in whole mount retinas double immunostained against collagen IV and laminin. As expected a disorganization, evidenced by the reduction in the colocalization of collagen IV and laminin, was observed in arteriolar annuli (Fig 36). The overlap coefficient and colocalization rate, two parameters used to quantify colocalization (Manders et al., 1993; Zinchuk et al., 2007; Bratic et al., 2011), indicated that the decrease of colocalization found in arteriolar annuli was statistically significant (overlap coefficient: arteriolar annuli = 0.8831±0.037 VS adjacent vessel wall = 0.9794±0.0029; $p = 0.0327$. Colocalization rate: arteriolar annuli = 64.38±6.66% VS adjacent vessel wall = 96.41±2.64%; $p = 0.0015$).

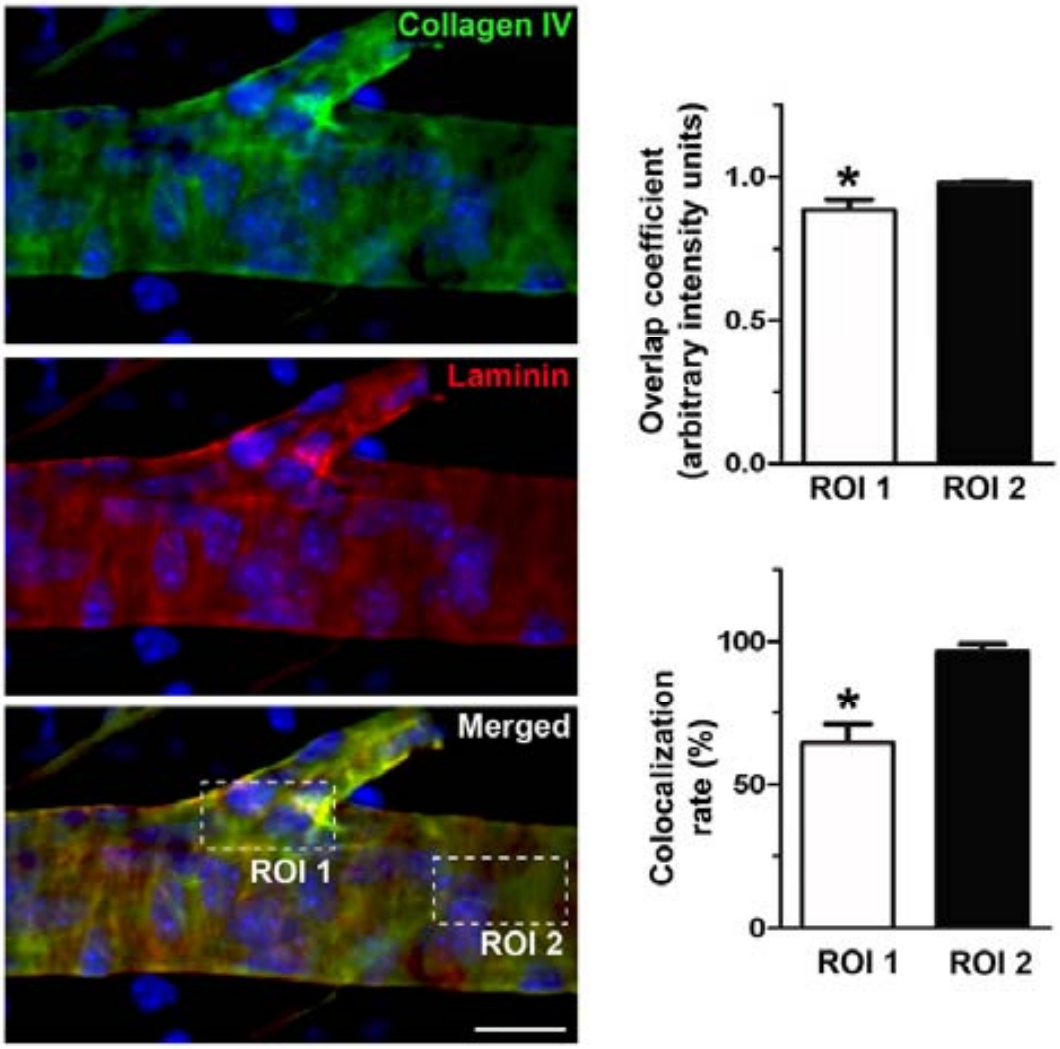


**Figure 36: Analysis of colocalization in annuli basement membrane.** Double immunohistochemistry with antibodies against collagen IV (green) and laminin (red) were performed in whole mount retinas to analyze colocalization with confocal microscopy. As bar graphs show overlap coefficient and colocalization rate, two parameters used to quantify colocalization, were diminished in arteriolar annuli. Differences between colocalization in arteriolar annuli a regular vascular wall was statistically significant. ROI 1: Arteriolar annuli; ROI 2: Regular arteriolar wall; Asterisk: $p < 0.05$. Scale bar: 17.5 μm.

| Protein | Basement membrane IN annuli | Basement membrane OUT annuli |
|---|---|---|
| Collagen IV | ++ | + |
| Laminin | ++ | + |
| Fibronectin | ++ | + |

**Table 3:** Comparative table of protein expression between basement membrane in the arteriolar annuli and in the adjacent vascular wall

Taken together, our results indicate a distinctive molecular and cellular phenotype in arteriolar annuli in comparison with other vascular localizations (Table 4). Thus, suggesting a specific function for arteriolar annuli in mouse retina.

| Protein | Endothelial cells | ICs | Smooth muscle cells |
|---|---|---|---|
| CD34 | + | - | - |
| CD31 | - | - | - |
| NADPH diaphorase | + | - | - |
| vWF | + | - | - |
| C-kit | - | - | - |
| Ano1 | - | + | - |
| CD44 | - | + | - |
| PDGF-Rβ | - | ++ | + |
| NG2 | - | ++ | + |
| Connexin 43 | + | + | + |
| F-actin | - | + | ++ |
| α-SMA | - | - | + |
| β-actin | - | + | - |
| Nestin | - | + | - |
| Vimentin | - | - | - |
| Desmin | - | - | - |

**Table 4:** Recapitulative table of molecular phenotype in cells of arteriolar annuli.

### A.4 Functional analysis of arteriolar annuli

Autoregulation is an important functional characteristic of the retinal circulation (Pannarale et al., 1996). Although many studies have demonstrated

the capacity of the retina to maintain constant blood flow despite variations of perfusion pressure (Riva, 1981; Pournaras, 2008; Kur 2012), the presence of specific sites of blood flow regulation within retinal vasculature is still under discussion.

In the middle of the last century, arteriolar annuli were proposed to regulate blood flow acting as sphincter-like structures (Thuránszky, 1957). However, the evidence for such activity has been not yet elucidated, because studies in retinal vascular dynamics do not evidence vascular constrictions at the arteriolar branch points (Friedman et al., 1964). Our results studying flat mounted indian ink injected retinas evidenced a spontaneous and specific contractile activity in arteriolar annuli (Fig. 37A and B). Unlike what happens with the distal segments of the side-arm branch that they did not constrict (Fig. 37A and B). These results completely agree with the observations of Yu and coworkers (2005), who observed similar activities in the arteriolar branching points of pig retina.

Ultrastructural analysis, as we have already seen, evidenced the absence of a true sphincter in arteriolar annuli (Fig. 33A), since multilayered smooth muscle cell structures surrounding arteriolar branches have never been observed. However, the arteriolar annuli morphological analysis showed reoriented smooth muscle cells that are able to reduce vascular lumen by bulging ICs and endothelial cells (Figs. 33C and D) to the vascular lumen. Although these structures could not be considered as “true” sphincters, these results suggest the existence of sphincter activity at the arterial annuli. Pouiseuille’s law, governing laminar flow, demonstrates an inverse exponential

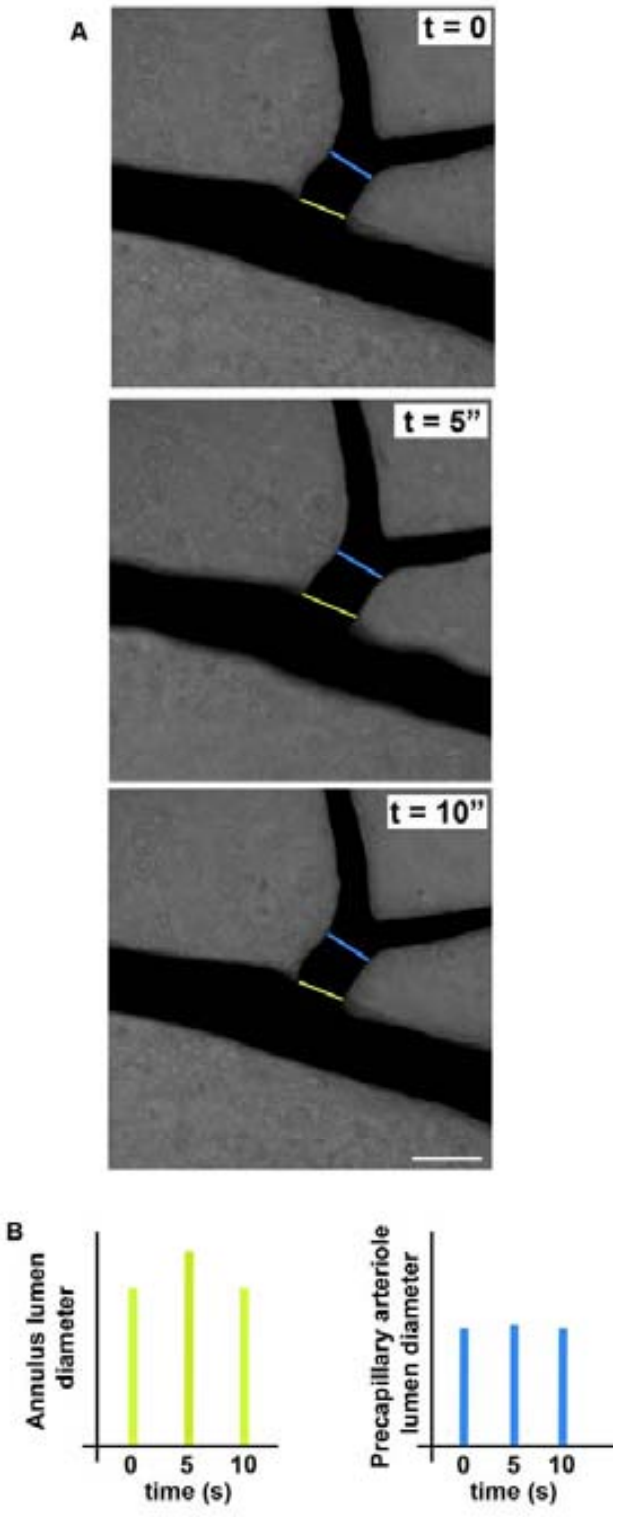


**Figure 37: Analysis of arteriolar annuli spontaneous sphincter-like activity.** (A) Time lapse images of arteriolar side-arm branch evidenced spontaneous constrictions and dilations of arteriolar annuli. By contrast, the more distant region of the branch did not noticeably constrict. (B) Graphical representation of vascular lumen diameters evidenced that sphincter-like activity was restricted to arteriolar annuli. Images were acquired every 5 seconds. Scale bar: 62.69 μm.

relationship between fluidic resistance and vessel diameter (Guyton and Hall, 2006). Slight reductions in lumen diameter could cause great modifications in blood flow (Guyton and Hall, 2006). Hence, our results suggest that arteriolar annuli may play a significant role in regulation of blood flow in the capillary network.

### A.4.1 Calcium events

Arterial contraction is due to increases of intracellular calcium concentration in smooth muscle cells (Lamboley et al., 2005). ICCs have been shown to generate calcium oscillations in the middle cerebral artery, indicating that they participate in the rhythmical activity of arteries (Harhun et al., 2009). To analyze calcium dynamics in arteriolar annuli, flat mounted retinas were stained with the calcium sensitive dye fluo-4 (Fig. 38). Preliminary *in* vivo scanning laser confocal studies showed that without external stimuli, ICs and smooth muscle cells of arteriolar annuli showed little or no calcium activity (Fig. 38B and C). These results are in accordance with those previously reported by Pucovský (2010), who observed very low calcium activity in arterial ICCs. Low calcium activity in the arterial annuli could be produced by the NO activity, as it has been previously described for the intestinal ICCs (Bayguinov et al, 2010). The increased capacity of endothelial cells in the annuli to produce NO (Fig. 7C) can be a cause of the decline of annuli calcium activity. This fact would inhibit the annuli contraction, maintaining the opening of the lumen at the branching site ensuring the blood flow.

Histamine triggers the release of calcium from internal stores causing a transient rise of cytosolic calcium in smooth muscle cells (Kotlikoff et al., 1987). In addition, histamine causes an acceleration of pacemaker activity and calcium slow waves of ICCs (Hashitani and Lang, 2010). Histamine administration on cultured retinas caused a transient rise in cytosolic calcium of both ICs and smooth muscle cells of arteriolar annuli (Fig. 38B and C). In contrast, endothelial cells did not show calcium activity in response to the drug administration (Fig. 38B and C).

**Figure 38: Analysis of calcium dynamics in arteriolar annuli.** (A) Representative image of arteriolar annuli during calcium analyses. Doted line outlines the retinal arteriole. Coloured lines encircle cells under study: interstitial cell (green), smooth muscle cell (red), endothelial cell (yellow) and glial cell (blue). (B) Colour coded confocal microscopy images evidenced changes in Fluo 4 fluorescence emission before (left image) and after (right image) histamine administration. Purple correspond to low emission and pink indicates high fluorescence. (C) Representative traces of calcium transient changes in response to histamine administration. As can be seen, histamine caused a transient calcium rise in glial (blue line), smooth muscle (red line) and interstitial (green line) cells, whereas no change in calcium concentration was observed in endothelial cells (yellow). (D) Normalization of intensity values demonstrated different calcium dynamics between interstitial (green line) and smooth muscle (red line) cells. Scale bars: A = 15.05 μm; B = 31.71 μm.

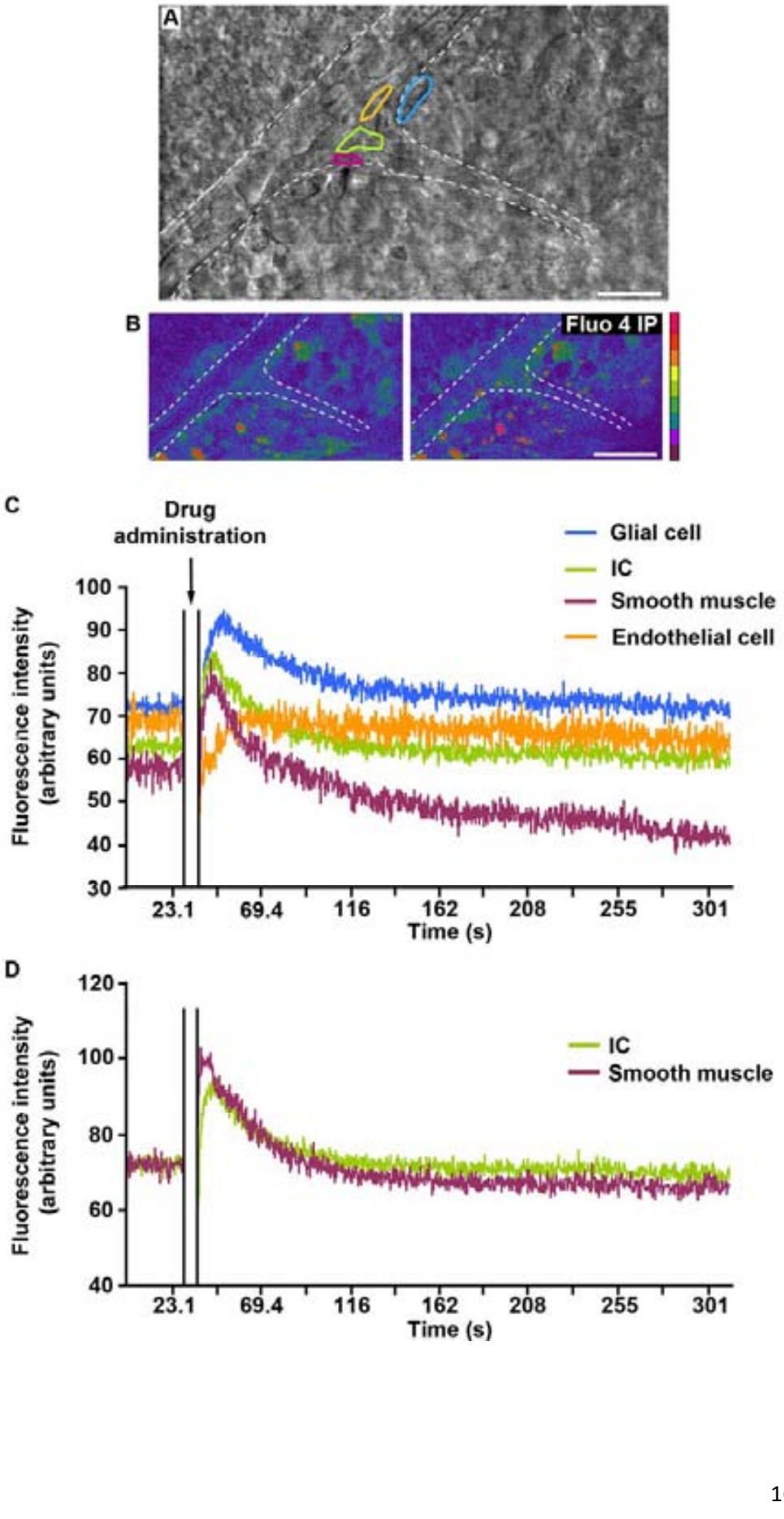
A
B
Fluo 4 IP
C
Drug
administration
Glial cell
IC
Smooth muscle
Endothelial cell
Fluorescence intensity
(arbitrary units)
100
90
80
70
60
50
40
30
23.1
69.4
116
162
208
255
301
Time (s)
D
IC
Smooth muscle
Fluorescence intensity
(arbitrary units)
120
100
80
60
40
23.1
69.4
116
162
208
255
301
Time (s)

Vascular ICCs and smooth muscle cells show marked differences in intracellular calcium events that indicate different physiological roles (Harhun et al., 2005). As figure 38C shows, annuli ICs showed longer-lasting calcium events than smooth muscle cells. This result agrees with previous calcium analyses in mesenteric arterial ICCs (Pucovský et al., 2003). In addition, smooth muscle cells displayed calcium events of higher intensity than ICs in arteriolar annuli, as evidenced when fluorescence intensity values were normalized to compare the intensity of calcium changes (Fig. 38D).

Calcium release in ICCs causes a depolarization that leads to an activation of calcium activated chloride channels (Harhun et al., 2005), and this seems to be critical for smooth muscle function in many tissues (Huang et al., 2009; McGabon et al., 2009). In order to test if calcium rises in annuli ICs and smooth muscle cells corresponded to contractile activity, arteriolar diameter in histamine treated retinas was assessed. As expected, time-lapse imaging of Indian ink injected retinas evidenced that histamine caused transient

---

**Figure 39: Arteriolar annuli contraction in response to histamine administration.** (A) Histamine administration during time-lapse analysis of Indian ink injected retinas caused specific long-lasting transient contraction of arteriolar annuli. (B) By contrast, no contractile activity was observed in dichotomous branching in response to histamine administration. (A) and (B) correspond to confocal microscopy time-lapse analysis images. Images were taken every 2 seconds. t = 0: histamine administration; t = 1: 150 seconds after histamine administration; t = 3: 250 seconds after histamine administration. Scale bars: A = 14.50 μm; B = 14.60 μm.

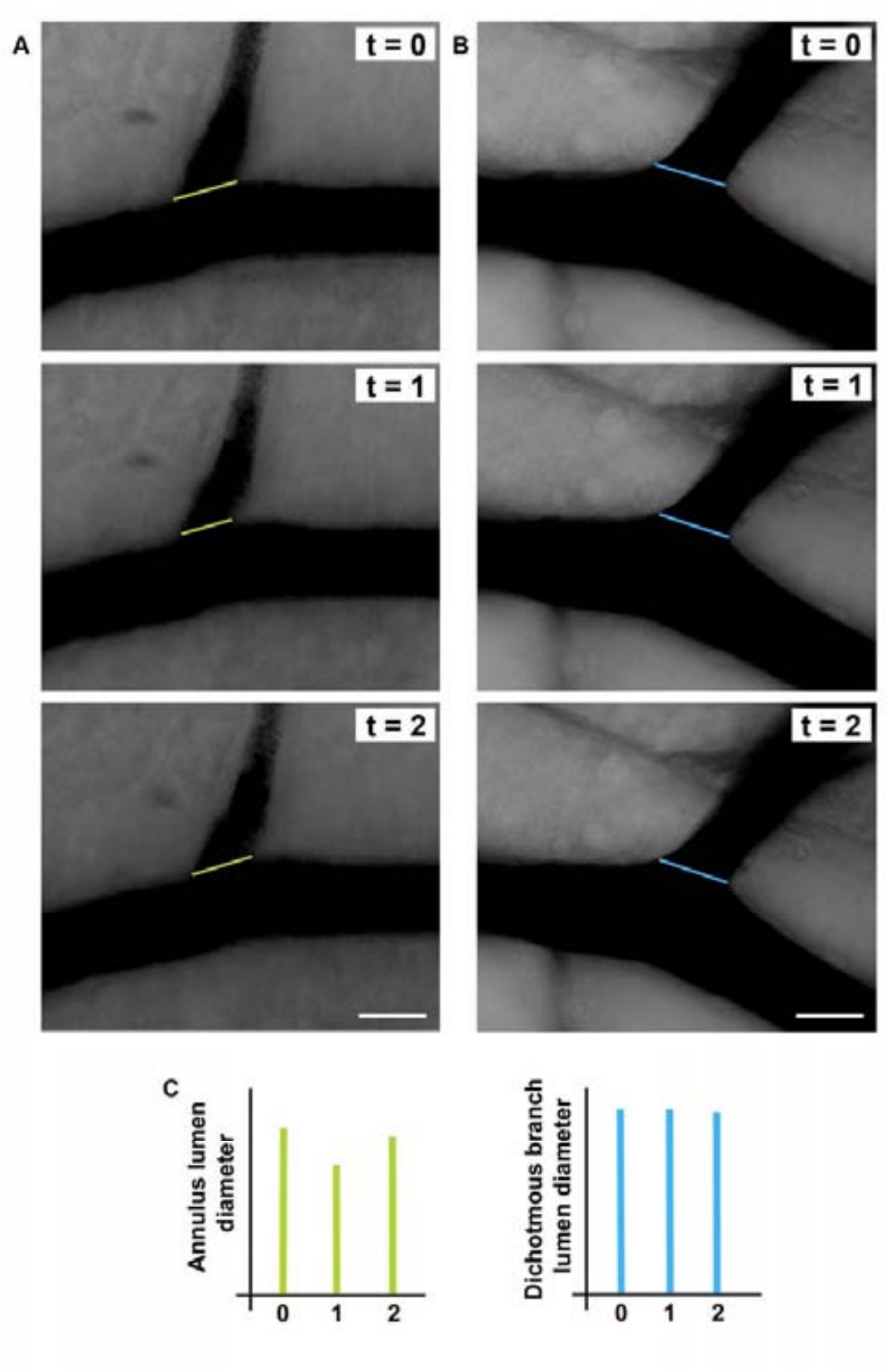
A
t = 0
t = 1
t = 2
B
t = 0
t = 1
t = 2
C
Annulus lumen diameter
0
1
2
Dichotmous branch lumen diameter
0
1
2

contractions in arteriolar annuli (Fig 39A and C). By contrast, arteriolar dichotomous branching sites did not contract either spontaneously or in response to histamine administration (Fig. 39B and C). Thus, suggesting a specific contractile activity of arteriolar annuli in response to this vasoactive molecule.

Taken togeteher, our results in calcium dynamics, the expression of calcium-activated chloride channels in annuli ICs, evidenced by Ano1 expression (Fig. 24B), and the specific contractile activity in response to histamine administration, suggest that ICs could play a role in the regulation of vascular tone in the arterial annuli.

Perivascular glial cells close to arteriolar annuli also showed transient rises of intracellular calcium in response to histamine administration (Fig. 38B and C). Metea and Newman (2007) have reported that glial cells respond to increased neuronal activity by increasing their intracellular calcium levels and, as a consequence, releasing vasoactive substances to generate vasoconstriction or vasodilation.

### A.4.2 Neurovascular coupling

Retinal function requires a finely tuned blood flow regulation in order to match local metabolic needs (Pournaras et al., 2008). According to this, increased neuronal activity in a localized region of the retina evokes increased blood flow to that region, in a phenomenon called functional hyperaemia (Riva

et al., 2005). Due to its location in close contact with both neurons and blood vessels, glial cells have been proposed to mediate this response (Metea and Newman, 2006). Thus, a coordinated interaction between neurons, glia and vascular cells is needed, forming what has been called neurovascular unit (Metea and Newman, 2007).

Analysis of whole mount retinas from nestin-GFP transgenic mice revealed the existence of GFP-positive perivascular cells emitting processes that entered to the arteriolar annuli through gaps in the basement membrane, evidenced by collagen IV inmunolabeling (Fig. 40A). Cellular processes crossing basement membrane were in close contact with annuli ICs (Fig. 40A). As expected by our previous results (Fig. 30C), triple immunohistochemistry labeling collagen IV, GS and GFP in retinas from nestin-GFP mice revealed that processes crossing the blood vessel basement membrane corresponded to Müller cells (Fig. 40B).

Glial cells respond to increased neuronal activity by releasing vasoactive substances (Metea and Newman, 2007). Such vasoactive substances include NO (Goldstein et al., 1996; Haverkamp et al., 1999) and arachidonic acid metabolites (Mishra et al., 2011). In gastrointestinal tract, NO released from nerve terminals acts over ICCs, which in turn transmit an electrical response to smooth muscle cells via gap junctions (Iino et al., 2008). Our results could indicate that ICs in arteriolar annuli, which are in close contact with Müller cells (Fig. 40A and B) and smooth muscle cells (Fig. 23), may play a key role as mediators in neurovascular coupling.

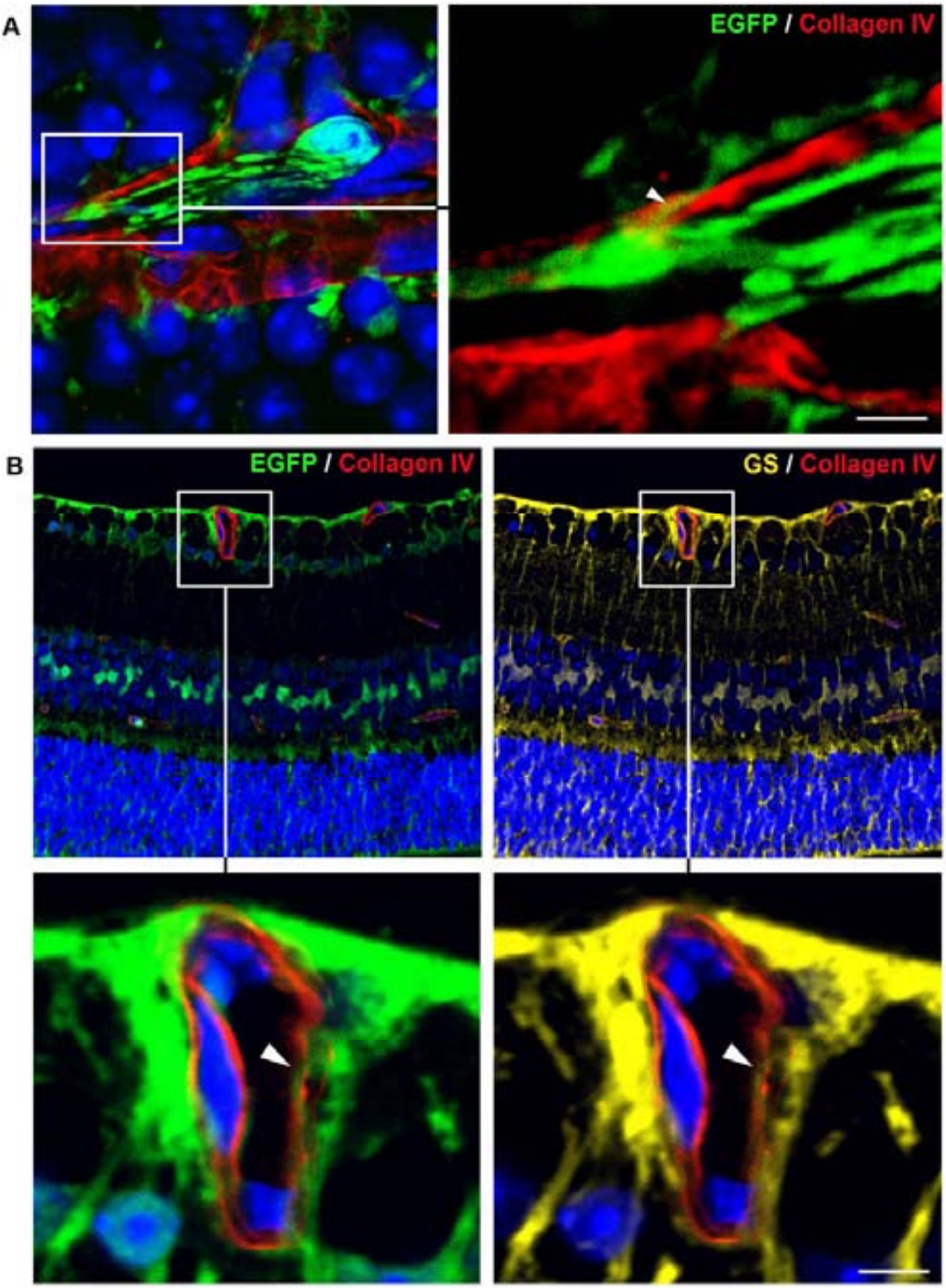
A
EGFP / Collagen IV
B
EGFP / Collagen IV
GS / Collagen IV

### A.4.3 Function during experimental hypoxia

Functional magnetic resonance imaging has shown that local stimulation of neuronal activity in an certain area of the retina results in increased blood flow largely confined to that area (Duong et al., 2002; Srienc et al., 2010), demonstrating that retina possesses mechanisms for functional hyperemia (Kur et al., 2012). Sphincter-like vasoconstrictions of vascular branching sites in the retina have been proposed to underlie a controlled closing of certain collateral branches to maximize blood flow to other areas (Metea and Newman, 2007).

Previous results of our group have demonstrated the presence of arterio-arteriolar shunts in the mouse retinal vasculature (Ramos et al., 2013). In these areas, arterioles communicate directly to each other by a network of capillaries (Fig.41A and B). The analysis of the distribution of arteriolar annuli showed an increased number in the arterio-arteriolar shunts areas (Fig. 41C). These results indicating a specific distribution of arteriolar annuli suggest an increased capacity to regulate blood flow at arterio-arteriolar shunts.

---

**Figure 40: Analysis of neurovascular coupling.** (A) Whole mount retinas from nestin-EGFP mice were immunolabelled with anti-colagen IV antibody (red) and analyzed by confocal microscopy. As micrograph show, processes from perivascular nestin positive cells crossed basement membrane to contact annuli interstitial cells (arrowhead). (B) Triple immunolabeling of paraffin sections using antibodies against collagen IV (red), EGFP (green) and GS (yellow) evidenced that processes crossing basement membrane (arrowhead) corresponded to Müller cells. Nuclei counterstain: Hoeshct. Scale bars: A = 2.68 μm; B = 6.49 μm.

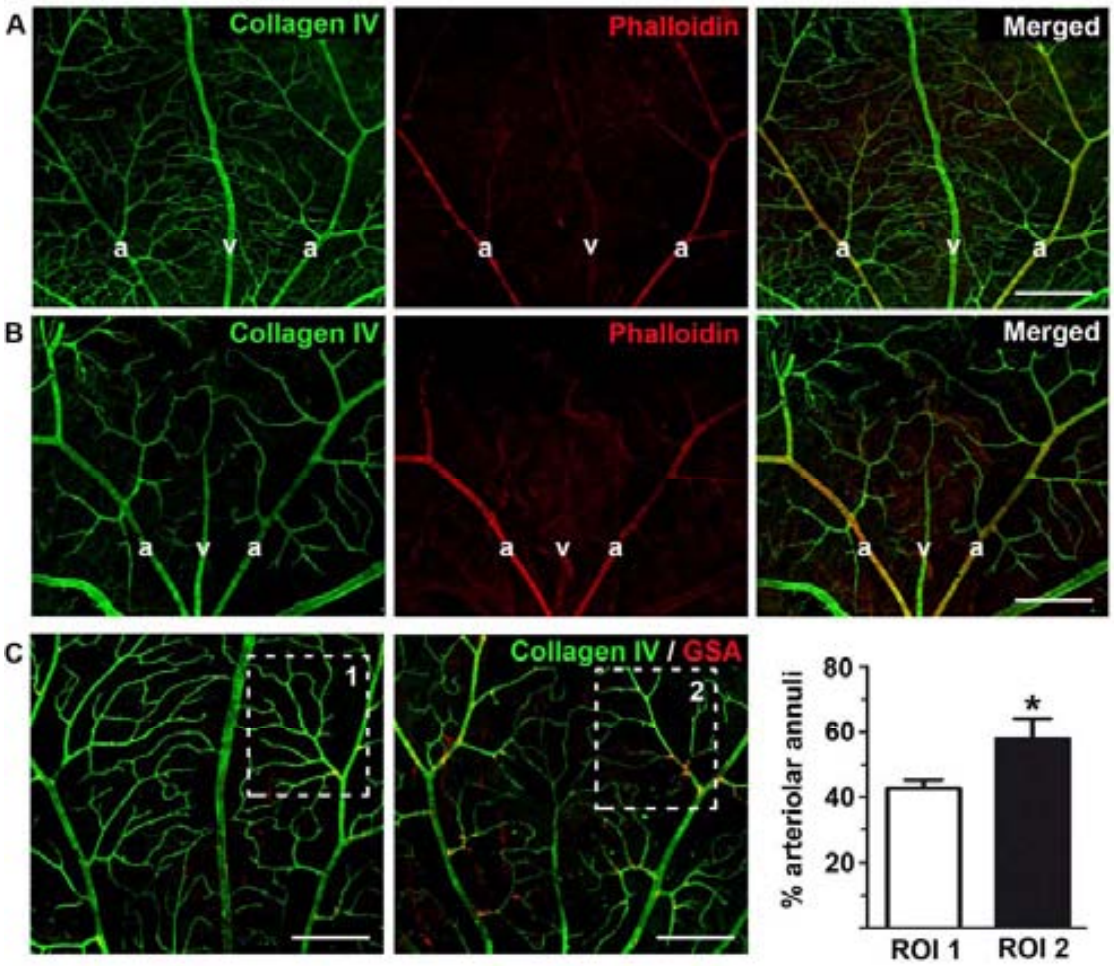


**Figure 41: Analysis of the presence of arteriolar annuli in arterio-arteriolar shunts.** (A) Normally, arterioles communicate with venules through a meshwork of capillaries. (B) However, direct communications between arteries were also observed. (A) and (B) correspond to confocal micrsocopy images of whole mount retinas immunostained with anitcollagen IV (green) to evidence retinal vasculature. Phalloidin labeling (red) was used to mark smooth muscle cells. Note that phalloidin is less abundant in venules and almost inexistent in capillaries. (C) *Griffonia simplicifolia* (GSA) staining evidenced a increased number of arteriolar annuli occurring in arterio-arteriolar shunts (image on the right) when compared to regular vascular pattern (micrograph on the left). Bar graphs show that differences in annuli number were statistically significant. a: arteriole; v: venule; ROI 1: arteriolar branches in a regular vascular area; ROI 2: arteriolar branches of arterio-arteriolar shunt; asterisk: $p < 0.05$. Scale bars: A = 302.69 μm; B = 287.56 μm; C = 295 μm.

To test this hypothesis, a mouse model of retinal hypoxia induced by a partial chirurgical ligature of common carotid arteries, was intravenously injected with pimonidazole (Fig. 42). Pimonidazole is a chemical compound that specifically binds thiol-containing proteins in hypoxic cells (Varia et al., 1998), and it has been widely used as a marker of retinal hypoxia (Gooyer et al., 2006; Wright et al., 2010; Mowat et al., 2010). Immunohistochemical detection of pimonidazole showed a great reduction in the number of hypoxic cells in the

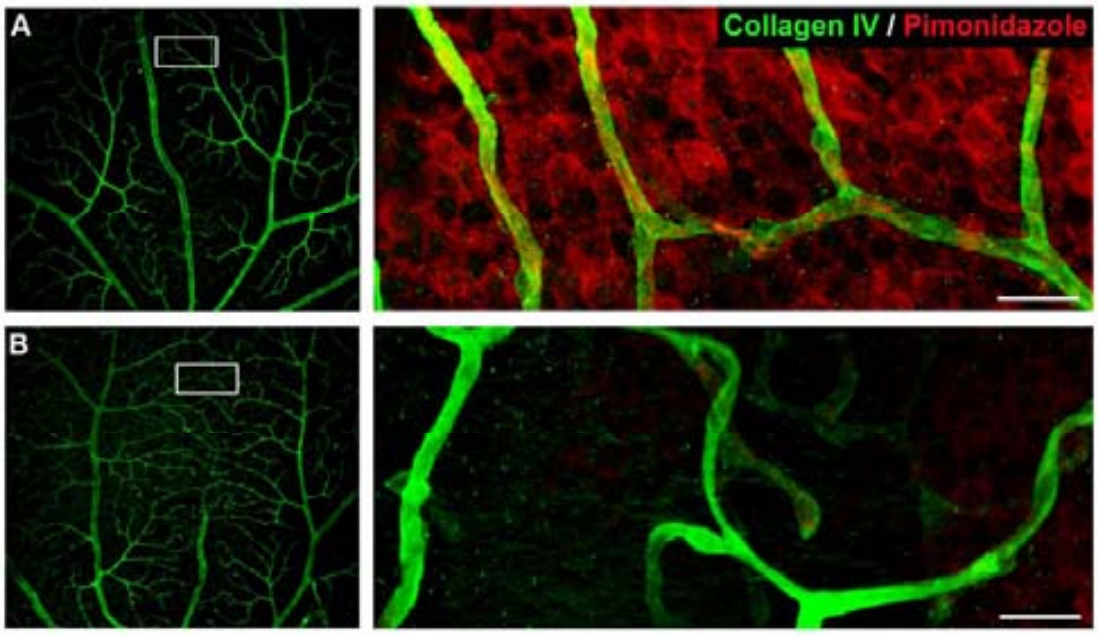


**Figure 42: Analysis of arteriolar annuli function during experimental hypoxia.** (A) Immunodetection of pimonidazole (red) in whole mount retinas from a mouse model of retinal hypoxia, showed that most cells located in areas were retinal arterioles communicate with venules were hypoxic. (C) By contrast, in areas were arterio-arteriolar shunts occurred the number of hypoxic cells was greatly reduced. Arterio-arteriolar shunts are related to an increased presence of arteriolar annuli, suggesting a role of these structures in directing blood flow to certain areas. Scale Bars: A = 28.15 μm; B = 27.79 μm.

arterio-arteriolar shunts, when compared with areas where arterioles communicate directly with venules (Fig. 42A and B). Thus, retinal areas resistant to hypoxia are associated with an increased presence of arteriolar annuli (Fig 41C), suggesting that blood flow can be directed to this specifically protected areas by specific contraction and dilatation of the arterial annuli sphincters.

# B. ALTERATIONS OF ARTERIOLAR ANNULI DURING RETINOPATHY

Retinal blood flow is altered in many diseases affecting the eye, including diabetic retinopathy (Ashton, 1953; Clermont and Bursell, 2007; Pournaras et al., 2008), hypertensive retinopathy (Ramalho and Dollery, 1968), glaucoma (Flammer et al., 2002) and age-related macular degeneration (Kur et al., 2012). Our previous results suggest a role of arteriolar annuli in the maintenance and regulation of retinal blood flow. Thus, alterations of arteriolar annuli could be implicated in the impairment of retinal circulation during retinopathy.

## B.1. Diabetic retinopathy

Diabetes mellitus is one of the most common chronic diseases in the world, and its prevalence is expected to increase to affect 500 million people in 2030 (Shaw et al., 2010). Type 2 diabetes, a disease closely associated with lifestyle and obesity, accounts for almost 90% of global cases of diabetes and is becoming a global pandemic (Zimmet et al., 2001). Diabetic retinopathy, a common and specific microvascular complication of diabetes (Tapp et al., 2003; Cheung et al., 2010), is one of the main causes of acquired blindness in the western world (Cai and Bulton, 2002; Ahmed et al., 2010). Hallmarks of diabetic retinopathy include many vascular alterations (Ramos et al, 2013).

Animal models have become an essential tool for the understanding diabetic retinopathy pathogenesis. In this regard, to analyze alterations of arteriolar annuli during diabetic retinopathy, retinas from db/db mice were studied.

db/db (*Lepr*$^{db}$) mice, homozygous for a mutation in the gene encoding the OB-R receptor for leptin (Chen et al., 1996), spontaneously develop type 2 diabetes (Coleman and Hummel, 1967). As expected, 8 month old db/db mice showed increased body weight (Fig. 43A) and blood glucose levels (Fig. 43B), when compared with age-matched control mice. In retinas from db/db mice, signs of diabetic retinopathy such as atrophy of inner and outer nuclear layers (Fig. 43C) as well as glial reactivation (Fig. 43D) were evident. To assess alterations of arteriolar annuli during type 2 diabetes, whole mount retinas from db/db mice were labeled with *Griffonia simplicifolia* (Fig. 44). As figure 44 evidences, annuli ICCs from diabetic retinas showed a marked decrease in lectin binding. Confocal quantification of fluorescence intensity demonstrated that differences in lectin binding between arteriolar annuli from db/db and control mice retinas were statistically significant (Flourescence intensity in diabetic arteriolar annuli = 54.48 $\pm$ 4.74 VS fluorescence intensity in control arteriolar annuli = 97.92 $\pm$ 9.73; p = 0.0009). Since *Griffonia simplicifolia* stains glycogen (Fig. 3), these results suggest that glycogen content is reduced in annuli ICs of db/db mice. This result is reinforced by previous experiments indicating that insulin resistance in type 2 diabetes is closely associated with a defect in the activation of glycogen synthase, driving to impaired glucose storage as glycogen (Vaag et al., 1991).

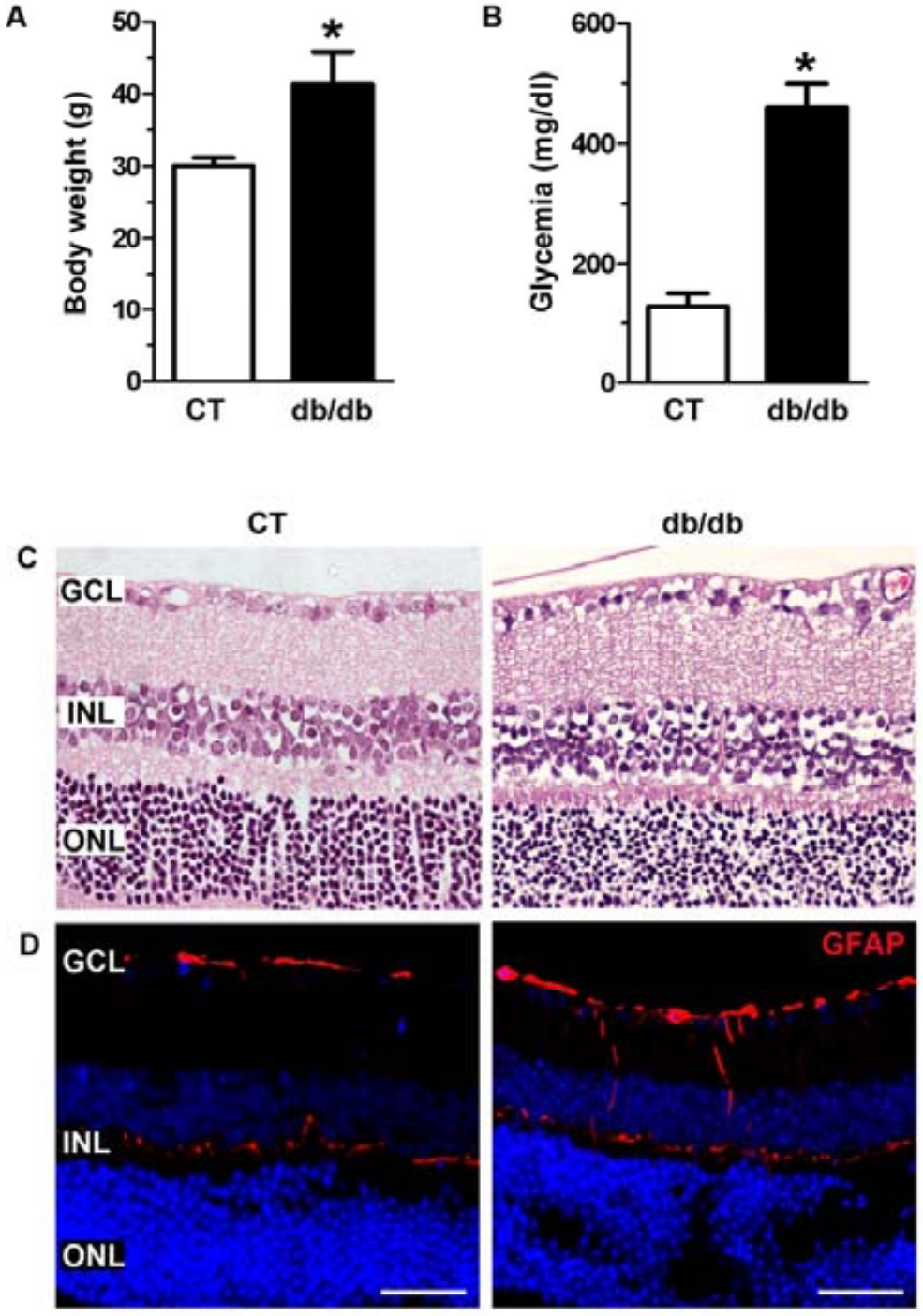


**Figure 43: Analysis of retinas from db/db mice.** (A) As bar graphs show, db/db mice were obese and hyperglycaemic. (B) Haematoxilin/eosin stained paraffin sections of db/db mice retinas showed a decreased number of cells in both inner and outer nuclear layers. (C) Glial reactivation was evident in retinas from db/db mice immunostained with an antibody against GFAP. Nuclei counterstain: Hoescht. CT: Control mice. Magnification A: 400x; Scale bars: D (left panel) = 121.72 μm; D (right panel) = 39.10 μm.

ICC damage is closely associated to smooth muscle changes and seems to be implicated in diabetic intestinal motility disorders in db/db mice (Yamamoto et al., 2007; Huizinga et al., 2009). According with this reasoning, the alteration observed in the retinal ICs of db/db mice could be a cause for

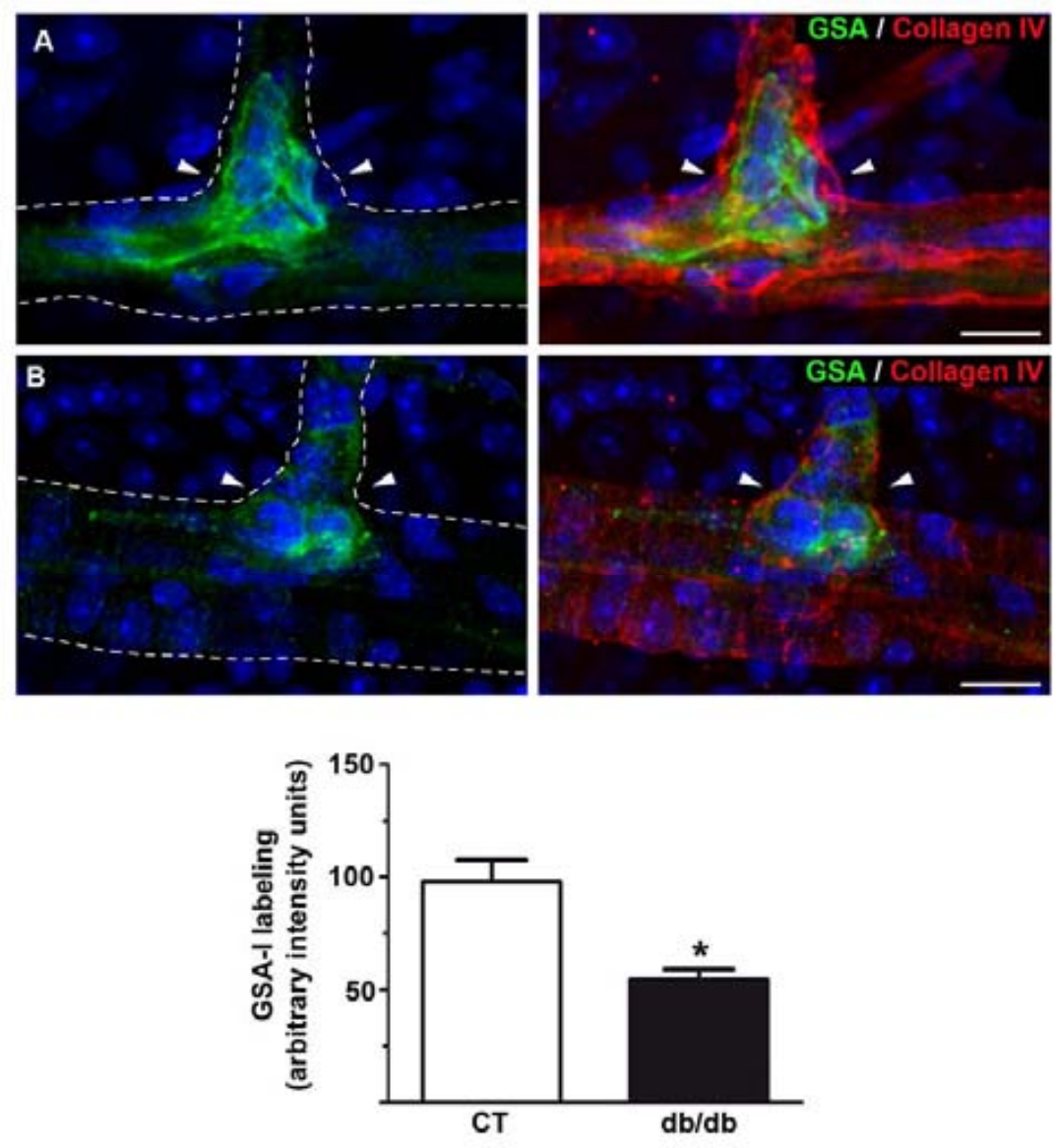


**Figure 44: Analysis of arteriolar annuli during diabetic retinopathy.** Whole mount retinas from control (A) and db/db (B) mice were labelled with *Griffonia simplicifolia* (GSA) (green) and anti-collagen IV (red) to analyze annuli morphological alterations during type 2 diabetes. A great reduction of *Griffonia simplicifolia* labelling was evident in annuli of db/db mice retinas. (C) Bar graphs evidence that differences in GSA labelling were statistically significant. Nuclei counterstain: hoescht. Arrowhead: arteriolar annuli; Asterisk: $p < 0.05$. Scale bars: A = 11.34 μm; B = 15.59 μm.

the induction of impaired blood flow during diabetic retinopathy, since our results have previously suggested a role of annuli ICs in retinal calcium dynamics, vasomotor responses and blood flow regulation (Fig. 38).

## B.2 Hypertensive retinopathy

Hypertension is a condition that affects one billion people worldwide (Grosso et al., 2005). Sustained elevation of blood pressure induces a greater risk for cardiovascular diseases (Porta et al., 2005). The retina is especially sensitive to sustained elevations of blood pressure, even during bening hypertension (Garner et al., 1975). Each 10 mmHg increase in mean arterial pressure produces a reduction of 6 microns in retinal arteriolar diameters (Wong et al., 2005).

In order to study the alterations of arteriolar annuli during hipertensive retinopathy, retinas from 8 to 11 month-old KAP transgenic mice were analyzed. KAP transgenic mice overexpress the kidney androgen-regulated protein (KAP) driven by its own promoter (pKAP2-KAP) in a cell- and androgen- restricted manner (Tornavaca et al., 2009). As expected, tail-cuff measurements of arterial pressure have shown that KAP transgenic male mice develop hypertensive phenotype at 4 months of age. In these mice, arterial pressure increases from 4 to 6 months, stabilizing at 7 months of age (data not shown).

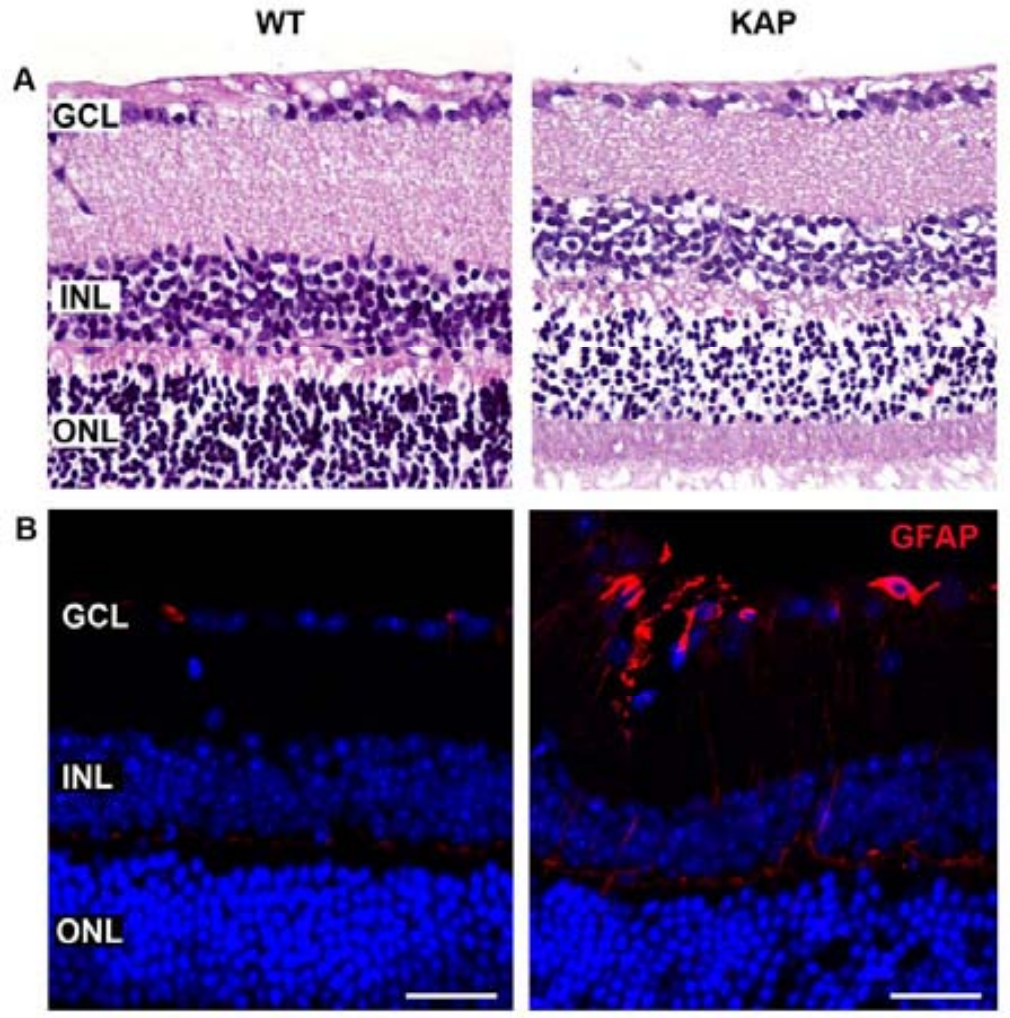


**Figure 45: Analysis of retinas from KAP transgenic mice.** (A) Paraffin sections stained with haematoxylin and eosin evidenced a great reduction in cell number of transgenic retinas when compared with wild type mice. (B) Immunostaining of paraffin sections with an anti-GFAP antibody showed glial reactivation in retinas from transgenic mice. Nuclei counterstain: Hoescht. WT: Wild type; GCL: ganglion cell layer; INL: Inner nuclear layer; ONL: Outer nuclear layer. Magnification A: 400x; Scale bars: B (left) = 32.32 μm; B (right) = 27.58 μm.

Retinas from KAP transgenic mice showed an apparent reduction in cell number (Fig. 45A) and glial activation (Fig. 45B), both signs indicative of retinopathy (Francke et al., 2003; Calandrella et al., 2007; Fletcher et al., 2010). More detailed arteriolar analysis using immunohistochemical labeling of α-SMA

demonstrated increased wall thickness in KAP transgenic mice (Fig. 46A). Moreover, collagen IV immunohistochemistry of whole mount retinas showed focal arteriolar narrowing and arteriolar nicking in KAP transgenic mice (Fig 46B).

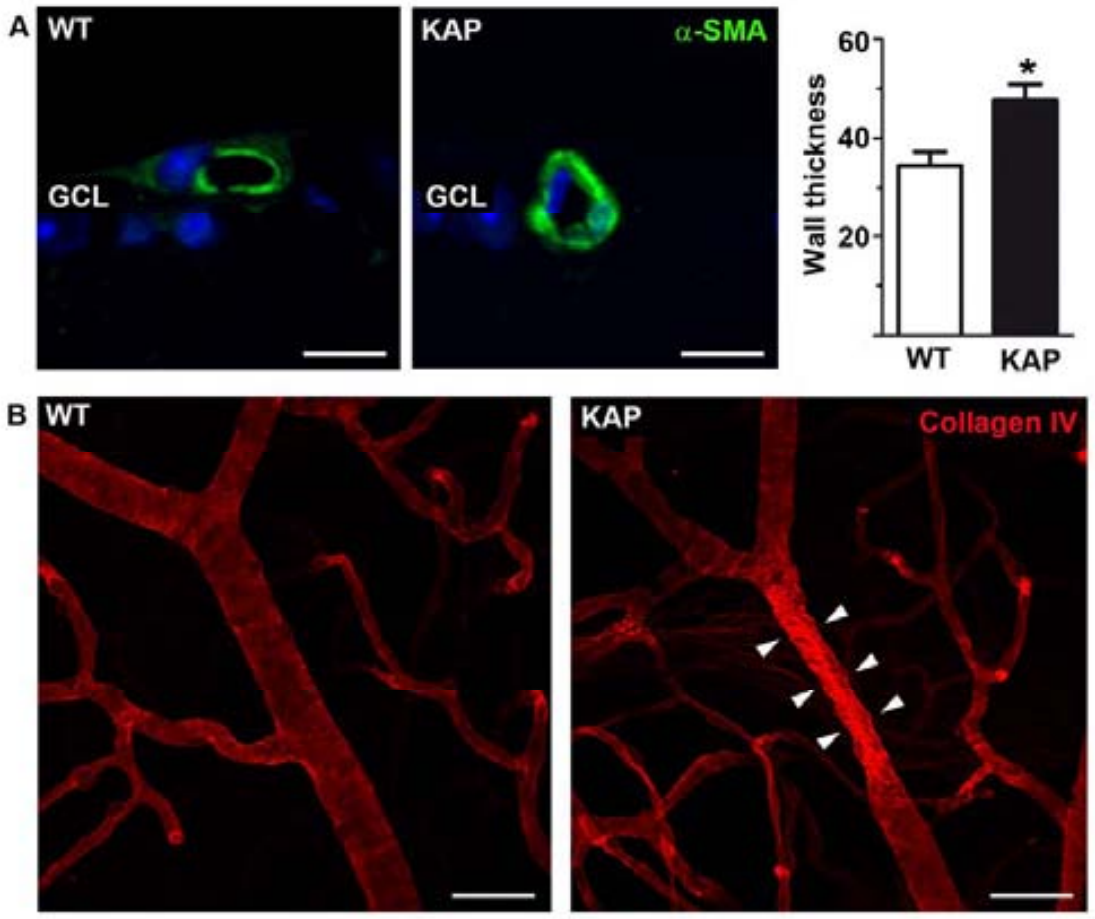


**Figure 46: Analysis of retinal vasculature in KAP transgenic mice.** (A) Immunohistochemical detection of a-smooth muscle actin (-SMA) in paraffin sections of wild type (left image) and KAP transgenic (micrograph on the right) mice showed an increase in the media layer of hypertensive mice vasculature. Bar graph evidences that differences in wall thickness were statistically significant ($p < 0.05$; $n = 4$). (B) Confocal microscopy studies in whole mount retinas immunostained with anti-collagen IV (red) antibody evidenced focal narrowing in arterioles of KAP transgenic mice. WT: Wild type; GCL; Ganglion cell layer; Arrowhead: focal arteriolar narrowing. Scale bars: A (WT) = 9.70 μm; A (KAP) = 9.48 μm; B (WT) = 39.40 μm; B (KAP) = 38.32 μm.

All these vascular changes observed in KAP transgenic mice are compatible with mild hypertensive retinopathy (Grosso et al., 2005; Wong and McIntosh, 2005).

To assess alterations of arteriolar annuli during hypertensive retinopathy, double immunohistochemistry against Ano1 and collagen IV was performed on whole mount retinas from KAP transgenic mice (Fig. 47). The expression of Ano1 was markedly diminished in annuli ICs from KAP transgenic mice (Fig. 47B), when compared with age-matched control littermates (Fig. 47A). Thus, our results suggest a loss of function of calcium-activated chloride channels in annuli ICs in the KAP transgenic mouse. These results are in accordance with recent studies demonstrating that Ano1 expression in basilar artery is down-regulated during hypertension (Wang et al., 2012).

Calcium-activated chloride channels of ICCs, and therefore Ano1, are required for pacemaker activity and proper smooth muscle contraction (Huang et al., 2009). In fact, studies in Ano1 knockout mice have demonstrated that the absence of Ano1 results in greatly reduced smooth muscle contraction (Huang et al., 2009). In retina, the first event when pressure rises is a general contraction of retinal arterioles (Garner et al., 1975). In hypertensive KAP transgenic mice, the reduction of Ano1 could be a cause for malfunction of arteriolar annuli and consequently produce an alteration of retinal blood flow.

Grande and coworkers (2011) have demonstrated that specific overexpression of KAP gene in the kidney proximal tubule induces hypertension by increased oxidative stress with activation of the renin-angiotensin system

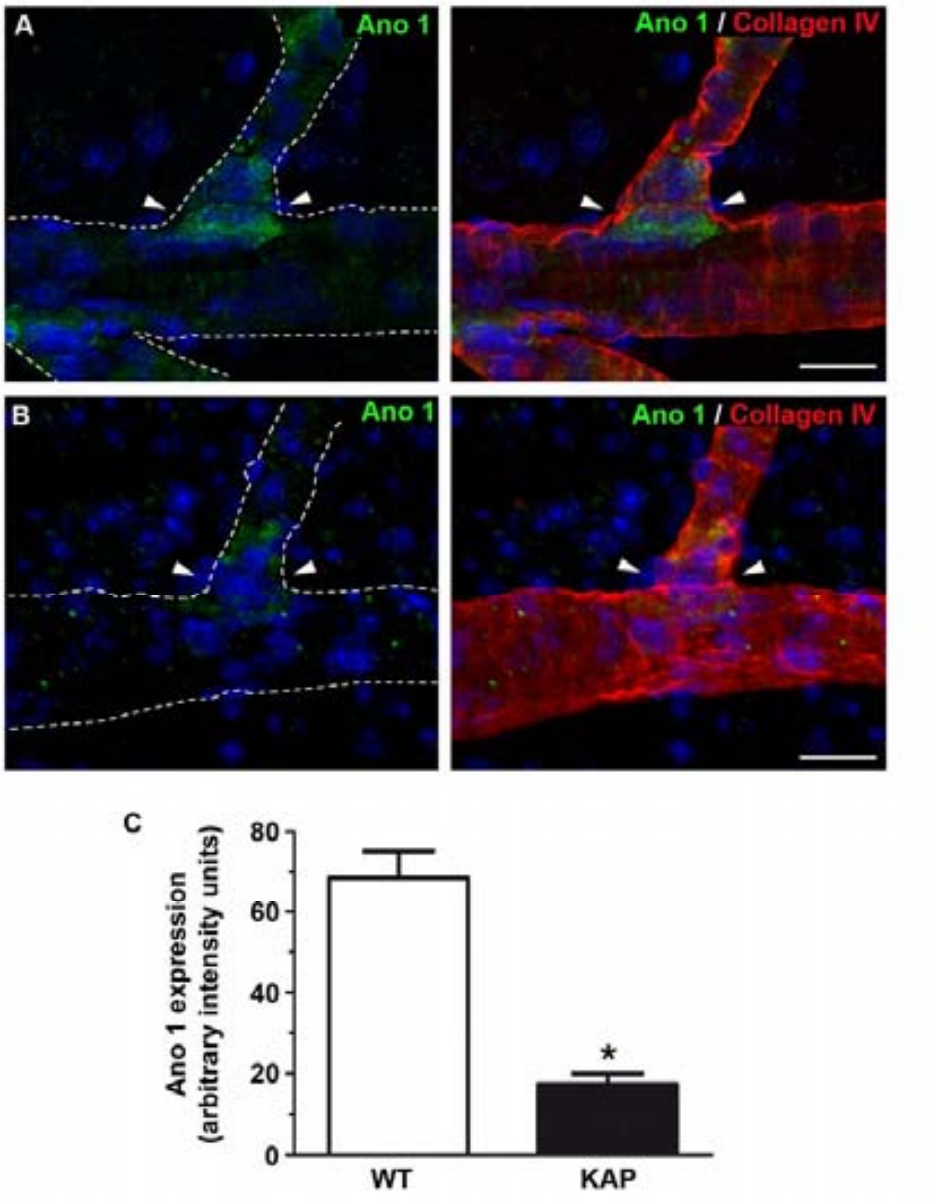


**Figure 47: Alterations of arteriolar annuli during hypertensive retinopathy.** Alterations of arteriolar annuli were assessed by double immunohistochemistry labelling anoctamin 1 (Ano 1) (green) and collagen IV (red) in whole mount retinas from wild type (A) and KAP transgenic mice (B). Confocal microscopy quantification of fluorescence intensity evidenced a great decrease of Ano 1 expression in KAP transgenic mice (B) when compared with wild type mice (A). (C) Differences in Ano 1 expression were statistically significant, as shown in bar graphs. Nuclei counterstain: ToPro 3. Arrowhead: Arteriolar annuli; Asterisk: $p< 0.05$. Scale bars: A = 17.41 μm; B = 15.50 μm.

and the sympathetic nervous system. Oxidative stress has been demonstrated to produce alterations of ICCs in gastrointestinal tract, driving to motility disorders (Choi et al., 2008; Izbeki et al., 2010). Thus, oxidative stress during hypertension in KAP transgenic mice could be one of the causes to produce damage in retinal annuli ICs.

## C. ARTERIOLAR ANNULI IN HUMAN RETINA

The existence of arteriolar annuli in human retina has been poorly documented and, due to the lack of specialized immunohistochemistry studies, the arteriolar annuli itself have not been always properly defined (Lee, 1976; Ma, 1994). Moreover, most of the authors studying this structure in different species could not detect it in man (Kuwabara and Cogan, 1960; Henkind and De Oliveira, 1968; Pournaras et al., 2008).

*Griffonia simplicifolia* specific labeling unequivocally demonstrated the presence of arteriolar annuli in human retina (Fig. 48). Moreover, preliminary studies in a retina from a diabetic donor suggest a decrease in the labeling of this lectin during diabetic retinopathy (Fig. 48 Donor 2). Thus, our results confirm the presence of arteriolar annuli in human retina suggesting, as happens in mouse, a role in the regulation of retinal blood flow. In addition, our preliminary studies on a human diabetic retina have showed similar alterations to those observed in retinas from db/db mice (Fig. 44).

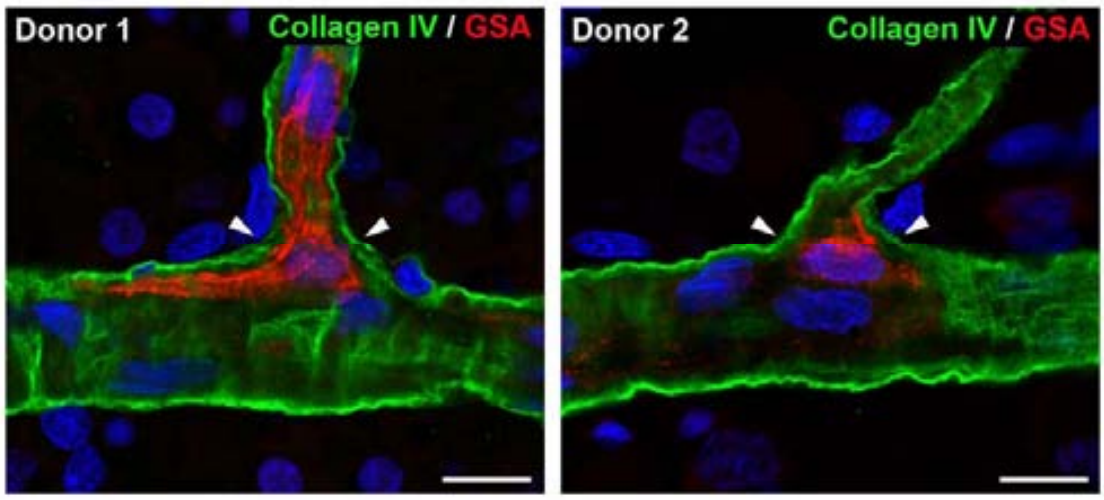


**Figure 48: Arteriolar annuli in human retina.** Labelling of *Griffonia simplicifolia* (GSA) (red) showed the presence of arteriolar annuli in human retinas. Moreover, GSA labelling was decreased in arteriolar annuli of a diabetic donor (Donor 2) when compared with a healthy retina (Donor 1). Retinal vasculature was evidenced by immunohistochemistry against collagen IV (green). Nuclei counterstain: ToPro3. Micrographs acquired by means of confocal microscopy analysis of whole mount retinas. Arrowheads: Arteriolar annuli. Scale bars: A = 13.28 μm; B = 13.25 μm.

## D. GENERAL DISCUSSION

Due to the lack of autonomous innervation, retinal blood flow is mainly controlled by local regulatory events (Firbas et al., 2005). Arteriolar annuli have been involved in retinal blood flow regulation (Pannarale et al., 1996). Our results have confirmed the presence of arteriolar annuli in mouse retina, appearing as a conical hypercellular structure of intensely PAS stained material (Fig. 12). Lectin specific binding and salivary amylase digestion have determined that specific PAS stain is mainly due to increased glycogen content in cells forming the arteriolar annuli (Fig. 14).

Detailed morphological analyses of arteriolar annuli have evidenced that vascular wall components show a distinctive structural and molecular phenotype. In this regard endothelial cells show decreased expression of CD31 (Fig. 18B), together with enhanced NADPH diaphorase (Fig. 18C) and vWF (Fig. 20A) expression. Thus, suggesting that annuli endothelial cells are able to induce vasodilatation and to maintain an antithrombotic milieu. Smooth muscle cells in the annuli appeared reoriented embracing the origin of the collateral arteriole (Fig. 33C and D). This particular disposition could indicate a sphincter-like activity by bulging annuli cells to the arteriolar lumen. In addition, ultrastuctural analysis evidenced the existence of peg-and-socket junctions between smooth muscle cells of arteriolar annuli (Fig. 33B). This result suggests a stretch-coordinated annuli contraction. Furthermore, a possible

reinforcement of basement membrane was evidenced by increased expression of its main components, including collagen IV, laminin and fibronectin (Fig. 35). A diminished colocalization of collagen IV and laminin (Fig. 36), together with differences observed in ultrastructure (Fig. 34), suggest a change in the organization of basement membrane in arteriolar annuli.

ICs have been described as a new cell population in the arteriolar annuli. Cell lineage of vascular interstitial cells is still under discussion, since some authors have reported a close relation between arterial ICC-like and smooth muscle cells (Pucovský et al., 2007). However, annuli ICs showed a morphology matching the “gold standard” ultrastructural features established for intestinal ICC identification (Huizinga et al., 1997). In addition, annuli presumptive ICCs expressed specific markers of ICCs, such as Ano1 (Fig. 24B), CD44 (Fig. 24C) and nestin (Fig. 31), although c-kit expression could not be observed (Fig. 24A). A distinctive pattern of distribution of F-actin filaments (Fig. 26A), together with an increased expression of β-actin (Fig. 28) and a lack of α-SMA (Fig. 26B) allowed further differentiation between annuli ICs and vascular smooth muscle cells.

Annuli ICs also expressed PDGF-Rβ (Fig. 25A) and NG2 (Fig. 25B), two widely used pericyte markers (Pfister et al., 2008). However, pericytes are only found in precapillary arterioles, capillaries and venules (Pucovský et al., 2007) while annuli ICs were located in the main retinal arteriolar branching sites. Moreover, ultrastructure of annuli ICs does not correspond to that of pericytes.

Thus, these facts make unlikely the possibility that annuli ICs belong to pericyte or smooth muscle cell types.

ICCs regulate motility of gastrointestinal tract by means of three well-accepted functions (Formey et al., 2011). Similarly, our results suggest that annuli ICCs perform functions of:

**(1) Pacemaker activity:** ICCs controls the frequency and propagation of contractile activity by periodic calcium release that, in turn, induces rhythmic depolarization in the electrically coupled smooth muscle cells (Yoneda et al., 2001; Popescu et al., 2005; Huang et al., 2009). Annuli ICCs showed structural and molecular features important for this pacemaker activity, such as the expression of the PDGF-Rβ (Fig. 25A), the calcium-activated chloride channel subunit Ano1 (Fig. 24B) and the gap junction protein connexin 43 (Fig. 23C).

**(2) Neuromodulation:** physiological experiments have evidenced a key role of ICCs as mediators of intestinal nitrergic neurotransmission (Iino et al., 2008). Annuli endothelial cells (Fig. 18C) and ICs (Fig. 25C) showed increased NADPH diaphorase activity. Thus, the modulation of annuli activity by NO is also suggested.

**(3) Mechanotransduction:** mechanical distortion of ICCs increases pacemaker activity (Huizinga et al., 2009). Annuli ICs have shown an

increased expression of CD44 (Fig 24C). Cell adhesion molecules, such as CD44, couple extracellular matrix and nuclear matrix scaffolds by means of cytoskeleton filaments (Ingber, 1997). Thus, mechanical changes in basement membrane can be transmitted to the nucleus triggering biochemical responses (Ingber, 1997). Moreover, CD44 has been implicated in the adhesion of cells to basement membrane proteins laminin and fibronectin (Underhill, 1992), which are overexpressed in arteriolar annuli (Fig. 24B and C). Annuli ICs also showed high expression of nestin (Fig. 31), an intermediate filament, known to act as a modulator of mechanical strength by coordinating cytoskeleton dynamics. Thus, annuli ICs show structural and molecular features suggesting that these cells, subjected to a mechanical deformation, could act as mechanotransducers leading to specific cellular responses.

Taken together, our results suggest that arteriolar annuli are endowed with specific molecular, structural and functional characteristics which allow them playing a key role in the retinal blood flow regulation.

Vascular alterations are related to many retinopathies, including diabetic and hypertensive retinopathy (Kur et al., 2012; Wong et al., 2005). The analyisis of arteriolar annuli in db/db mice evidenced impaired glycogen storage in annuli ICs (Fig. 44). In addition, our studies in KAP transgenic mice retinas evidenced

a decreased expression of Ano1 in annuli ICCs during hypertensive retinopathy (Fig. 47), suggesting a loss of function of calcium-activated chloride channels. Thus, alterations observed in the retinal ICs could induce an impaired function of arteriolar annuli driving to dysregulation of blood flow during retinopathy.

*Griffonia simplicifolia* evidenced the presence of arteriolar annuli in human retina (Fig. 36). Moreover, annuli ICs from a diabetic donor showed a decreased binding of this lectin (Fig. 48), as happened in db/db mice (Fig. 44). Thus our results suggest a similar role of arteriolar annuli in human and mouse retinal blood flow regulation in health and disease.

# *CONCLUSIONS*

1. 55% of arteriolar branches in mouse retina show annuli.

2. Arteriolar annuli are found more frequently in the central retina.

3. The increased PAS positive staining observed in arteriolar annuli match the high expression of several carbohydrates, as evidenced by lectin histochemistry.

4. Amylase retinal digestion, previous to GS lectin staining, indicates that glycogen accumulates in annuli cells.

5. Three types of cells are localized at the arteriolar annuli: endothelial, interstitial (ICs) and smooth muscle cells.

6. Annuli endothelial cells display a specific molecular phenotype characterized by the decreased expression of CD31. No differences are observed in CD34 expression.

7. Ultrastructural analysis of arteriolar annuli shows two endothelial cell subpopulations. A subtype I, with characteristics of activated endothelial cells, and subtype II having the morphological features observed in endothelial cells under increased shear stress.

8. von Willebrand factor and Weibel-Palade bodies accumulate in the cytoplasm of annuli endothelial cells. Thus, suggesting that endothelial cells maintain an antithrombotic milieu at the arteriolar annuli.

9. The increased expression of NADPH diaphorase in annuli endothelial cells could indicate a predominance of vasodilatation at the arteriolar annuli.

10. Blood retinal barrier is preserved at the arteriolar annuli.

11. At ultrastructural level, ICs have multiple long thin cytoplasmatic processes, multilobulated nuclei, numerous caveolae and large mitochondria. All these morphological features are similar to those presented by Intersticial Cajal cells.

12. Annuli ICs molecular phenotype is characterized by the expression of Ano 1, CD44, PDGF-Rβ, NG2 and NADPH diaphorase, and the absence of c-kit expression. Thus, confirming that ICs are a special subtype of Intersticial Cajal cells.

13. Annuli ICs present gap junctions that allow communication with smooth muscle and endothelial cells, as evidenced by transmission electron microscopy and connexin 43 expression.

14. In contrats to β-actin that is upregulated, α-actin is downregulated in annuli ICs, suggesting that these cells do not contract.

15. The stem cell marker nestin is specifically expressed in the annuli ICs.

16. Smooth muscle cells do not form a true sphincter at the arteriolar annuli. Only a single layer of smooth muscle cells is lining the annuli. However, their specific arrangement surrounding the annuli, allows the vascular closure by bulging ICs and endothelial cells into the lumen.

17. Annuli smooth muscle cells are coupled by peg and socket junctions, suggesting a coordinated mechanism of contraction.

18. The ultrastructural analysis evidenced a great thickening of the basement membranes at the arteriolar annuli. Collagen IV, laminin and fibronectin are increased and diferentially organized.

19. In vivo visualization shows a localized contracting activity at the arteriolar annuli.

20. ICs and smooth muscle cells show different intracellular calcium events during annuli contraction.

21. Annuli ICs are in close contact with Müller cells and annuli smooth muscle cells, suggesting a role of these cells in neurovascular coupling.

22. In mouse retina there are specific regions resistant to hypoxia. Increased presence of arteriolar annuli is associated with these areas.

23. Decreased GSA binding at the arterial annuli is observed in a model of diabetes type II (db/db mice), suggesting an impaired glycogen storage during diabetic retinopathy.

24. Decreased expression of Ano1 at the arterial annuli is observed in a model of hypertension (KAP mice), suggesting a deficiency of the annuli contraction during hypertensive retinopathy.

25. Arterial annuli are present in man retina. Preliminary results may suggest its alteration during retinopathy.

26. Final conclusion: Retinal arteriolar annuli display specific structural, molecular and functional features, suggesting an important role of these structures as discrete sites for blood flow regulation during health and retinopathy.

# *BIBLIOGRAPHY*

- Agrawal PK, Agarwal LP, Tandon HD. **Retinal vasculature in mammalia.** *Indian Journal of Ophtalmology* **(1968)** 16(1): 3-11.

- Ahmed KA, Muniandy S and Ismail IS. **Type 2 Diabetes and Vascular Complications: A pathophysiologic view.** *Biomedical Research* **(2010)** 21(2): 147-155

- Aird WC. **Mechanisms of Endothelial Cell Heterogeneity in Health and Disease.** *Circulation Research* **(2006)** 98:159-162.

- Aird WC. **Phenotypic heterogeneity of the endothelium: I. Structure, function, and mechanisms.** *Circulation Research* **(2007)** 100(2): 158-73.

- Aird WC. **Endothelial Cell Heterogeneity.** *Cold Spring Harbor Laboratory Press* **(2012)** 2: a006429 1-13.

- Allen PG, Shuster CB, Käs J, Chaponnier C, Janmey A and Herman IM. **Phalloidin Binding and Rheological Diffreneces among Actin Isoforms.** *Biochemistry* **(1996)** 35: 14062-14069.

- Alm A and Bill A. **Ocular and optic nerve blood flow at normal and increased intraocular pressures in monkeys (*Macaca irus*): a study with radioactively labelled microspheres including flow determinations in brain and some other tissues.** *Experimental Eye Research* **(1973)** 15(1): 15-29.

- Al-Shabrawey M, El-Remessy A, Gu X, Brooks SS, Hamed MS, Huang P, Caldwell RB. **Normal vascular development in mice deficient in endothelial NO synthase: possible role of neuronal NO synthase.** *Molecular Vision* **(2003)** 9: 549-558.

- Amir S, Edelstein K. **A blocker of nitric oxide synthase, NG-nitro-L-arginine methyl ester, attenuates light-induced Fos protein expression in rat suprachiasmatic nucleus.** *Neuroscience Letters* **(1997)** 224(1): 29-32.

- Anderson B, McIntosh HD. **Retinal Circulation.** *Annual Review of Medicine* **(1967)** 18: 15-26.

- Anderson RG. **The caveolae membrane system.** *Annual Review of Biochemistry* **(1998)** 67: 199-225.

- Ando A, Yang A, Nambu H and Campochiaro PA. **Blockade of Nitric-Oxide Syntahse Reduces Choroidal Neovascularization.** *Molecular Pharmacology* **(2002)** 62(3): 539-544

- Armulik A, Genové G, Betsholtz C. **Pericytes: developmental, physiological, and pathological perspectives, problems, and promises.** *Developmental Cell* **(2011)** 21(2): 193-215.

- Ashton N. **Arteriolar involvement in diabetic retinopathy.** *The British journal of ophthalmology* **(1953)** 37(5): 282-292.

- Bayguinov PO, Henning GW and Smith TK. **$Ca^{2+}$ imaging of activity in ICC-MY during local mucosal reflexes and the colonic migrating motor complex in the murine large intestine.** *Journal of Physiology* **(2010)** 588(Pt22): 4453-4474.

- Bergers G, Song S. **The role of pericytes in blood-vessel formation and maintenance.** *Neuro-Oncology* **(2005)** 7(4): 452-464.

- Bois RM. **The organization of contractile apparatus of vertebrate smooth muscle.** *The Anatomical Record* **(1973)** 177(1): 61-77.

- Bratic A, Wredenberg A, Grönke S, Stewart JB, Mourier A, Ruzzenente B, Kukat C, Wibom R, Habermann B, Partridge L and larsson NG. **The Bicoid Stability Factor Controls Polyadenylation and Expression of Specific Mitochondrial mRNAs in *Drosophila melanogaster.*** *PLOS Genetics* **(2011)** 7(10): e1002324

- Bristow EA, Griffiths PG, Andrews RM, Johnson MA and Turnbull DM. **The Distribution of Mitochondrial Activity in Relation to Optic Nerve Structure.** *Archives of Ophtalmology.* **(2002)** 120(6): 791-796.

- Bobryshev YV. **Subset of cells immunopositive for neurokinin-1 receptor identified as arterial interstitial cells of Cajal in human large arteries.** *Cell and Tissue Research* **(2005)** 321(1): 45-55.

- Cai J and Bulton M. **the pathogenesis of diabetic retinopathy: old concepts and new questions.** *Eye* **(2002)** 16: 242-260.

- Calabrese G, Fernandez de Recondo M, Recondo E, Wainstok de Calmanovici R. **Platelet endothelial cell adhesion molecule-1 expression during mouse postimplantation development.** *Cellular and Molecular Biology (Noisy-le-grand)* **(1998)** 44(3): 537-541.

- Calandrella N, Scarsella G, Pescosolido N, Risuleo G. **Degenerative and apoptotic events at retinal and optic nerve level after experimental induction of ocular hypertension.** *Molecular and Cellular Biochemistry* **(2007)** 301(1-2): 155-163.

- Chakravarty U, Stitt AW, McNally J, Bailie JR, Hoey EM and Duprex P. **Nitric oxide synthase activity and expression in retinal capillary endothelial cells and pericytes.** *Current Eye Research* **(1995)** 14: 285-294.

- Chen H, Charlat O, Tartaglia LA, Woolf EA, Weng X, Ellis SJ, Lakey ND, Culpepper J, Moore KJ, Breitbart RE, Duyk GM, Tepper RI, Morgenstern JP. **Evidence that the diabetes gene encodes the leptin receptor: identification of a mutation in the leptin receptor gene in db/db mice.** *Cell* **(1996)** 84(3): 491-495.

- Chen L, Yang P and Kijlstra A. **Distribution, markers, and functions of retinal microglia.** *Ocular Immunology and Inflammation*. **(2002)** 10: 27-39.

- Cheung N, Mitchell P, Wong TY. **Diabetic retinopathy.** *Lancet* **(2010)** 376(9735): 124-136.

- Choi KM, Gibbons SJ, Nguyen TV, Stoltz GJ, Lurken MS, Ordog T, Szurszewski JH and Farrugia G. **Heme Oxygenase-1 Protects Interstitial Cells of Cajal from Oxidative Stress and Reverses Diabetic gastroparesis.** *Gastroenterology* **(2008)** 135(6): 2055-2064.

- Cines DB, Pollak ES, Buck CA, Loscalzo J, Zimmerman GA, McEver RP, Pober JS, Wick TM, Konkle BA, Schwartz BS, Barnathan ES, McCrae KR, Hug BA, Schmidt AM, Stern DM. **Endothelial cells in physiology and in the pathophysiology of vascular disorders.** *Blood* **(1998)** 91(10): 3527-3561.

- Ciontea SM, Radu E, Regalia T, Ceafalan L, Cretoiu D, Gherghiceanu M, Braga RI, Malincenco M, Zagrean L, Hinescu ME, Popescu LM. **C-kit immunopositive interstitial cells (Cajal-type) in human myometrium.** *Journal of Cellular and Molecular Medicine* **(2005)** 9(2): 407-420.

- Clermont AC, Bursell SE. **Retinal blood flow in diabetes.** *Microcirculation* **(2007)** 14(1): 49-61.

- Coleman DL, Hummel KP. **Studies with the mutation, diabetes, in the mouse.** *Diabetologia* **(1967)** 3(2): 238-248.

- Cooper JA. **Effects of cytochalasin and phalloidin on actin.** *The Journal of cell biology* **(1987)** 105(4): 1473-1478.

- Cooper GM and Hausman RE. **Paredes celulares, matriz extracellular e interacciones celulares (Chapter 14)** pp. 571-599. *Ed. Marbán.* 5TH Edition **(2010).**

- Coultas L, Chawengsaksophak K, Rossant J. **Endothelial cells and VEGF in vascular development.** *Nature* **(2005)** 438(7070): 937-45.

- Cross PC and Mercer KL. **Cell and Tissue Ultrastructure. A Functional Perspective.** *Ed. W.H. Freeman and Company.* 6TH Edition **(1993).**

- Cunha-Vaz JG. **The blood-retinal barriers**. *Documenta Ophthalmology* **(1976)** 41(2): 287-327.

- Dahl E, Nelson E. **Electron microscopi observations on human intracranial arteries. Arteries. II. Innervation.** *Archives of neurology* **(1964)** 10: 158-164.

- Daniel EE. **Communication between interstitial cells of Cajal and gastrointestinal muscle.** *Neurogastroenterology and Motility: the official journal of the European Gastrointestinal Motility Society* **(2004)** 16 Suppl 1: 118-22.

- Dawson TM, Bredt DS, Fotuhi M, Hwang PM, Snyder SH. **Nitric oxide synthase and neuronal NADPH diaphorase are identical in brain and peripheral tissues.** *Proceedings of the National Academy of Sciences of the United States of America* **(1991)** 88(17): 7797-801.

- De Angelis K, Irigoyen MC, Morris M. **Diabetes and cardiovascular autonomic dysfunction: application of animal models.** *Autonomic neuroscience : basic & clinical* **(2009)** 145(1-2): 3-10.

- Dealey C and van De Voorde J. **Regulatory mechanisms in the retinal and choroidal circulation.** *Ophtalmic Research*. **(2000)** 32(6): 249-256.

- Debray H, Decout D, Strecker G, Spik G, Montreuil J. **Specificity of twelve lectins towards oligosaccharides and glycopeptides related to N-glycosylproteins.** *European journal of biochemistry / FEBS* **(1981)** 117(1): 41-55.

- D'Orléans-Juste P, Claing A, Télémaque S, Maurice MC, Yano M, Gratton JP. **Block of endothelin-1-induced release of thromboxane A2 from the guinea pig lung and nitric oxide from the rabbit kidney by a selective ETB receptor antagonist, BQ-788.** *British journal of pharmacology* **(1994)** 113(4): 1257-1262.

- Dräger UC, Edwards DL, Barnstable CJ. **Antibodies against filamentous components in discrete cell types of the mouse retina.** *The Journal of Neuroscience* **(1984)** 4(8): 2025-2042.

- Dreher Z, Robinson SR and Distler C. **Müller cells in vascular and avascular retinae: A survey of seven mammals.** *Journal of Compartive Neurology.* **(1992)** 323(1): 59-80.

- Dumortier J, Daemi N, Pourreyron C, Anderson W, Bellaton C, Jacquier M-F, Bertrand S, Chayvialle J-A, Remy L. **Loss of epithelial differentiation markers and acquisition of vimentin expression after xenograft with laminin-1 enhance migratory and invasive abilities of human colon cancer cells LoVo C5.** *Differentiation* **(1998)** 63(3): 141-150.

- Duong TQ, Ngan SC, Ugurbil K, Kim SG. **Functional magnetic resonance imaging of the retina.** *Investigate Ophthalmoly & Visual Science* **(2002)** 43(4): 1176-1181.

- Duquette RA, Shmygol A, Vaillant C, Mobasheri A, Pope M, Burdyga T, Wray S. **Vimentin-positive, c-kit-negative interstitial cells in human and rat uterus: a role in pacemaking?** *Biology of Reproduction* **(2005)** 72(2): 276-83.

- Evans WH, Martin PE. **Gap junctions: structure and function (Review).** *Molecular Membrane Biology* **(2002)** 19(2): 121-136.

- Farrugia G. **Interstitial cells of Cajal in health and disease.** *Neurogastroenterology and motility : the official journal of the European Gastrointestinal Motility Society* **(2008)** 20 Suppl 1: 54-63.

- Faulstich H, Zobeley S, Rinnerthaler G, Small JV. **Fluorescent phallotoxins as probes for filamentous actin.** *Journal of muscle research and cell motility* **(1988)** 9(5): 370-383.

- Flammer J, Orgül S, Costa VP, Orzalesi N, Krieglstein GK, Serra LM, Renard JP, Stefánsson E. **The impact of ocular blood flow in glaucoma.** *Progress in Retinal and Eye Research* **(2002)** 21(4): 359-393.

- Fletcher EL, Downie LE, Hatzopoulos K, Vessey KA, Ward MM, Chow CL, Pianta MJ, Vingrys AJ, Kalloniatis M, Wilkinson-Berka JL. **The significance of neuronal and glial cell changes in the rat retina during oxygen-induced retinopathy.** *Documenta ophthalmologica. Advances in ophthalmology* **(2010)** 120(1): 67-86.

- Félétou M. **The Endothelium: Part 1: Multiple Functions of the Endothelial Cells—Focus on Endothelium-Derived Vasoactive Mediators.** *San Rafael (CA): Morgan & Claypool Life Sciences* **(2011)**. Integrated Systems Physiology: from Molecule to Function to Disease.

- Formey A, Buscemi L, Boittin FX, Bény JL, Meister JJ. **Identification and functional response of interstitial Cajal-like cells from rat mesenteric artery.** *Cell and tissue research* **(2011)** 343(3): 509-519.

- Fourman J and Moffat DB. **The effect of intra-arterial cushions on plasma skimming in small arteries.** *Journal of Physiology.* **(1961)** 158: 374-380.

- Fraga CH, True LD and Kirk D. **Enhanced expression of the mesenchymal marker, vimentin, in hyperplastic versus normal human prostatic epithelium.** *The Journal of Urology* **(1998)** 159 (1): 270-274.

- Francke M, Uhlmann S, Pannicke T, Goczalik I, Uckermann O, Weick M, Härtig W, Wiedemann P, Reichenbach A, Bringmann A. **Experimental dispase-induced retinopathy causes up-regulation of P2Y receptor-mediated calcium responses in Müller glial cells.** *Ophthalmic Research* **(2003)** 35(1): 30-41.

- Frank RN, Turczyn TJ, Das A. **Pericyte coverage of retinal and cerebral capillaries.** *Investigative Ophthalmology & Visual Science* **(1990)** 31(6): 999-1007.

- Frank PG, Pavlides S, Lisanti MP. **Caveolae and transcytosis in endothelial cells: role in atherosclerosis.** *Cell and Tissue Research* **(2009)** 335(1): 41-47.

- Friedman E, Smith TR and Kuwabara T. **Retinal microcirculation in vivo.** *Investigative Ophtalmology* **(1964)** 3(2): 217-226.

- Fuchs E, Cleveland DW. **A structural scaffolding of intermediate filaments in health and disease.** *Science* **(1998)** 279(5350): 514-519.

- Funk RH. **Blood supply of the retina.** *Ophtalmic Research* **(1997)** 29(5): 320-325.

- Furuse M, Fujimoto K, Sato N, Hirase T, Tsukita S, Tsukita S. **Overexpression of occludin, a tight junction-associated integral membrane protein, induces the formation of intracellular multilamellar bodies bearing tight junction-like structures.** *Journal of Cell Science* **(1996)** 109( Pt 2): 429-35.

- Gardiner TA, Archer DB, Curtis TM, Stitt AW. **Arteriolar involvement in the microvascular lesions of diabetic retinopathy: implications for pathogenesis.** *Microcirculation* **(2007)** 14(1): 25-38.

- Gardner TW, Antonetti DA, Barber AJ, LaNoue KF, Levison SW and The Penn State Retina Research Group. **Diabetic Retinopathy: more than meets the eye.** *Survey of Ophtalmology* **(2002)** 47(2): s253-s261.

- Gardner TW, Antonetti DA, Barber AJ, Lieth E, Tarbell JA. **The molecular structure and function of the inner blood-retinal barrier. Penn State Retina Research Group.** *Documenta Ophthalmologica* **(1999)** 97(3-4): 229-237.

- Garner A, Ashton N, Tripathi R, Kohner EM, Bulpitt CJ, Dollery CT. **Pathogenesis of hypertensive retinopathy. An experimental study in the monkey.** *The British journal of ophthalmology* **(1975)** 59(1): 3-44.

- Gartner IP and Hiatt JL. **Texto atlas de Histologia.** McGraw Hill Interamericana EM-H, Ed. **(1997).**

- Gee KR, Brown KA, Chen WN, Bishop-Stewart J, Gray D, Johnson I. **Chemical and physiological characterization of fluo-4 Ca(2+)-indicator dyes.** *Cell Calcium* **(2000)** 27(2): 97-106.

- Gelse K, Pöschl E, Aigner T. **Collagens – structure, function and biosynthesis.** *Advanced Drug Delivery Reviews* **(2003)** 55(12): 1531-1546.

- Germer A, Biedermann B, Wolburg H, Schuck, Grosche J, Kuhrt H, Reichelt W, Schousboe A, Paasche G, Mack AF and Reichenbach A. **Distribution of mitochondria within Müller cells-I. Correlation with retinal vascularization in different mammalian species.** *Journal of Neurocytology.* **(1998)** 27(5): 329-345.

- Gerrity RG, Richardson M, Somer JB, Bell FP, Schwartz CJ. **Endothelial Cell Morphology in Areas of In Vivo Evans Blue Uptake in the Aorta of Young Pigs**. II. **Ultrastructure of the Intima in Areas of Differing Permeability to Proteins.** *American Journal of Pathology* **(1977)** 89(2): 313-334.

- Gherghiceanu M, Popescu LM. **Interstitial Cajal-like cells (ICLC) in human resting mammary gland stroma. Transmission electron microscope (TEM) identification.** *Journal of cellular and molecular medicine* **(2005)** 9(4): 893-910.

- Giepmans BN, Feiken E, Gebbink MF, Moolenaar WH. **Association of connexin43 with a receptor protein tyrosine phosphatase.** *Cell Communication & Adhesion* **(2003)** 10(4-6): 201-205.

- Goldstein IM, Ostwald P, Roth S. **Nitric oxide: a review of its role in retinal function and disease.** *Vision Research* **(1996)** 36(18): 2979-2994.

- Gomez-Pinilla PJ, Gibbons SJ, Bardsley MR, Lorincz A, Pozo MJ, Pasricha PJ, Van de Rijn M, West RB, Sarr MG, Kendrick ML, Cima RR, Dozois EJ, Larson DW, Ordog T, Farrugia G. **Ano1 is a selective marker of interstitial cells of Cajal in the human and mouse**

**gastrointestinal tract. American journal of physiology.** *Gastrointestinal and liver physiology* **(2009)** 296(6): G1370-1381.

- Gooyer TE, Stevenson KA, Humphries P, Simpson DA, Gardiner TA and Stitt AW. **Retinopathy is reduced during experimental diabetes in a mouse model of outer retinal degeneration.** *Investigative Ophthalmology and Visual Science* **(2006)** 47(12): 5561-5568.

- Goupille O, Saint Cloment C, Lopes M, Montarras D, Robert B. **Msx1 and Msx2 are expressed in sub-populations of vascular smooth muscle cells.** *Developmental Dynamics* **(2008)** 237(8): 2187-2194.

- Grande MT, Pascual G, Riolobos AS, Clemente-Lorenzo M, Bardaji B, Barreiro L, Tornavaca O, Meseguer A, López-Novoa JM. **Increased oxidative stress, the renin-angiotensin system, and sympathetic overactivation induce hypertension in kidney androgen-regulated protein transgenic mice.** *Free Radical Biology & Medicine* **(2011)** 51(10): 1831-1841.

- Grosso A, Veglio F, Porta M, Grignolo FM, Wong TY. **Hypertensive retinopathy revisited: some answers, more questions.** *The British journal of ophthalmology* **(2005)** 89(12): 1646-1654.

- Guyton AC and Hall JE. **Textbook of medical physiology.** *Ed. Elsevier Inc.* 11$^{TH}$ edition. **(2006)**.

- Haefliger IO, Meyer P, Flammer J and Lüscher TF. **The vascular endothelium as a regulator of the ocular circulation: A new concept in ophthalmology?** *Survey of Ophthalmology* **(1994)** 39(2): 123-132.

- Hammes HP, Martin S, Federlin K, Geisen K, Brownlee M. **Aminoguanidine treatment inhibits the development of experimental diabetic retinopathy.** *Proceedings of the National Academy of Sciences of the United States of America* **(1991)** 88(24): 11555-11558.

- Hathaway DR, March KL, Lash JA, Adam LP and Wilensky RL. **Vascular smooth muscle. A review of the molecular basis of contractility.** *Circulation* **(1991)** 83: 382-390.

- Hardy DO, Ge RS, Catterall JF, Hou YT, Penning TM, Hardy MP. . *Endocrinology* **(2000)** 141(5): 1608-1617.

- Harhun MI, Pucovský V, Povstyan OV, Gordienko DV and Bolton TB. **Interstitial cells in the vasculature.** *Journal of Cellular and Molecular Medicine* **(2005)** 9(2): 232-243.

- Harhun MI, Szewczyk K, Laux H, Prestwich SA, Gordienko DV, Moss RF, Bolton TB. **Interstitial cells from rat middle cerebral artery belong to smooth muscle cell type.** *Journal of Cellular and Molecular Medicine* **(2009)** 13(11-12): 4532-4539.

- Hassell JR, Leyshon WC, Ledbetter SR, Tyree B, Suzuki S, Kato M, Kimata K, Kleinman HK. **Isolation of two forms of basement membrane proteoglycans.** *The Journal of biological chemistry* **(1985)** 260(13): 8098-8105.

- Hashitani H, Lang RJ. **Functions of ICC-like cells in the urinary tract and male genital organs.** *Journal of cellular and molecular medicine* **(2010)** 14(6A): 1199-1211.

- Haverkamp S, Kolb H, Cuenca N. **Endothelial nitric oxide synthase (eNOS) is localized to Müller cells in all vertebrate retinas.** *Vision Research* **(1999)** 39(14): 2299-2303.

- Haynes BF, Telen MJ, Hale LP, Denning SM. **CD44--a molecule involved in leukocyte adherence and T-cell activation.** *Immunolology Today* **(1989)** 10(12): 423-428.

- Heidger PM Jr, Van Orden DE, Farley DB. **Electron microscopic and histochemical characterization of intra-arterial cushions of the rat and porcine uterine vascular bed.** *Acta Anatomica* **(1983)** 117(3): 239-247.

- Henkind P, De Oliveira LF. **Retinal Arteriolar Annuli.** Investigative *Ophtalmology and Visual Science* **(1968)** 7(5): 584-591.

- Hennigar RA, Mayfield RK, Harvey JN, Ge Z-H, Sens DA. **Lectin detection of renal glycogen in rats with short-term streptozotocin-diabetes.** *Diabetologia* **(1987)** 30(10): 804-811.

- Hennigar RA, Schulte BA, Spicer SS. **Histichemical detection of glycogen using *Griffonia simplicifolia* agglutinin II.** *The Histochemical Journal* **(1986)** 18(11-12): 589-596.

- Henry CBS, DeFouw DO. **Differential Lectin Binding to MIcrovascular Endothelial Glycoconjugates uring Normal Angiogenesis in the Chick Chorioallantoic Membrane.** *Microvascular Research* **(1995)** 49(2): 201-211.

- Herman IM, D'Amore PA. **Microvascular pericytes contain muscle and nonmuscle actins.** *The Journal of Cell Biology* **(1985)** 101(1): 43-52.

- Herrmann H and Aebi U. **Intermediate filaments and their associates: multitalented structural elements specifying cytoarchitecture and cytodynamics.** *Current Opinion in Cell Biology* **(2000)** 12: 79-90.

- Herrmann H and Aebi U. **Intermediate filaments: molecular structure, assembly mechanism, and integration into functionally distinct intracellular Scaffolds.** *Annual review of biochemistry* **(2004)** 73: 749-89.

- Hinescu ME, Ardeleanu C, Gherghiceanu M and Popescu LM. **Interstitial Cajal-like cells in human gallbladder.** Journal of Molecular Histology **(2007)** 38(4): 275-284.

- Hinescu ME, Popescu LM. **Interstitial Cajal-like cells (ICLC) in human atrial myocardium.** *Journal of cellular and molecular medicine* **(2005)** 9(4): 972-975.

- Hinescu ME, Gherghiceanu M, Mandache E, Ciontea SM and Popescu LM. **Interstitial Cajal-like cells (ICLC) in atrial myocardium: ultrastructural and immunohistochemical characterization.** *Journal of Cellular and Molecular Medicine* **(2006)** 10(1): 243-257.

- Hinescu ME, Popescu LM, Gherghiceanu M, Faussone-Pellegrini MS. **Interstitial Cajal-like cells in rat mesentery: an ultrastructural and immunohistochemical approach.** *Journal of cellular and molecular medicine* **(2008)** 12(1): 260-270.

- Hirase T, Staddon JM, Saitou M, Ando-Akatsuka Y, Itoh M, Furuse M, Fujimoto K, Tsukkita S and Rubin LL. **Occludin as a possible determinant of tight junction permeability in endothelial cells.** *Journal of Cell Science* **(1997)** 110: 1603-1613.

- Hirata Y, Emori T, Eguchi S, Kanno K, Imai T, Ohta K, Marumo F. **Endothelin receptor subtype B mediates synthesis of nitric oxide by cultured bovine endothelial cells.** *The Journal of clinical investigation* **(1993)** 91(4): 1367-1373.

- Hoffman M and Monroe III DM. **A Cell-based Model of Hemostasis.** *Thrombosis and Haemostasis* **(2001)** 85: 958-965.

- Hoffmann A, Gloe T, Pohl U and Zahler S. **Nitric oxide enhances de novo formation of endothelial gap junctions.** *Cardiovascular research* **(2003)** 60: 421-430.

- Hoffmann JJ and Iruela-Arispe. **Notch expression patterns in the retina: An eye on receptor-ligand distribution during angiogenesis.** *Gene Expression Patterns* **(2007)** 7: 461-470.

- Hojo M, Ohtsuka T, Hashimoto N, Gradwohl G, Guillemot F, Kageyama R. **Glial cell fate specification modulated by the bHLH gene Hes5 in mouse retina.** *Development* **(2000)** 127(12): 2515-22.

- Holash JA, Stewart PA. **The relationship of astrocyte-like cells to the vessels that contribute to the blood-ocular barriers.** *Brain Research* **(1993)** 629(2): 218-224.

- Holder JW, Elmore E, Barrett JC. **Gap junction function and cancer.** *Cancer Research* **(1993)** 53(15): 3475-3485.

- Holländer H, Makarov F, Dreher Z, van Driel D, Chan-Ling T and Stone J. **Structure of the microglia of the retina: sharing and division of labour between astrocytes and Müller cells.** *Journal of Comparative Neurology.* **(1991)** 313(4): 587-603.

- Hope BT, Michael GJ, Knigge KM, Vincent SR. **Neuronal NADPH diaphorase is a nitric oxide synthase.** *Proceedings of the National Academy of Sciences of the United States of America* **(1991)** 88(7): 2811-2814.

- Huang F, Rock JR, Harfe BD, Cheng T, Huang X, Jan YN, Jan LY. **Studies on expression and function of the TMEM16A calcium-activated chloride channel.** *Proceedings of the National Academy of Sciences of the United States of America* **(2009)** 106(50): 21413-21418.

- Huizinga JD, Thuneberg L, Vanderwinden JM, Rumessen JJ. **Interstitial cells of Cajal as targets for pharmacological intervention in gastrointestinal motor disorders.** *Trends in Pharmacological Sciences* **(1997)** 18(10): 393-403.

- Huizinga JD, Robinson TL and Thomsen L. **The search of the origin of rhythmicity in intestinal contraction; from tissue to single cells.** *Neurogastrenterolgy and Motility* **(2000)** 12: 3-9.

- Huizinga JD, Faussone-Pellegrini MS. **About the presence of interstitial cells of Cajal outside the musculature of the gastrointestinal tract.** *Journal of cellular and molecular medicine* **(2005)** 9(2): 468-473.

- Huizinga JD, Zarate N, Farrugia G. **Physiology, injury, and recovery of interstitial cells of Cajal: basic and clinical science.** *Gastroenterology* **(2009)** 137(5): 1548-1556.

- Huizinga JD, Lammers WJEP, Mikkelsen HB, Zhu Y and Wang XY. **Toward a Concept of Stretch Coupling in Smooth Muscle: A Thesis by Lars Thuneberg on Contractile Activity in Neonatal Interstitial Cells of Cajal.** *The Anatomical Record* **(2010)** 293(9): 1543-1552.

- Hungerford JE, Owens GK, Argraves WS, Little CD. **Development of the aortic vessel wall as defined by vascular smooth muscle and extracellular matrix markers.** *Developmental Biology* **(1996)** 178(2): 375-392.

- Ignarro LJ. Nitric oxide. **A novel signal transduction mechanism for transcellular communication.** *Hypertension* **(1990)** 16(5): 477-483.

- Iino S, Horiguchi K, Nojyo Y. **Interstitial cells of Cajal are innervated by nitrergic nerves and express nitric oxide-sensitive guanylate cyclase in the guinea-pig gastrointestinal tract.** *Neuroscience* **(2008)** 152(2): 437-448.

- Ikebe T, Shimada T, Ina K, Kitamura H and Nakatsuka K. **The three-dimensional architecture of retinal blood vessels in kk mice, with special reference to the smooth muscle cells and pericytes.** *Journal of Electron Microscopy*. **(2001)** 50(2): 125-132.

- Inoue A, Yanagisawa M, Kimura S, Kasuya Y, Miyauchi T, Goto K, Masaki T. **The human endothelin family: three structurally and pharmacologically distinct isopeptides predicted by three separate genes.** *Proceedings of the National Academy of Sciences of the United States of America* **(1989)** 86(8): 2863-7.

- Ishikawa T. **Fine structure of retinal vessels in man and the macaque monkey.** *Investigative Ophthalmology* **(1963)** 2: 1-15.

- Isshiki M, Ying YS, Fujita T and Anderson RGW. **A Molecular Sensor Detects Signal Transduction from Caveolae in Living Cells.** *The Journal of Biological Chemistry* **(2002)** 277(45): 43389-43398.

- Izbeki F, Asuzu DT, Lorincz A, Bardsley MR, Popko LN, Choi KM, Young DL, Hayashi Y, Linden DR, Kuro-o M, Farrugia G, Ordog T. **Loss of Kitlow progenitors, reduced stem cell factor and high oxidative stress underlie gastric dysfunction in progeric mice.** *The Journal of physiology* **(2010)** 588(Pt 16): 3101-3117.

- Kanaya H, Takeya R, Takeuchi K, Watanabe N, Naihe J and SUmimoto H. **Fhos2, a novel formin-related actin-organizing protein, probably associates with nestin intermediate filament.** *Genes to Cells* **(2005)** 10: 665-678.

- Keith CG, Cunha-Vaz JG, Shakib M. **Studies on the effects of osmotically active substances on the circulation and structure of the retina. I. Observations in vivo.** *Investigative Ophthalmology* **(1967)** 6(2): 192-197.

- Kivelä T, Uusitalo M. **Structure, development and function of cytoskeletal elements in non-neuronal cells of the human eye.** *Progress in Retinal and Eye Research* **(1998)** 17(3): 385-428.

- Knott R and Forrester JV. **Diabetic eye disease. In Textbook of diabetes.** *Eds. Pickup J Williams G.* **(2003).**

- Kotlikoff MI, Murray RK, Reynolds EE. **Histamine-induced calcium release and phorbol antagonism in cultured airway smooth muscle cells.** *The American journal of physiology* **(1987)** 253(4 Pt 1): C561-C566.

- Krueger M and Bechmann I. **CNS pericytes: Concepts, misconceptions, and a way out.** *Glia* **(2010)** 58(1): 1-10.

- Kur J, Newman EA, Chan-Ling T. **Cellular and physiological mechanisms underlying blood flow regulation in the retina and choroid in health and disease.** *Progress in Retinal and Eye Research* **(2012)** 31(5):3 77-406.

- Kuwabara T, Cogan DG. **Studies of Retinal Vascular Patterns Part I. Normal Architecture.** *Archives of Ophtalmology* **(1960)** 64(6): 904-911.

- Lamboley M, Pittet P, Koenigsberger M, Sauser R, Bény JL, Meister JJ. **Evidence for signaling via gap junctions from smooth muscle to endothelial cells in rat mesenteric arteries: possible implication of a second messenger.** *Cell Calcium* **(2005)** 37(4): 311-320.

- Laties AM. **Central retinal artery innervation. Absence of adrenergic innervation to the intraocular branches.** *Archives of Ophthalmology* **(1967)** 77(3): 405-409.

- Leamey CA, Protti DA and Dreher B. **Eye, retina, and Visual System of the Mouse. Chapter 3: Comparative Survey of the Mammalian Visual System with Reference to the mouse.** Ed Chalupa LM and Williams RW. The Mit Press. **(2008)** 510-524.

- Lee JH, Park HS, Shin JM, Chun MH, Oh SJ. **Nestin expressing progenitor cells during establishment of the neural retina and its vasculature.** *Anatomy & cell biology* **(2012)** 45(1): 38-46.

- Lee SH. **Retinal Vascular Patterns: Part I. A/V crossings, argyrophilic perivascular network, exogenous retinal vasculitis and arterial annulus.** *Journal of the Korean Ophthalmological Society* **(1976)** 17(2): 127-135.

- Lee SH, Hungerford JE, Little CD and Iruela-Arispe ML. **Proliferation and Differentiation od Smooth Muscle Cell Precursors Occurs Simultaneously During the Development of the Vessel Wall.** *Developmental Dynamics* **(1997)** 209: 342–352.

- Li S, Li T, Luo Y, Yu H, Sun Y, Zhou H, Liang X, Huang J, Tang S**. Retro-orbital injection of FITC-dextran is an effective and economical method for observing mouse retinal vessels.** *Molecular Vision* **(2011)** 17: 3566-3573.

- Loewenstein A. **Cushion cells in retinal precapillaries and capillaries.** *Nature* **(1947)** 159 (4059): 229.

- Lopes M, Goupille O, Saint Cloment C, Robert B. **Msx1 is expressed in retina endothelial cells at artery branching sites.** *Biology Open* **(2012)** 1(4): 376-84.

- Luksch A, Garhöfer G, Imhof A, Polak K, Polska E, Dormer GT, Anzenhofer S, Wolzt M and Schmetterer L. **Effect of inhalation of different mixtures of $O_2$ and $CO_2$ on retinal blood flow.** *British Journal of Ophtalmology*. **(2002)** 86: 1143-1147.

- Luna G, Lewis GP, Banna CD, Skalli O, Fisher SK. **Expression profiles of nestin and synemin in reactive astrocytes and Müller cells following retinal injury: a comparison with glial fibrillar acidic protein and vimentin.** *Molecular Vision* **(2010)** 16: 2511-2523.

- Ma JX. **Retinal arteriolar annulus and its function.** *Zhonghua Yan Ke Za Zhi* **(1994)** 30(2): 89-91.

- Maeda H, Yamagata A, Nishikawa S, Yoshinaga K, Kubayashi S, Nishi K and Nishikawa SI. **Requirement of c-kit for development of intestinal pacemaker system.** *Development NK* **(1992)** 116: 369-375.

- Manders EMM, VErbeek FJ, Aten JA. **Measurment of co-localization of objects in dual-color confocal images.** *Journal of Microscopy* **(1993)** 169(3): 375-382.

- Masuda H, Kawamura K, Nanjo H, Sho E, Komatsu M, Sugiyama T, Sugita A, Asari Y, Kobayashi M, Ebina T, Hoshi N, Singh TM, Xu C, Zarins CK. **Ultrastructure of endothelial cells under flow alteration.** *Microscopy Research and Technique* **(2003)** 60(1): 2-12.

- Matsuura T, Yamamoto T**. An electron microscope study of arteriolar branching sites in the normal gastric submucosa of rats and in experimental gastric ulcer.** *Virchows Archiv. A, Pathological Anatomy and Histopathology* **(1988)** 413(2): 123-131.

- Maureen A, McCall N and Gregg RG. **Neurotransmission in the mouse retina. In: Eye, Retina, and Visual System of the Mouse.** pp. 175-188. *Eds. Chalupa LM and Williams RW.* The Mit Press. **(2008)**

- May CA, Lütjen-Drecoll E. **Morphology of the murine optic nerve**. *Investigative Ophthalmology & Visual Science.* **(2002)** 43(7): 2206-2212.

- McCall MA, Peachey NS and Gregg RG. **Neurotransmission in the mouse retina. In: Eye, retina, and Visual System of the Mouse.** pp.175-187. *Eds. Chalupa LM and Williams RW. The Mit Press.* **(2008).**

- McGahon MK, Needham MA, Scholfield CN, McGeown JG, Curtis TM. **Ca2+-activated Cl- current in retinal arteriolar smooth muscle.** *Investigative ophthalmology & visual science* **(2009)** 50(1): 364-371.

- Mendes-Jorge L, Llombart C, Ramos D, López-Luppo M, Valença A, Nacher V, Navarro M, Carretero A, Méndez-Ferrer S, Rodriguez-Baeza A, Ruberte J. **Intercapillary bridging cells: immunocytochemical characteristics of cells that connect blood vessels in the retina.** *Experimental Eye Researc.* **(2012)** 98: 79-87.

- Metea MR, Newman EA. **Glial cells dilate and constrict blood vessels: a mechanism of neurovascular coupling.** *The Journal of neuroscience : the official journal of the Society for Neuroscience* **(2006)** 26(11): 2862-2870.

- Metea MR, Newman EA. **Signalling within the neurovascular unit in the mammalian retina.** *Experimental physiology* **(2007)** 92(4): 635-40.

- Metea MR, Newman EA. **Signalling within the neurovascular unit in the mammalian retina.** *Experimental Physiology* **(2007)** 92(4): 635-640.

- Meyer-Rüsenberg B, Pavlidis M, Stupp T and Thanos S. **Pathological changes in human retinal ganglion cells associated with diabetic and hypertensive retinopathy.** *Graefe's Archive for Clinical and Experimental Ophthalmology* **(2006)** 245(7): 1009-1018.

- Michalczyk K, and Ziman M. **Nestin structure and predicted function in cellular cytoskeletal organization.** *Histology and Histopathology* **(2005)** 20: 665-671.

- Michaux G, Cutler DF. **How to roll an endothelial cigar: the biogenesis of Weibel-Palade bodies.** *Traffic* **(2004)** 5(2): 69-78.

- Mignone JL, Kukekov V, Chiang AS, Steindler D, Enikolopov G. **Neural stem and progenitor cells in nestin-GFP transgenic mice.** *The Journal of comparative neurology* **(2004)** 469(3): 311-324.

- Minshall RD, Sessa WC, Stan RV, Anderson RG, Malik AB. **Caveolin regulation of endothelial function.** American Journal of Physiology. *Lung Cellular and Molecular Physiology* **(2003)** 285(6): L1179-1183.

- Mishra A, Hamid A and Newman EA. Oxygen modulation of neurovascular coupling in the retina. *PNAS* (2011) 108(43): 17827-17831.

- Miyagami M, Katayama Y. **Angiogenesis of glioma: evaluation of ultrastructural characteristics of microvessels and tubular bodies (Weibel-Palade) in endothelial cells and immunohistochemical findings with VEGF and p53 protein.** *Medical Molecular Morphology* **(2005)** 38(1): 36-42.

- Moffat DB, Creasey M. **The fine structure of the intra-arterial cushions at the origins of the juxtamedullary afferent arterioles in the rat kidney.** *Journal of Anatomy* **(1971)** 110(3): 409-419.

- Morcos Y, Hosie MJ, Bauer HC, Chan-Ling T. **Immunolocalization of occludin and claudin-1 to tight junctions in intact CNS vessels of mammalian retina.** *Journal of Neurocytology* **(2001)** 30(2): 107-123.

- Morel E, Meyronet D, Thivolet-Bejuy F, Chevalier P**. Identification and distribution of interstitial Cajal cells in human pulmonary veins.** *Heart rhythm : the official journal of the Heart Rhythm Society* **(2008)** 5(7): 1063-1067.

- Mowat FM, Luhmann UF, Smith AJ, Lange C, Duran Y, Harten S, Shukla D, Maxwell PH, Ali RR, Bainbridge JW. **HIF-1alpha and HIF-2alpha are differentially activated in distinct cell populations in retinal ischaemia.** *PLoS One* **(2010)** 5(6): e11103.

- Nabika TS, Paul A, Velletri S, Lovenberg WS and Beavens MA. **Increase in Cytoslic Calcium and Phosphoinositide Metabolism Indcuced by Angiotensin and [Arg] Vasopressin in Vascular Smooth Muscle Cells.** *The Journal of Biological Chemistry* **(1985)** 260(8): 4661-4670.

- Nagaoka T, Sakamoto T, Mori F, Sato E and Yoshida A. **The Effect of Nitric Oxide on Retinal Blood Flow during Hypoxia in Cats.** *Investigative Ophtalmolgy and Visual Science* **(2002)** 43(9): 3037-3044.

- Nehls V, Drenckhahn D. **Heterogeneity of microvascular pericytes for smooth muscle type alpha-actin.** *The Journal of cell biology* **(1991)** 113(1): 147-154.

- Newman E. and Reichenbach A. **The Müller cell: a functional element of the retina.** *Trends in Neurosciences* **(1996)** 19(8): 307-312.

- Ninomiya H, Masui M. **Vasculature of the orbital rete in the Japanese deer (Cervus nippon).** *Veterinary Ophthalmology* **(1999)** 2(2): 107-112.

- Ninomiya H, Inomata T. **Microvasculature of the hamster eye: scanning electron microscopy of vascular corrosion casts.** *Veterinary Ophthalmology* **(2005)** 8(1): 7-12.

- Ninomiya H, Kuno H. **Microvasculature of the rat eye: scanning electron microscopy of vascular corrosion casts.** *Veterinary Ophthalmology* **(2001)** 4(1): 55-59.

- Okabe M, Ikawa M, Kominami K, Nakanishi T, Nishimune Y. **'Green mice' as a source of ubiquitous green cells.** *FEBS Letters* **(1997)** 407(3): 313-319.

- Owens GK, Kumar MS and Wamhoff BR. **Molecular Regulation of Vascular Smooth Muscle Cell Differentiation in Development and Disease.** *Physiological Reviews* **(2004)** 84: 767-801.

- Page C, Rose M, Yacoub M, Pigott R**. Antigenic heterogeneity of vascular endothelium.** *The American Journal of Pathology* **(1992)** 141(3): 673-683.

- Palade GE and Bruns RR. **Structural modulations of plasmalemmal vesicles.** *Journal of Cell Biology* **(1968)** 37(3): 633-649.

- Pannarale L, Onori P, Ripani M, Gaudio E. **Precapillary patterns and perivascular cells in the retinal microvasculature. A scanning electron microscope study.** *Journal of Anatomy* **(1996)** 188(3): 693-703.

- Palmer RM, Ferrige AG, Moncada S. **Nitric oxide release accounts for the biological activity of endothelium-derived relaxing factor.** *Nature* **(1987)** 327(6122): 524-526.

- Paques M, Tadayoni R, Sercombe R, Laurent P, Genevois O, Gaudric A and Vicaut E. **Structural and hemodynamic analisys of the mouse retinal microcirculation.** *Investigative Ophtalmology and Visual Science.* **(2003)** 44(11): 4960-4967.

- Pezzone MA, Watkins SC, Alber SM, King WE, de Groat WC, Chancellor MB, Fraser MO. **Identification of c-kit-positive cells in the mouse ureter: the interstitial cells of Cajal of the urinary tract.** American journal of physiology. *Renal physiology* **(2003)** 284(5): F925-F929.

- Pfister F, Feng Y, vom Hagen F, Hoffmann S, Molema G, Hillebrands JL, Shani M, Deutsch U, Hammes HP. **Pericyte migration: a novel mechanism of pericyte loss in experimental diabetic retinopathy.** *Diabetes* **(2008)** 57(9): 2495-2502.

- Planat-Bernard V, Menard C, Andre M, Puceat M Perez A, Garcia-Verdugo J, Penicaud and Casteilla L. **Spontaneous cardiomyocyte differentiation from adipose tissue stromal cells.** *Circulation Research* **(2004)** 94: 223-229.

- Popescu LM, Hinescu ME, Ionescu N, Ciontea SM, Cretoiu D and Ardeleanu C. **Interstitial cells of Cajal in pancreas.** *Journal of Cellular and Molecular Medicine* **(2005)** 9(1): 169-190.

- Popescu LM, Ciontea SM, Cretoiu D, Hinescu ME, Radu E, Ionescu N, Ceausu M, Gherghiceanu M, Braga RI, Vasilescu F, Zagrean L and Ardeleanu C. **Novel type of interstitial cell (Cajal-like) in human fallopian tube.** *Journal of Cellular and Molecular Medicine* **(2005)** 9(2): 479-523.

- Popescu LM, Ciontea SM and Cretoiu D. **Interstitial Cajal-Like Cells in Human Uterus and Fallopian Tube.** *Annals of the New York Academy of Sciences* **(2007)** 1101(Reproductive Biomechanics): 139-165.

- Popescu LM, Gherghiceanu M, Manole CG and Faussone-Pellegrini MS. **Cardiac renewing: interstitial Cajal-like cells nurse cardiomyocyte progenitors in epicardial stem cell niches.** *Journal of Cellular and Molecular Medicine* **(2009)** 13(5): 866-886.

- Porat RM, Grunewald M, Globerman A, Itin A, Barshtein G, Alhonen L, Alitalo K, Keshet E. **Specific induction of tie1 promoter by disturbed flow in atherosclerosis-prone vascular niches and flow-obstructing pathologies.** *Circulation Research* **(2004)** 94(3): 394-401.

- Porta M, Grosso A, Veglio F. **Hypertensive retinopathy: there's more than meets the eye.** *Journal of Hypertens* **(2005)** 23(4): 683-696.

- Pournaras CJ, Donati G, Kapetanios AD, Redard M, Bochatay-Piallat ML, Gabbiani G. **Myofibroblasts and retinal fibrovascular membranes.** *Klinische Monatsblätter für Augenheilkunde* **(1998)** 212(5): 356-8.

- Pournaras CJ, Rungger-Brändle E, Riva CE, Hardarson SH, Stefansson E. **Regulation of retinal blood flow in health and disease.** *Progress in Retinal and Eye Research* **(2008)** 27(3): 284-330.

- Povstyan OV, Gordienko DV, Harhun MI, Bolton TB. **Identification of interstitial cells of Cajal in the rabbit portal vein.** *Cell Calcium* **(2003)** 33(4): 223-39.

- Presnell JK, Schreibman MP. **Animal Tissue Techniques.** *Ed. Gretchen L. Humanso.* 5th edition **(1997)**.

- Pucovský V, Moss RF, Bolton TB. **Non-contractile cells with thin processes resembling interstitial cells of Cajal found in the wall of guinea-pig mesenteric arteries.** *The Journal of physiology* **(2003)** 552(Pt 1): 119-133.

- Pucovský V, Harhun MI, Povstyan OV, Gordienko DV, Moss RF and Bolton TB. **Colse relation of arterial ICC-like cells to the contractile phenotype of vascular smooth muscle cell.** *Journal of Cellular and Molecular medicine* **(2007)** 11(4): 764-775.

- Pucovský V, Moss RF, Bolton TB. **Potentiation of carbachol-induced detrusor smooth muscle contractions by beta-adrenoceptor activation.** *European journal of pharmacology* **(2009)** 606(1-3): 191-198.

- Pucovský V. **Interstitial cells of blood vessels**. *TheScientificWorldJournal* **(2010)** 10: 1152-1168.

- Puro DG. **Retinovascular pathophysiology: New experimental approach/new insights.** *Progress in Retinal and Eye Research.* **(2012)** 31(3): 258-270.

- Ramalho PS, Dollery CT. **Hypertensive retinopathy. Caliber changes in retinal blood vessels following blood-pressure reduction and inhalation of oxygen.** *Circulation* **(1968)** 37(4): 580-588.

- Ramos D, Navarro M, Mendes-Jorge L, Carretero A, Lopez-Luppo M, Nacher V, Rodridguez-Baeza A, Ruberte J. **The use of confocal laser microscopy to analyze mouse retinal blood vessels.** *Confocal laser Microscopy. Principles and applications in medicine, biology, and the food sciences(1$^{st}$ ed), ed. Neil Lagali* **(2013)** Chapter 2: 19-37, INTECH

- Ripodas A, de Juan JA, Roldán-Pallarés M, Bernal R, Moya J, Chao M, López A, Fernández-Cruz A, Fernández-Durango R. **Localisation of endothelin-1 mRNA expression and immunoreactivity in the retina and optic nerve from human and porcine eye. Evidence for endothelin-1 expression in astrocytes.** *Brain Research* **(2001)** 912(2): 137-143.

- Risco JM, Nopanitaya W. **Ocular microcirculation. Scanning electron microscopic study.** *Investigative Ophthalmology & Visual Science* **(1980)** 19(1): 5-12.

- Riva CE, Grunwald JE and Petrig BL. **Autoregulation of human retinal blood flow. An investigation with laser Doppler velocimetry.** *Investigative Ophtalmology and Visual Science*. **(1986)** 27(12): 1706-1712.

- Riva CE, Logean E, Falsini B. **Visually evoked hemodynamical response and assessment of neurovascular coupling in the optic nerve and retina.** *Progress in retinal and eye research* **(2005)** 24(2): 183-215.

- Riva CE, Sinclair SH, Grunwald JE. **Autoregulation of retinal circulation in response to decrease of perfusion pressure.** *Investigative ophthalmology & visual science* **(1981)** 21(1 Pt 1): 34-38.

- Roitt I, Brostoff J and Male D. **Immunology**. (6th ed.). London: Ed. Mosby **(2001)**.

- Rootman J. **Vascular system of the optic nerve head and retina in the pig.** *British Journal of Ophtalmology* **(1971)** 55(12): 808-819.

- Rouget C. **Mémoire sur le Developpement, L'estructure et les Propriétés Physiologiques des Capillaires Sanguins et Lymphatiques.** *Archives de Physiologie Normale et Pathologique* **(1873)** 5(6): 603-671

- Rucker HK, Wynder HJ, Thomas WE. **Cellular mechanisms of CNS pericytes.** *Brain Research Bulletin* **(2000)** 51(5): 363-369.

- Saint-Geniez M, D'Amore PA. **Development and pathology of the hyaloid, choroidal and retinal vasculature.** *The International Journal Developmental Biology* **(2004)** 48(8-9): 1045-1058.

- Saint-Geniez M, Maldonado AE and D'Amore PA. **VEGF Expression and Receptor Activation in the Choroid during Development and in the Adult.** *Investigative Ophtamologu and Visual Science*. **(2006)** 47(7): 3135-3142.

- Sanders KM, Ordög T, Ward SM. **Physiology and pathophysiology of the interstitial cells of Cajal: from bench to bedside. IV. Genetic and animal models of GI motility disorders caused by loss of interstitial cells of Cajal.** *America Journal Physiology. Gastrointestinal and Liver Physiology* **(2002)** 282(5): G747-756.

- Sanders KM, Ward SM. **Interstitial cells of Cajal: a new perspective on smooth muscle function.** *The Journal of Physiology* **(2006)** 576(Pt 3): 721-726.

- Santhaman L, Berkowitz DE and Belkin AM. **Nitric-oxide regulates non-classical secretion of tissue transglutaminase.** *Communictaive and Integrative Biology* **(2011)** 4(5): 584-586.

- Schaller O. **Illustrated Veterinary Anatomical Nomenclature.** pp. 35-60. Ed. Enke. **(1992)**.

- Schneeberger EE, Lynch RD. **Tight junctions. Their structure, composition, and function.** *Circulation Research* **(1984)** 55(6): 723-733.

- Schneider RK, Püllen A, Kraman R, Bornemann J, Knüchel R, Neuss S and Perez-Bouza A. **Long-term survival and characterization of human umbilical cord-derived mesenchymal stem cells on dermal equivalents.** *Differentiation* **(2010)** 79 (3): 182-193.
- Selby R, Starzl TE, Yunis E, Brown BI, Kendall RS, Tzakis A. **Liver transplantation for type IV liver disease.** *The New England Journal of Medicine* **(1991)** 324 (1): 39-42.

- Senis YA, Richardson M, Tinlin S, Maurice DH, Giles AR. **Changes in the pattern of distribution of von Willebrand factor in rat aortic endothelial cells following thrombin generation in vivo.** *British Journal of Haematology* **(1996)** 93(1): 195-203.

- Sergeant GP, Hollywood MA, McCloskey KD, Thornbury KD and McHale NG. **Specialised pacemaking cells in the rabbit urethra.** *Journal of Physiology* **(2000)** 526(2): 359-366.

- Sergeant GP, Thornbury KD, McHale NG, Hollywood MA. **Interstitial cells of Cajal in the urethra.** *Journal of cellular and molecular medicine* **(2006)** 10(2): 280-291.

- Shah V, Haddad FG, Garcia-Cardena G, Frangos JA, Mennone A, Groszmann RJ, Sessa WC. **Liver sinusoidal endothelial cells are responsible for nitric oxide modulation of resistance in the hepatic sinusoids.** *Journal of Clinical Investigation* **(1997)** 100(11): 2923-2930.

- Sharon N, Lis H. **Legume lectins--a large family of homologous proteins.** *FASEB journal : official publication of the Federation of American Societies for Experimental Biology* **(1990)** 4(14): 3198-3208.

- Shaw JE, Sicree RA, Zimmet PZ. **Global estimates of the prevalence of diabetes for 2010 and 2030.** *Diabetes Research and Clinical Practice* **(2010)** 87(1): 4-14.

- Siemerink MJ, Klaassen I, Vogels IM, Griffioen AW, Van Noorden CJ, Schlingemann RO. **CD34 marks angiogenic tip cells in human vascular endothelial cell cultures.** *Angiogenesis* **(2012)** 15(1): 151-163.

- Simionescu M, Simionescu N, Palade GE. **Segmental differentiations of cell junctions in the vascular endothelium. The microvasculature.** *The Journal of Cell Biology* **(1975)** 67(3): 863-885.

- Simionescu M, Simionescu N. **Functions of the endothelial cell surface.** *Annual review of physiology* **(1986)** 48:279-293.

- Simoens P, De Schaepdrijver L, Lauwers H. **Morphologic and clinical study of the retinal circulation in the miniature pig. A: Morphology of the retinal microvasculature.** *Experimental Eye Research* **(1992)** 54(6): 965-973.

- Sircar K, Hewlett BR, Huizinga J, Chorneyko K, Berezin I and Riddle RH. **Interstitial Cells of Cajal as Precursors of Gastrointestinal Stromal Tumors.** *American Journal of Surgical Pathology* **(1999)** 23(4): 377-389.

- Smith RS, Hawes NL, Chang B and Nishina PM. **Retina. In: Systematic evaluation of the mouse eye.** pp 195-225.**(2002).**

- Soboleski MR, Oaks J, Halford WP. **Green fluorescent protein is a quantitative reporter of gene expression in individual eukaryotic cells.** *FASEB journal : official publication of the Federation of American Societies for Experimental Biology* **(2005)** 19(3): 440-442.

- Sobotta J and Becher H. **Atlas de Anatomía Humana.** *Eds. Ferner H, Staubesand J.* Munich: Ediciones Toray. **(2000).**

- Sokolovsky M, Ambar I, Galron R. **A novel subtype of endothelin receptors.** *The Journal of biological chemistry* **(1992)** 267(29): 20551-20554.

- Srienc AI, Kurth-Nelson ZL, Newman EA**. Imaging retinal blood flow with laser speckle flowmetry.** *Frontiers in Neuroenergetics* **(2010)** 2. pii: 128.

- Soto Abánades CI, Ríos Blanco JJ, Barbado Hernández FJ. **Interstitial cells of Cajal: another contribution to modern medicine.** *Revista clínica española* **(2008)** 208(11): 572-574.

- Strege PR, Ou Y, Sha L, Rich A, Gibbons SJ, Szurszewski JH, Sarr MG, Farrugia G. **Sodium current in human intestinal interstitial cells of Cajal.** *American journal of physiology. Gastrointestinal and liver physiology* **(2003)** 285(6): G1111-G1121.

- Suciu L, Popescu LM, Gherghiceanu M. **Human placenta: de visu demonstration of interstitial Cajal-like cells.** *Journal of cellular and molecular medicine* **(2007)** 11(3): 590-597.

Suciu L, Popescu LM, Regalia T, Ardelean A, Manole CG. **Epicardium: interstitial Cajal-like cells (ICLC) highlighted by immunofluorescence.** *Journal of cellular and molecular medicine* **(2009)** 13(4): 771-777.

- Sunni S, Geer JC, Kent SP. **Staining in normal and ischemic human myocardium. A study of myoglobin, IgG, glycogen, and diastase-PAS.** *Archives of Pathology and Laboratory Medicine* **(1984)** 108(8): 649-653.

- Takagi C, King GL, Takagi H, Lin YW, Clermont AC, Bursell SE. **Endothelin-1 action via endothelin receptors is a primary mechanism modulating retinal circulatory response to hyperoxia.** *Investigative ophthalmology & visual science* **(1996)** 37(10): 2099-2109.

- Tapp RJ, Shaw JE, Harper CA, de Courten MP, Balkau B, McCarty DJ, Taylor HR, Welborn TA, Zimmet PZ and AusDiab Study Group. **The prevalence of and factors associated with diabetic retinopathy in the Australian population.** *Diabetes Care* **(2003)** 26(6): 1731-1737.

- Thomas D, Tovey SC, Collins TJ, Bootman MD, Berridge MJ, Lipp P. **A comparison of fluorescent Ca2+ indicator properties and their use in measuring elementary and global Ca2+ signals.** *Cell Calcium* **(2000)** 28(4): 213-223.

- Thorin E, Shreeve SM. **Heterogeneity of vascular endothelial cells in normal and disease states.** *Pharmacology & Therapeutics* **(1998)** 78(3): 155-166.

- Thuneberg L. **Interstitial cells of Cajal: intestinal pacemaker cells?** *Advances in anatomy, embryology, and cell biology* **(1982)** 71: 1-130.

- Thuneberg L, Peters S. **Toward a concept of stretch-coupling in smooth muscle. I. Anatomy of intestinal segmentation and sleeve contractions.** *The Anatomical Record* **(2001)** 262(1): 110-124.

- Thuránzsky K. **Der Blutkreislau der Netz.** *Verlag der Ungarischen Akademie der Wissenschaften* **(1957)**

- Timpl R, Rhode H, Robey PG, Rennard SI, Foidart JM and Martin GR. **Laminin—a glycoprotein from basement membranes.** *Journal of Biological Chemistry* **(1979)** 254(19): 9933-9937.

- Timpl R, Dziadek M, Fujiwara S, Nowack H, Wick G. **Nidogen: a new, self-aggregating basement membrane protein.** *European journal of biochemistry / FEBS* **(1983)** 137(3): 455-465.

- Torihashi S, Horisawa M, Watanabe Y. **c-Kit immunoreactive interstitial cells in the human gastrointestinal tract.** *Journal of the Autonomic Nervous System* **(1999)** 75(1): 38-50.

- Tornavaca O, Pascual G, Barreiro ML, Grande MT, Carretero A, Riera M, Garcia-Arumi E, Bardaji B, González-Núñez M, Montero MA, López-Novoa JM, Meseguer A. **Kidney androgen-regulated protein transgenic mice show hypertension and renal alterations mediated by oxidative stress.** *Circulation* **(2009)** 119(14): 1908-1917.

- Tso MO, Shih CY. **Disruption of blood-retinal barrier in ocular hypotony: preliminary report.** *Experimental Eye Research* **(1976)** 23(2): 209-16.

- Tsujimura T, Makiishi-Shimobayashi C, Lundkvist J, Lendhal U, Nakasho K, Sugihara A, Iwasaki T, Mano M, Yamada N, Yamashita K, Toyosaka A and Terada N. **Expression of the Intermediate Filament Nestin in Gastronintestinal Stromal Tumors and Interstitial Cells of Cajal.** *The American Journal of Pathology* **(2001)** 158(3): 817-823.

- Underhill C. **CD44: the hyaluronan receptor.** *Journal of Cell Science* **(1992)** 103( Pt 2): 293-298.

- Vaag A, Skött P, Damsbo P, Gall MA, Richter EA, Beck-Nielsen H. **Effect of the antilipolytic nicotinic acid analogue acipimox on whole-body and skeletal muscle glucose metabolism in patients with non-insulin-dependent diabetes mellitus.** *The Journal of clinical investigation* **(1991)** 88(4): 1282-1290.

- Vaheri A, Mosher DF. **High molecular weight, cell surface-associated glycoprotein (fibronectin) lost in malignant transformation.** *Biochimica et Biophysica Acta* **(1978)** 516(1): 1-25.

- van Mourik JA, Romani de Wit T, Voorberg J. **Biogenesis and exocytosis of Weibel-Palade bodies.** *Histochemistry and Cell Biology* **(2002)** 117(2): 113-22.

- Vanderwinden J-M, Gillard K, De Laet M-H, Messam CA and Schiffmann SN. **Distribution of the intermediate filament nestin in the muscularis propria of the human gastrointestinal tract.** *Cell and Tissue Research* **(2002)** 309: 261-268.

- Varia MA, Calkins-Adams DP, Rinker LH, Kennedy AS, Novotny DB, Fowler WC Jr, Raleigh JA. **Pimonidazole: a novel hypoxia marker for complementary study of tumor hypoxia and cell proliferation in cervical carcinoma.** *Gynecologic Oncology* **(1998)** 71(2): 270-277.

- Venturini CM, Knowles RG, Palmer RM, Moncada S. **Synthesis of nitric oxide in the bovine retina.** *Biochemical and biophysical research communications* **(1991)** 180(2): 920-925.

- Vincent SR, Hope BT. **Neurons that say NO.** *Trends in Neurosciences* **(1992)** 15(3): 108-113.

- Vinores SA. **Assessment of blood-retinal barrier integrity.** *Histology and Histopathology* **(1995)** 10(1): 141-154.

- Vischer UM. **von Willebrand factor, endothelial dysfunction, and cardiovascular disease.** *Journal of Thrombosis and Haemostaisis: JTH* **(2006)** 4(6): 1186-1193.

- Walker GJ, Whelan WJ. **The mechanisms of carbohydrase action. 7. Stages in the salivary α-amylosis of amylose, amylopectin and glycogen.** *Biochemical Journal* **(1960)** 76(2): 257-263.

- Wang M, Yang H, Zheng LY, Zhang Z, Tang YB, Wang GL, Du YH, Lv XF, Liu J, Zhou JG, Guan YY. **Downregulation of TMEM16A calcium-activated chloride channel contributes to cerebrovascular remodeling during hypertension by promoting basilar smooth muscle cell proliferation.** *Circulation* **(2012)** 125(5): 697-707.

- Wangsa-Wirawan ND and Linsenmeier RA. **Retinal Oxygen: Fundamental and Clinical Aspects.** *Archives of Ophtalmology* **(2003)** 121(4): 547-557.

- Weibel ER, Palade GE. **New cytoplasmatic components in arterial endothelia.** *The Journal of Cell Biology* **(1964)** 23: 101-112.

- Whelan NL, Subramanian R, Jin J and Keith IM. **Intramyocardial Arterial Cushions of Coronary Vessels in Animals and Humans: Morphology, Occurrence and Relation to Heart Disease.** *Journal of Vascular Research* **(1996)** 33: 209-224.

- Winkler BS. **A quantitative assessment of glucose metabolism in the isolated rat retina.** In: Christen Y, Doly M and Droy-LefaixMT, eds. *Les Seminaires Ophtalmogiques d'IPSEN: Tome 6, Vision et Adaptation*. New York, NY: Elsevier Science Inc **(1995)**: 78-96.

- Wise NG. **The retinal circulation.** *Eds. Harper & Row: New York.* 1st edition. **(1971).**

- Wong TY, McIntosh R. **Hypertensive retinopathy signs as risk indicators of cardiovascular morbidity and mortality.** *British Medical Bulletin* **(2005)** 73-74: 57-70.

- Worth NF, Campbell GR, Rolfe BE. **A role for rho in smooth muscle phenotypic regulation.** *Annals of the New York Academy of Sciences* **(2001)** 947: 316-322.

- Wright WS, McElhatten RM, Messina JE, Harris NR. **Hypoxia and the expression of HIF-1alpha and HIF-2alpha in the retina of streptozotocin-injected mice and rats.** *Experimental Eye Research* **(2010)** 90(3): 405-412.

- Wurmser AE, Nakashima K, Summers RG, Toni N, D'Amour KA, Lie DC, Gage FH. **Cell fusion-independent differentiation of neural stem cells to the endothelial lineage.** *Nature* **(2004)** 430(6997): 350-356.

- Wu KK, Thiagarajan P. **Role of endothelium in thrombosis and hemostasis.** *Annual Review of Medicine* **(1996)** 47: 315-331.

- Xue L, Ding P, Xiao L, Hu M, Hu Z. **Nestin is induced by hypoxia and is attenuated by hyperoxia in Müller glial cells in the adult rat retina.** *International journal of experimental pathology* **(2011)** 92(6): 377-381.

- Xue LP, Lu J, Cao Q, Hu S, Ding P, Ling EA. **Müller glial cells express nestin coupled with glial fibrillary acidic protein in experimentally induced glaucoma in the rat retina.** *Neuroscience* **(2006)** 139(2): 723-732.

- Yamamoto T, Watabe K, Nakahara M, Ogiyama H, Kiyohara T, Tsutsui S, Tamura S, Shinomura Y and Hayashi N. **Disturbed gastrointestinal motility and decreased interstitial cells of Cajal in diabetic *db/db* mice.** *Journal of Gastroenterology and Hepatology* **(2008)** 23(4): 660-667.

- Yin J and Chen JDZ. **Interstitial Cells of Cajal Review Series: Roles of interstitial cells of Cajal in regulating gastrointestinal motility: *in vitro versus in vivo* studies.** *Lournal of Molecular Medicine* **(2008)** 12(4): 1118-1129.

- Yu B, Han J, He YT, Guo S, Li SF, Mei F. **Immunohistochemical study of CD44 immunopositive cells in the muscular layers of the gastrointestinal tract in adult guinea pigs and mice.** *Acta Histochemica* **(2009)** 111(4): 382-390.

- Yu DY, Cringle SJ, Su EN and YU PK. **Sphincter-like Activity in Retinal Arterioles Feeding the Deeper Capillary Layer in Pig.** *Current Eye Resarch* **(2005)** 30: 781-787

- Zarins CK, Giddens DP, Bharadvaj BK, Sottiurai VS, Mabon RF, Glagov S. Carotid bifurcation atherosclerosis. **Quantitative correlation of plaque localization with flow velocity profiles and wall shear stress.** *Circulation Research* **(1983)** 53(4): 502-14.

- Zimmet P, Alberti KG, Shaw J. **Global and societal implications of the diabetes epidemic.** *Nature* **(2001)** 414(6865): 782-787.

- Zinchuk V, Zinchuk O, Okada T. **Quantitative Colocalization Analysis of Multicolor Confocal Immunofluorescence Microscopy Images: Pushing Pixels to Explore Biological Phenomena.** *Acta Histochemica et Cytochemica* **(2007)** 40(4): 101-111.